Adaptive Filters

for

Two to Four Wire Conversion

in

Telephony

by

Colm Ward B.Sc. (Eng.)

A thesis submitted to the University of Keele for the

Degree of Doctor of Philosophy.

August, 1983

Signal Processing Group,

Department of Physics,

University of Keele,

Keele,

Staffordshire,

England.

TO ELLEN RYRIE

ABSTRACT

The problem of inaccurate two to four wire conversion is considered, and a comprehensive survey of the transhybrid responses of 1845 subscribers' lines is carried out.

Results on the optimum performance achieved by line matching techniques are presented, and a simulator which is capable of simulating actual transhybrid responses is described.

The theory of continuous analog recursive adaptive filters is developed, and use of a filtered error signal is shown to considerably simplify their implementation. A simple method of estimating the gradients of the error surface is proposed. A method of modelling the behaviour of the filters is described and used to investigate the effects of these simplifications.

Various filter structures are investigated in terms of suitability for use in an adaptive hybrid. The implementation of 3 types of analog adaptive filter is described, and the effects of circuit imperfections are investigated. Results are presented for the performance of the filters. A 1st order filter, having a single pole and zero, is shown to provide adequate cancelled return loss against simulated lines. However, the dynamic performance of this filter is shown to be inadequate unless it converges from a set of stored initial conditions. It is concluded that implementation of an analog adaptive hybrid is impractical.

The effects of the process of A/D and D/A conversion on the complexity required of a digital adaptive filter are investigated. It is shown that these effects can be simply compensated.

The implementation of an experimental digital recursive adaptive filter is described, and results are presented for the performance of filters of various orders against subscribers' lines. It is shown that a first order pole-zero filter gives adequate static and dynamic performance when using an adaptive step size algorithm. The implementation of the digital adaptive hybrid is discussed.

ACKNOWLEDGEMENTS

My research colleagues Andy, Steve, Ambi, Aladdin and Kamran, for stimulating, if sometimes irreverent, suggestions.

My family and friends for their interest and encouragement

and Ellen, for undeserved tolerance and understanding.

CONTENTS

CHAPTER 1

INTRODUCTION

1.1 An Historical Introduction

The development of the all-digital local exchange has created
a need for more accurate conversion between the 2 wire system used to
connect the subscriber to the exchange, and the 4 wire system used
within the remainder of the telephone network. To highlight this
need it is instructive to consider some stages in the evolution of
the present telephone network.

When the telephone receiver and transmitter were invented by
A.G. Bell in 1876, the only methods of switching between electrical
connections were mechanical. Transmission was limited to the use of
wire, with no possibility of amplification. Thus all the likely
components of a telephone system were suitable for bi-directional
transmission, and almost all early telephone systems used only a
single pair of wires to carry signals in both directions of
transmission. The invention of the triode valve in 1906 introduced
the possibility of amplification on long-distance circuits, and
because the valve could only transmit signals in one direction, 4
wire transmission began to be introduced for long-distance telephony.
A 2 to 4 wire converter, often referred to as a hybrid, was used to
split a bi-directional channel into separate transmit and receive
channels. Initially these hybrids were used in repeaters for 2 wire
submarine cables, but when modulation and demodulation techniques
became possible, it was increasingly attractive to use full 4 wire
circuits for all long-distance telephony.

The telephone network thus evolved with a mixture of 2 wire

and 4 wire circuits, with the 2 wire circuits predominating for local and short-distance communication. This remained the case until the development of electronic switching techniques in 1959, which initiated the spread of 4 wire switching into the local telephone network. With the advent of the digital local exchange, using uni-directional electronic switching, the 2 to 4 wire conversion must now take place at the interface to the subscriber's line in the local exchange.

1.2 The 2 to 4 Wire Converter

Early 2 to 4 wire converters used a balanced bridge circuit with two centre-tapped transformers, however for the purposes of this thesis, the 2 to 4 wire converter which will be considered is the active circuit shown in Figure 1.1. The balance impedance (Zb), the terminating impedances (Ztl and Ztb), and the input impedance of the subscriber's line (Zi) form a bridge type circuit. The signal at the 4 wire receive input port is buffered by the amplifier A1 and applied to both arms of the bridge, while the 4 wire transmit output signal is formed from the difference of the signals at the mid-points of the arms. When the ratios:-

$$\frac{Zi(s)}{Ztl(s)+Zi(s)} \quad \text{and} \quad \frac{Zb(s)}{Zb(s)+Ztb(s)}$$

are equal, the bridge is said to be balanced, and none of the 4 wire receive input signal appears at the 4 wire transmit output. The signal applied to the subscriber's line is however a scaled version of the 4 wire receive input signal. Signals applied to the 2 wire port 'see' an input impedance equal to the terminating impedance Ztl, since the output impedance of amplifier A_1 is considered to be zero. These signals appear at the 4 wire transmit output, scaled by the gain of the differencing amplifier A_2.

The transfer function between the 4 wire receive input and the 4 wire transmit output, known as the transhybrid transfer function, is given by:-

$$H(s) = \frac{A_1 A_2 Zt(s)}{Zt(s)+Zb(s)} \frac{Zb(s)-Zi(s)}{Zi(s)+Zt(s)} \qquad 1.1$$

assuming that $Ztl(s) = Ztb(s) = Zt(s)$.

The condition of perfect balance, given by $Zb(s) = Zi(s)$, is difficult to achieve in practice, since in general no two subscribers' lines have exactly the same input impedances. Thus where a single balance impedance is used for all lines, its value is the result of a compromise, and in general the transhybrid transfer function is non-zero.

The maximum magnitude of the transhybrid transfer function encountered in the network depends on the spread of values of the line input impedances which the hybrid is required to match. The drop in the position within the heirarchy of the telephone system at which the 2 to 4 wire conversion takes place, has resulted in larger spreads of line input impedances to be balanced. This results in difficulty in achieving the required value of transhybrid loss. The effects of this finite transhybrid loss are discussed in Section 1.4. The purpose of the terminating impedance Zt is discussed in the following section and the concept of sidetone is introduced.

1.3 Control of Sidetone

In the subscriber's telephone it is necessary to connect both a microphone and an earpiece to a 2 wire local line. A simple series connection of the two elements results in the subscriber's speech being heard locally in the earpiece. This effect is known as sidetone, and it can be controlled by using a hybrid in the

telephone, as shown in the simplified diagram of Figure 1.2.

Voltages produced at the microphone cause currents to flow in opposite directions in windings W1 and W2. If Zb, the balance impedance, is equal to Zis, the input impedance of the line, as seen at the subscriber's end, then these currents are equal. If N1 = N2, then under these conditions no voltage is induced in winding W3, and no sidetone is heard in the earpiece. The level of sidetone produced in the earpiece thus depends on the input impedance of the line, which in turn depends on the terminating impedance used in the 2 to 4 wire converter at the exchange. The level of sidetone can therefore be controlled by fixing the value of the terminating impedance used in the hybrid.

1.4 The Effects of Imperfect 2 to 4 Wire Conversion

Figure 1.3 shows a simplified connection between two subscribers using 4 wire transmission. It can be seen that the two hybrids are connected 'back to back', and that the transhybrid transfer functions form a closed loop with the transmission paths CD and EF. Since it is desirable that paths CD and EF have low loss, the stability of the loop is critically dependant on the transhybrid losses. A measure of the stability of the system is given by the minimum transhybrid loss over the bandwidth 300 Hz to 3.4 kHz, and is referred to as the stability return loss (SRL).

If both hybrids have low values of SRL, then the loop may oscillate or 'sing' at a frequency where the total loop phase shift is a multiple of 2π. Even when the losses are sufficient to prevent this oscillation, the quality of the connection can nonetheless be seriously degraded, and the connection may sound 'hollow'.

From Figure 1.3 it can also be seen that insufficient

transhybrid loss at subscriber B's end of the the connection results in subscriber A's speech being returned via the path DEFA. This effect is known as 'talker echo', and provided that the loop is stable and the net delay around the loop is small, it is masked by sidetone in A's earpiece. If in addition subscriber A's hybrid has insufficient loss, then subscriber B hears A's speech initially via CDB, and later via CDEFCDB. This effect is known as 'listener echo', and it is masked by the original speech, if the loop delay is small. The average return loss due to a subscriber's line and hybrid over the frequency range 500 Hz to 2.5 kHz provides a measure of the level of both talker and listener echo, and is therefore known as the echo return loss (ERL).

Many studies of the effects of echo on the subjective quality of telephone connections have been undertaken. Early work in this field concentrated on the effects of long time delays because of the use of cables with low propogation velocities. The introduction of synchronous (or geo-stationary) satellites for communications re-awakened interest in this field. Riesz and Klemmer (1963), found that even round-trip delays as large as 1.2 S did not result in much dissatisfaction among inexperienced users when no echo was present. It was found however, that users who had been exposed to a delay of 2.4 S later reported considerable dissatisfaction, even with circuits having a delay of 0.6 S.

Emling and Mitchell (1963), noted that large round-trip delays altered the normal pattern of conversation, increasing the tendancy for both speakers to talk simultaneously. It was also noted that responses to one piece of conversation were sometimes mistaken for interruptions to a later (and possibly different) subject, and that this could lead to considerable confusion. Emling and Mitchell also reported on the results of a previous study on the combined

effects of delay and echo. This study showed that as the round- trip delay is increased, then higher values of ERL are necessary to achieve the same level of customer satisfaction. More recent work (CCITT, 1972) has verified these conclusions, although much higher values of ERL were found to be required to give only a small probability of objectionable echo occuring.

Bunker, Scida and Mc. Cabe (1979), concluded that for round-trip delays of up to 4 mS, such as may be encountered in the local network, a minimum SRL of 4 dB is required at each hybrid. Even with delays as low as 2 mS, and with 4 dB SRL however, only 50 % of subjects rated a test connection as 'good', with 90 % rating the connection as 'good' or 'fair'.

Cavanaugh, Hatch and Neigh (1980) reported that for connections with short time delays, a frequency weighted measure of the echo path loss provided better agreement with subjective testing of listener echo than that provided by the SRL or the ERL.

Techniques for controlling the objectionable effects of echo and instability are considered in the following sections.

1.5 Echo Control on Circuits with Small Propogation Delays

The network loss plan was originally developed in the United States to control echo on long-distance telephone circuits via loaded cable (Huntley, 1953). In this scheme sufficient loss was included in all long-distance circuits to render the effects of echo unnoticable. For each L dB loss introduced into the forward transmission paths, the echo level is reduced by 2L dB. Using this technique it was possible to achieve adequate performance on 99 % of calls for lines with propogation delays up to 45 mS. The plan was made obsolete by the introduction of low propogation delay

transmission systems.

The recent introduction of PCM transmission has again required that loss be inserted in the 4 wire loop, since the system otherwise provides 0 dB insertion loss irrespective of transmission distance. This loss must be introduced in the analog part of the 4 wire circuit, and this strategy has the effect of imposing stringent restrictions on the loss which can be ircurred on the subscriber's line without breaching loudness specifications.

The trade off between between loudness and echo control is particularly acute on circuits with long 2 wire lines, which may have considerable loss, and whose input impedances are difficult to match using simple balance impedances. In these cases a solution is to achieve better minimum SRL by using complex balance impedances rather than the normal balance resistor (Ames, 1981).

1.6 Echo Control on Circuits with Large Propogation Delays

Insertion of loss into the transmission path, and better balancing of the hybrid, are incapable of achieving the very high levels of ERL required for satisfactory communication via 4 wire circuits with large propogation delays. When synchronous satellites are used to provide inter-continental links, for example, the round trip propogation delay can be as large as 1 S. The additional return loss required is conventionally provided at international switching centres by means of echo suppression or echo cancellation.

1.6.1 Echo Suppression

The first attempts to control echo on links with large propogation delays made use of a simple voice switching technique to

detect speech in one 4 wire path and open the other path. Figure 1.4 shows two half echo suppressors connected at traffic-concentrated points between subscribers A and B. Because the suppressors are situated at traffic-concentrated points, so that they can be shared between many subscribers, there are small delays (D1 and D2) in the paths between the suppressors and the nearest hybrids. These delays are known as end-delays.

When speech from subscriber B is present at point E, then switch Sw1 is opened and potential echo signals are prevented from returning to B. For proper control of the echo, switch Sw1 should remain open for a small 'hangover' period after speech has ceased at point E. This hangover period can result in the first few syllables of speech from subscriber A (the near-end speaker), being lost, if A begins to speak immediatly on hearing a pause in B's speech. To counteract this near-end speech or 'double talking' problem, modern echo suppressors use 'break-in' detectors to ensure that the forward transmission path is closed immediatly a subscriber speaks. This modification removes echo suppression during double talking however. The problems of echo suppression and the techniques used in the design of echo suppressors were well documented by Brady and Helder (1963).

The switching and chopping of speech resulting from the use of echo suppressors was found by Riesz and Klemmer (1963) to be more objectionable than the original echo in some cases. Emling and Mitchel (1963) also pointed out that where two or more full echo suppressors are used with delay between them, then both forward transmission paths can be simultaneously blocked under some circumstances (a phenomenon known as 'lock-out'). To avoid this possibility it is necessary to ensure that only one full echo suppressor is used on any possible connection.

An alternative method of echo suppression was proposed by Mitchell and Berkley (1971). This method consisted of modelling the transhybrid loss over a number of frequency bands by variable attenuators, as shown in Figure 1.5. The 4 wire receive input to the hybrid was connected to the inputs of a set of filter banks and attenuators, and peak detectors estimated the peak amplitude of the echo signal in each frequency band. The peak detector outputs were used to control variable centre-clippers, which removed the echo components in each band from the 4 wire transmit output. It was reported that this technique operated successfully with ERL as low as 6 dB, and without the need to disable the centre-clippers when near-end speech was present. This approach requires 3 band-pass filters to model the echo path over each band, and no mechanism was proposed for automatically adjusting the attenuators.

1.6.2 Echo Cancellation

The aforementioned problems with echo suppressors led to an interest in methods of echo reduction without switching or inserting loss. It was initially suggested by Kelly and Logan (see Becker and Rudin, 1966), that the echo path response be modelled by an analog transversal filter, and that the output of the filter be subtracted from the signal in the return path to achieve echo cancellation. This scheme is shown in Figure 1.6. The output of the subtractor can then be used to control the tap weights of the filter in such a way as to cause the filter response to converge to an accurate model of the echo path response. This technique had been used by Lucky (1965), to cancel intersymbol interference in data transmission, and the combination of the transversal filter and the tap weight control circuitry became known as an adaptive filter. The amount of echo

An alternative method of echo suppression was proposed by Mitchell and Berkley (1971). This method consisted of modelling the transhybrid loss over a number of frequency bands by variable attenuators, as shown in Figure 1.5. The 4 wire receive input to the hybrid was connected to the inputs of a set of filter banks and attenuators, and peak detectors estimated the peak amplitude of the echo signal in each frequency band. The peak detector outputs were used to control variable centre-clippers, which removed the echo components in each band from the 4 wire transmit output. It was reported that this technique operated successfully with ERL as low as 6 dB, and without the need to disable the centre-clippers when near-end speech was present. This approach requires 3 band-pass filters to model the echo path over each band, and no mechanism was proposed for automatically adjusting the attenuators.

1.6.2 Echo Cancellation

The aforementioned problems with echo suppressors led to an interest in methods of echo reduction without switching or inserting loss. It was initially suggested by Kelly and Logan (see Becker and Rudin, 1966), that the echo path response be modelled by an analog transversal filter, and that the output of the filter be subtracted from the signal in the return path to achieve echo cancellation. This scheme is shown in Figure 1.6. The output of the subtractor can then be used to control the tap weights of the filter in such a way as to cause the filter response to converge to an accurate model of the echo path response. This technique had been used by Lucky (1965), to cancel intersymbol interference in data transmission, and the combination of the transversal filter and the tap weight control circuitry became known as an adaptive filter. The amount of echo

cancellation achieved by the adaptive filter is known as the echo return loss enhancement (ERLE), and it is measured by:-

$$ERLE = 10\log_{10}(Pd/Pe)$$
1.2

where Pd and Pe are the powers of the 4 wire transmit output signal and the error signal respectively, over the bandwidth 500 Hz to 2.5 kHz.

An early attempt at echo cancellation by Miura et al (1968), measured the impulse response of the echo path by injecting an impulse into the 'go' side, and observing the signal received from the return side. This procedure was carried out once on initiation of a call, and the resulting echo path model was held constant until the call was terminated. It was realised however, that in many cases the echo path is time varying. This can occur when carrier transmission is used with imperfectly synchronised local oscillators, resulting in slow periodic variations in the echo path response. This effect is known as 'phase-roll'. Time variation in the echo path response occurs more commonly when calls are transferred from one telephone to another. For these reasons it was necessary to develop echo cancellers which could continuously track variations in the echo path, and this effectively ruled out methods which depended on the injection of test signals. The echo canceller proposed by Kelly and Logan used only the 'go' and the 'return ' signals to estimate the echo path response, and almost all echo cancellers developed after 1968 used this technique in one form or another. In the following sections the major developments in echo cancellers are briefly reviewed.

1) Becker and Rudin (1966)

Becker and Rudin developed an analog echo canceller based on a tapped delay line transversal filter, and the tap weights were adjusted so as to minimise the mean-square error between the filter

output and the signal in the 'go' path. This was achieved by cross correlating the delayed input signal with the error signal, and using the result to add or subtract a fixed amount from the tap weigth setting. 20 dB ERLE against simulated echo path responses was reported, and this performance was maintained during double talking.

2) Sondhi and Presti (1966) and Sondhi (1967)

Sondhi proposed an analog echo canceller similar to that of Becker and Rudin, but using a non-linear function of the instantaneous error signal in controlling the tap weights. This system was shown to converge to an estimate of the echo path faster than that of Becker and Rudin, however the use of an instantaneous error criterion resulted in the filter tap weights diverging during double talking. To overcome this effect Sondhi proposed a simple near-end speech detector, similar to those used in echo suppressors, which disabled the tap weight adjustment circuitry during double talking. Computer simulations of the canceller predicted about 20 dB ERLE.

3) Kato et al (1971)

Kato et al developed a digital echo canceller using a transversal filter, based on a recirculating shift register, to model the echo path. Non-linear functions of the error signal and of the delayed input signal samples were used to control the filter coefficients. This simplified the implementation of the canceller and improved its convergence. The canceller also included a means of measuring and synthesising the fixed end-delay. Cancellation of up to 20 dB was reported for the 216-coefficient filter with simulated echo path delays of 12 mS.

4) Mackechnie (1970)

MacKechnie proposed a means of achieving very fast convergence of a transversal digital echo canceller in order to

output and the signal in the 'go' path. This was achieved by cross correlating the delayed input signal with the error signal, and using the result to add or subtract a fixed amount from the tap weigth setting.   20 dB ERLE against simulated echo path responses was reported, and this performance was maintained during double talking.

2) Sondhi and Presti (1966) and Sondhi (1967)

Sondhi proposed an analog echo canceller similar to that of Becker and Rudin, but using a non-linear function of the instantaneous error signal in controlling the tap weights. This system was shown to converge to an estimate of the echo path faster than that of Becker and Rudin, however the use of an instantaneous error criterion resulted in the filter tap weights diverging during double talking. To overcome this effect Sondhi proposed a simple near-end speech detector, similar to those used in echo suppressors, which disabled the tap weight adjustment circuitry during double talking. Computer simulations of the canceller predicted about 20 dB ERLE.

3) Kato et al (1971)

Kato et al developed a digital echo canceller using a transversal filter, based on a recirculating shift register, to model the echo path. Non-linear functions of the error signal and of the delayed input signal samples were used to control the filter coefficients. This simplified the implementation of the canceller and improved its convergence. The canceller also included a means of measuring and synthesising the fixed end-delay. Cancellation of up to 20 dB was reported for the 216-coefficient filter with simulated echo path delays of 12 mS.

4) Mackechnie (1970)

MacKechnie proposed a means of achieving very fast convergence of a transversal digital echo canceller in order to

output and the signal in the 'go' path. This was achieved by cross correlating the delayed input signal with the error signal, and using the result to add or subtract a fixed amount from the tap weigth setting. 20 dB ERLE against simulated echo path responses was reported, and this performance was maintained during double talking.

2) Sondhi and Presti (1966) and Sondhi (1967)

Sondhi proposed an analog echo canceller similar to that of Becker and Rudin, but using a non-linear function of the instantaneous error signal in controlling the tap weights. This system was shown to converge to an estimate of the echo path faster than that of Becker and Rudin, however the use of an instantaneous error criterion resulted in the filter tap weights diverging during double talking. To overcome this effect Sondhi proposed a simple near-end speech detector, similar to those used in echo suppressors, which disabled the tap weight adjustment circuitry during double talking. Computer simulations of the canceller predicted about 20 dB ERLE.

3) Kato et al (1971)

Kato et al developed a digital echo canceller using a transversal filter, based on a recirculating shift register, to model the echo path. Non-linear functions of the error signal and of the delayed input signal samples were used to control the filter coefficients. This simplified the implementation of the canceller and improved its convergence. The canceller also included a means of measuring and synthesising the fixed end-delay. Cancellation of up to 20 dB was reported for the 216-coefficient filter with simulated echo path delays of 12 mS.

4) Mackechnie (1970)

MacKechnie proposed a means of achieving very fast convergence of a transversal digital echo canceller in order to

output and the signal in the 'go' path. This was achieved by cross correlating the delayed input signal with the error signal, and using the result to add or subtract a fixed amount from the tap weigth setting. 20 dB ERLE against simulated echo path responses was reported, and this performance was maintained during double talking.

2) Sondhi and Presti (1966) and Sondhi (1967)

Sondhi proposed an analog echo canceller similar to that of Becker and Rudin, but using a non-linear function of the instantaneous error signal in controlling the tap weights. This system was shown to converge to an estimate of the echo path faster than that of Becker and Rudin, however the use of an instantaneous error criterion resulted in the filter tap weights diverging during double talking. To overcome this effect Sondhi proposed a simple near-end speech detector, similar to those used in echo suppressors, which disabled the tap weight adjustment circuitry during double talking. Computer simulations of the canceller predicted about 20 dB ERLE.

3) Kato et al (1971)

Kato et al developed a digital echo canceller using a transversal filter, based on a recirculating shift register, to model the echo path. Non-linear functions of the error signal and of the delayed input signal samples were used to control the filter coefficients. This simplified the implementation of the canceller and improved its convergence. The canceller also included a means of measuring and synthesising the fixed end-delay. Cancellation of up to 20 dB was reported for the 216-coefficient filter with simulated echo path delays of 12 mS.

4) Mackechnie (1970)

MacKechnie proposed a means of achieving very fast convergence of a transversal digital echo canceller in order to

output and the signal in the 'go' path. This was achieved by cross correlating the delayed input signal with the error signal, and using the result to add or subtract a fixed amount from the tap weigth setting. 20 dB ERLE against simulated echo path responses was reported, and this performance was maintained during double talking.

2) Sondhi and Presti (1966) and Sondhi (1967)

Sondhi proposed an analog echo canceller similar to that of Becker and Rudin, but using a non-linear function of the instantaneous error signal in controlling the tap weights. This system was shown to converge to an estimate of the echo path faster than that of Becker and Rudin, however the use of an instantaneous error criterion resulted in the filter tap weights diverging during double talking. To overcome this effect Sondhi proposed a simple near-end speech detector, similar to those used in echo suppressors, which disabled the tap weight adjustment circuitry during double talking. Computer simulations of the canceller predicted about 20 dB ERLE.

3) Kato et al (1971)

Kato et al developed a digital echo canceller using a transversal filter, based on a recirculating shift register, to model the echo path. Non-linear functions of the error signal and of the delayed input signal samples were used to control the filter coefficients. This simplified the implementation of the canceller and improved its convergence. The canceller also included a means of measuring and synthesising the fixed end-delay. Cancellation of up to 20 dB was reported for the 216-coefficient filter with simulated echo path delays of 12 mS.

4) Mackechnie (1970)

MacKechnie proposed a means of achieving very fast convergence of a transversal digital echo canceller in order to

achieve good tracking of echo paths with significant phase-roll. The
method proposed to treat the input and error signal samples in
blocks, and the coefficient adjustment algorithm was used iteratively
to further refine the coefficient values over each data block. This
scheme was implemented by Demytko and Mackechnie (1973), and a
similar implementation was later reported by Demytko and English
(1977). The latter implementation also used non-linear functions in
updating the filter coefficients, and it was found that these
functions, together with the averaging inherent in the block
treatment of the signal samples, rendered the use of a near-end
speech detector unnecessary. Up to 25 dB cancellation of echo was
reported, however this canceller inserted a not insignificant added
delay into the echo path, due to the block treatment of the samples.

5) Hoge (1975)

The digital echo canceller proposed by Hoge used an optimised
gradient gain or step size in updating the coefficients of an
adaptive transversal filter. The optimised gradient gain gave the
fastest possible convergence, and the optimum gain was shown to be
proportional to the power of the signal in the 'go' path. A
recursive algorithm was suggested for estimating the power in the
near-end signal, and this estimate was used to reduce the gradient
gain during double talking, without disabling adaption completely.
It was reported that during simulated double talking, with equal
speech powers from both speakers, this canceller was capable of
providing 10 dB ERLE within 2 syllables of speech.

6) Mark and Yeung (1976)

This digital echo canceller used an adaptively quantised error
signal, and the quantiser range-factor was used as the gradient gain
in the coefficient adjustment algorithm. In this way the gradient
gain was made proportional to the amplitude of the error signal. The

adaptive quantiser included a variable dead-band, which reduced the sensitivity of the coefficient adjustment algorithm to noise.

7) Horna (1977)

Horna developed a digital echo canceller using pseudo-logarithmic coding to simplify multiplications. Two adaptive thresholds were used to control the coefficient updating algorithm, and the use of non-linear functions simplified the implementation of the canceller. A simple double talk detector was used to inhibit updating of the coefficients when near-end speech was present, and an adaptive centre-clipper was used to remove any residual echo.

8) Ochiai et al (1977)

To overcome the problems of double talking, Ochiai et al proposed the use of two digital transversal filters, one of whose coefficients were updated using an instantaneous error squared criterion with optimised gradient gain. The other filter was used to synthesise the echo path and provide the cancellation signal. The synthesising filter was updated from the adapting filter only under strict conditions. This strategy prevented divergence of the echo path model between the onset of near-end speech and its detection. This echo canceller gave 25 dB cancellation against simulated echo paths, and it was possible to prevent updating of the echo path model for near-end speech levels as low as 20 dB below the far-end level.

9) Duttweiler (1978)

Duttweiler described the implementation of a digital echo canceller using an optimised gradient gain. The speed of the multiplier used in this canceller was such that a single 128-coefficient filter could be time-shared between 12 channels, thus significantly reducing the per-channel costs. The canceller used floating point arithmetic, with only single bit mantissae signals used in updating the coefficients. A simple near-end speech detector

was used to disable adaption during double talking. An integrated circuit version of this canceller was reported by Duttweiler and Chan (1980).

1.7 Per-Line Echo Control:- The Adaptive 2 to 4 Wire Converter

The echo cancellers discussed in the previous section have been designed for use at points in the telephone network with the highest possible traffic concentration. Typically this involves siting the cancellers at international switching centres which are linked by channels with large propogation delays. This strategy allows the costs of large and sophisticated cancellers to be spread over very many telephone circuits. The disadvantage of this approach is that in general the echo canceller is required to model echo paths consisting of large end-delays.

The aim of this research is to investigate the possibilities of providing the cancellation of the unwanted echo signal at the local exchange. This has the advantage that the complexity of the canceller can be considerably reduced, since it no longer has to model the end-delay. It is estimated that this step alone would reduce the complexity of the canceller by a factor of 3 or 4.

The main advantage of this approach however, is that the use of a canceller in the local exchange would allow the transmission performance of the 2 wire local exchange to be achieved by a 4 wire digital exchange. Thus the attenuation which is necessary for echo control in the digital exchange could be removed. This would allow the use of more lossy or longer subscribers' lines, while still achieving the same loudness levels in the network.

A further advantage of this approach is that if sufficient echo cancellation can be achieved, then it will be possible to use a

single purely resistive balance impedance for all subscribers' lines.
In the following paragraphs the options for the provision of the
required cancellation are outlined, and the advantages and
disadvantages of each option are discussed.

1) **Option 1:** Figure 1.7 shows the echo canceller sited at a traffic-
concentrated point in the local exchange, where it is assumed that
the D/A and A/D conversion takes place via an intermediate sampling
rate. Thus the band-limiting function is split between an analog
filter and a digital filter for each transmission direction
(Tattersall and Carey, 1979). The combination of analog and digital
filter should have a sharp high frequency cut off to meet the
required filtering specification (CCITT, recommendation G712), and it
will therefore have a long impulse response. Furthermore, the
digital filter must include a high-pass function, which also requires
a long impulse response. In addition to the unknown transhybrid
transfer function, the canceller must model the responses of all 4
filters. Since the responses of the digital filters are known and
time invariant, and they provide most of the band-limiting function,
considerable savings in canceller complexity will result if they are
modelled by a fixed digital filter, as shown in Figure 1.8. The
responses of the analog filters are imprecisely known due to
component tolerances, and they may be susceptible to ageing. Thus
the adaptive filter must model the impulse responses of the analog
filters, convolved with that of the 2 to 4 wire converter. Siting
the echo canceller at this point in the exchange has the advantage
that its cost can be shared over many subscribers' lines, and
consequently its complexity can be reasonably high. However it will
be seen that further simplifications are possible.

2) **Option 2:** If the echo canceller is sited as shown in Figure 1.9,
then it must model the responses of the analog filters and the

transhybrid response. In this case the canceller operates at the intermediate sampling frequency, and must be provided on a per-line basis. For this approach to be feasible the adaptive filter should be simple, and preferably suitable for integration with the D/A and A/D converters and digital filters (the codec) in a single integrated circuit. This combination of adaptive filter, codec and 2 to 4 wire converter can be referred to as a digital adaptive hybrid.

3) Option 3: The response which the adaptive filter must model is further simplified if it is sited as shown in Figure 1.10. In this case the adaptive filter should be analog, since the overhead of separate A/D and D/A conversion would be impractical. The use of a sampled analog adaptive filter would probably require the use of analog anti-aliasing filters, whose responses would have to be compensated by the adaptive filter. Therefore the adaptive filter should be analog and continuous, i.e. unsampled. For this option to be feasible, the adaptive filter should be suitable for integration with the other analog components in a subscriber's line interface chip (SLIC).

1.8 The Structure of this Thesis

In this introductory chapter it has been seen that the transhybrid response determines the <u>minimum</u> complexity of the adaptive filter required to achieve good echo cancellation. Chapter 2 therefore describes an investigation into the nature of the transhybrid responses of a sample of 1845 subscribers' lines.

Chapter 3 describes the design and implementation of a line and hybrid simulator based on the techniques of Chapter 2. The simulator is used in the remainder of this thesis to test the performance of the proposed adaptive 2 to 4 wire converters.

The theory of continuous analog recursive adaptive filters is described in Chapter 4, and a method of analysis of the convergence of these filters is developed. Chapter 5 describes the implementation of two prototype analog recursive adaptive filters. Results are also presented for the performance of the filters against subscribers' lines. The implementation of an adaptive hybrid using these filters is discussed.

The problems of implementing a digital adaptive hybrid are described in Chapter 6, and the effects of the intermediate sampling rate and the analog filters on the complexity of the required adaptive filter are analysed. Chapter 7 describes the theory and implementation of an experimental digital recursive adaptive filter. The latter part of Chapter 7 reports results obtained for the performance of digital recursive adaptive filters of various complexities against subscribers' lines.

Overall conclusions from this study are given in Chapter 8.

The theory of continuous analog recursive adaptive filters is described in Chapter 4, and a method of analysis of the convergence of these filters is developed. Chapter 5 describes the implementation of two prototype analog recursive adaptive filters. Results are also presented for the performance of the filters against subscribers' lines. The implementation of an adaptive hybrid using these filters is discussed.

The problems of implementing a digital adaptive hybrid are described in Chapter 6, and the effects of the intermediate sampling rate and the analog filters on the complexity of the required adaptive filter are analysed. Chapter 7 describes the theory and implementation of an experimental digital recursive adaptive filter. The latter part of Chapter 7 reports results obtained for the performance of digital recursive adaptive filters of various complexities against subscribers' lines.

Overall conclusions from this study are given in Chapter 8.

Figure 1.1: Active 2 to 4 Wire Converter
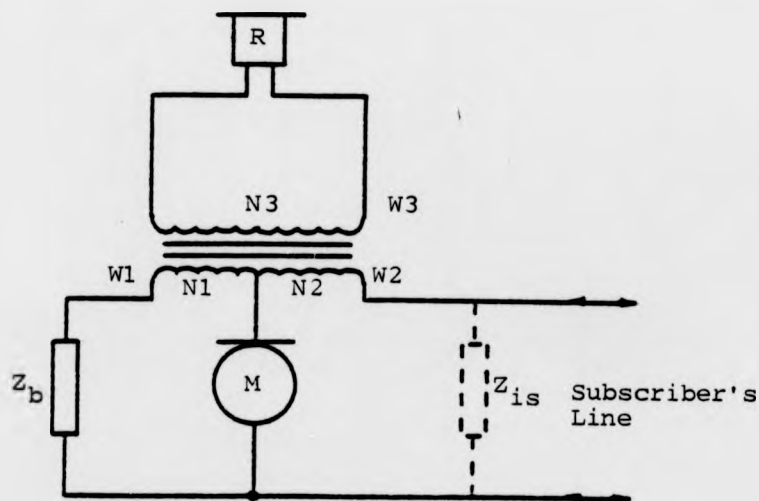
Figure 1.2: Simplified Diagram of a Telephone
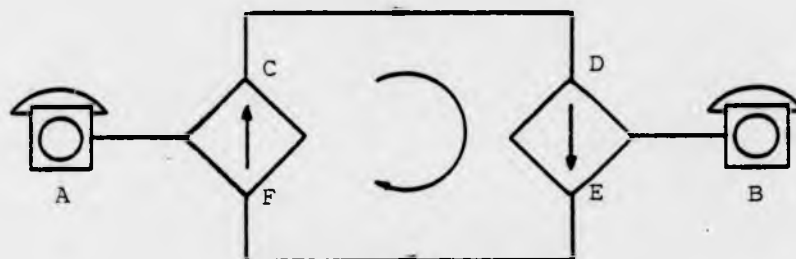
Figure 1.3: Simplified Connection Between 2 Subscribers
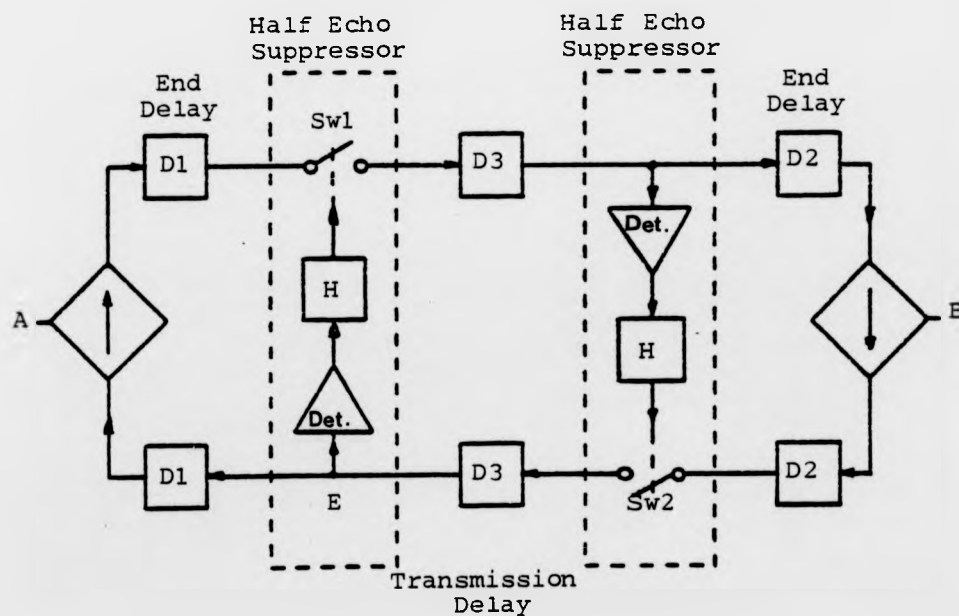
Figure 1.4: A Simple Echo Suppressor
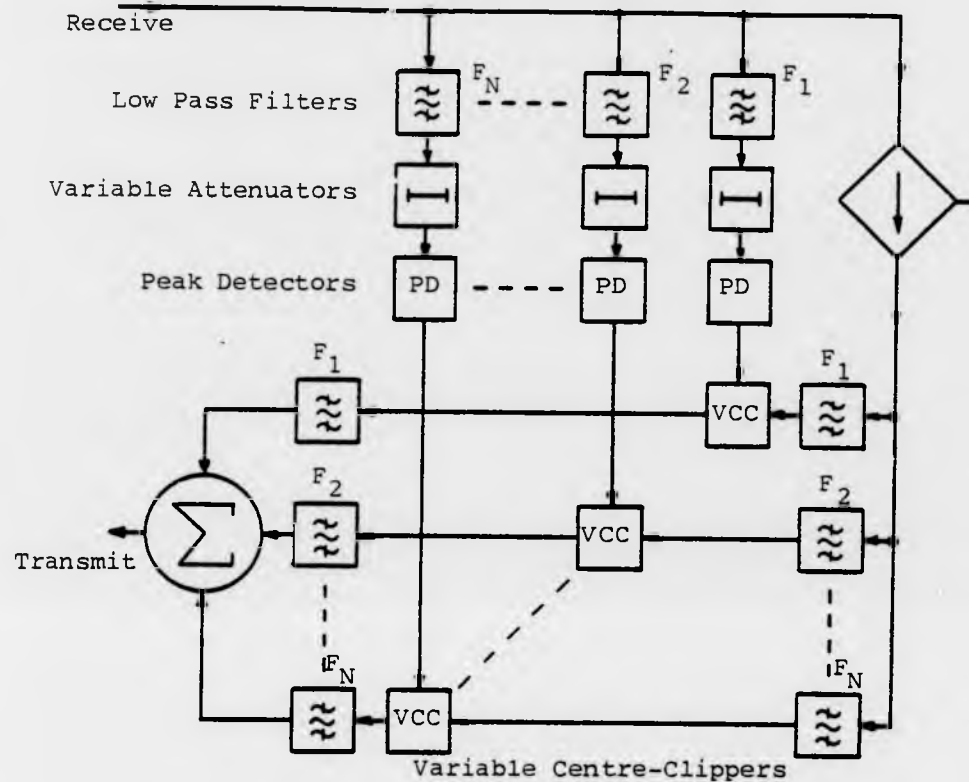
Figure 1.5: An Echo Suppressor Using Centre Clipping
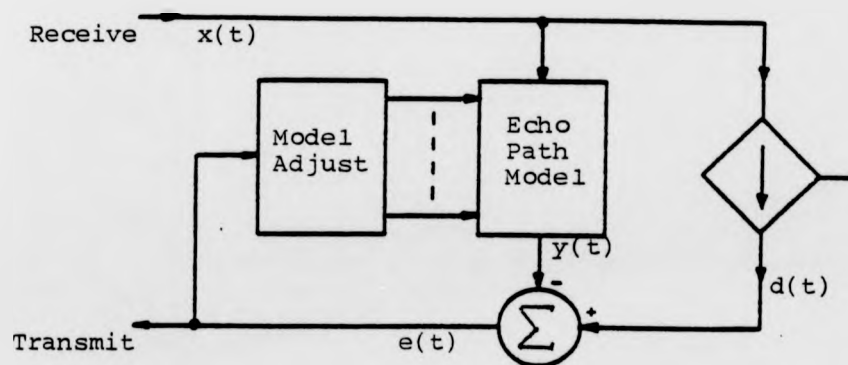
Figure 1.6: Simplified Representation of an Echo Canceller
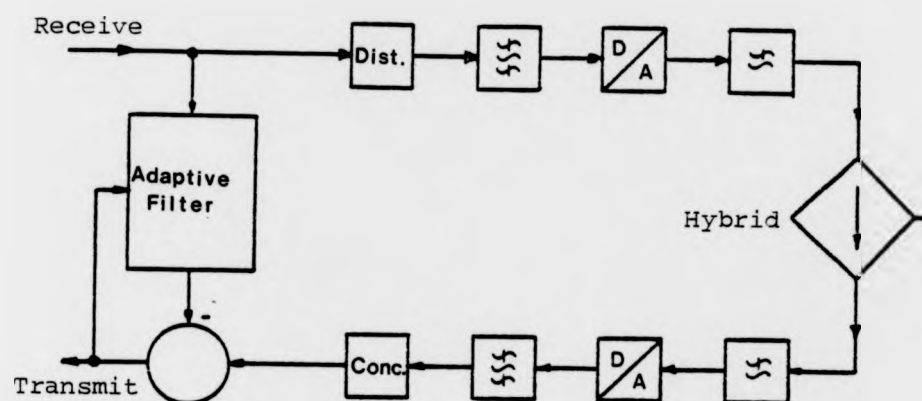
Figure 1.7: An Echo Canceller Sited at
a Traffic Concentrated Point
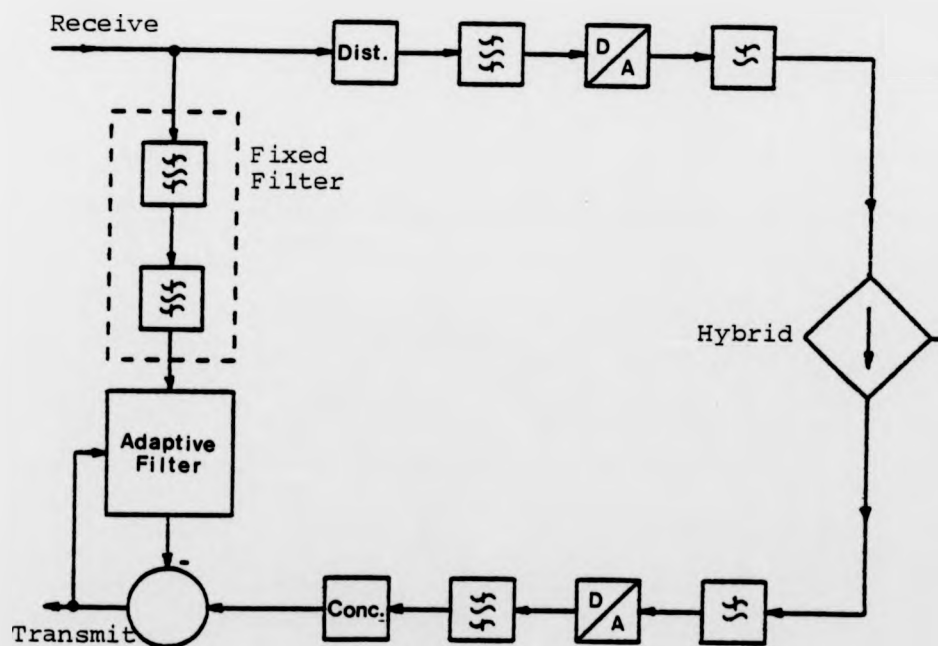
Figure 1.8: Use of a Fixed Digital Filter to Reduce
the Complexity of the Echo Canceller
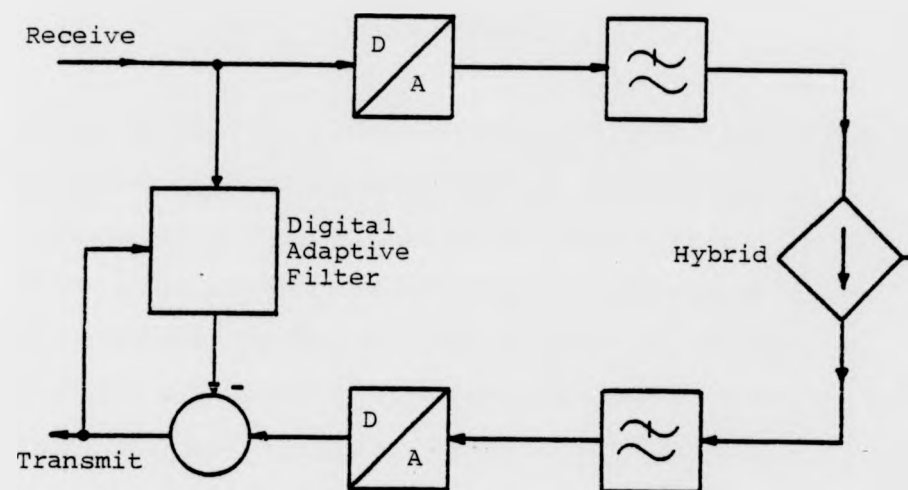
Figure 1.9: Cancellation at the Intermediate Sampling Rate
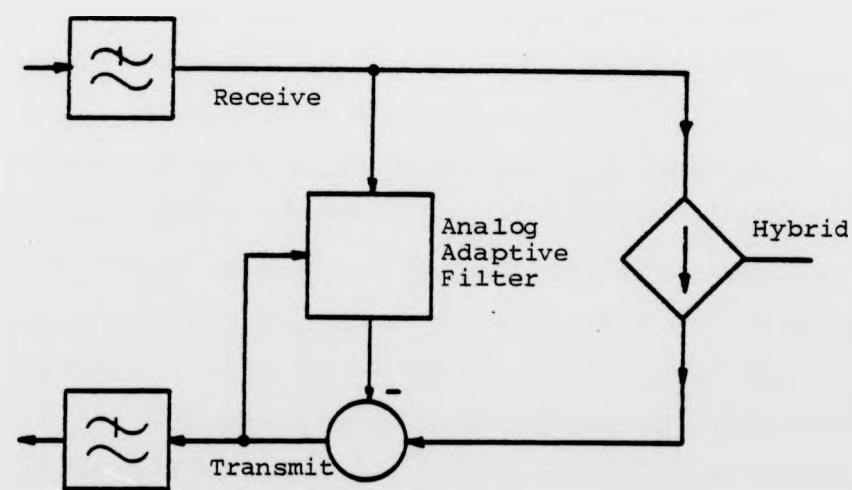
Figure 1.10: Analog Echo Cancellation

CHAPTER 2

THE LINE SURVEY

In the previous chapter the problem of 2 to 4 wire conversion was seen to depend on accurately matching the hybrid balance impedance to the input impedance of the subscriber's line. Knowledge of the nature and range of input impedances of subscribers' lines is thus a pre-requisite for any attempt to design balance impedances. In Section 1 of this chapter the input impedances of a sample of 1845 subscribers' lines are studied, and the information gained is used in the design of balance impedances.

In Section 2 the previous impedance survey is broadened to examine the transhybrid frequency and impulse responses which result from various combinations of hybrid balance and terminating impedances. This information is used to estimate the best performance likely to be attained by the use of various hybrid balancing strategies.

In Chapter 1 it was shown that echo cancelling techniques can be used to improve the overall return loss across the hybrid. In particular, use of a transversal type echo canceller requires knowledge of the length of time for which the transhybrid impulse response has significant values. Thus in the latter part of Section 2 the length of the transhybrid impulse responses are studied.

In the final section of this chapter the results described in the first two sections are used to estimate the number of distinct balance impedances necessary to achieve a given minimum stability return loss specification. This information is vital in determining the feasibility of any technique for automatic or manual selection of balance networks.

2.1 The Line Impedance Survey

In this subsection a computer-based analysis of the impedance seen at the exchange of a sample of 1845 subscribers' lines is described. Each line's input impedance is calculated from its load impedance by repeated use of the transmission line equations. The results of the analysis are presented in the form of scatter plots of input impedances at five frequencies in the band 200 Hz to 3.5 kHz. The effect of the characteristics of the various types of cable on the line input impedance is investigated. The mean line input impedance at each frequency is computed and the results used to design optimum balance impedances.

2.1.1 The Data Base

The data base for the line survey consists of information on the composition and lengths of 1845 typical subscribers' lines. An initial sample of data on 1796 lines was obtained, and this sample is biased to include a higher proportion of long lines than the national sample of 18000 lines from which it was derived. This data had been collected by British Telecom to carry out an exchange line costing survey. The maximum length of line in the 1796 line sample is approximately 8 km. It was felt that this maximum line length did not reflect the extreme line lengths which are encountered in local networks in rural areas, and for this reason data on a further 49 very long lines were added to the survey data base, bringing the maximum line length to approximately 20 km. The additional data was added to the end of the file containing the initial 1796 line data, so that it is possible to examine the effects of removing the extremely long lines from the data base. The input impedance of each

line can be expected to be strongly dependant on the length of the line, and as a preliminary to the line survey, the cumulative distribution of the lengths of the lines in the complete data base were calculated. This distribution is shown in Figure 2.1.

A typical subscriber's line, consisting of N cable sections of various lengths, is shown in Figure 2.2. The data for each line consists of a line number and information about the lengths and types of each cable section. The use of this data to calculate the line input impedance is described in the following sections.

2.1.2 The Line Load Impedance

To obtain realistic results from the survey, the impedance used in the calculation as a load at the subscriber's end of the line should be the input impedance of the subscriber's apparatus in the off-hook position. It is known however, that the input impedance of the most common subscriber's apparatus, the 706-type telephone, is highly variable. This is due to the use of a carbon-granule microphone, whose impedance, although mainly resistive, varies with the orientation of the handset. A conditioning procedure has been specified by CCITT (recommendation P75) to allow the measurement and comparison of telephone characteristics, but even using this technique it was found to be difficult to obtain repeatable results for the telephone impedance. Repeatable measurement of the telephone impedance requires that the microphone be replaced by an equivalent resistance. While this technique gives an estimate of the impedance presented by the telephone to the line, it does not represent the extremes of load impedance encountered in the network, where no standard conditioning is applied to the microphone before use. Moreover, when lines are shared between subscribers, or where an

extension has been fitted, or where modems are in use, the load impedance can differ considerably from that of the telephone.

The problem of specifying the input impedance of the telephone is compounded by the use of a regulating network, containing a thermistor, to lower the sensitivity of the telephone on short lines. The input impedance of the telephone depends on the thermistor's resistance, which in turn depends on the line current. On longer lines the line current is such that the regulating network is inactive, and this is also the case where constant current line feed has been introduced.

For the purposes of this survey, it was decided to use the impedance of the average subscriber's telephone, at 32 mA line current, as the load impedance for the lines. This impedance has been tabulated at 14 frequencies in the audio band as a result of earlier investigations carried out by British Telecom.

2.1.3 Calculation of Line Input Impedances

Referring to Figure 2.2, the input impedance of the nth line section is given by the transmission line equation:-

$$Zi_n(\omega) = ZO_n(\omega) \; \frac{Zi_{n-1}(\omega)+ZO_n(\omega)\tanh(\gamma_n(\omega)l_n)}{ZO_n(\omega)+Zi_{n-1}(\omega)\tanh(\gamma_n(\omega)l_n)} \qquad 2.1$$

where

$Zi_n(\omega)$ is the input impedance of the nth line section

$Zi_{n-1}(\omega)$ is the input impedance of the n-1th line section

$ZO_n(\omega)$ is the characteristic impedance of the nth line section

$\gamma_n(\omega)$ is the propogation coefficient of the nth line section

l_n is the length of the nth line section, and

ω is the angular frequency.

To calculate the imput impedance presented by the line to the

exchange at frequency ω, equation 2.1 is used in the following manner:-

Starting at the subscriber's end of the line, the length and type of the first line section is read from the data base. The decimal code for the section type (say type k) is used to look-up the line constants R, G, L and C for that type of cable. $ZO_k(\omega)$ and $\gamma_k(\omega)$ are calculated using equations 2.2 and 2.3 below:-

$$ZO_k(\omega) = \sqrt{\frac{R_k + j\omega L_k}{G_k + j\omega C_k}} \qquad 2.2$$

$$\gamma_k(\omega) = \sqrt{(R_k + j\omega L_k)(G_k + j\omega C_k)} \qquad 2.3$$

The input impedance of the first section of line is then calculated using equation 2.1 with $Zi_0(\omega) = Zl(\omega)$, the line load impedance. The procedure is repeated for each line section, the input impedance of one section becoming the load impedance of the next, until the input impedance of the final line section has been calculated.

2.1.4 Results of the Line Impedance Survey

Scatter plots of the 1845 line input impedances calculated using the average 706-type telephone as the load impedance, for frequencies of 200 Hz, 500 Hz, 1 kHz, 2 kHz and 3.5 kHz are shown in Figures 2.3 to 2.7 respectively. A number of general observations can be made on these results.

1) Each plot shows the line input impedances diverging from a point which represents the load impedance at that frequency. From equation 2.1, as 1 approaches zero, $\tanh(\gamma(\omega)l)$ approaches zero, and the line input impedance tends towards the load impedance. Thus points near the apex of the plots represent short lines.

2) In all of the plots it is evident that there are two average trends, which become more spiral in character as the frequency is

increased. To investigate this effect further, the input impedances at 500 Hz of a single section of each type of cable in the data base were plotted. Each test line was loaded with 600 Ω, and the impedances were plotted for section lengths between 100 m and 10 km. The results of this experiment are shown in Figure 2.8, where each cable type is identified by its decimal code written beside the input impedance point corresponding to a section length of 10 km. From Figure 2.8 it can be seen that there are two broad classifications of cable, the input impedance of some types being approximately equal to the load impedance (types .12, .17, .25 and .7), while the input impedances of the remaining types describe spiral curves as the section length is increased. This result can be explained by considering the characteristic impedance of a transmission line with G = 0, from equation 2.2:-

$$ZO(\omega) = \sqrt{L/C} \sqrt{1-jR/\omega L} \qquad\qquad 2.4$$

If the line is very lossy, or working at a very low frequency, then $R/\omega l > 1$ and ZO can be approximated by:-

$$ZO(\omega) \approx \sqrt{-j} \sqrt{R/\omega C} \left(1+j\omega L/2R\right) \qquad\qquad 2.5$$

In Table 2.1 the line constants for all 17 types of cable in the data base are tabulated (all types have G = 0) and it can be seen that with the exception of type .7 (a lossless test cable), all the cables are lossy. If however $R/\omega l \gg 1$, then equation 2.5 can be further simplified to:-

$$ZO(\omega) \approx \sqrt{-j} \sqrt{R/\omega C} = \sqrt{R/\omega C} \; \underline{/-45°} \qquad\qquad 2.6$$

Figure 2.8 thus shows that most of the cable types at lengths of 10 km have input impedances close to a line representing impedances with angle -45°, and that the magnitude of the impedances along this line are approximately given by $\sqrt{R/\omega C}$. These values are also tabulated in Table 2.1. This result shows that for most of the cable types, the input impedances of the cables are approximately equal to

the characteristic impedances, for lengths above 10 km. This result is supported by the following calculation of the minimum length of cable which can be considered electrically long:-

$Z_i \approx Z_0$ when $\tanh(\gamma l) \approx 1$, from equation 2.1, but:-

$$\tanh(\gamma l) = \frac{e^{\gamma l} - e^{-\gamma l}}{e^{\gamma l} + e^{-\gamma l}} \qquad\qquad 2.7$$

If the condition that $\tanh(\gamma l) \approx 1$ is taken to be:-

$$e^{\gamma l} > 10 e^{-\gamma l} \qquad\qquad 2.8$$

then the requirement that the cables be electrically long is:-

$$l > \frac{\ln(10)}{2\alpha}, \text{ since } \gamma = \alpha + j\beta \qquad\qquad 2.9$$

where for lossy lines:-

$$\alpha \approx \sqrt{\omega RC/2} \qquad\qquad 2.10$$

The length l_1, the approximate length for the cable to be electrically long at 500 Hz, is also tabulated in Table 2.1. From this table it is clear that l_1 is the feature which distinguishes between the two broad classifications of cable evident in Figure 2.8.

This analysis shows that the two average trends in the line input impedance scatter plots are due to a predominance of two particular cable types in the makeup of the lines in the data base, and that the distance along either of the average curves is proportional to the length of the line. It is also evident from this analysis that there is considerable variation in the characteristic impedances of the various cable types, and the consequences of this result will be discussed in Section 2.2.6.

3) At 200 Hz (Figure 2.3), the effect of most of the subscribers' lines is to add a largely resistive component in series with the load impedance to form the input impedance. The concentration of points near the value of the load impedance indicates that most of the lines are electrically short at this frequency. Some lines however show significant change in the reactive component of the input impedance,

compared with that of the load.

4) At 500 Hz (Figure 2.4) the line input impedances have larger reactive components, and the spread of values is greater than at 200 Hz.   At high frequencies the line input impedances tend to concentrate near the ends of the spiral curves, showing that at these frequencies most of the lines are electrically long.

The difficulty of accurately matching the input impedances of the lines is illustrated by the observation that at the lower end of the speech band the best match is given by the load impedance, while at the upper end of the band the best match is the characteristic impedance.   The best possible performance can therefore be obtained if the load impedance is constrained to an estimate of the average characteristic impedance of the lines in the data base, so that each line appears infinite in length and can be accurately matched by the average characteristic impedance.   This is demonstrated by the use of the 3-element network of Figure 2.9.   This network approximates the average line's characteristic impedance as a function of frequency, and the line input impedance scatter plots using this network as the load are shown in Figures 2.10 to 2.14.   It can be seen from these figures that at the higher frequencies the scatter of the points is much reduced, however at the low frequencies there is still a large variation in line input impedance.

2.1.5 Design of Balance Impedances

In attempting to design balance networks, at least four possible objectives are identifiable:-

1) Maximise the SRL of the worst case line.

2) Maximise the ERL of the worst case line.

3) Maximise the SRL averaged over all lines.

4) Maximise the ERL averaged over all lines.

Choice between options 1 or 2 and 3 or 4 is effectively a choice between maximising the minimum quality of service, and maximising the average quality of service. Best possible performance could be achieved by choosing option 4, subject to a restriction on the worst case SRL. To achieve any of these objectives it is necessary to calculate the transhybrid return loss for each line in the data base.

In this section balance impedances are designed to match the average input impedance of each line at five frequencies, averaged over all 1845 lines in the survey. Further averaging in frequency also takes place, since it is not necessarily desirable to match the 5 average impedance points exactly, and it may not even be possible with a simple balance network. This approach is similar to option 4, and in Section 2.2 the average and worst case ERL and SRL achieved by the designed impedances are investigated.

1) Balance Impedance with the Telephone as the Load

The mean line input impedance at each of the five frequencies, where the load impedance is that due to the 706-type telephone, is shown in Figure 2.15. The locus of the impedance with varying frequency can be seen to approximate to a semicircle in the impedance plane. A semicircular impedance locus is synthesised by the 3-element network of the type shown in Figure 2.9. The semicircle is centered on the point $(R_1+R_2/2, 0)$, and has radius $R_2/2$. The position of the impedance on this locus is dependent on the product $\omega C_2 R_2$, and can be conveniently specified by the angle θ (Figure 2.15), where:-

$$\theta = -\tan^{-1}(\omega C_2 R_2) \qquad\qquad 2.11$$

Thus the procedure for obtaining the optimum balance impedance is as follows; the average line input impedance at each of the frequencies of interest is plotted on the impedance plane, and

the semicircle which provides the best fit is chosen and plotted. This allows the values of R_1 and R_2 to be deduced. Points on the semicircle providing the closest fit to the average impedance points at each frequency are chosen. Using the measured angles θ, the frequency ω and the value of R_2, the optimum value of C_2 at each frequency is then calculated. The value of C_2 used for the optimum balance impedance is the average of the C_2 values for each frequency. Figure 2.15 shows the derivation of the balance impedance which best matches the average input impedance of the 1845 lines with the 706-type telephone as the load. The average line input impedance points are denoted by '.', and the points on the locus chosen to match these points are denoted by 'x'. The average C_2 value is 0.12 µF, and the values of the optimum balance network thus are; R1 = 275 Ω, R2 = 810 Ω, C2 = 0.12 µF.

2) Balance Impedance with an Optimised Load

In Section 2.1.4 it was shown that the scatter of input impedance points is reduced when the load impedance is an estimate of the mean line characteristic impedance. In theory the optimum balance impedance in this case is identical to the load impedance. Using the technique described above however, an optimum balance impedance given by; R1 = 320 Ω, R2 = 1075 Ω, C2 = 0.21 µF was chosen. This result is due to the large spread in line input impedances at low frequencies, even when the load is the three element network, as shown in Section 2.1.4 (Figure 2.10).

3) The Optimum Balance Resistor

The value of the single balance resistor which minimises the difference between the balance and input impedances over the speech band can be shown to be:-

$$Rb_{opt} = \frac{\int_{\omega_2}^{\omega_1} Re[Zi(\omega)]d\omega}{\omega_2 - \omega_1} \qquad 2.12$$

where $\omega_2 - \omega_1$ is the speech bandwidth and $Z_i(\omega)$ is the input impedance of the line to be balanced. The above value of balance resistor does not necessarily maximise the value of the resulting transhybrid loss however, as can be seen by considering the case where Zi is purely reactive. The expression for the value of the balance resistor which maximises the transhybrid loss is considerably more complicated than equation 2.12, and for this reason the derivation of the optimum balance resistor for all lines is included in Section 2.2.6.

2.1.6 Circles of Constant Return Loss

In the previous section the design of balance networks using a graphical technique was discussed. This technique can be considerably refined by the use of circles of constant return loss. A circle, or in general a contour, of constant return loss is a line joining those input impedance points in the complex impedance plane which will give a certain value of return loss with a particular 2 to 4 wire converter at a given frequency. Thus the equation for the contours of constant return loss for the 2 to 4 wire converter discussed in Section 2.2.2 can be found by solving the equation:-

$$\left| \frac{2\ Zt(\omega)}{Zt(\omega)+Zb(\omega)} \frac{Zb(\omega)-Zi(\omega)}{Zt(\omega)+Zi(\omega)} \right| = A \qquad 2.13$$

for $Zi(\omega)$, the line input impedance, where A is the required return loss value, ω is the frequency at which the return loss is required and $Zt(\omega)$ and $Zb(\omega)$ are the 2 to 4 wire converter terminating and balance impedances respectively. The solution to equation 2.13 is given by:-

$$\left[\operatorname{Re}[Zi(\omega)] - \operatorname{Re}[Zb(\omega)] \left(\frac{1+\alpha^2}{1-\alpha^2} \right) \right]^2 + \left[\operatorname{Im}[Zi(\omega)] - \operatorname{Im}[Zb(\omega)] \left(\frac{1+\alpha^2}{1-\alpha^2} \right) \right]^2$$

$$= \frac{4|Zb(\omega)\alpha^2|}{(1-\alpha^2)^2} \qquad\qquad 2.14$$

where

$$\alpha = \frac{A|Zb(\omega)+Zt(\omega)|}{|2Zt(\omega)|} \qquad\qquad 2.15$$

Equation 2.14 describes a circle of centre:-

$$C = \left(\operatorname{Re}[Zb(\omega)] \left[\frac{1+\alpha^2}{1-\alpha^2} \right], \operatorname{Im}[Zb(\omega)] \left[\frac{1+\alpha^2}{1-\alpha^2} \right] \right)$$

with radius:-

$$R = \frac{2|Zb(\omega)|\alpha}{1-\alpha^2}$$

in the impedance plane.

Figure 2.16 shows the 10 dB return loss circle superimposed on the scatter plot of line impedances at 200 Hz, when the load impedance is a three element network with values, $R_1 = 370$ Ω, $R_2 = 620$ Ω, $C_2 = 0.31$ μF, and the balance and terminating impedances are identical to the load impedance. Values of Zi lying inside the circle give values of return loss greater than 10 dB at this frequency, while points lying outside the circle give values of return loss less than 10 dB. It can be seen from Figure 2.16 that a significant number of lines lie outside the circle, and that the value of balance impedance chosen is such that the centre of the circle does not lie close to the mean input impedance of the lines at this frequency.

Circles of constant return loss are a useful aid in designing balance impedances, as they allow the performance of a proposed balance impedance to be gauged. The fact that this is possible only at single frequencies limits the application of constant return loss circles however, and in the next section an alternative method of

gauging the effectiveness of balance networks is discussed.

2.2 The Transhybrid Response Survey

In Section 2.1 the design of optimum balance networks was
discussed. Any optimum balance impedance is however a compromise
between the wide range of input impedances to be matched. It is
therefore essential to determine the minimum SRL and ERL which can be
achieved by the use of a single optimum balance network, since this
will determine the stability of the worst case line. In this section
the line input impedance calculations are extended to calculate the
the transhybrid frequency response due to any combination of load
impedance, line characteristics and 2 to 4 wire converter. ERL
and SRL are calculated and a fast Fourier transform technique is used
to calculate the transhybrid impulse response from the frequency
response. Cumulative distributions of ERL and SRL are presented, and
these results are used to determine the best performance possible as
a result of optimising the hybrid balance impedance and the input
impedance of the telephone. Cumulative distributions of impulse
response length are also presented and used to determine the
feasibility of cancelling the unwanted hybrid output by means of a
transversal echo canceller.

2.2.1 The Input Impedance of the Subscriber's Line

Calculation of the transhybrid impulse response requires that
the transhybrid frequency response be specified at 129 equispaced
points in the range 0 to 4 kHz, as explained in Section 2.2.5. The
line input impedance must therefore be calculated at these 129 points
also.

Data on the input impedance of the average subscriber's apparatus are available only at 15 points in the required range, and it is necessary to interpolate between these points to fully specify the load impedance. The fact that the initial 15 points are unevenly spaced from 0 to 4 kHz restricts the number of suitable curve fitting techniques. Of the two most common approaches, curve fitting with cubic splines is superior to fitting with a polynomial where the curve represented by the initial data has many peaks and troughs (Naglib, 1977). For this reason a least-squares cubic spline curve fitting technique was used. The results of the curve fitting are shown in Figures 2.17 and 2.18, where the original points are denoted by '+'.

The line input impedance is calculated using equation 2.1 as described in Section 2.1.3, with the exception that the characteristic impedance and propogation coefficient for each line type are obtained directly from a precomputed table. In the next section the calculation of the transhybrid response, using the line input impedance, is described. It is assumed that the subscriber's line is provided with the required line current via a constant current source, which presents a high impedance to the line and whose effect can therefore be ignored. Ringing current is assumed to be applied to the line via a relay or other switch whose effect can also be ignored. The input impedance of the subscriber's line can therefore be assumed to be the impedance presented to the 2 wire port of the 2 to 4 wire converter.

2.2.2 The 2 to 4 Wire Converter

The 2 to 4 wire converter used in this survey is that of Figure 1.1, whose transhybrid response is:-

$$H(\omega) = \frac{A1A2Zt(\omega)}{Zt(\omega)+Zb(\omega)} \frac{Zb(\omega)-Zi(\omega)}{Zi(\omega)+Zt(\omega)} \qquad 2.16$$

assuming $Ztl(\omega) = Ztb(\omega) = Zt(\omega)$. The gains A1 and A2 are calculated to give no insertion loss between either the 4 wire receive and 2 wire ports, or between the 2 wire port and 4 wire transmit port, assuming that the line is correctly terminated, i.e. $Zt(\omega) = Zi(\omega)$. Thus A2 = 1 and A1 = 2.

Choosing the values of A1 and A2 in this manner means that under certain circumstances there may be a net transhybrid gain however, assuming $Zt(\omega) = Zb(\omega)$, then the worst case return loss is 0 dB. This occurs when $Zi(\omega) = \infty$, or when $Zi(\omega) = 0$, i.e. when the subscriber's line is either 'open circuit' or 'short circuit'.

Having calculated the line input impedance as described earlier, the transhybrid response is calculated at the required frequencies using equation 2.16. The values of $Zb(\omega)$ and $Zt(\omega)$ used in the survey are specified by the values of the components of a 3-element network of the form of Figure 2.9. Throughout the remainder of this thesis $Zb(\omega)$ and $Zt(\omega)$ will be specified by the values of the components R1, R2 and C2.

2.2.3 ERL and SRL Distributions

The ERL and SRL, as defined in Section 1.4, are calculated using equations 2.17 and 2.18 below:-

$$ERL = \frac{1}{65} \sum_{i=17}^{81} 10\log_{10}\left|H(i\Delta\omega)\right|^2 \qquad 2.17$$

$$SRL = Max\{10\log_{10}\left|H(i\Delta\omega)\right|^2\}, \quad 11 < i < 110 \qquad 2.18$$

The values of ERL and SRL for each line are calculated and stored. As the most useful indicator of the performance of any combination of load impedance and hybrid is the percentage of lines having return loss greater than a given value, the results for ERL and SRL are

presented in the form of cumulative distributions. The mean and standard deviation of the ERL and SRL values are also calculated, as are the minimum values of ERL and SRL.

2.2.4 Results of the Transhybrid Frequency Response Survey

The results of the transhybrid frequency response survey are presented in detail below, and for convenience they are also summarised at the end of this section.

1) Resistive Balance Impedance

Figures 2.19 to 2.21 show the variation in mean ERL, mean SRL, minimum ERL and minimum SRL with the value of the balance resistor in the hybrid, where the terminating impedance is the 3-element network; $R1 = 370 \, \Omega$, $R2 = 620 \, \Omega$, $C2 = 0.31 \, \mu F$. In all cases the load impedance is the input impedance of the 706-type telephone. The value of the balance resistor which maximises both the minimum ERL and the minimum SRL is $620 \, \Omega$, while the value which maximises the mean ERL is $740 \, \Omega$. Choice of the optimum balance resistor thus involves a trade off of mean return loss in the local network in favour of increased minimum return loss. This trade off is most critical in the case of mean ERL, which is reduced by 1.7 dB to improve minimum ERL by 1 dB and minimum SRL by 0.5 dB. Since the 'singing margin', or the overall stability of the worst line in the network is of paramount importance, it can be concluded that the optimum value of balance resistor is $620 \, \Omega$. This value is in close agreement with the present standard balance resistance of $600 \, \Omega$.

2) Complex Balance Impedance

The effect on the cumulative return loss distributions of changing the balance impedance from $600 \, \Omega$ (curve a) to the 3-element network $R1 = 370 \, \Omega$, $R2 = 620 \, \Omega$, $C2 = 0.31 \, \mu F$ (curve b), is shown in

Figure 2.22. It is evident that the use of the complex balance impedance considerably improves the lower values of ERL and SRL, while the higher values are decreased. Thus the standard deviations of the ERL and SRL distributions are reduced from 4.9 dB to 1.48 dB and from 3.09 dB to 0.97 dB respectively, while the mean ERL and SRL are increased from 11.3 dB to 14.27 dB and from 8.46 dB to 11.12 dB respectively. The minimum ERL and SRL are increased from 5.0 dB to 9.5 dB and from 3.0 dB to 6.0 dB. Examination of the results for individual longer lines in the survey reveals that it is these lines which show the improvement in return loss, while the shorter lines show the degradation in return loss. This effect occurs because 600 Ω matches the input impedance of the telephone quite well, and thus matches the input impedance of the short lines. The 3-element network provides a closer match to the input impedances of the longer lines.

The cumulative return loss distributions for the balance network; R1 = 275 Ω, R2 = 810 Ω, C2 = 0.12 μF (curve a), whose design was described in Section 2.1.5, are shown superimposed on the distributions for the previous complex balance impedance (curve b), in Figure 2.23. By considering the crossover points of the curves it can be seen that the use of this new balance impedance improves the ERL for 93% of the lines in the survey, and the SRL for 95% of the lines. The minimum SRL is unchanged, although the minimum ERL is decreased by 3.0 dB. In changing the values of the complex balance impedance, the mean ERL and SRL are increased from 14.27 dB to 20.04 dB and from 11.12 dB to 15.52 dB respectively. The standard deviations of ERL and SRL however, are increased from 1.47 dB to 5.91 dB and from 0.97 dB to 3.0 dB respectively. This result shows that significant improvements in mean return loss are possible by redesigning the present standard complex balance impedance, however

these improvements are achieved at the cost of a 3 dB decrease in the minimum ERL.

3) Terminating Impedance

Figure 2.24 shows the effect of changing the terminating impedance from the three element network R1 = 370 Ω, R2 = 620 Ω, C2 = 0.31 μF (curve a), to a single resistor of 600 Ω (curve b), with the balance resistor in each case being 600 Ω. The differences in the return loss distributions are negligable for low values of return loss, although for most lines some improvement is obtained by using the complex terminating network. Altering the terminating impedance alters the level of sidetone produced in the subscriber's earpiece, as described in Section 1.3, and for this reason no further investigations into its effect on return loss were conducted.

4) Line Load Impedance

Figure 2.25 shows the effect of changing the load impedance used in the survey from the input impedance of the telephone (curve a), to that of the network; R1 = 370 Ω, R2 = 620 Ω, C2 = 0.31 μF (curve b), where the balance and terminating impedances are identical to the latter load impedance. It can be seen that the already high values of return loss are further improved, but that the minimum return loss is unchanged. Thus the mean ERL and SRL increase from 14.27 dB to 18.3 dB and from 11.12 dB to 14.47 dB respectively. The standard deviations of ERL and SRL also increase in consequence. On investigation, the lines at the low SRL end of the distribution with $Z1 = Zb = Zt$, were generally found to be the longer lines. The lines whose SRL are lowest however, are those whose composition is in some way unusual. For example, the line with the lowest SRL consists of a single 4.7 km section of 0.63 type cable. This result reflects the wide spread of cable caracteristic impedances discussed in Section 2.1.3.

Using the balance impedance designed in Section 2.1.5 for the case where the load impedance is that of the 3-element network, the return loss distributions are as shown in Figure 2.26. The mean ERL and SRL are 24 dB and 17.7 dB respectively, and the minimum SRL is 8.0 dB, while the minimum ERL is 9.0 dB. This result indicates the best possible performance which can be achieved using optimised load and balance impedances, although it could perhaps be slightly improved by adjusting the balance impedance to match more closely the lines with low SRL, at the expense of those with high SRL.

A summary of the above results is given in Table 2.2, which shows the values of minimum ERL, minimum SRL, mean ERL, mean SRL, and the standard deviations of the ERL and SRL, for various combinations of balance, terminating and load impedances.

2.2.5 Calculation of the Transhybrid Impulse Response

This section describes the calculation of transhybrid impulse responses using the inverse discrete Fourier transform (IDFT). The equation for the IDFT can be written as:-

$$h(nT) = \Delta\omega \sum_{k=0}^{N-1} H(jk\omega_s/N)e^{j2\pi kn/N} \qquad n = 0....N-1 \qquad 2.19$$

where the transhybrid frequency response is represented by N values $\Delta\omega$ rads/sec apart, between $-\omega_s/2$ and $\omega_s/2$, ω_s being the sampling frequency. The equation gives N values of the transhybrid impulse response, spaced T seconds apart, where $T = 2\pi/\omega_s$. In Appendix Al the derivation of equation 2.19 is explained, and the the effect of non-rectangular window functions is discussed.

A well documented algorithm for the efficient computation of equation 2.19 is the inverse fast Fourier transform. In the case of the line survey a standard inverse fast Fourier transform routine is

used, and the negative half of the complex frequency spectrum is equated to the complex conjugate of the positive half, to ensure a purely real set of impulse response samples. The frequency sampling interval is chosen to be:-

$$\Delta\omega = 2\pi\ 4000/128 = 2\pi\ 31.25\ \text{rads/sec} \qquad\qquad 2.20$$

Thus the transhybrid frequency response is represented by 129 samples over the range 0 to 4 kHz, and this allows calculation of impulse response samples at 0.125 mS intervals up to time T = 32 mS. Using the rectangular window function the resulting time resolution is 2 sample periods or 0.25 mS, while if either the Hanning or the Hamming windows are used the resolution is 4 sample periods or 0.5 mS.

2.2.6 Measurement of Transhybrid Impulse Response Length

The length of the transhybrid impulse response determines the number of taps required in an adaptive transversal filter to cancel the unwanted signal at the hybrid output. Theoretically, since the transhybrid impulse response is due to a continuous analog system whose response varies with frequency, the adaptive filter would require an infinite number of taps to achieve perfect cancellation. A lesser number of taps is required if imperfect cancellation is acceptable. To examine the relationship between the degree of cancellation and the number of taps required, consider an example in which the the transhybrid response is of the second order. The reponse can thus be written as:-

$$h(t) = e^{-at}\text{Cos}(\omega_0 t), \qquad t > 0 \qquad\qquad 2.21$$

The process of cancelling the impulse response can be visualised as removing its initial portion. Assume for example that the transversal filter can accurately model $h(t)$ up to time t_1, when the envelope of $h(t)$ has decayed to A times its peak value, where A < 1.

used, and the negative half of the complex frequency spectrum is equated to the complex conjugate of the positive half, to ensure a purely real set of impulse response samples. The frequency sampling interval is chosen to be:-

$$\Delta\omega = 2\pi \ 4000/128 = 2\pi \ 31.25 \ \text{rads/sec} \qquad\qquad 2.20$$

Thus the transhybrid frequency response is represented by 129 samples over the range 0 to 4 kHz, and this allows calculation of impulse response samples at 0.125 mS intervals up to time $T = 32$ mS. Using the rectangular window function the resulting time resolution is 2 sample periods or 0.25 mS, while if either the Hanning or the Hamming windows are used the resolution is 4 sample periods or 0.5 mS.

2.2.6 Measurement of Transhybrid Impulse Response Length

The length of the transhybrid impulse response determines the number of taps required in an adaptive transversal filter to cancel the unwanted signal at the hybrid output. Theoretically, since the transhybrid impulse response is due to a continuous analog system whose response varies with frequency, the adaptive filter would require an infinite number of taps to achieve perfect cancellation. A lesser number of taps is required if imperfect cancellation is acceptable. To examine the relationship between the degree of cancellation and the number of taps required, consider an example in which the the transhybrid response is of the second order. The reponse can thus be written as:-

$$h(t) = e^{-at} Cos(\omega_0 t), \qquad t > 0 \qquad\qquad 2.21$$

The process of cancelling the impulse response can be visualised as removing its initial portion. Assume for example that the transversal filter can accurately model $h(t)$ up to time t_1, when the envelope of $h(t)$ has decayed to A times its peak value, where $A < 1$.

The residual impulse response then is:-

$$h_c(t) = U(t-t_1)e^{-at}Cos(\omega_0 t) \qquad\qquad 2.22$$

and ignoring the delay due to the delayed unit step function $U(t-t_1)$, this can be written as:-

$$h'_c = Ae^{-at}Cos(\omega_0(t-t_1)) \qquad\qquad 2.23$$

Thus the amplitude of the transhybrid impulse response has been decreased by a factor of A. This relationship between attenuation and time to decay to some fraction of peak impulse response amplitude is due to the nature of the exponential function, and is approximately true for all impulse responses due to real, stable systems. Calculating the time taken for the envelope of each transhybrid impulse response to decay below various percentages of its peak value thus allows the number of taps necessary to achieve a given improvement in ERL to be estimated. For example, if a particular impulse response envelope decayed to 10% of its peak value in 1 mS, then an adaptive filter with an 8 kHz sampling rate would require 8 taps to achieve 20 dB ERLE.

In the line survey the times taken for the transhybrid impulse responses to decay below 5%, 1% and 0.5% of their peak are calculated. These times are then analysed to form cumulative distributions of decay times. The results of the analysis of impulse response decay times for various combinations of line load impedance and hybrid terminating and balance impedances are presented in Section 2.2.7.

2.2.7 Results of the Transhybrid Impulse Response Survey

In Appendix A1 the use of non-rectangular frequency window functions in calculating the transhybrid impulse response is discussed. Results of testing the impulse response decay time

calculation are also presented in Appendix A1, and it is shown that
the use of the Hamming window gives greater accuracy at the low
impulse response amplitudes than the rectangular window function.
For this reason the Hamming window function is used in calculating
transhybrid impulse responses. A copy of the Fortran program used to
calculate transhybrid impulse responses is given in Appendix A2.

The distribution of the decay times to 5%, 1% and 0.5% of
peak impulse response value for the 1845 lines, with complex
terminating impedance and 600 Ω balance impedance is shown in Figure
2.27, where the load impedance is the input impedance of the 706-type
telephone. The distributions of times to 5% and 1% of peak are
discontinuous, implying that the impulse responses have either very
short time constants, or relatively long time constants, but that no
lines have decay times to 5% or 1% of peak between approximately 1 mS
and 3 mS. These discontinuities were found to be due to the nature
of the telephone impedance used as the load impedance in the survey.
In particular, when the peaks in both the real and the imaginary
parts of the impedance at low frequency (Figures 2.17 and 2.18) were
eliminated, the distributions became smooth, as shown in Figure 2.28.
Similarly, as will be seen later, when the 3-element network is used
as the load impedance, the distributions are also continuous.
Measurements of the impedance of a telephone verified the existence
of the low frequency peaks, and the use of an alternative
interpolation technique on the original impedance data was found also
to produce discontinuities. It would thus appear that the
discontinuities evident in the impulse response decay distributions
accurately reflect the nature of the transhybrid impulse response.

The longest decay time to 5% of peak of Figure 2.27 is
approximately 12 mS, and thus to provide 26 dB ERLE for all lines, an
adaptive transversal filter with a sampling frequency of 8 kHz would

require approximately 96 taps. It is apparent from Figure 2.27 that considerably fewer taps would be adequate for most lines, since 85% of impulse responses decay to less than 5% of peak within 1 mS.

Figure 2.29 shows the corresponding impulse response decay time distributions when the balance impedance is changed from 600 Ω to the 3-element network; R1 = 370 Ω, R2 = 620 Ω, C2 = 0.31 μF. In this case the decay times to 5% and 1% of peak are shortened, while the decay times to 0.5% of peak are lengthened. The longest time to 5% of peak with the complex balance impedance is approximately 4 mS.

When the load impedance is identical to the balance and terminating impedances used in Figure 2.29 (R1 = 370 Ω, R2 = 620 Ω, C2 = 0.31 μF), the decay time distributions are as shown in Figure 2.30. The times to 5%, 1% and 0.5% are all shortened considerably, i.e. the impulse responses have become more impulse like, in this case the maximum time to decay to 5% of peak is 1.6 mS.

2.3 Multiple Balance Networks

The results of Section 2.2.4 show that using a single optimised balance network, the highest minimum SRL which can be achieved is 6 dB. A possible strategy for improving on this figure is to manually or automatically select a single balance network from one of a range of fixed balance networks. A factor of vital importance in determining the feasibility of this approach is the number of distinct balance impedances required to obtain a given minimum SRL in the network. This information can be obtained by combining the transhybrid response survey with the balance impedance design technique described in Section 2.1.5.

To find the the number of balance impedances required to achieve X dB minimum SRL, the value of the single balance resistor

(Rm) which maximises the number of lines having SRL greater than X dB is first found. This value can be found from cumulative distributions of SRL for various values of balance resistor close to the optimum single balance resistor. Using the value of Rm obtained in this manner, a subset of lines having SRL less than X dB when matched with Rm is formed, and Rm is chosen as the first balance impedance in a multiple balance network. A new balance impedance Zb_1 is designed for this subset of lines, as described in Section 2.1.5 and this impedance is chosen as the second balance impedance required. A further subset of lines having SRL less than X dB when matched with Zb_1 is then selected from the previous subset, and the procedure is repeated until sufficient balance networks have been designed to achieve SRL greater than X dB for all lines, when matched with one or other of the balance networks.

When using this technique, care must be taken to ensure that groups of line impedances which lie in distinct areas of the impedance plane are not averaged, as this would produce a balance impedance which matches none of the groups well. Similarly, care must be taken to ensure that a balance impedance which eventually matches only a small number of lines is not designed on the basis of averaging the impedances of a much larger number of lines.

The result of the above procedure, carried out for a minimum SRL of 10 dB, is recorded in Table 2.3. To achieve this value of minimum SRL three distinct balance impedances are necessary, although two of the networks are required only for a small number of lines.

As the value of the minimum SRL is increased, the procedure for estimating the required number of balance impedances becomes difficult to use, as at each stage only small numbers of lines are brought within the specified value of minimum SRL, although many lines are used in averaging to obtain each balance impedance. The

number of balance impedances necessary can be expected to increase sharply with the minimum SRL required however, and using the 3-element balance impedance it may not even be possible to achieve very high values of minimum SRL.

Line type	R (Ω/km)	L (mH/km)	C (μF/km)	R/ωL	$\sqrt{R/\omega C}$	l_1 (m)
.11	65	0.6	58.0	34.5	597	473
.12	32	2.5	4.7	4.1	1472	2368
.17	19	2.5	4.7	2.4	1134	2587
.21	42	0.6	90.0	22.3	385	472
.25	9	2.5	5.1	1.1	749	5070
.31	290	0.6	52.0	154	1332	236
.32	435	0.6	50.0	231	1664	197
.40	273	0.6	50.0	144	1318	249
.41	120	0.6	49.0	64	883	379
.50	168	0.6	50.0	89	1034	317
.51	281	0.6	62.0	149	1201	220
.61	225	0.6	38.0	119	1373	314
.63	109	0.6	50.0	58	833	393
.81	111	0.6	64.0	59	743	345
.90	55	0.6	50.0	29	592	554
.70	0	50.0	18.0	0	0	∞
.75	169	0.0	47.0	∞	1070	326

Table 2.1 Characteristics of the types of cable encountered
in the line survey, at 500 Hz.

Z1	706-Type	706-Type	706-Type	706-Type	370Ω 620Ω 0.31µF	370Ω 620Ω 0.31µF
Zb	600Ω	370Ω 620Ω 0.31µF	275Ω 810Ω 0.12µF	600Ω	370Ω 620Ω 0.31µF	320Ω 1075Ω 0.21µF
Zt	370Ω 620Ω 0.31µF	370Ω 620Ω 0.31µF	370Ω 620Ω 0.31µF	600Ω	370Ω 620Ω 0.31µF	370Ω 620Ω 0.31µF
Mean ERL	11.3	14.3	20.0	11.2	18.3	23.9
Mean SRL	8.46	11.1	15.5	8.1	14.5	17.7
Minimum ERL	5.0	9.5	6.5	5.0	9.5	9.0
Minimum SRL	3.0	6.0	6.0	3.0	6.0	8.0
Std.Dev ERL	4.19	1.48	5.91	4.36	4.31	4.6
Std.Dev SRL	3.09	0.97	3.0	3.05	3.6	2.45

Table 2.2 A summary of the results of the transhybrid frequency response survey.

Z1	706-Type	706-Type	706-Type	706-Type	370Ω 620Ω 0.31µF	370Ω 620Ω 0.31µF
Zb	600Ω	370Ω 620Ω 0.31µF	275Ω 810Ω 0.12µF	600Ω	370Ω 620Ω 0.31µF	320Ω 1075Ω 0.21µF
Zt	370Ω 620Ω 0.31µF	370Ω 620Ω 0.31µF	370Ω 620Ω 0.31µF	600Ω	370Ω 620Ω 0.31µF	370Ω 620Ω 0.31µF
Mean ERL	11.3	14.3	20.0	11.2	18.3	23.9
Mean SRL	8.46	11.1	15.5	8.1	14.5	17.7
Minimum ERL	5.0	9.5	6.5	5.0	9.5	9.0
Minimum SRL	3.0	6.0	6.0	3.0	6.0	8.0
Std.Dev ERL	4.19	1.48	5.91	4.36	4.31	4.6
Std.Dev SRL	3.09	0.97	3.0	3.05	3.6	2.45

Table 2.2 A summary of the results of the transhybrid frequency response survey.

Balance Impedance			Number of lines with SRL > 10dB	Number of lines remaining
R1 (Ω)	R2 (Ω)	C2 (µF)		
670	0		397	1448
225	950	0.107	1394	54
145	1005	0.29	54	0

Table 2.3   Number of balance impedances required to achieve SRL greater than 10 dB.
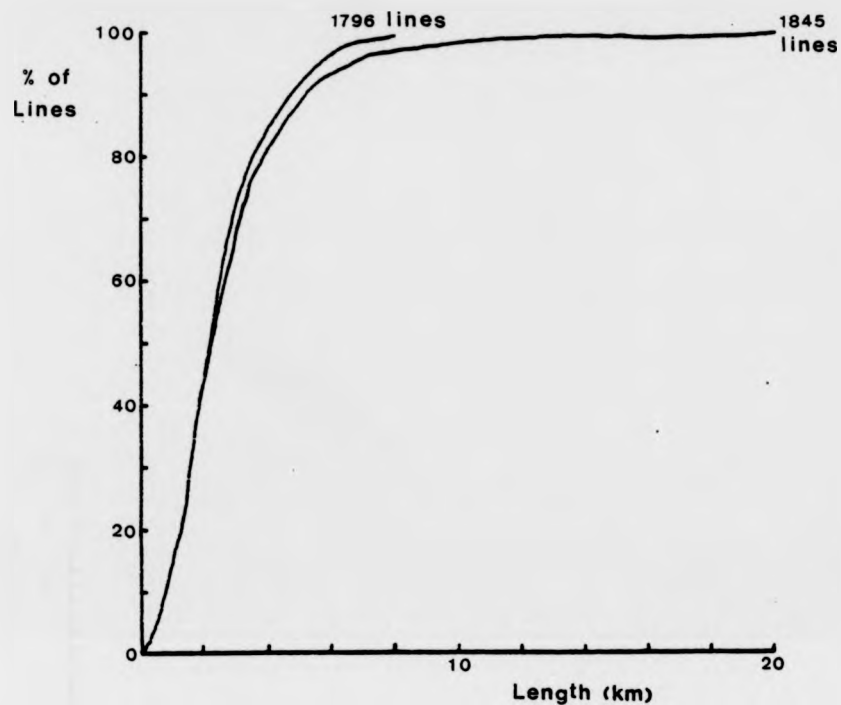
Figure 2.1: Cumulative Distribution of Line Lengths
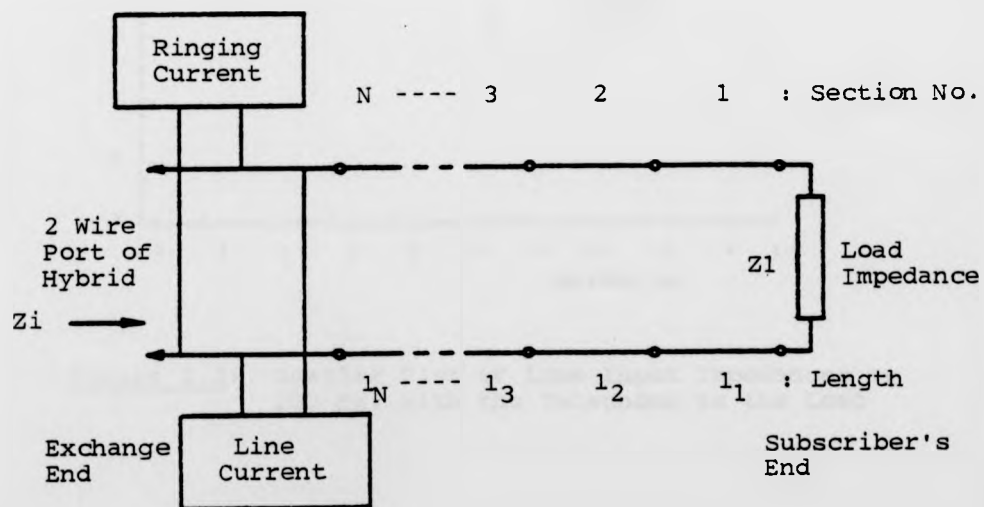
Figure 2.2: A Typical Subscriber's Line

Figure 2.3: Scatter Plot of Line Input Impedances at 200 Hz, with the Telephone as the Load
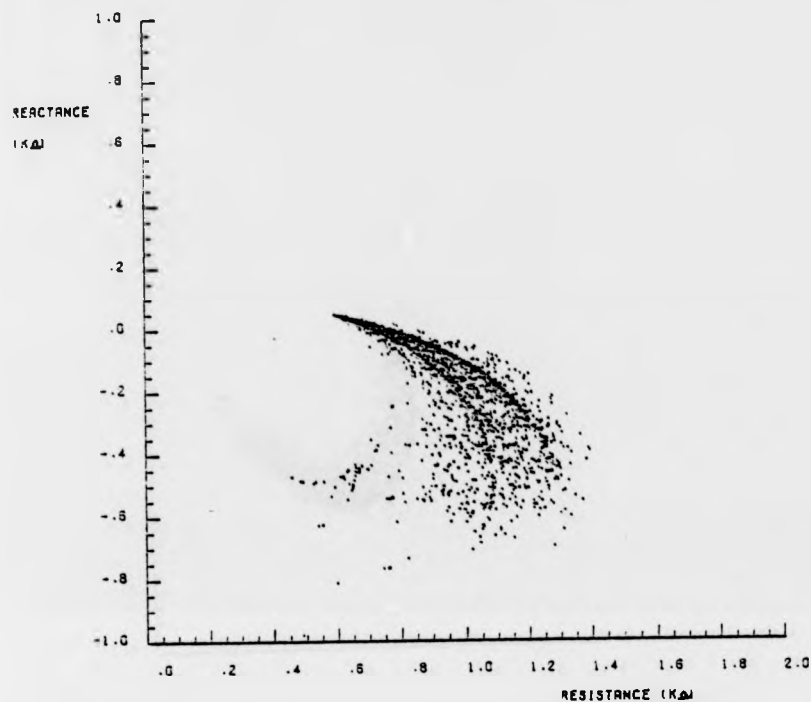
Figure 2.4: Scatter Plot of Line Input Impedances at 500 Hz, with the Telephone as the Load
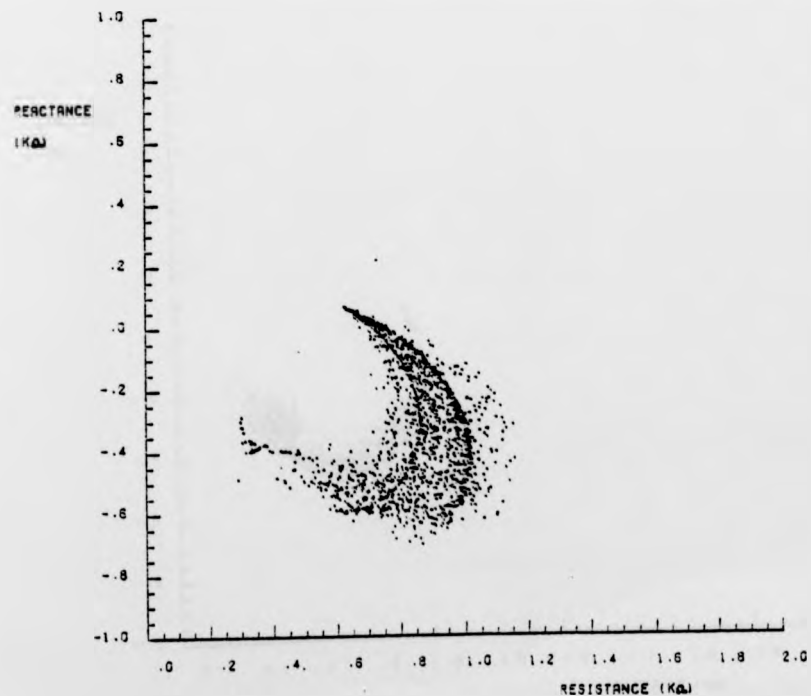
Figure 2.5: Scatter Plot of Line Input Impedances at 1 kHz, with the Telephone as the Load
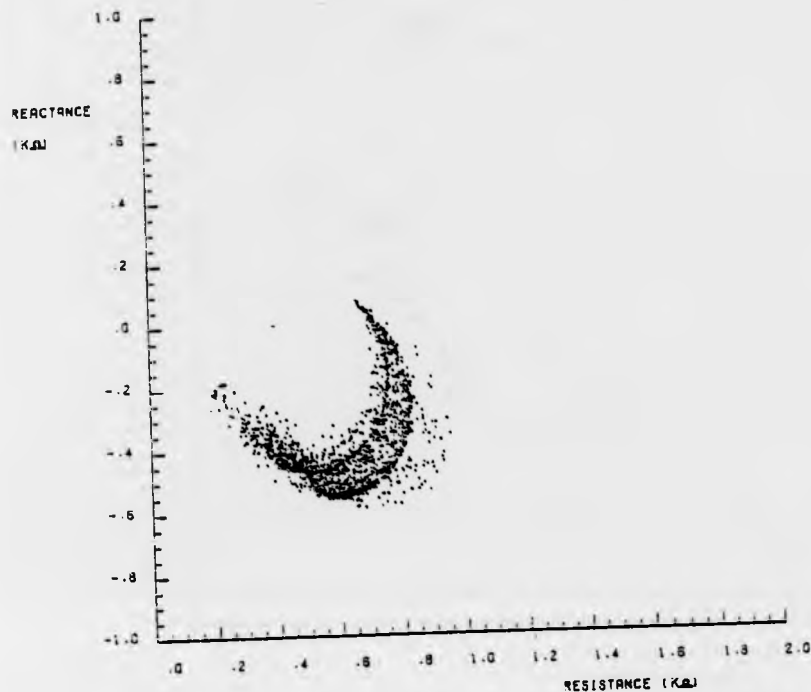
Figure 2.6: Scatter Plot of Line Input Impedances at 2 kHz, with the Telephone as the Load
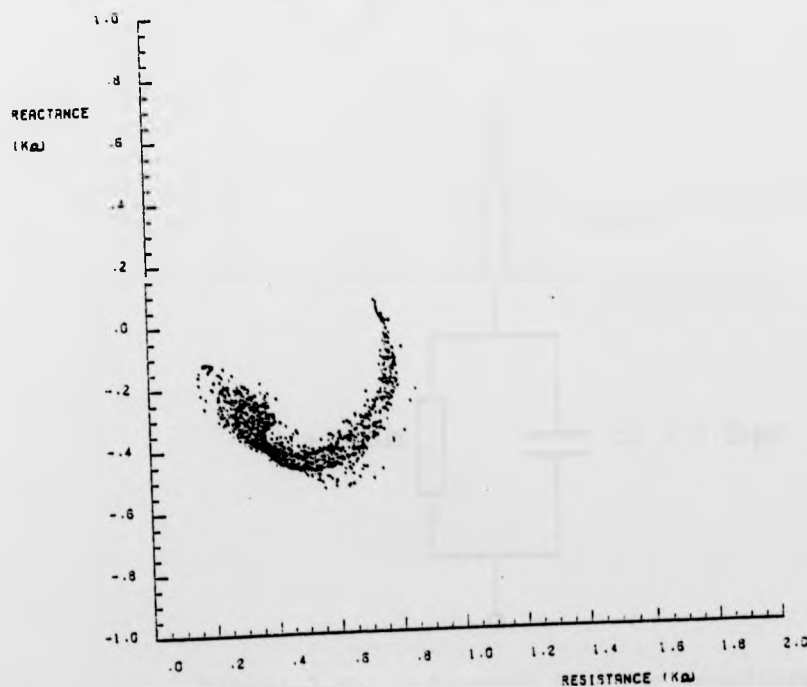
Figure 2.7: Scatter Plot of Line Input Impedances at 3.5 kHz, with the Telephone as the Load
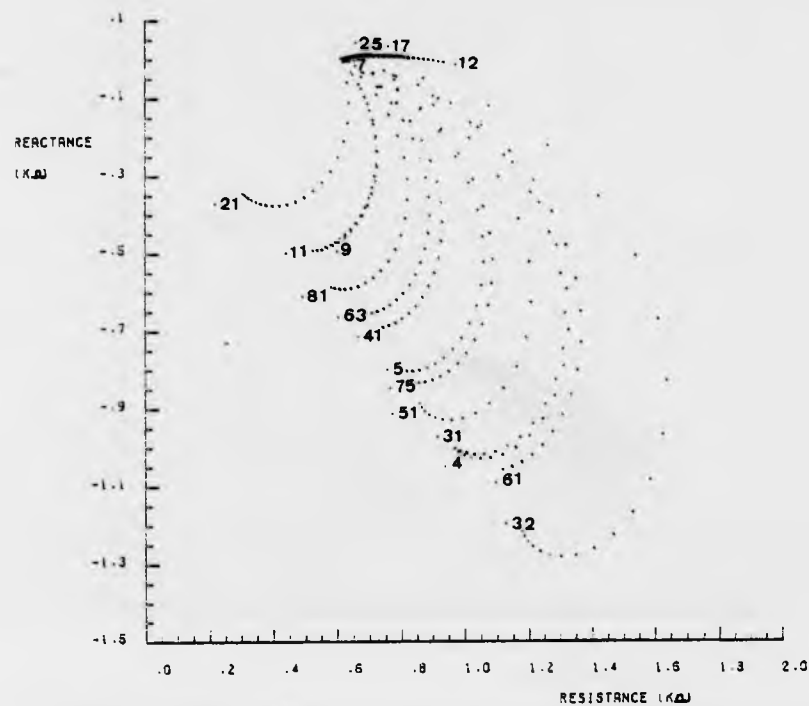
Figure 2.8: Variation of Input Impedance with Line Length for all Types of Cable at 500 Hz
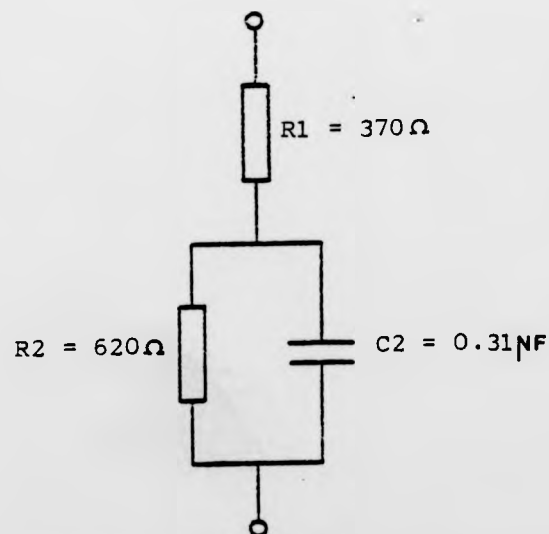
Figure 2.9: 3-Element Balance Impedance
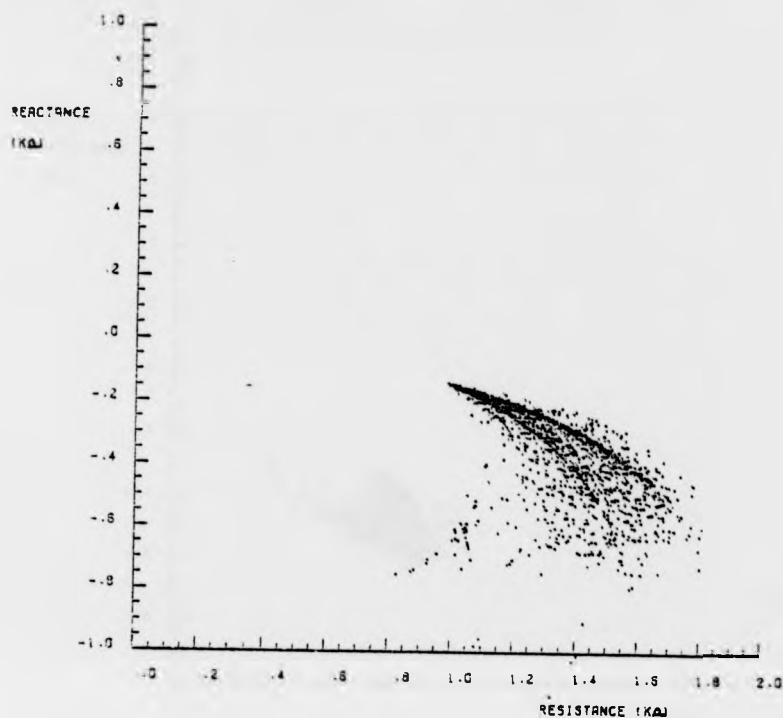
Figure 2.10: Scatter Plot of Line Input Impedances at 200 Hz, with the 3-Element Load Impedance
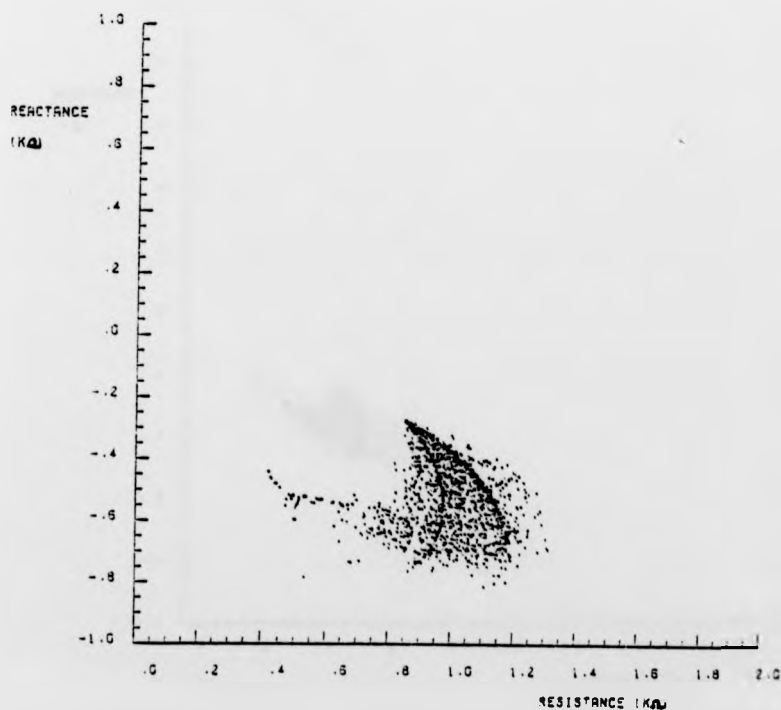
Figure 2.11: Scatter Plot of Line Input Impedances at 500 Hz, with the 3-Element Load Impedance
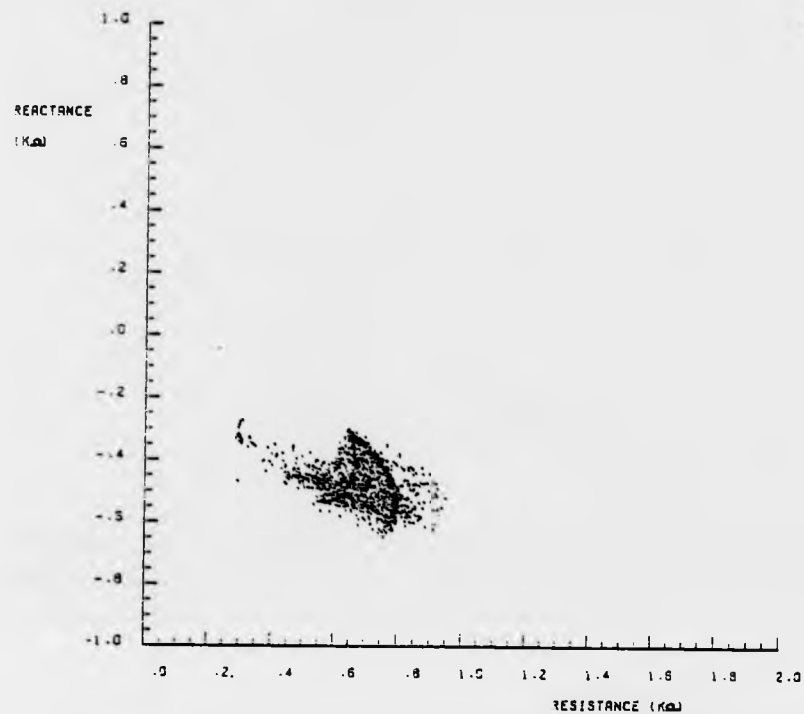
Figure 2.12: Scatter Plot of Line Input Impedances at 1 kHz, with the 3-Element Load Impedance
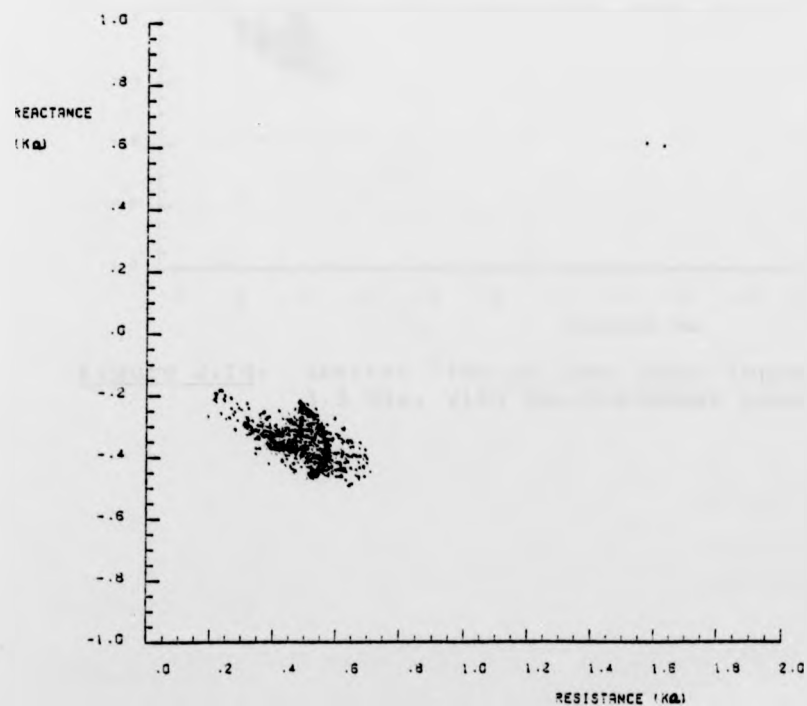
Figure 2.13: Scatter Plot of Line Input Impedances at 2 kHz, with the 3-Element Load Impedance
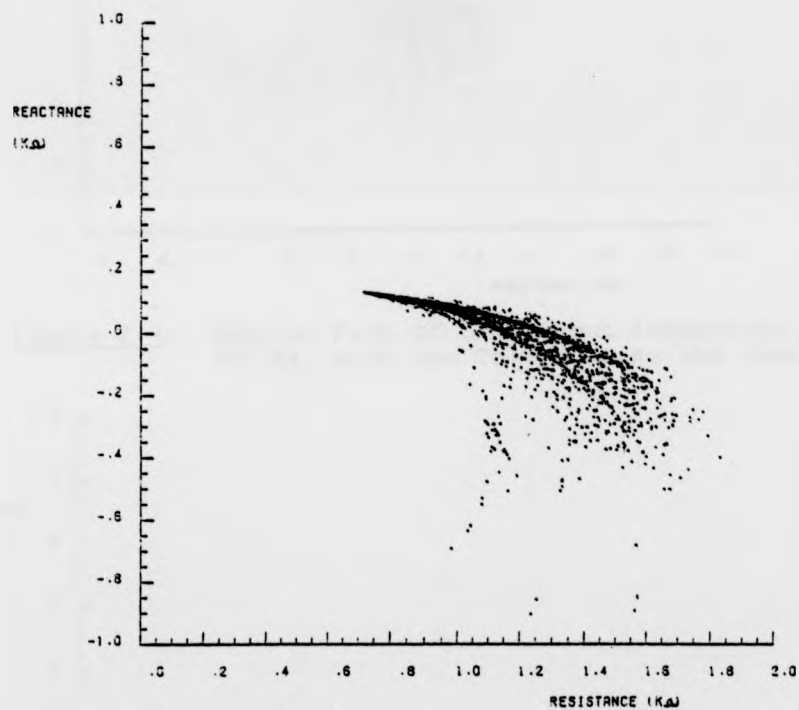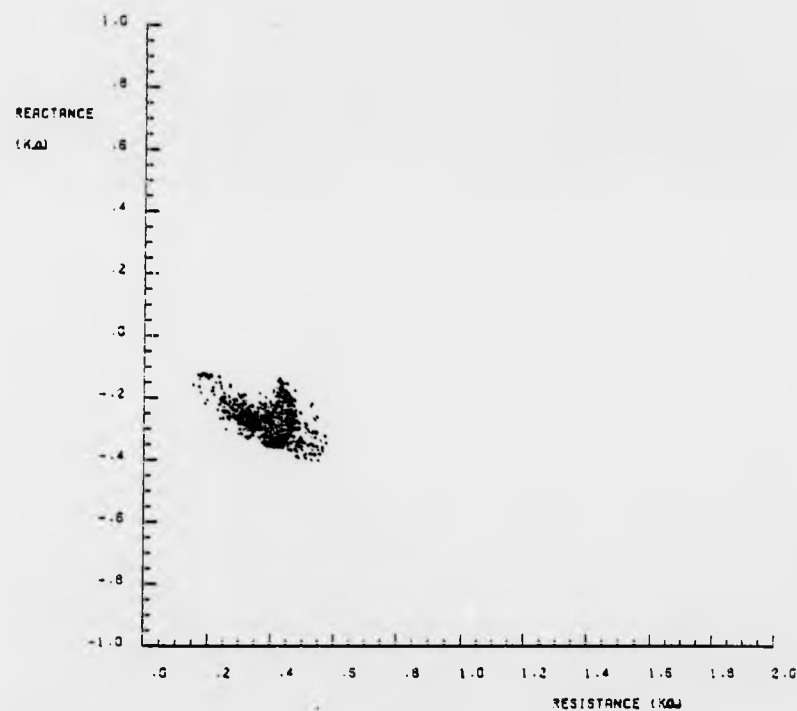
Figure 2.14: Scatter Plot of Line Input Impedances at 3.5 kHz, with the 3-Element Load Impedance
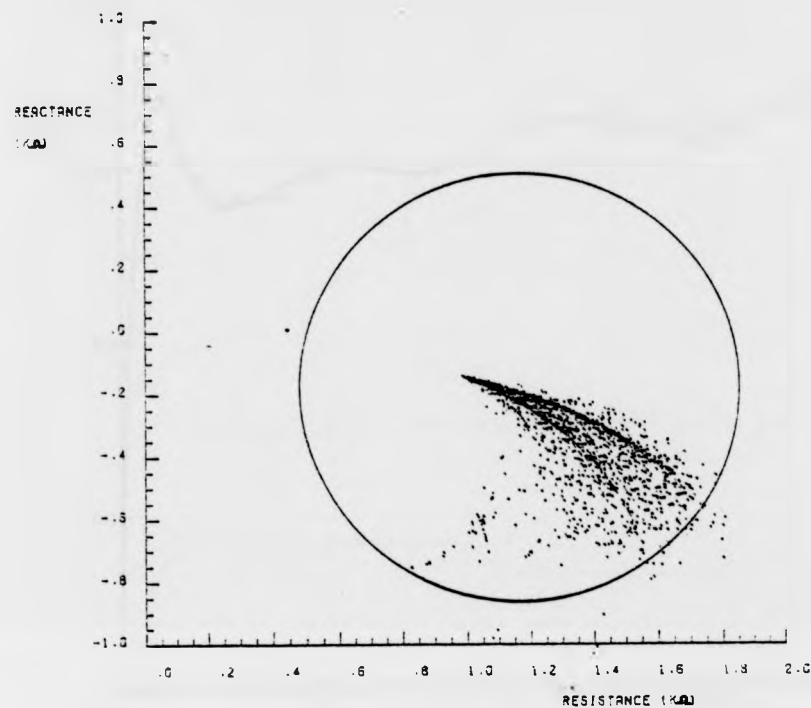
Figure 2.16: A 10 dB Circle of Constant Return Loss Superimposed on the Scatter Plot of Line Input Impedances at 200 Hz, with the 3-Element Load Impedance

. = Line input
   impedance points

+ = 3-element
   impedance points
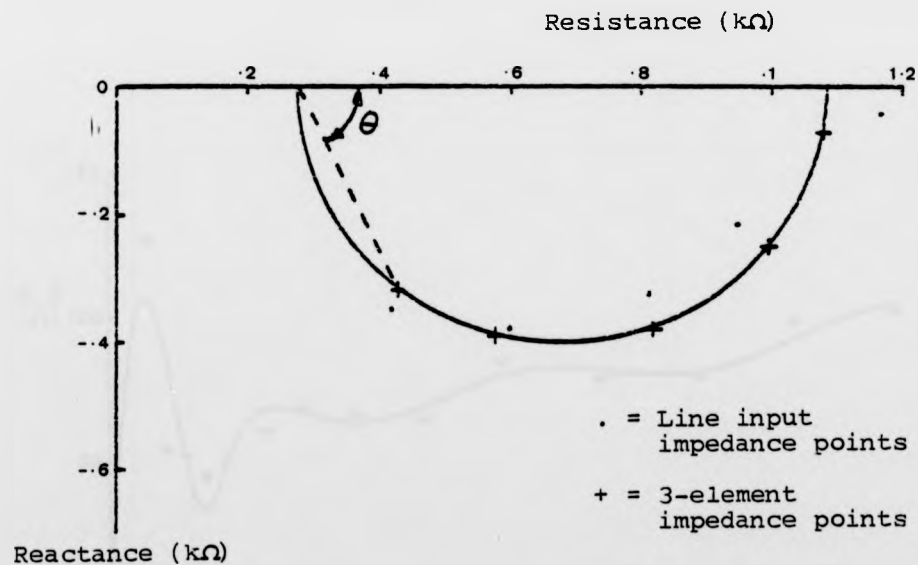
Figure 2.15: The Mean Line Input Impedance at 5 Frequencies
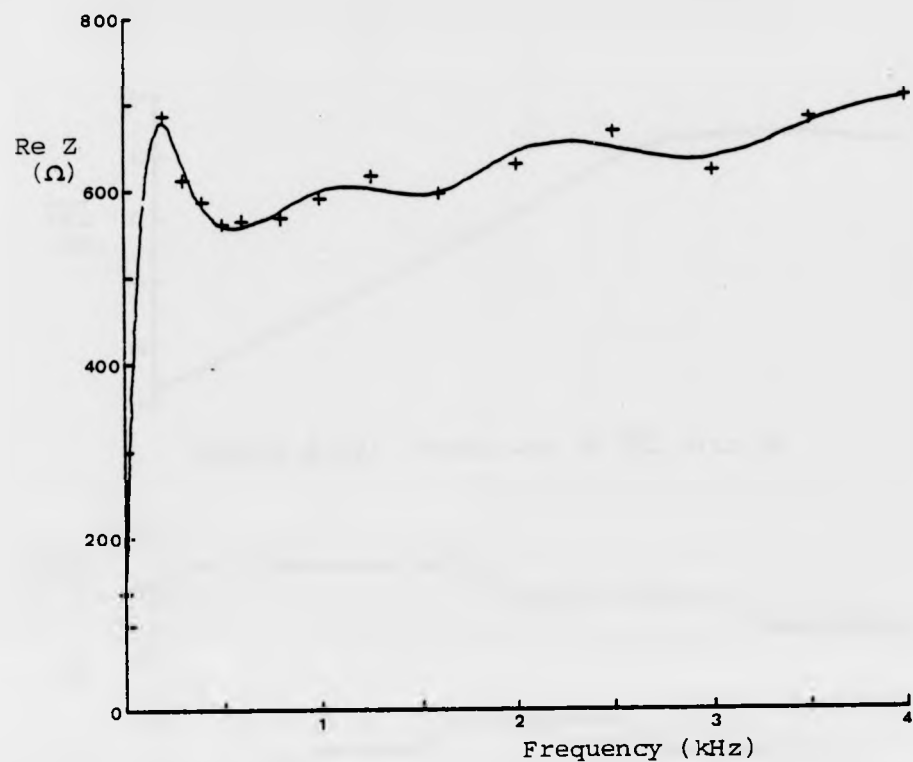
Figure 2.17: Interpolation of the Real Part of the Telephone Impedance
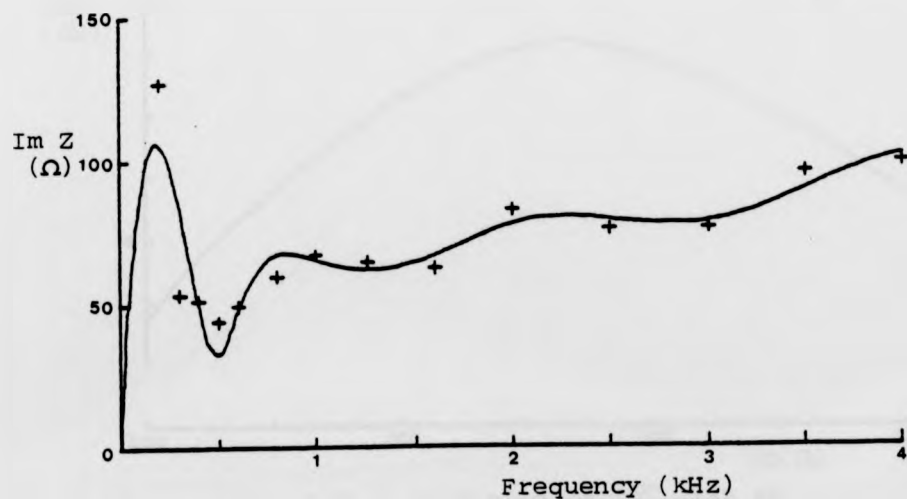
Figure 2.18: Interpolation of the Imaginary Part of the Telephone Impedance
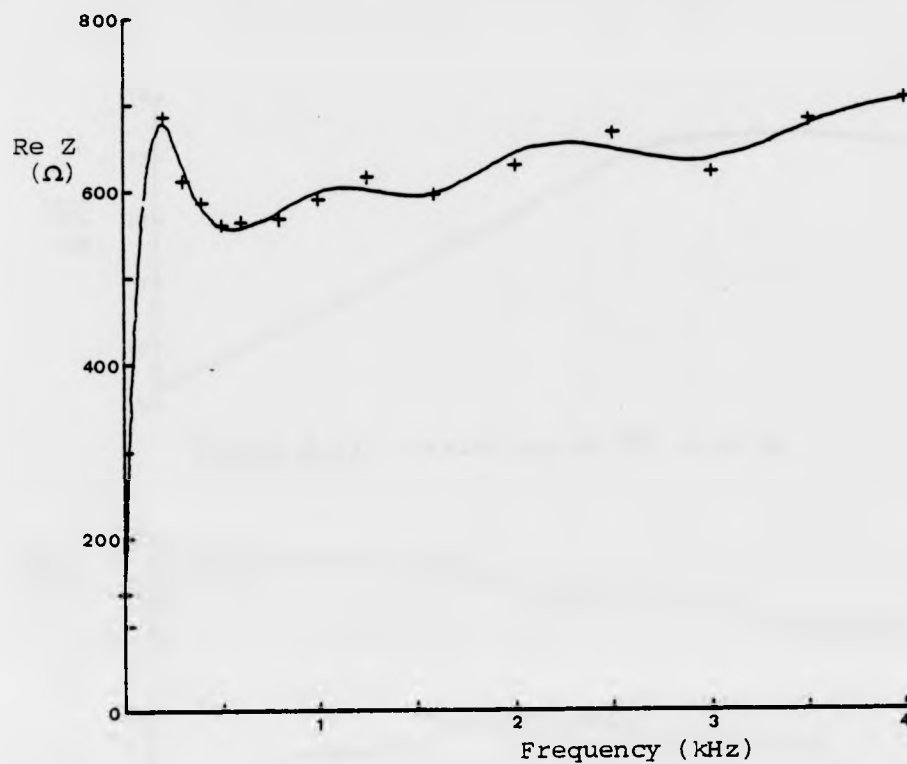
Figure 2.17: Interpolation of the Real Part of the Telephone Impedance
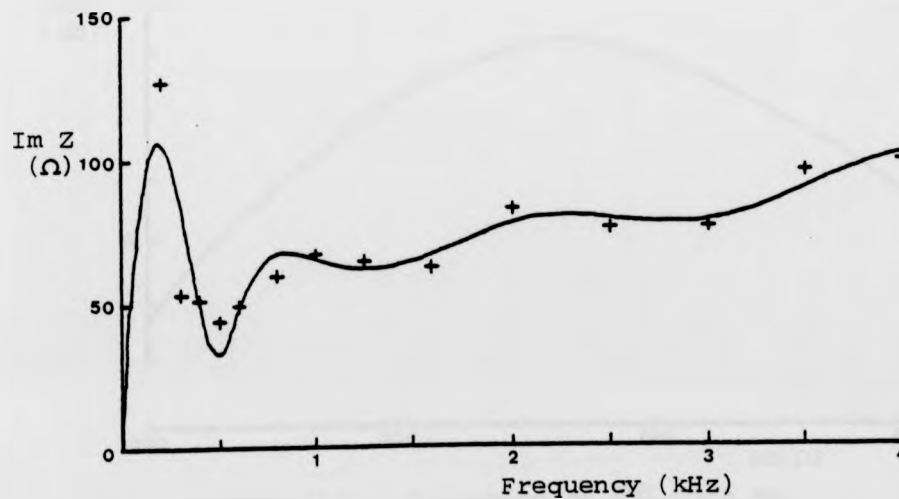
Figure 2.18: Interpolation of the Imaginary Part of the Telephone Impedance
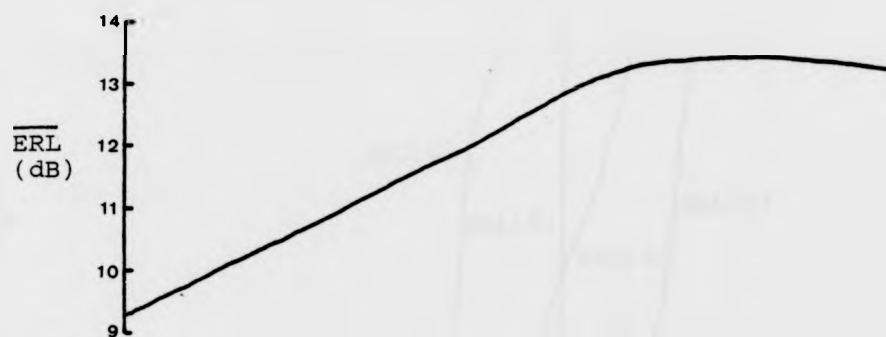
Figure 2.19: Variation of $\overline{ERL}$ with Rb
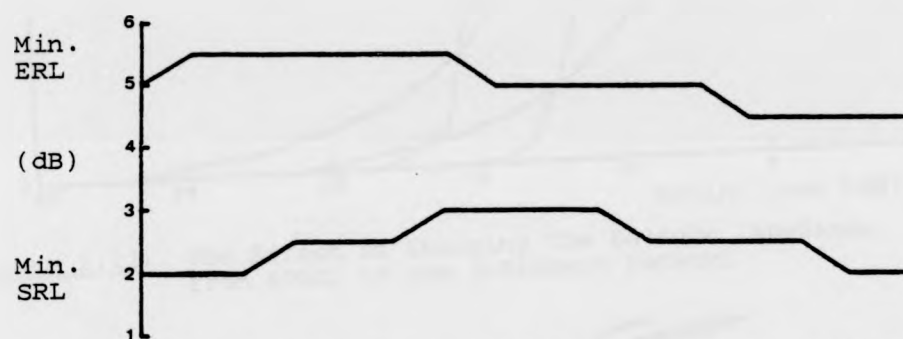
Figure 2.20: Variation of Minimum ERL and SRL with Rb
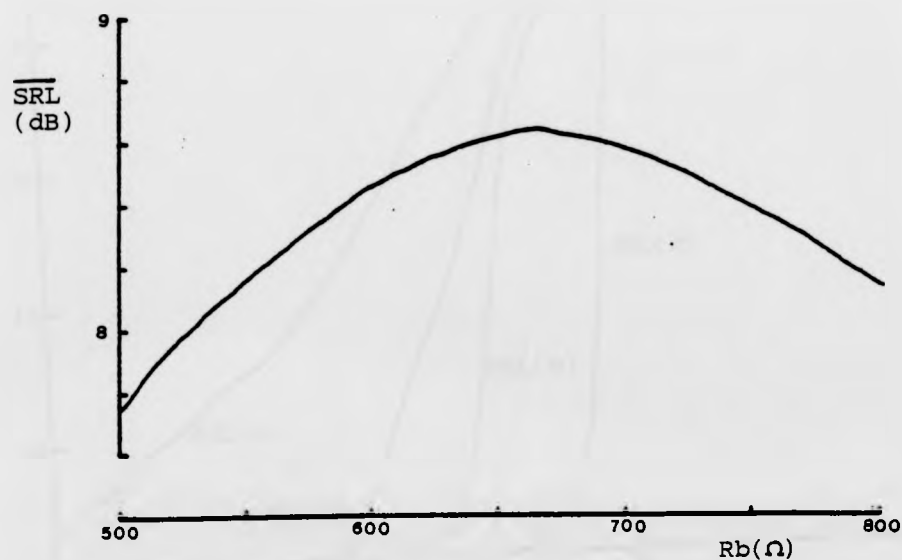
Figure 2.21: Variation of $\overline{SRL}$ with Rb
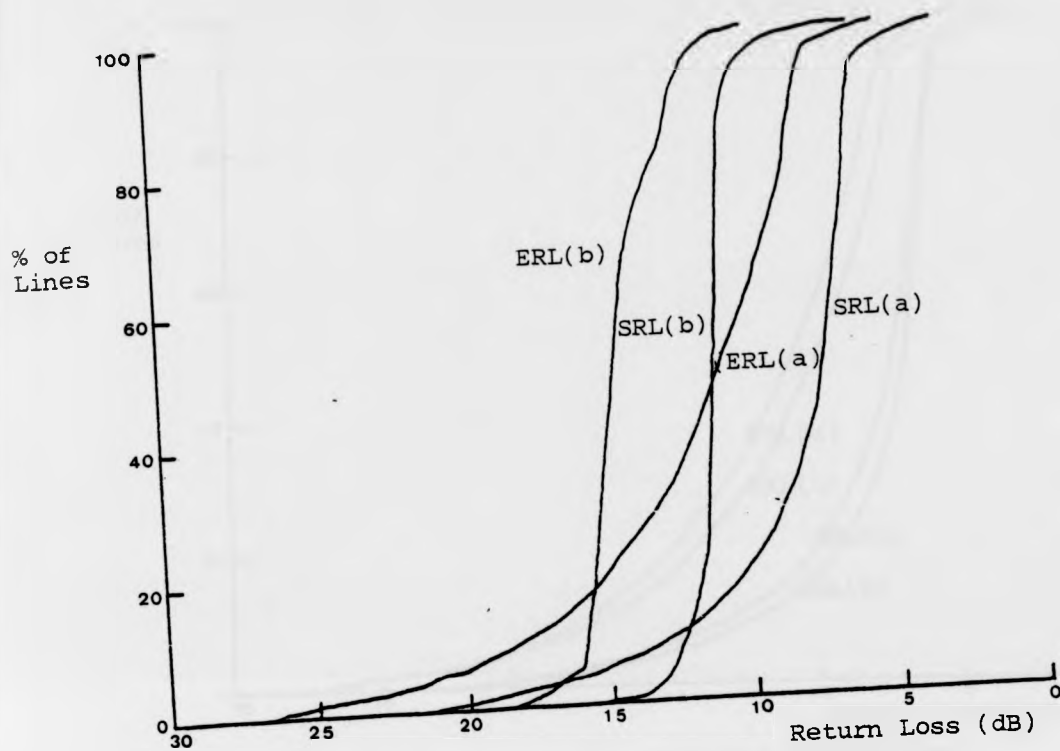
Figure 2.22: The Effect of Changing the Balance Impedance from 600Ω to the 3-Element Network
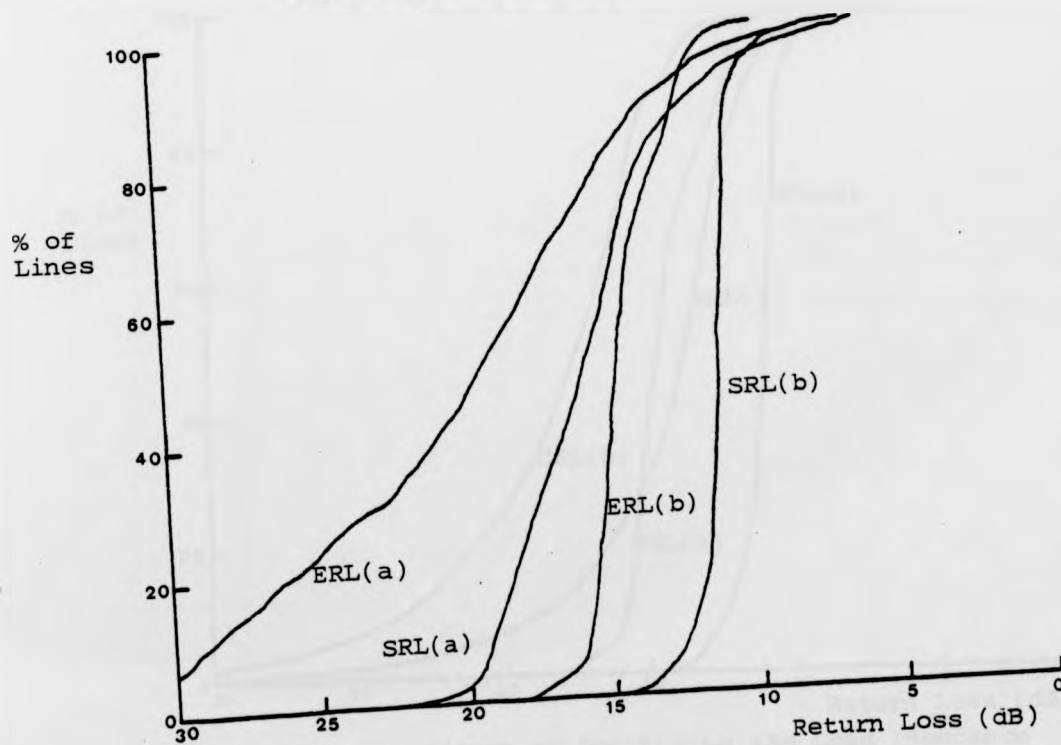
Figure 2.23: The Effect of Optimising the 3-Element Balance Network
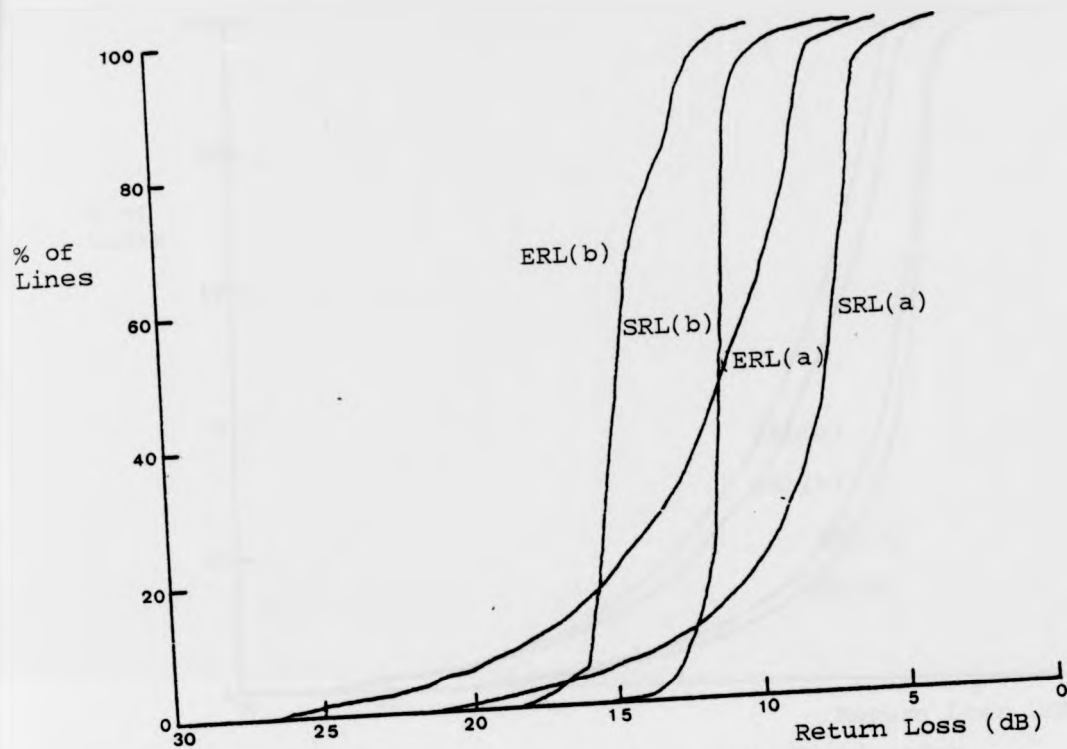
Figure 2.22: The Effect of Changing the Balance Impedance from 600Ω to the 3-Element Network
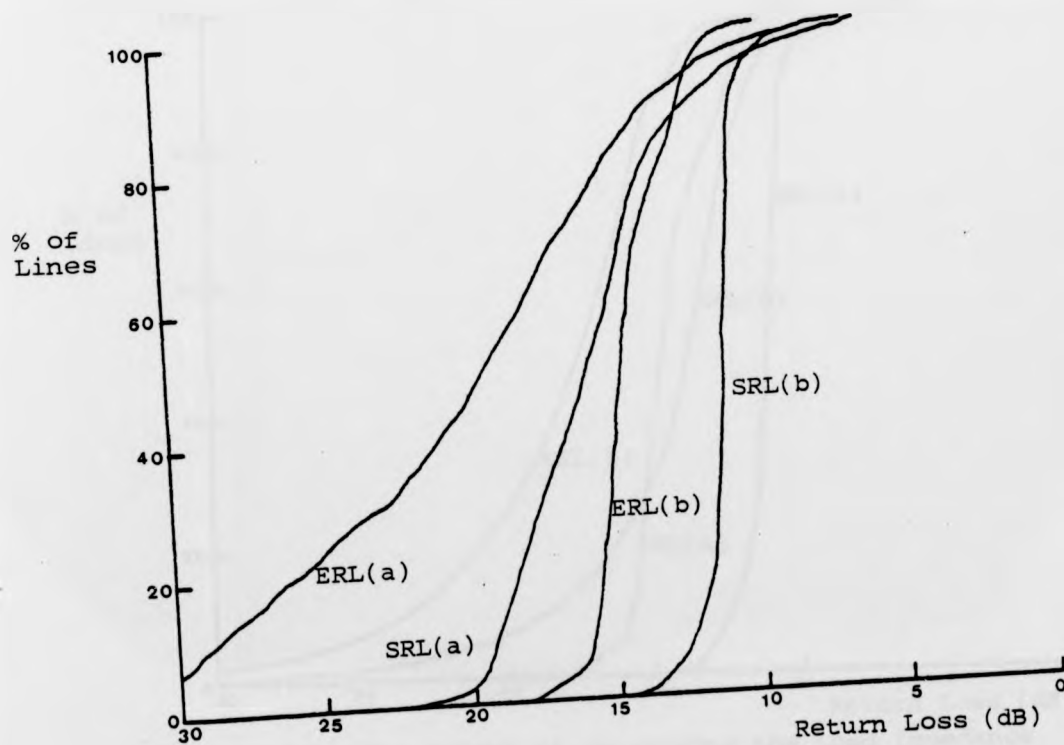
Figure 2.23: The Effect of Optimising the 3-Element Balance Network
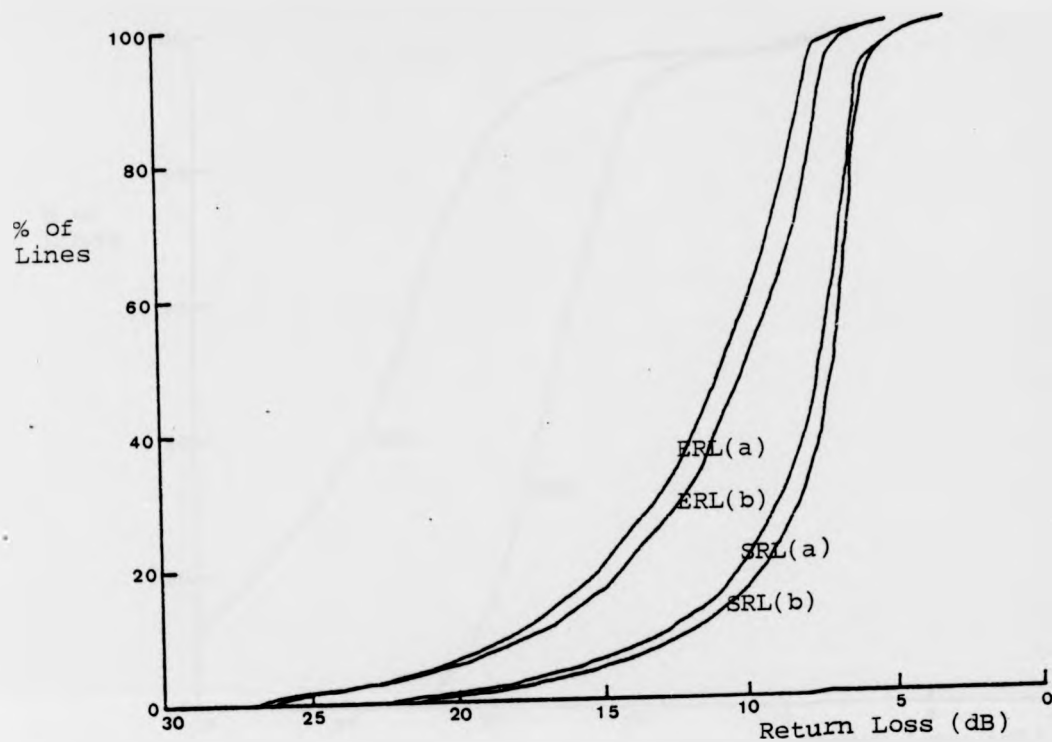
Figure 2.24:   The Effect of Changing the Terminating
               Impedance from 600Ω to the 3-Element Network
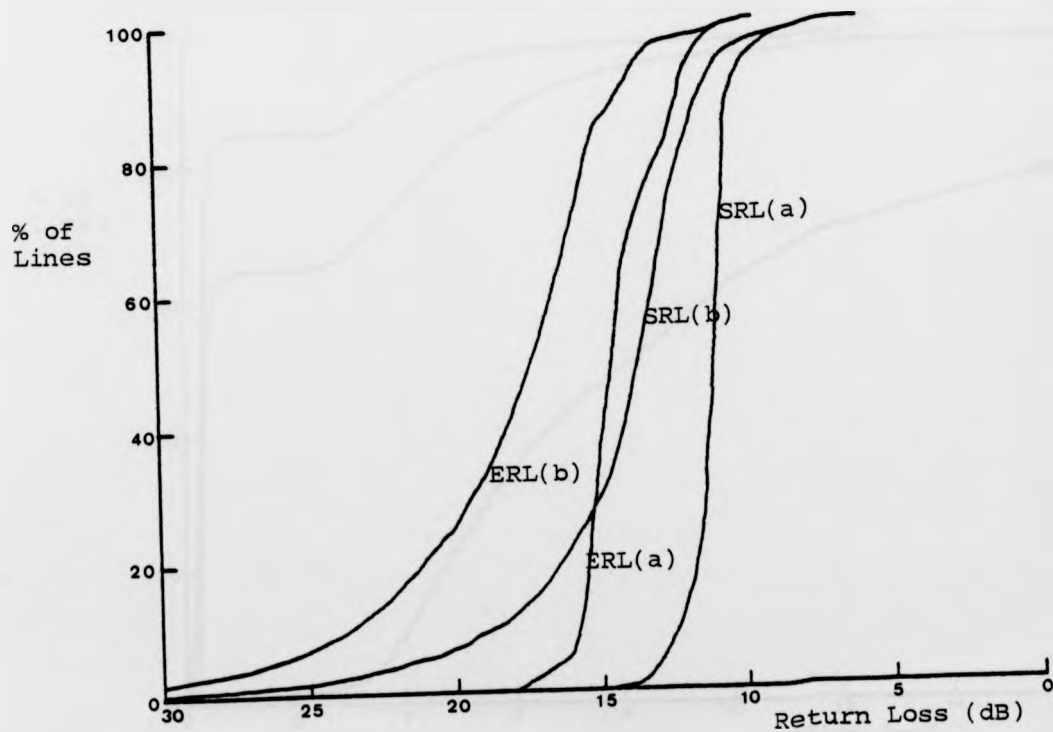
Figure 2.25:   The Effect of Optimising the Load Impedance
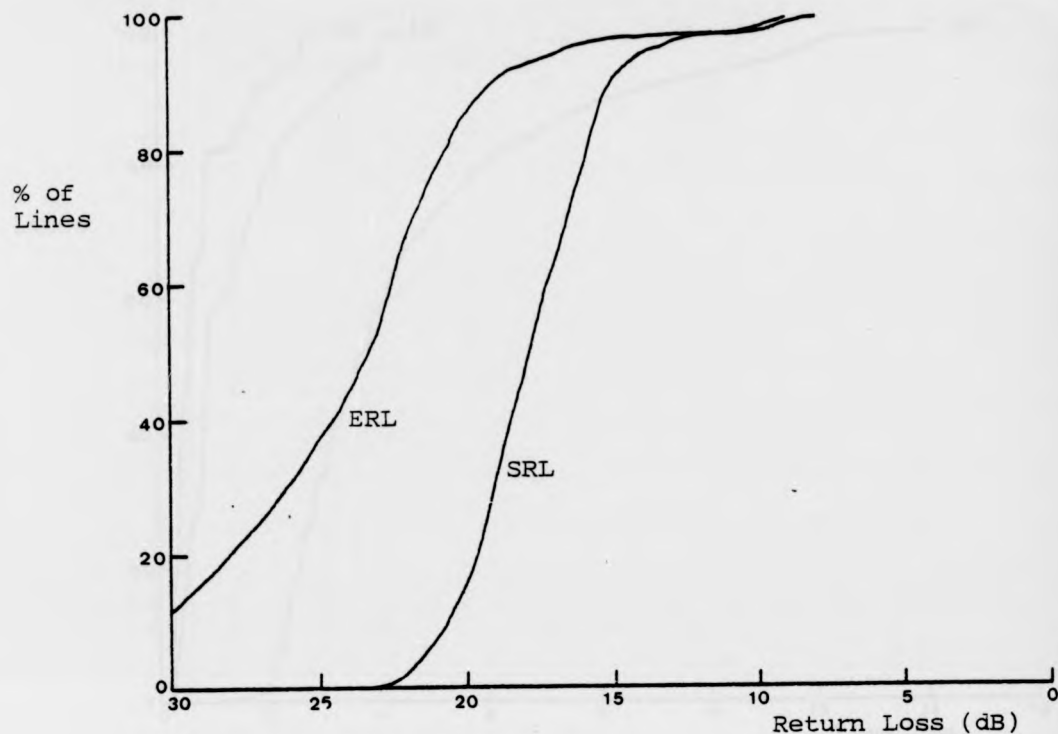
Figure 2.26: ERL and SRL Distributions with
Optimised Load and Balance Impedances
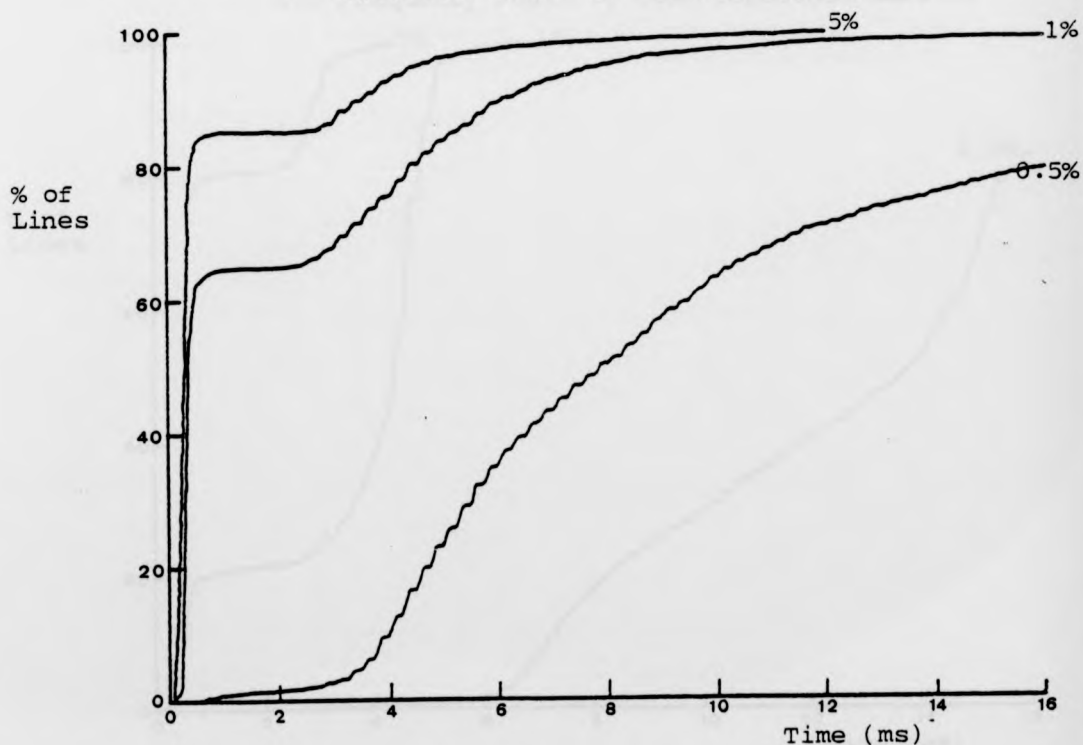
Figure 2.27: Distribution of Transhybrid
Impulse Response Decay Times with
the Telephone as the Load Impedance
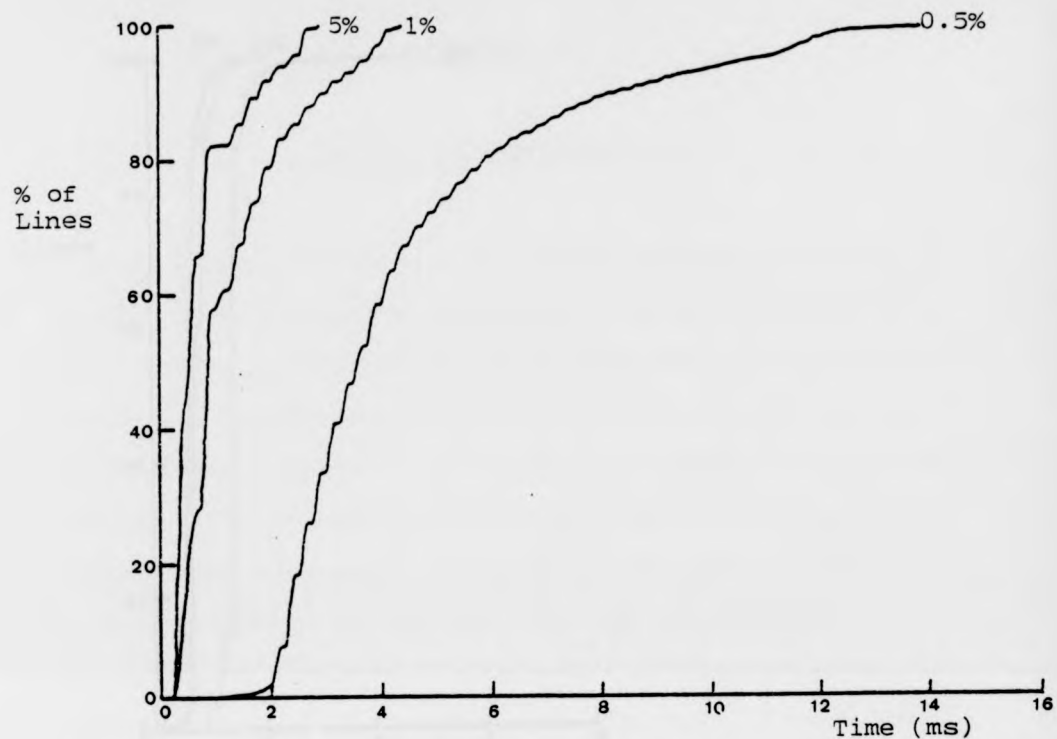
Figure 2.28:   Impulse Response Decay Time Distribution with
Low Frequency Peaks of Load Impedance Removed
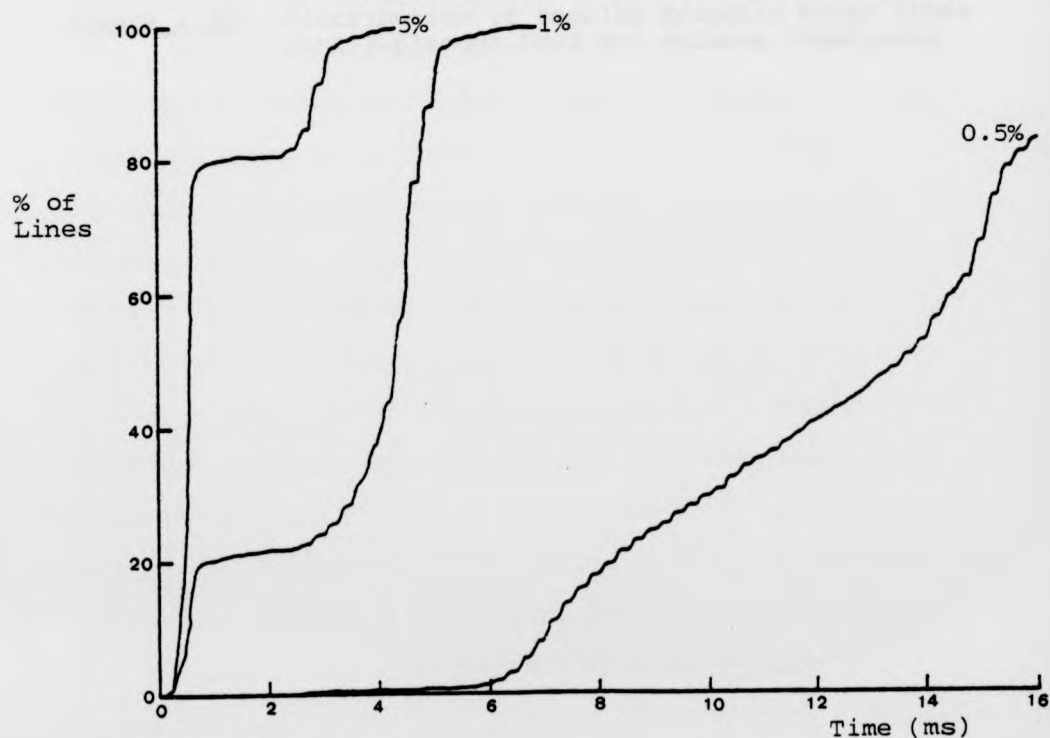
Figure 2.29:   Distribution of Impulse Response Decay
Times with Complex Balance Impedance
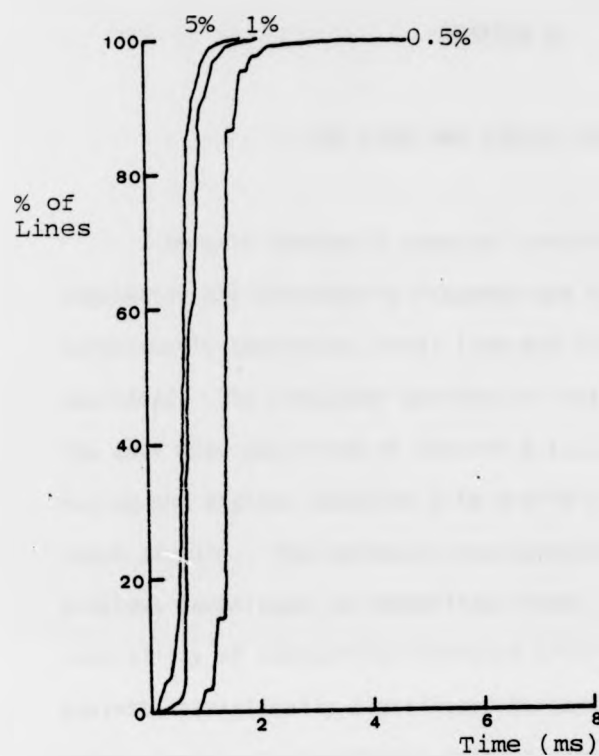
Figure 2.30: Distribution of Impulse Response Decay Times
with 3-Element Load and Balance Impedances

CHAPTER 3

THE LINE AND HYBRID SIMULATOR

In this chapter a computer controlled system capable of
simulating the transhybrid response due to any combination of
subscriber's apparatus, local line and fixed 2 to 4 wire converter is
described. The simulator operates in real-time and when used with
the data base described in Section 2.1.1, it enables testing of both
analog and digital adaptive 2 to 4 wire converters with realistic
input signals. The system is considerably more flexible than
previous techniques for modelling lines, and it provides the
possibility of conducting automated trials of adaptive hybrids
against statistically significant numbers of lines. The simulator
can be used to test adaptive balance circuits by simulating the
response of one arm of the converter, as shown in Figure 3.1.

The simulator consists of an 128th order digital transversal
filter whose coefficients are down-loaded from a computer, as shown
in Figure 3.2. The coefficients are calculated as described in
Section 2.2.5 and loaded into the simulator's coefficient store. The
required transfer function can then be simulated without further
intervention of the computer. In the following sections the
operation of the simulator is described and the design of ancillary
filtering and compensation circuits is discussed. In Section 3.6 the
accuracy of the simulator is measured against known frequency
responses.

3.1 Loading Transhybrid Impulse Responses

The computer (LSI-11) is interfaced to the simulator using a DRV-11 interface card. This card allows 4 bi-directional input-output ports to be addressed by the computer as part of its memory, the addresses of the ports being selected by means of jump leads on the card. The 3 ports used to interface to the simulator are designated as follows:-

PORT 1 : Control Port : This port is used to control the operation of the simulator. By writing the appropriate control words to the port the computer can switch the simulator between its 3 modes, as shown in Table 3.1. The reset mode is used to initialise all timing and control signals, usually following 'switch on'. In the halt mode the simulator is halted and the computer can access the coefficient store, via the other 2 ports, to load a new set of simulator coefficients. In the run mode the simulator operates independently of the computer and simulates the required response, as explained in Section 3.2.

PORT 2 : Data Port : This port is used to write coefficient values into the coefficient store when the simulator has been placed in the halt mode.

PORT 3 : Address Port : This port is used to address locations in the simulator's coefficient store during coefficient loading.

Thus, to load a new set of coefficient values into the coefficient store, the computer halts the simulator via the control port. The address of the first coefficient to be loaded is then output to the address port, and the coefficient value is output to the data port. The computer bus timing signals are used to strobe the coefficient into the store, and the address of the next coefficient to be loaded is output by the computer. Having loaded

all 128 coefficients within the coefficient store, the control port

is used to restart simulation with the new coefficient set.

Coefficient loading is controlled by an assembly language program

(Macro-11) which can be called as a subroutine from a Fortran program

which calculates the coefficient values. A listing of the load macro

is given in Appendix A2.

3.2 Simulation of Transhybrid Responses

The 128th order digital transversal filter whose response

simulates the transhybrid response, is of the recirculating shift

register type (Rabiner and Gold, 1975). A digital filter evaluates

the discrete convolution:-

$$y_{nT} = \sum_{i=0}^{N-1} h_{iT} x_{(n-i)T} \qquad 3.1$$

where y_{nT} and x_{nT} are the output and input samples at time $t = nT$

respectively, h_{iT} is the sample of the impulse response of the system

at time $t = iT$, i.e. the ith filter coefficient, N is the number of

samples used to represent the system's impulse response, and T is the

time between samples.

To implement this discrete convolution, during one input

sampling period, the recirculating shift register (RSR in Figure 3.2)

recirculates all of the 128 most recent input samples, which appear

sequentially on the RSR output. The RSR clock is also used to clock

a counter, which sequences the coefficient store (RAM) through all of

its locations. The synchronisation is arranged so that the

multiplier and accumulator (MAC) is presented with an input sample

and the corresponding impulse response coefficient simultaneously.

These are multiplied together and accumulated with the 127 other

sample-coefficient products by the MAC (TRW, 1979). Thus the set of

128 coefficients is convolved with the delayed input samples to form an output sample. Both the coefficients and the input samples are represented by 12-bit 2's complement numbers in parallel form, and the products are accumulated in a 27-bit register, allowing 3 bits 'headroom' for the accumulation. Having performed the convolution given by equation 3.1, the output sample is rounded to 12 bits and clocked into an output register.

To facilitate testing of the simulator, a circuit was designed to inject an impulse into the input of the filter once in every 128 input sample periods. This allows the impulse response of the simulator to be displayed on an oscilloscope for verification.

In Figure 3.3 an example of the timing of the simulator and its associated A/D and D/A conversion circuits is given. For convenience the example is in terms of a 4th order transversal filter, and it can be seen that there is an overall delay of 2 sample periods through the simulator. A complete circuit diagram of the simulator is given in Appendix A3.

3.3 Simulator Sampling Rate and Filtering Requirements

The frequency response of a digital filter is periodic about the sampling frequency, and the presence of the so called image bands in the spectrum of the output signal would interfere with the operation of an adaptive filter which was attempting to cancel the output of the simulator. To attenuate the image bands it is necessary to filter the output of the simulator as shown in Figure 3.4. This filter is known as a reconstruction filter, since it serves to reconstruct the analog signal from its samples. For minimum distortion of the simulated response, the response of the reconstruction filter should be flat, with approximately linear

phase, in the passband. This allows the phase response of the filter to be compensated for by the introduction of an appropriate delay in the adaptive filter path. Analog filters with the desired type of response do exist, notably Bessel and Gaussian filters (Zverev, 1967), but they have very poor attenuation characteristics. An alternative approach to the problem is to use 2 filters with identical responses, one at the simulator output and the other in the adaptive filter path, as shown in Figure 3.5. The net effect of this approach is that the input signal x(t) is filtered before being applied to either the adaptive filter or the simulator, and assuming that the filter has sufficient rejection of the image bands, the adaptive filter attempts to match the simulator's response in the passband only. By increasing the sampling frequency used in the simulator, the filtering requirements are relaxed, and the task of designing 2 filters with identical amplitude and phase responses in the passband is facilitated.

Assuming a simulator sampling rate of 16 kHz, and a passband of 3.6 kHz, then the lower band edge of the lowest frequency image band falls at 12.4 kHz. The sample and hold circuit at the simulator output has an effective transfer function of:-

$$Sh(\omega) = \frac{Sin(\omega T/2)}{\omega T/2} \qquad 3.2$$

where T is the sampling period. At 12.4 kHz this function contributes approximately 12 dB attenuation, and therefore for 30 dB net image band rejection, the filter should provide at least 18 dB attenuation at this frequency, i.e. a 3rd order Butterworth or Tchebichef filter is sufficient. Both types of filter have good attenuation characteristics, however, of the two types, Butterworth filters have lower group delay (and hence introduce less phase distortion), are maximally flat in the pasband, and are also less sensitive to component inaccuracies (Zverev, 1967). Since this last

factor is important if two identical filters are to be designed, a third order Butterworth filter was chosen for image band rejection.

A third order Butterworth or Tchebichef filter can be implemented using an extension of the standard Sallen and Key second order section (Ambikairajah, 1981). This method was chosen for implementation of the reconstruction filters because it requires only a single operational amplifier for each filter.

The responses of the 2 filters are shown in Figure 3.6, and it can be seen that the responses have been matched to better than 0.1 dB in the passband.

3.4 Compensation for the Fixed Delay of the Simulator

In Section 3.1 it was shown that the combination of simulator and A/D converter has a fixed delay of 2 sample periods. To compensate for this delay it is necessary to introduce an equal delay into the adaptive filter path. The compensating delay must be introduced before the input to the adaptive filter, rather than at its output, to avoid introducing a delay into the parameter control path of the adaptive filter. The required delay is achieved by connecting 3 pairs of sample and holds in cascade, as shown in Figure 3.7. The first pair of sample and holds hold a sample for 1 clock cycle, with effectively 1 clock cycle to acquire the sample, and the remaining pairs each delay the held sample by a further clock period. The advantage of this technique is that the acquisition period is invisible at the output of the delay. A conventional sample and hold, with visible acquisition time, would introduce unwanted distortion into the adaptive filter path.

3.5 Compensation for the Effects of a Non-Rectangular Frequency Window

In Appendix A1 it is shown that to achieve sufficient accuracy in calculating impulse responses from frequency responses, it is necessary to use a non-rectangular window in the frequency domain. Use of other than a rectangular window distorts the simulated frequency and phase response however, and an analog circuit is used to compensate for this distortion in the LHS. Comparison of the the window functions:-

$$W1(f) = 0.54+0.46Cos(2\pi f/f_s) : Hamming \qquad 3.3$$

$$W2(f) = 0.5(1.0+Cos(2\pi f/f_s)) : Hanning \qquad 3.4$$

with f_s = 16 kHz, shows that over the band of interest the Hamming window introduces less amplitude distortion than the Hanning window. The time domain responses of these windows have the same main-lobe widths (4/Fs), but the first side-lobe of the Hamming window is smaller in amplitude than that of the Hanning window. Although for the Hanning window the other side-lobes are smaller in amplitude than those of the Hamming window, the Hamming window was chosen because of its lower attenuation in the passband. For comparison the time responses of both window functions are shown in Figure 3.8.

The Hamming frequency window, with the first zero at 16 kHz, gives an attenuation of 3.8 dB at 3.4 kHz, and this 'droop' can be compensated by an under-damped second order section. The 2nd order section introduces some phase distortion, however, and it is necessary to restrict the phase lag of the compensation circuit. The optimum 2nd order section was found to be specified by ζ = 0.1 and ω_0 = 6 kHz, where the response of the section is given by:-

$$R(s) = \frac{1}{1+(2\zeta s/\omega_0)+(s/\omega_0)^2} \qquad 3.5$$

Table 3.2 shows the response of the compensation network compared

with that of the Hamming window, for a sampling frequency of 16 kHz.
The maximum error between the responses over the passband is 0.6 dB
at 3.4 kHz, while the maximum phase shift introduced by the section
is 9.5° at 3.4 kHz. The effect of this phase shift is that if an
adaptive filter models the simulated transhybrid response accurately,
then the SRL enhancement (SRLE) is limited to 15.6 dB at 3.4 kHz. To
achieve higher SRLE the adaptive filter must also model the phase
distortion produced by the compensation circuit. If the SRLE is
lower than 15.6 dB, then this indicates that the adaptive filter is
unable to accurately match the simulated response. The compensation
circuit will have a lesser effect on the ERLE, since this is an
average figure obtained over lower frequencies, where the phase
distortion is less.

The response of a Sallen and Key section, designed to realise
the required transfer function, together with the reciprocal of the
window droop, and the theoretical response of the Sallen and Key
section, is shown in Figure 3.9. It can be seen that the actual
compensation circuit has a resonant frequency which is slightly lower
than the nominal design frequency. The resultant improvement in
compensation is obtained at the expense of greater phase lag in the
compensation circuit.

In Appendix A1 it is also shown that the Hamming window
causes the initial samples of the calculated impulse response to be
'smeared out', effectively into the final portion of the response.
The final calculated impulse response sample, using a Hamming window,
thus represents energy of the true impulse response which has been
smeared out by the main lobe of the Hamming time function, and should
be included in the initial portion of the simulated impulse response
for accurate simulation. This effect occurs because the frequency
window represents an unrealisable system, i.e. it introduces

frequency-dependent attenuation, but no phase shift. The resulting calculated impulse response is also unrealisable, and should be shifted circularly one sample to the right to form a realisable impulse response. This procedure is equivalent to delaying the simulator output, and a further delay of 1 sample period is introduced into the delay compensation circuit of Section 3.4 to compensate for this effect.

3.6 Results of Testing the Line and Hybrid Simulator

As the line and hybrid simulator (LHS) is a programmable transversal filter, the performance of the hardware can be verified by designing an 128th order transversal filter to a given specification, implementing the filter on the LHS, and verifying its response. Using a standard filter design program (Mc. Clellan et al, 1972), a filter with the following specifications was designed:-

Filter order = 128

Sampling frequency = 32 kHz

Cutoff frequency = 3.4 kHz

Transition bandwidth = 600 Hz

Passband ripple = 0.01 dB

Stopband attenuation = 58 dB

The frequency response of this filter, implemented by loading the coefficients calculated by the filter design program into the LHS, at sampling rates of 8, 16 and 32 kHz, is shown in Figure 3.10. The impulse response of the filter, operating at 32 kHz, is shown in Figure 3.11.

To test the analog circuitry discussed earlier, a flat spectrum was windowed by the Hamming window and the inverse FFT taken. The resulting impulse response was shifted one place to the

right and loaded into the coefficient store. An error signal was formed by subtracting the output of the simulator's reconstruction filter from the output of the cascade of delay compensation circuit and the other reconstruction filter, where both paths had the same input signal. Figure 3.12 shows a plot of the resulting cancellation of the output of the simulator, as a function of frequency. It can be seen from the figure that as the frequency increases the phase shift due to the window compensation circuit decreases the accuracy of the simulator, but 15 dB SRLE is still possible at 3.4 kHz, as calculated in the previous section. The value of ERLE obtained with an input signal of white noise, bandlimited to 500 Hz to 2.5 kHz was 30.5 dB.

To complete the testing of the LHS, the transhybrid response due to a combination of load impedance, an artificial transmission line of various lengths, and a precision hybrid were measured. The line constants (R, L, G and C) of the artificial line were used to simulate the test lines on the LHS. The measured responses of the simulator, for the same test line lengths, are shown in Figure 3.13. Superimposed on Figure 3.13 are the equivalent test circuit responses at 500 Hz intervals, adjusted to allow for the effect of the sample and hold. Also superimposed on Figure 3.13 are the theoretical responses of the simulator, adjusted for the effect of the sample and hold. The error between the simulated responses and the desired responses is in part due to erors in calculating the frequency response to be simulated, i.e. due to errors between the calculated response and the desired response. These errors are due to inaccuracies in the information available to the simulator, e.g. line constants, hybrid characteristics, etc. The remaining error (between the calculated response and the actual response simulated) is simulation error. This error is worst when the response to be

simulated is low in amplitude, the maximum error being approximately
2 dB.   The main source of simulation error is likely to be inaccurate
compensation for the effects of the Hamming window.

simulated is low in amplitude, the maximum error being approximately
2 dB.   The main source of simulation error is likely to be inaccurate
compensation for the effects of the Hamming window.

simulated is low in amplitude, the maximum error being approximately 2 dB. The main source of simulation error is likely to be inaccurate compensation for the effects of the Hamming window.

Mode	Control Word	Status
Reset	-32768	All Timing Signals Reset
Run	0	Simulates Transhybrid Response
Halt	16384	Coefficient Loading

Table 3.1   Modes of the Line and Hybrid Simulator

Frequency (Hz)	Window Loss (dB)	Comp. Gain (dB)	Comp. Phase (°)
200	0.0	0.0	-0.4
1000	-0.3	0.2	-2.0
2000	-1.3	1.0	-4.3
3000	-2.9	2.4	-7.6
3400	-3.8	3.2	-9.5

Table 3.2   The Response of the Compensation Circuit Compared with
that of the Window
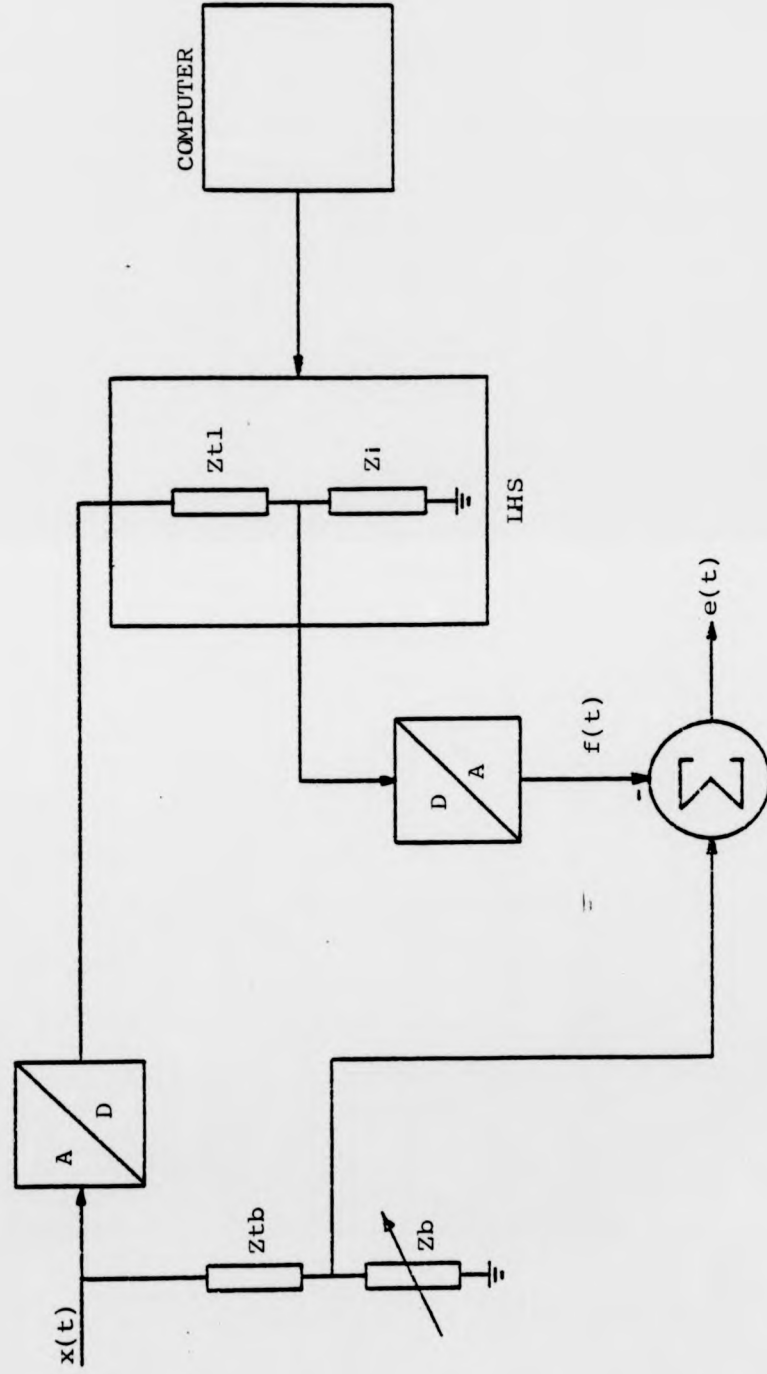
Figure 3.1: Use of the LHS in Testing Adaptive Balancing Hybrids
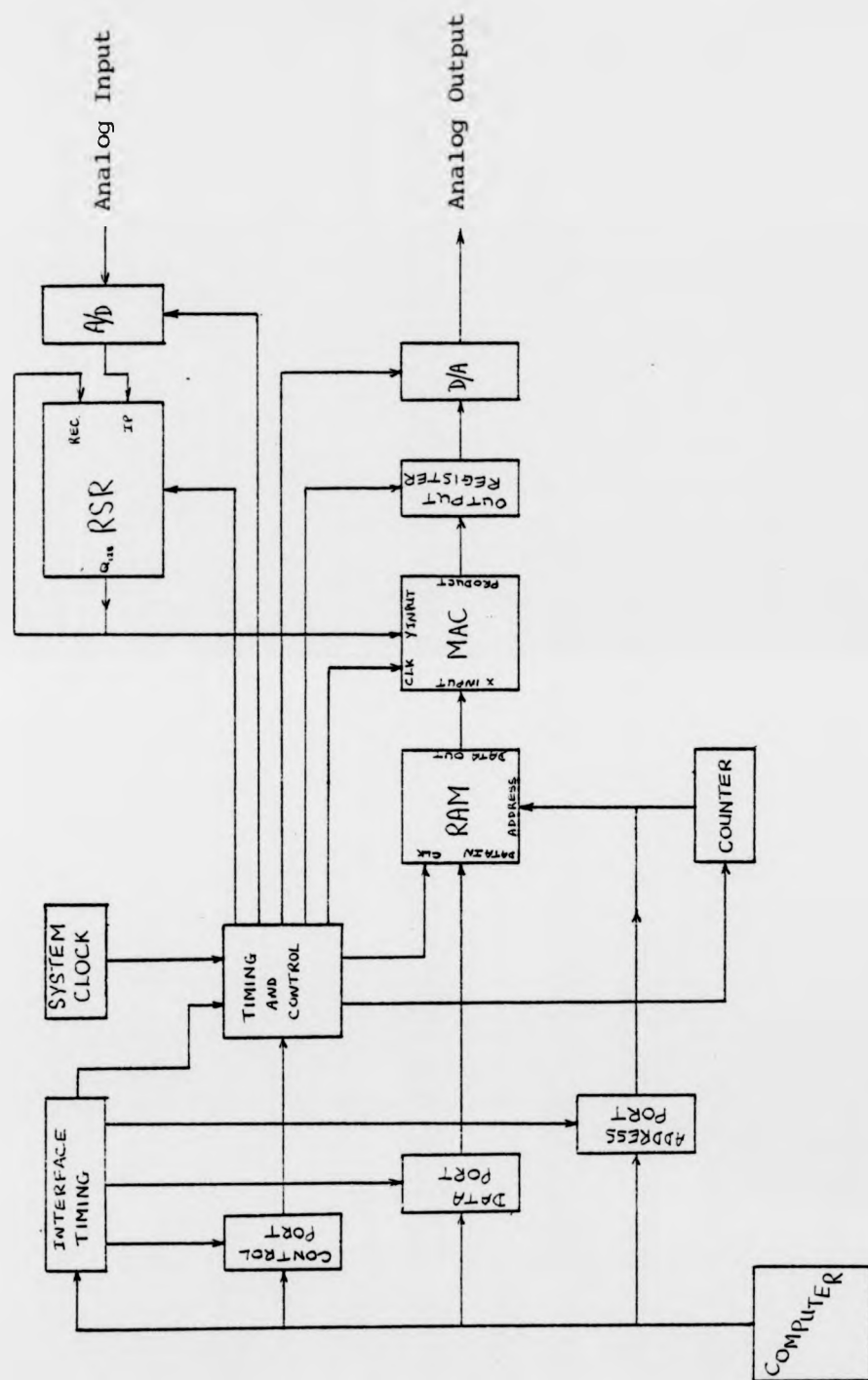
Figure 3.2: A Block Diagram of the IHS

Figure 3.3: Simplified Timing Diagram of the LHS
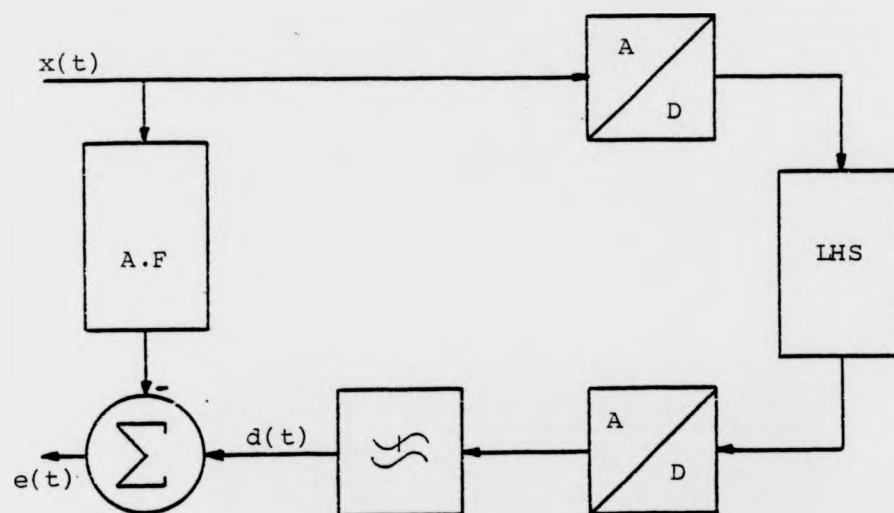
Figure 3.4:   The Analog Reconstruction
              Filter at the Output of the LHS
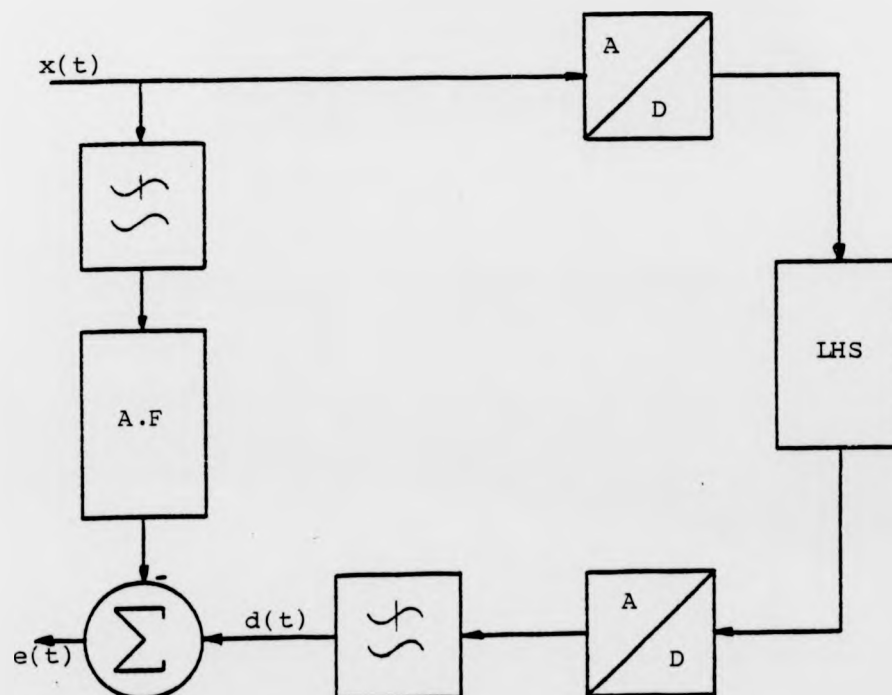
Figure 3.5:   The Use of 2 Reconstruction Filters

2dB

0 ⊢——————⊣ 1 kHz
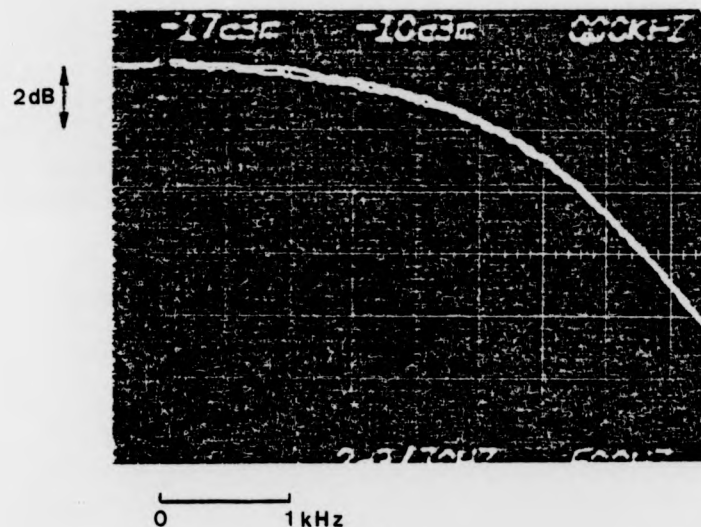
Figure 3.6: The Frequency Responses of
the Reconstruction Filters
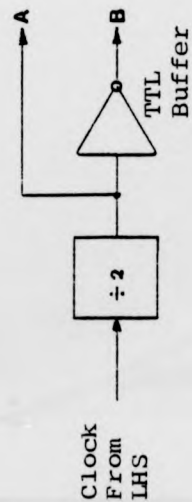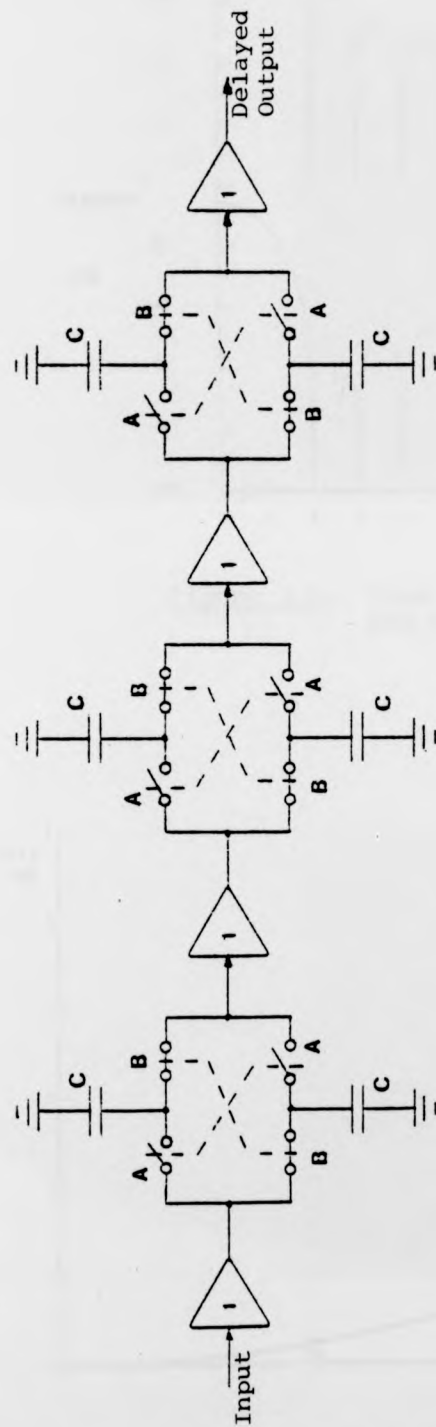
Figure 3.7: The Delay Compensation Circuit
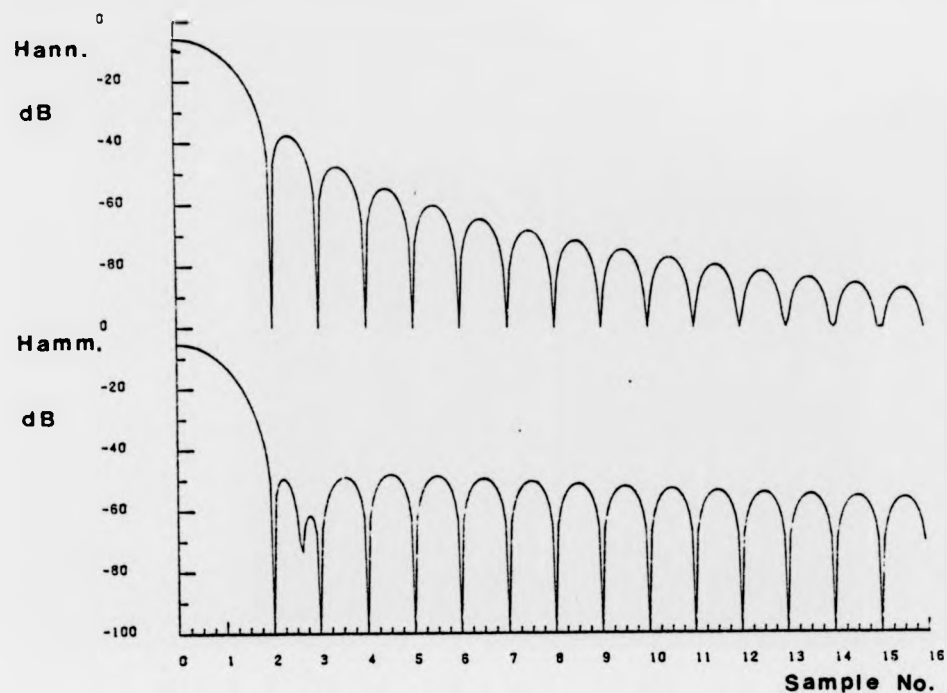
Figure 3.8:   Time Responses of the Hanning
and Hamming Frequency Windows
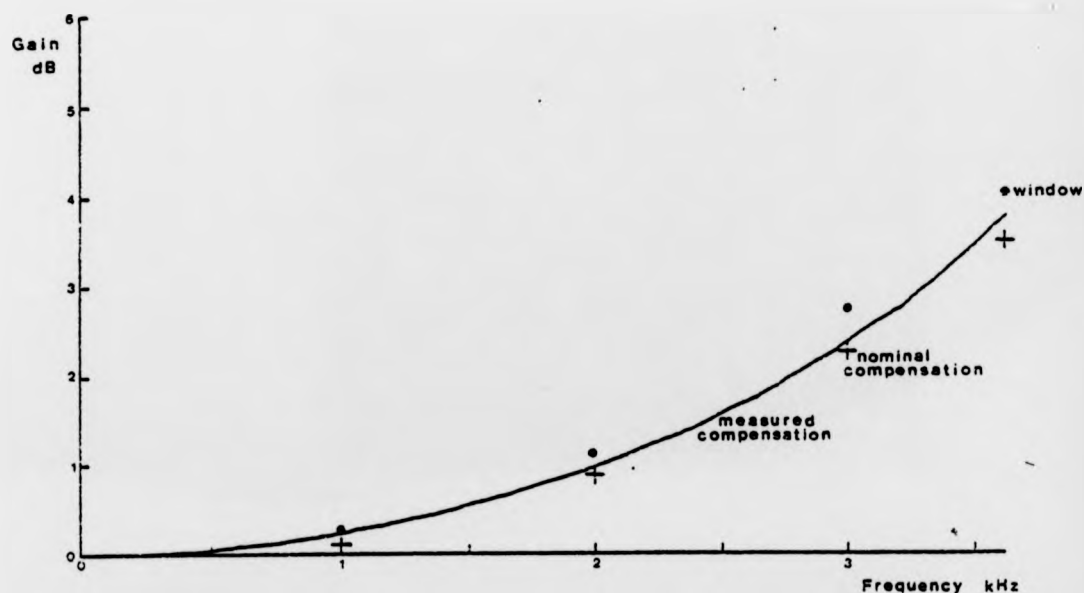
Figure 3.9:   Reciprocal of the Window "Droop" Compared
with the Response of the Compensating Filter

0 ⊢————————————⊣ 1 kHz
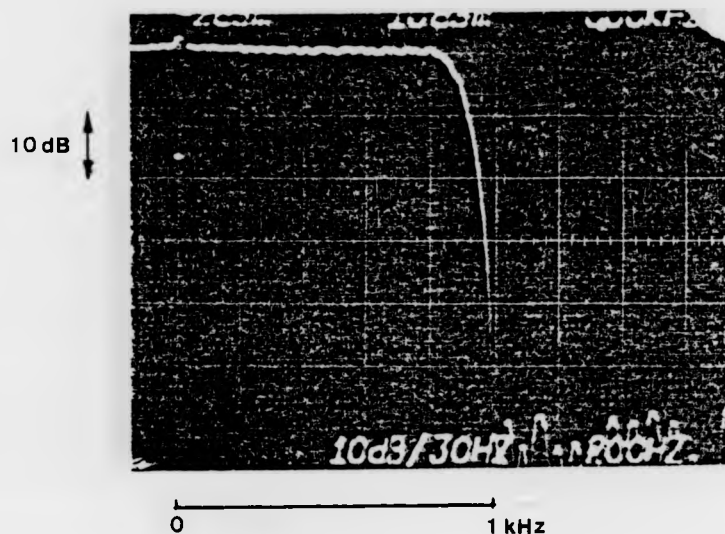
<u>Figure 3.10a</u>: Frequency Response of the Digital
Filter at 8 kHz Sampling Rate

0 ⊢————⊣ 1 kHz
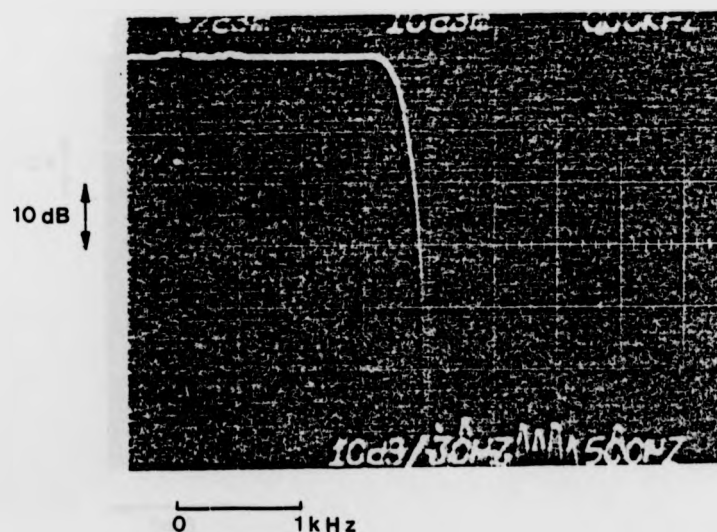
<u>Figure 3.10b</u>: Frequency Response of the Digital
Filter at 16 kHz Sampling Rate

10 dB

0   1 kHz
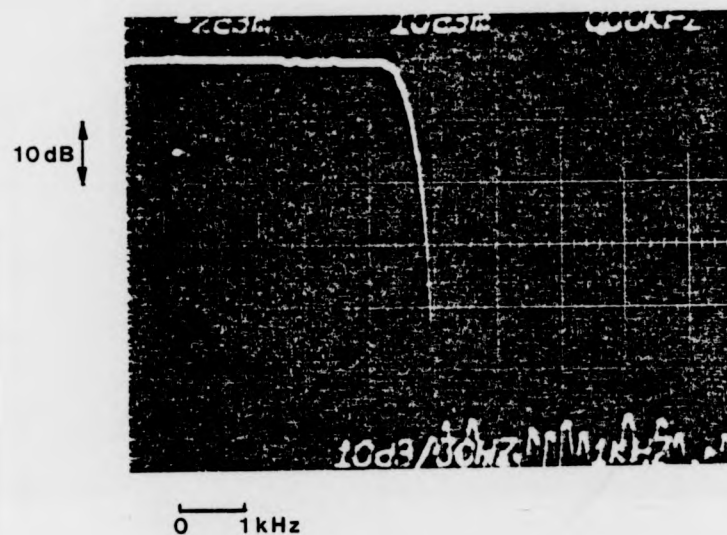
Figure 3.10c: Frequency Response of the Digital
               Filter at 32 kHz Sampling Rate

0·5V

1mS
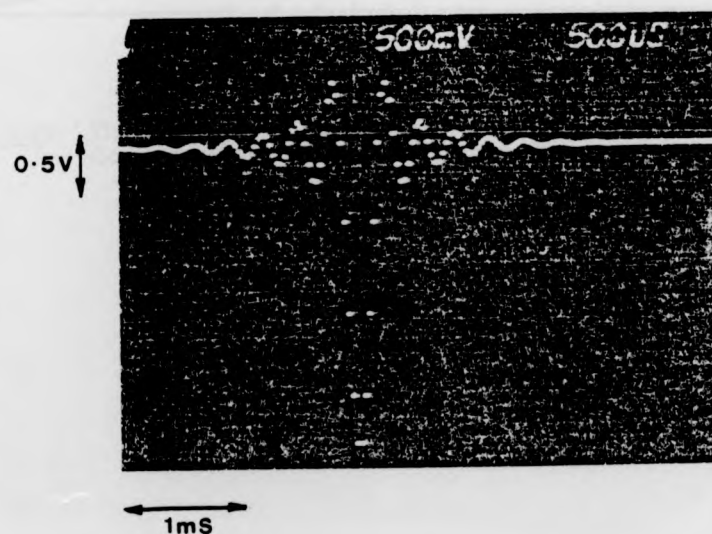
Figure 3.11: Impulse Response of the Digital
              Filter at 32 kHz Sampling Rate
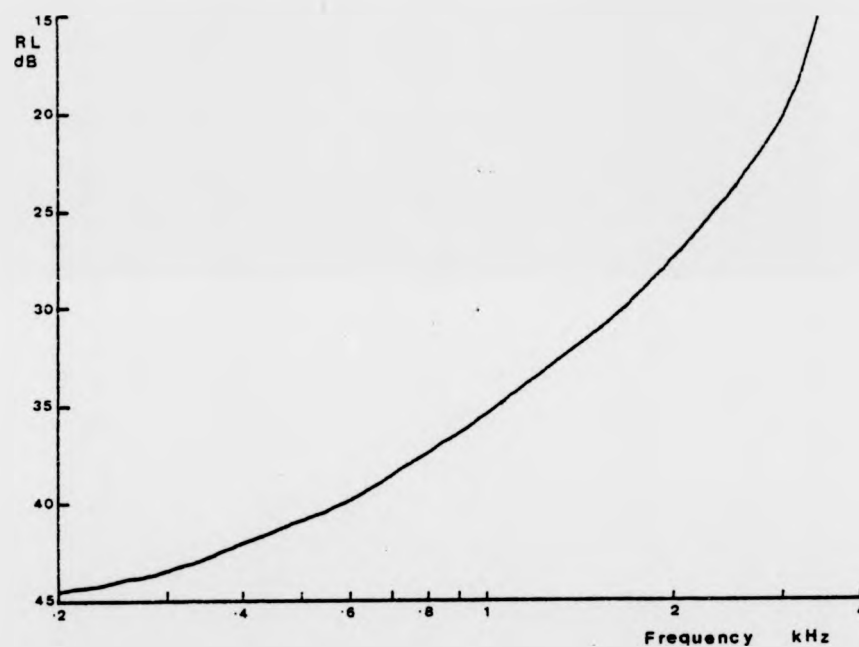
Figure 3.12: The Effect of the Phase Distortion of the Window
Compensation Circuit on the Accuracy of the LHS

Figure 3.13: Frequency Response of Simulated Test Lines
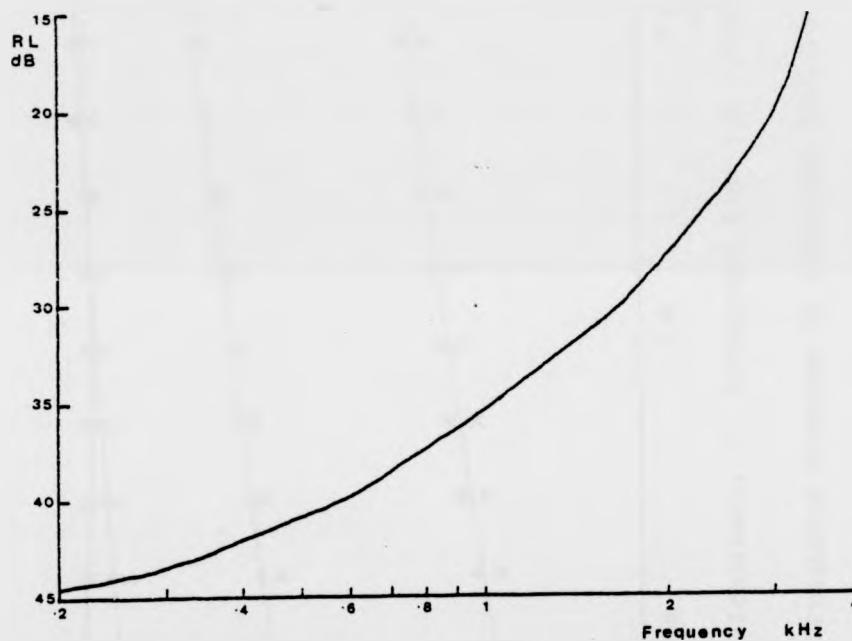
Key: Solid Line - Calculated ; x - Artificial Line ; △ - Simulator

Figure 3.12: The Effect of the Phase Distortion of the Window
Compensation Circuit on the Accuracy of the LHS

Key: Solid Line - Calculated ; x - Artificial Line ; △ - Simulator

Figure 3.13: Frequency Response of Simulated Test Lines

Figure 3.13: Frequency Response of Simulated Test Lines

Key: Solid Line - Calculated ; x - Artificial Line ; △ - Simulator
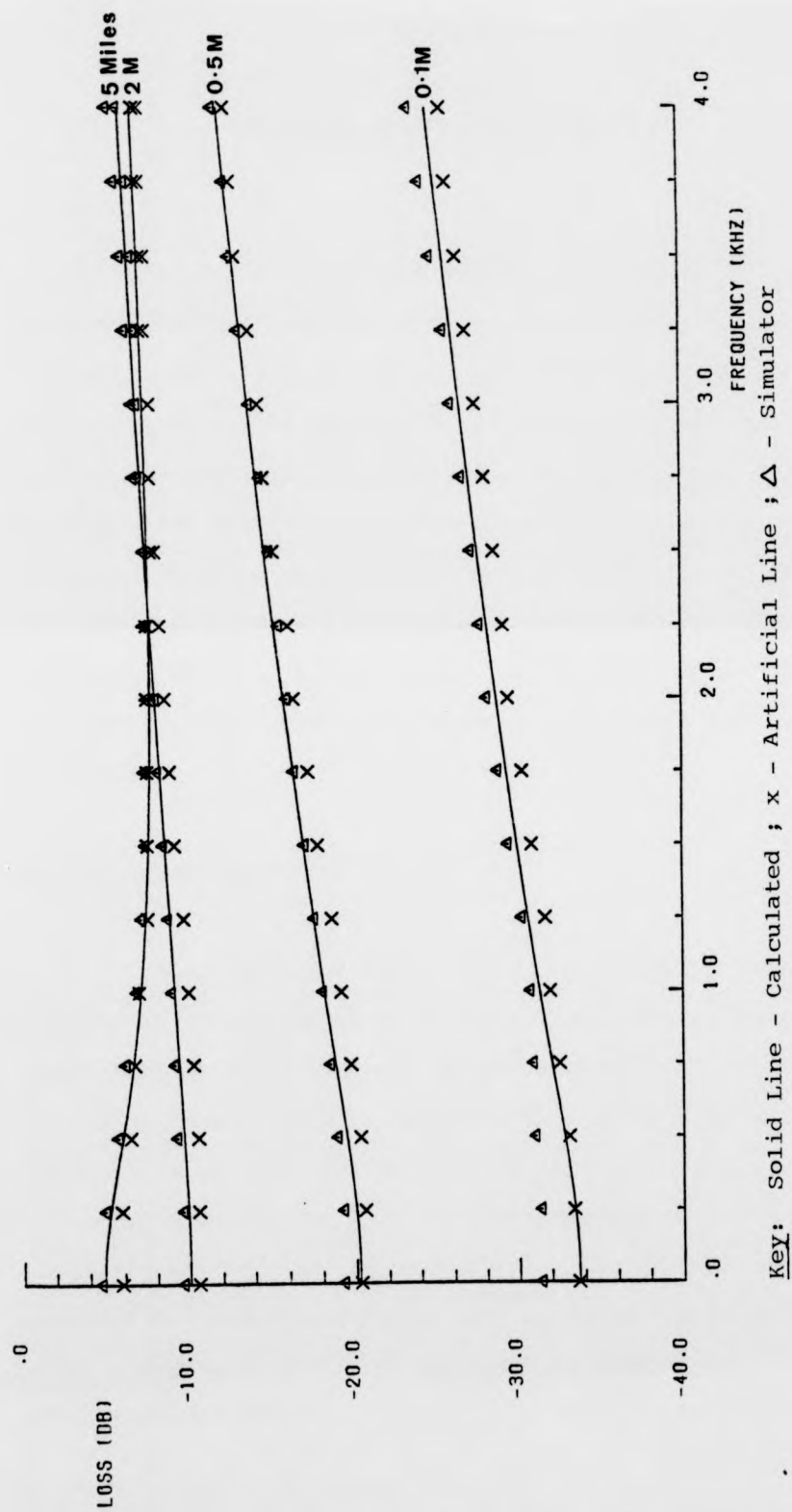
CHAPTER 4

CONTINUOUS ANALOG ADAPTIVE FILTERS

In Chapter 1 it was shown that the use of an analog unsampled adaptive filter for adaptive 2 to 4 wire conversion has a number of advantages. In Section 4.1 of this chapter the techniques and concepts to be used in the analysis and design of these filters are developed and explained. In Section 4.2 various new adaptive filter structures are investigated in terms of suitability for use in adaptive 2 to 4 wire converters and ease of implementation and adaption. In Section 4.3 a method of analysing the convergence of analog adaptive filters is developed, and the convergence properties of the most promising filter structures and algorithms are considered.

4.1 Analog Adaptive Filter Concepts

An adaptive filter with N controlling parameters, used in an adaptive 2 to 4 wire converter, is shown in Figure 4.1. The adaptive filter produces an estimate $y(t)$ of the desired signal $d(t)$, and the difference between these two signals forms an error signal $e(t)$. For best performance it is required that the adaptive filter find the particular values for its N controlling parameters which minimises some function $F[e(t)]$ of the error signal. A most useful error criterion is the mean-square error $\overline{e(t)^2}$, because this criterion can be translated directly into an equivalent frequency-domain criterion using Parseval's theorem:-

$$\overline{e(t)^2} = \int_{-\infty}^{\infty} |E(\omega)|^2 d\omega \qquad\qquad 4.1$$

Another possible error criterion, more often used in digital adaptive filtering, is the mean error magnitude $\overline{|e(t)|}$.

4.1.1 The Error Surface

As an aid in visualising the process of finding the optimum parameter values, it is useful to consider F[e(t)] as the error surface in N+1 dimensions, which gives the value of the error criterion F[e(t)] as a function of the N filter parameters, for given input signals. The problem of finding the N parameters then becomes that of finding the minimum in this error surface.

The properties of the error surface are central to the successful implementation of an adaptive filter, and some filter structures can be expected to have error surfaces more suited to adaption than others. In particular any error surface may have many minima, the smallest valued minimum being known as the global minimum, while the other minima are known as local minima. Surfaces with multiple minima are unsuitable for use with gradient or "hill-climbing" methods of finding the minimum, as there can be no guarantee that the minimum found is the global minimum, and in this sense performance would not be optimal.

Thus the most important property of the error surface is the number of minima it posesses. To find the number and positions of the minima and maxima, collectively known as stationary points, the partial derivative of the error criterion with respect to each filter parameter is equated to zero, forming a set of simultaneous equations. The solutions to this set of equations are the positions of the stationary points of the surface.

To illustrate these ideas, consider a hypothetical adaptive

filter consisting of a variable gain and a single real pole, whose position is variable, as shown in Figure 4.2. The transfer function of the filter is given by:-

$$G(\omega) = \frac{a_0}{1+j\omega b_1} \qquad \qquad 4.2$$

and the error surface is the value of the error criterion as a function of a_0 and b_1, for a given input signal. If the transhybrid response is $H(\omega)$, and the error criterion chosen is the total error power (mean-square error), then the error surface can be derived as follows:-

$$F[e(t)] = \overline{e^2(t)} = \int_{-\infty}^{\infty} |E(\omega)|^2 d\omega \qquad \qquad 4.3$$

For adaptive 2 to 4 wire conversion it is necessary only to minimise the average error power over the speech bandwidth (ω_1 to ω_2), and the limits of the integral can be set accordingly. Thus:-

$$F[e(t)] = 2\int_{\omega_1}^{\omega_2} |E(\omega)|^2 d\omega \qquad \qquad 4.4$$

For convenience the factor of 2 and the limits of integration are omitted in the remainder of this chapter. The error signal is:-

$$E(\omega) = D(\omega) - Y(\omega) = X(\omega)\{H(\omega) - a_0/(1+j\omega b_1)\}$$

and

$$|E(\omega)|^2 = |X(\omega)|^2$$
$$\frac{|H(\omega)|^2(1+\omega^2 b_1^2) + a_0^2 - a_0\{H(-\omega)(1-j\omega b_1) + H(\omega)(1+j\omega b_1)\}}{1+\omega^2 b_1^2}$$

If $H(\omega)$ is the response of a realisable system then:-

$$Re[H(\omega)] = Re[H(-\omega)]$$

and

$$Im[H(\omega)] = -Im[H(-\omega)]$$

thus:-

$$|E(\omega)|^2 = |X(\omega)|^2 \frac{|H(\omega)|^2(1+\omega^2 b_1^2)+a_0^2-2a_0\{Re[H(\omega)]-\omega b_1 Im[H(\omega)]\}}{1+\omega^2 b_1^2}$$

4.5

and the value of the error criterion is given by equation 4.4.

Equations 4.4 and 4.5 give the mean square error surface for this adaptive filter structure. The value of a_0 at the stationary point is given by the solution to the equation:-

$$\partial F[e(t)]/\partial a_0 = 0$$

Differentiating inside the integral sign, since:-

$$\frac{d}{dx}\int_B^A f(x,t)dt = \int \frac{\partial f(x,t)}{\partial x}dt + f(x,B)\frac{dB}{dx} - f(x,A)\frac{dA}{dx}$$

(Hildebrand, 1962)

gives the solution for a_0 as:-

$$a_0^* = \frac{\int \{Re[H(\omega)]-\omega b_1 Im[H(\omega)]\}|X(\omega)|^2/(1+\omega^2 b_1^2)\ d\omega}{\int |X(\omega)|^2/(1+\omega^2 b_1^2)\ d\omega}$$

4.6

This stationary point must correspond to a minimum, rather than a maximum, in the error surface, because $F(a_0)$ is quadratic and positive (equations 4.4 and 4.5), which excludes the possibility of the stationary point corresponding to a maximum of $F(a_0)$.

Equation 4.6 shows that for any given input signal, unknown system $H(\omega)$ and value of the parameter b_1, there is a single value of the parameter a_0 which minimises the mean-square error, i.e. in the parameter a_0 the error surface has a single unique minimum.

For the parameter b_1, setting $\partial F[e(t)]/\partial b_1 = 0$ gives:-

$$\int a_0 \omega |X(\omega)|^2 \{Im[H](1-b_1^2\omega^2)-b_1\omega(\ Re[H]-a_0)\}/(1+\omega^2 b_1^2)^2\ d\omega$$

$$= 0$$

4.7

This equation cannot be solved in general for the value of b_1 at the stationary point, however, because of the presence of terms in b_1^2 it is possible that there are two distinct values of b_1 which minimise the error criterion, i.e. multiple minima may exist. To further investigate the nature of the error surface, the equation of the

error contours can be derived and plotted, as explained in the next section.

4.1.2 Error Contours

For the two parameter adaptive filter, the error surface exists in three dimensions, however if the locus in the 2-parameter plane a_0, b_1 which gives a constant value of error criterion $F[e(t)]$ = E_1 is plotted, then this locus is known as the error contour for an error of E_1.   Error contours plotted for a number of distinct values of error criterion allow the shape and nature of the error surface to be accurately represented in 2 dimensions.   Thus for the adaptive filter of Figure 4.2, the error contour for a mean-square error of E_1 is obtained by solving the equation:-

$$a_0^2 \int |X(\omega)|^2/(1+\omega^2 b_1^2) \ d\omega$$

$$- 2a_0 \int |X(\omega)|^2 \{Re[H(\omega)]-\omega b_1 Im[H(\omega)]\}/(1+\omega^2 b_1^2) \ d\omega$$

$$+ \int |X(\omega)|^2 |H(\omega)|^2 d\omega \ - E_1 \ = 0 \qquad\qquad 4.8$$

for values of a_0, while b_1 is varied over a suitable range.   The error contour exists only for values of b_1 which give purely real solutions for a_0 in equation 4.8.

The shape of the error surface depends on the input signal spectrum $X(\omega)$, and if $X(\omega)$ is non-stationary, i.e. $X = X(\omega,t)$ then the error surface changes shape over time.   Since in the case of an adaptive filter used in an adaptive 2 to 4 wire converter, $X(\omega)$ is the spectrum of a speech signal, and speech can only be considered stationary over periods less than 10 mS (Rabiner and Schafer, 1978), the effects of non-stationarity cannot be ignored.   In considering error surfaces however, $X(\omega)$ is considered stationary and the effect of the movement of the surface is included in the analysis of the

adaption algorithm. The possible stationary values of the input
spectrum can be represented by the extremes:-

$$X(\omega) = \Delta(\omega \pm \omega_i) \; ; \; \text{sinusoidal input signal}$$

and

$$X(\omega) = 1 \; \text{if} \; \omega_1 < |\omega| < \omega_2$$
$$= 0 \; \text{otherwise} \; ; \; \text{wideband input signal}$$

Since the sinusoidal input case does not necessarily require matching
of the adaptive filter's response to that of the unknown system, it
can be regarded as a problem of lesser magnitude than the wideband
input case. Thus in the study of error surfaces a wideband input is
assumed. Figure 4.3 shows an example of an error contour plot for
the adaptive filter of Figure 4.2, where the unknown system is a
short circuit. For convenience the contours are evaluated as loci of
constant ERLE. The error surface can be seen to be "saddle shaped",
with a depression at the point (0,1) representing the single minimum
in the surface.

4.1.3. Reduced Error Surfaces

For adaptive filters with more than 2 controlling parameters,
the error contours can be plotted as a function of any two
parameters, while the values of the remaining parameters are
optimised. In particular any parameters in which the error surface
is quadratic can be considered to have their optimum values, without
obscuring the presence of local minima in the error surface. This
would not be the case if simple fixed cross sections of the surface
were considered. An error surface in which some quadratic parameters
have been eliminated in this manner is known as a reduced error
surface (Stearns, 1980). Error contour plots are a powerful tool in
the study of adaptive filters and extensive use will be made of such

plots in the remainder of this thesis.

4.1.4 Error Filtering

In the example of the 2 parameter adaptive filter discussed
earlier, it was seen that the presence of a denominator term
containing powers higher than 2 of the parameter b_1 contributed terms
of order greater than 1 in the expression for the error gradient.
This introduced the possibility of more than a single minimum in the
error surface.   The denominator term can be removed by filtering the
error signal by the transfer function $(1+j\omega b_1)$.   The filtered error
signal is then given by:-

$$E'(\omega) = E(\omega)(1+j\omega b_1) \qquad\qquad 4.9$$

This technique of error filtering was first suggested by Mantey
(1964), in the context of adaptive recursive digital filters.   The
equation for the filtered error criterion (filtered error power) is:-

$$F[e'(t)] = \int |X(\omega)|^2 (|H(\omega)|^2(1+\omega^2 b_1{}^2)+a_0{}^2$$
$$- 2a_0\{Re[H(\omega)]-\omega b_1 Im[H(\omega)]\}) \, d\omega \qquad\qquad 4.10$$

The positions of the stationary points of the modified error
criterion are given by:-

$$a_0{}^* = \frac{\int |X(\omega)|^2\{Re[H(\omega)]-\omega b_1 Im[H(\omega)]\} \, d\omega}{\int |X(\omega)|^2 d\omega} \qquad\qquad 4.11$$

and

$$b_1{}^* = \frac{-a_0\int \omega |X(\omega)|^2 Im[H(\omega)]d\omega}{\int |X(\omega)|^2 \omega^2 |H(\omega)|^2 d\omega} \qquad\qquad 4.12$$

Since $|E'(\omega)|^2$ is positive and quadratic in a_0 and b_1, unless $H(\omega)=0$,
then the above point $(a_0{}^*, b_1{}^*)$ represents a minimum.   When $H(\omega) = 0$
the minimum is known as a distributed minimum, since the value of b_1
is irrelevant (equation 4.10).   The effect of error filtering on the
error surface can be visualised by using the error contour plotting

technique described earlier. Figure 4.4 shows the filtered error contours for the 2 parameter adaptive filter when the unknown system is a short circuit. It can be seen by comparison with Figure 4.3 that in this case the position of the global minimum is unaltered, and that the modified error surface is quadratic in both a_0 and b_1.

4.1.4.1 The Effect of Error Filtering on the Position of the Minimum

When error filtering is used, the adaptive filter minimises the filtered error power rather than the power of the unfiltered error. In the following analysis it is shown that if the filter structure is such that the non-filtered error power can not be made zero, then the minima in the filtered and unfiltered error surfaces do not occur at the same point.

In general, for an adaptive filter with N+1 controlling parameters $a_0....a_N$, the mean square error surface can be written as:-

$$ES(a_0,....a_N) = \int |E(\omega,a_0,....a_N)|^2 d\omega$$

and the position of the minimum in the surface is given by the set of simultaneous equations:-

$$\int \frac{\partial |E(\omega,a_0,....a_N)|^2}{\partial a_k} d\omega = 0, \text{ for } k = 0,1,....N \qquad 4.13$$

The equation of the filtered error surface can be written as:-

$$ES'(a_0,....a_N) = \int |F(\omega,a_0,....a_N)|^2 |E(\omega,a_0,....a_N)|^2 d\omega$$

where $F(\omega,a_0,....a_N)$ is the error filtering function. The minimum in the filtered error surface is given by the set of simultaneous equations:-

$$\int |F(\omega,a_0,\ldots,a_N)|^2 \frac{\partial |E(\omega,a_0,\ldots,a_N)|^2}{\partial a_k} \, d\omega$$

$$+ \int |E(\omega,a_0,\ldots,a_N)|^2 \frac{\partial |F(\omega,a_0,\ldots,a_N)|^2}{\partial a_k} \, d\omega = 0 \qquad \qquad 4.14$$

for $k = 0,1,\ldots N$. For an error surface minimum which is independent
of the input signal bandwidth, the integrand of equation 4.13 must be
zero, i.e:-

$$\frac{\partial |E(\omega,a_0,\ldots,a_N)|^2}{\partial a_k} = 0$$

This condition also represents a solution in the error filtered case
only if the error power at the minimum is zero, i.e:-

$$|E(\omega,a_0,\ldots,a_N)|^2 = 0$$

since

$$\frac{\partial |F(\omega,a_0,\ldots,a_N)|^2}{\partial a_k} \neq 0 \quad \text{for all } k.$$

Thus when the adaptive filter is of sufficient order that the minimum
non-filtered error power is zero, then the position of the minimum is
unchanged by error filtering, irrespective of the input signal
bandwidth. If the adaptive filter is insufficient, then
$E(\omega,a_0,\ldots,a_N)$ evaluated at the values of a_k which are solutions to
equation 4.13 will be non-zero, and equations 4.14 and 4.13 will have
different solutions. Using error filtering thus changes the position
of the minimum in the error surface as well as changing the shape of
the error surface, if the adaptive filter is insufficient.

4.1.5 The Steepest Descent Algorithm

In the previous sections the concept of the error criterion
as a surface in N+1 dimensions (where N is the number of adaptive
filter controlling parameters) was discussed. A simple technique for

finding a minimum in a multi-variable function is the well-known steepest descent algorithm, and again the operation of the algorithm can best be understood by considering the function to be minimised as a surface. The task of the algorithm is to find a minimum in the surface. This is done by calculating (or estimating) the gradients of the error criterion with respect to each filter parameter, and adjusting the parameters in the direction of the negative gradient. Thus each parameter is adjusted in the direction which causes the error to decrease. When the gradients are all zero then no further adjustments are made, and the filter parameters are said to have converged to a minimum in the error surface.

A discrete time steepest descent algorithm for adjusting a filter parameter a_k can be written as:-

$$a_k(t+\Delta t) = a_k(t) - K \partial F[e(t)]/\partial a_k$$

where K is a step size factor and $\partial F[e(t)]/\partial a_k$ is the error gradient with respect to a_k. Rearranging and dividing by Δt gives:-

$$\frac{a_k(t+\Delta t)-a_k(t)}{\Delta t} = \frac{-K}{\Delta t} \frac{\partial F[e(t)]}{\partial a_k}$$

To obtain the continuous form of the algorithm $\Delta t \to 0$ and $K \to 0$, while $K/\Delta t \to A_k$, a constant. Thus:-

$$da_k(t)/dt = -A_k \partial F[e(t)]/\partial a_k \qquad\qquad 4.15$$

Simply expressed, the continuous time steepest descent algorithm sets the rate of change of each parameter equal to minus a constant times the error gradient for that parameter.

Solving equation 4.15 gives the required control function for the filter parameter a_k:-

$$a_k(t) = -A_k \int_{-\infty}^{t} \partial F[e(\tau)]d\tau/\partial a_k \qquad\qquad 4.16$$

It can be seen from equation 4.15 that for a given error gradient the factor A_k controls the speed of convergence of the algorithm.

A cross section of a hypothetical error surface is shown in Figure 4.5. This can be considered to be the error surface for the case when all the filter parameters except a_k are kept constant and the surface is assumed to have two minima and one maximum in a_k. Use of the steepest descent algorithm, where a_k has an initial starting point less than a_1, would cause the value of a_k to converge to the local minimum a_2, where the value of the error is greater than the error at the global minimum a_3. Successful use of the steepest descent algorithm thus requires that the error surface possess a single minimum.

For many adaptive filter structures the gradient terms required by the steepest descent algorithm may be difficult to obtain. In some cases an estimate of the gradient may be simply obtained, but if an estimate of the gradient is used then the sign of the true gradient must be preserved, in order that the parameters be adjusted in the correct direction. Similarly the gradient estimate must equal zero at the same point in the surface as the true gradient, ensuring that convergence to the same point occurs. The effect of approximating the true error gradient for the mean-square error criterion, is considered in the next section.

4.1.6 Gradient Estimates for the Steepest Descent Algorithm

The error gradient used to adapt a filter parameter a_k so as to minimise the mean-square error, using the steepest descent algorithm, is $\partial \overline{e^2}(t)/\partial a_k$. A signal which is proportional to this gradient is needed to control a_k according to equation 4.16. To produce this signal directly, a_k could be perturbed by a fixed small amount and the change in the error power would then be proportional to the required gradient. This process would involve complex

hardware, and a long period of averaging would be necessary to measure the mean error power before and after each perturbation. It is therefore of interest to devise a simplified method of estimating the error gradients, suitable for implementation in continuous analog circuitry.

In Appendix A.1 it is shown that, in an average sense, the gradient of the instantaneous error squared is equal to the gradient of the mean error squared, i.e:-

$$\overline{\partial e^2(t,a_k)/\partial a_k} = \overline{\partial e^2(t,a_k)}/\partial a_k \qquad\qquad 4.17$$

The derivation assumes that the error signal is statistically stationary, i.e. that $x(t)$ and $d(t)$ are stationary and that the loops controlling the filter parameters are open. Thus it is assumed that the filter parameters are not adjusted, i.e. that one merely wishes to know in which direction they should be adjusted out of academic interest. In Section 4.3 it will be shown that adjusting the parameters does not invalidate the gradient estimates.

The quantity on the left hand side of equation 4.17 is the average gradient of the instantaneous error squared. The process of averaging the gradient, if carried out, would considerably lengthen the time taken for the filter to adapt. A further simplification to the adaption circuits can be made by omitting the averaging indicated by equation 4.17. This can be expected to introduce noise into the gradient estimates, i.e. they will only be correct in an average sense, but the average direction in which the filter parameters are adjusted will therefore also be correct. These approximations are analogous to the standard method of approximating the error gradients in digital transversal adaptive filters (Widrow, 1966). Thus the control equation to minimise the mean-square error, for the parameter a_k, is:-

$$a_k(t) = -A_k \int_0^t e(\tau) \partial e(\tau)/\partial a_k \, d\tau \qquad\qquad 4.18$$

where the factor of 2 has been included with the constant A_k.

At a local or global minimum the average gradient estimate is zero, i.e. this gradient estimate causes the filter to converge to the same point in the error surface as the true error gradient. It will be shown in a later section that the use of this gradient estimate considerably simplifies the implementation of continuous analog adaptive filters.

In Section 4.1.1 the possibility of using the mean magnitude of the error signal as the error criterion was mentioned. Use of this criterion is of interest since it may result in simpler adaption circuits for the analog adaptive filters. Consider an adaptive filter in which it is required to minimise the mean magnitude of the error signal. In this case the true gradient is $\partial \overline{|e(t)|}/\partial a_k$ where a_k is the filter parameter to be adapted. This true gradient cannot be expressed in the frequency domain because of the non-linearity of the magnitude function, however if the approximation of equation 4.17 can be justified in this case, then an estimate for the gradient can be obtained as follows:-

$$\partial \overline{|e(t)|}/\partial a_k \approx \partial |e(t)|/\partial a_k = \text{Sgn}[e(t)]\partial e(t)/\partial a_k$$

where the averaging has been omitted. Using the steepest descent algorithm, the required control function for the a_k parameter is:-

$$a_k(t) = -A_k \int_0^t \text{Sgn}[e(\tau)]\partial e(\tau)/\partial a_k \, d\tau \qquad\qquad 4.19$$

Thus a non-linear function is introduced into the parameter control circuit in the adaptive filter, and in this case the multiplier which forms the product of equation 4.19 can be a simple polarity multiplier. In a similar manner, if only the sign of the gradient estimate were required in minimising the mean error squared, then the a_k control equation could be written as:-

$$a_k(t) = -A_k \int\limits_0^t Sgn[e(\tau)]Sgn[\partial e(\tau)/\partial a_k] \, d\tau \qquad\qquad 4.20$$

The multiplication indicated by the above equation can be performed by a simple exclusive-or type circuit, and this considerably simplifies the implementation of the circuits controlling the adaptive filter parameters. A fourth possible adaption algorithm can be formed by using a non-linear function in equation 4.18, i.e:-

$$a_k(t) = -A_k \int\limits_0^t e(\tau)Sgn[\partial e(\tau)/\partial a_k] \, d\tau \qquad\qquad 4.21$$

Use of non-linearities of the types indicated above are considered further in Section 4.3.

4.2 Adaptive Filter Structures

In Section 2.1.4 it was seen that the average input impedance of the lines in the line survey can be approximately matched by a three element network of the form of Figure 2.9. The result of Section 2.3 further showed that by using one of three balance networks of the same type, it is possible to achieve better return loss performance than that achieved by a single compromise network. These results suggest that the majority of lines are well matched by the 3-element network, and that the difficulty lies in matching all lines with a small number of such networks. In the following analysis it is shown that if the input impedance of the lines is that of a 3-element network whose values are variable, and if the balance and terminating impedances are purely resistive, then the transhybrid response consists of a variable gain, a pole and a zero, all of whose values are variable.

The transhybrid response is given by equation 2.16. Assuming Zt and Zb are resistive, and Zi is the input impedance of the 3 element network R1, R2 and C2, then the expression for the

transhybrid response is:-

$$H(s) = A \frac{\{1+(sC_2R_2(R_b-R_1)/(R_b-R_1-R_2))\}}{\{1+(sC_2R_2(R_t+R_1)/(R_t+R_1+R_2))\}}$$ 4.22

where A is a scaling factor, and H(s) has a gain, a pole and a zero, all of whose values are variable. Since the resistor values are positive, the pole is constrained to lie within the left-hand half of the s-plane, but the values of the gain and the zero can be either positive or negative.

If the terminating impedance Zt contains frequency selective components, then further poles or zeros can be introduced into H(s), but in general equation 4.22 represents the minimum complexity of the transhybrid response.

This analysis shows that an adaptive filter for use in an adaptive 2 to 4 wire converter should have a structure capable of synthesising at least a variable gain, a variable zero, and a variable pole. This result is used in the following sections as a criterion for judging the suitability of various adaptive filter structures for use in 2 to 4 wire conversion.

4.2.1 Parallel Form Adaptive Filters

Figure 4.6 shows a block diagram of an parallel form adaptive filter consisting of N+1 variable parameters $a_0....a_N$, and N frequency selective elements $G_1(s)....G_N(s)$. The transfer function of the adaptive filter can be written as:-

$$Y(s)/X(s) = a_0 + \sum_{i=1}^{N} G_i(s)a_i$$ 4.23

If the unknown system which the adaptive filter is attempting to model is H(s), then the mean square error can be written as:-

$$ES = \int |X(\omega)|^2 \{ |H(\omega)|^2 - 2Re[H(\omega)] \sum_{i=1}^{N} Re[G_i(\omega)]a_i$$

$$- 2Im[H(\omega)] \sum_{i=1}^{N} Im[G_i(\omega)]a_i + \sum_{j=1}^{N} a_j G_j(\omega) \sum_{i=1}^{N} a_i G_i(\omega) \} \, d\omega$$

ES is thus a quadratic function in all N+1 parameters, and the single unique value for each parameter which minimises ES can be found as in Section 4.1.1.

If the approximation of equation 4.17 is made then the gradient estimate becomes:-

$$\partial e^2(t)/\partial a_k = 2e(t)\partial e(t)/\partial a_k = -2e(t)g_k(t)$$

where $g_k(t)$ is the output of the kth frequency selective network. Thus the control algorithm for each filter parameter requires only a single multiplier and an integrator to produce the coefficient according to equation 4.18.

If the transfer functions $G_i(s)$ in the parallel form adaptive filter contain both poles and zeros, then the overall filter response will be capable of synthesising poles at any or all of the fixed positions of the poles of $G_i(s)$, and zeros whose positions are variable (equation 4.23). In this sense the performance of the parallel form adaptive filter is inefficient, since it would require a distinct $G_i(s)$ for each distinct pole in the transhybrid responses of all lines.

If the parallel form adaptive filter structure is used as shown in Figure 4.7 to form an adaptive 2 to 4 wire converter, then the G_is are the responses of potential dividers consisting of Z_t (the terminating impedance) and each of the N distinct balance impedances. This structure can thus have an effective balance impedance which is a linear combination of the N individual impedances. Dotter, De la Plaza et al (1980), used a parallel form adaptive filter with two distinct G_is to form an adaptive 2 to 4 wire converter, where the

filter parameters were $a_0 = \theta$ and $a_1 = 1-\theta$, and θ is a single adaption parameter. In a digital implementation it was found that 2-bit quantisation of θ gave 12 dB ERL against an artificial line, i.e. the full range of linear combinations of balance impedances was not required. Although this simplification reduces the circuit complexity required in the adaptive filter, it was shown in Chapter 2 that 3 distinct balance impedances would be necessary to achieve 12 dB minimum SRL. While this does not take account of the possibility of combinations of the 3 impedances, the restrictions on the positions of the poles in the parallel form adaptive filter makes it non-optimal for use in 2 to 4 wire conversion.

4.2.2 Series Form or Transversal Adaptive Filters

A block diagram of this type of adaptive filter structure is shown in Figure 4.8. The filter consists of cascaded networks $G_0(s)$ to $G_N(s)$ whose outputs are weighted by the filter parameters a_0 to a_N and summed to produce the adaptive filter output. The filter transfer function is:-

$$Y(s)/X(s) = \sum_{i=0}^{N} a_i \prod_{k=0}^{i} G_k(s) \qquad\qquad 4.24$$

When the the filter is used in the system identification mode, where the unknown system is $H(s)$, then the mean square error is:-

$$ES = \int |X(\omega)|^2 \{ |H(\omega)|^2 - H(\omega) \sum_{i=0}^{N} a_i \prod_{k=0}^{i} G_k(-\omega) - H(-\omega) \sum_{i=0}^{N} a_i \prod_{k=0}^{i} G_k(\omega)$$

$$+ \sum_{i=0}^{N} a_i \sum_{m=0}^{N} a_m \prod_{k=0}^{i} G_k(\omega) \prod_{l=0}^{m} G_l(-\omega) \} \, d\omega$$

The highest power of any filter parameter appearing in this equation is 2, and thus the error surface is quadratic in all parameters, irrespective of the nature of the networks $G_i(s)$. The gradient

estimates are:-

$$\partial e^2(t)/\partial a_k = 2e(t)\partial e(t)/\partial a_k = -2e(t)g_k(t) \qquad 4.25$$

where $g_k(t)$ is the output of the kth cascaded transfer function. The implementation of the steepest descent algorithm for this filter structure therefore requires a single multiplier and integrator per filter parameter.

The responses $G_k(s)$ should form an orthogonal set, so that the adaptive filter can model any possible transfer function. For example, if the cascade of networks $G_k(s)$ is replaced by a tapped delay line then an analog transversal adaptive filter results. This type of structure was first used as an echo-canceller by Sondhi (1967), although a modified algorithm was used to control the filter tap weights. Since that time all echo-cancellers have made use of the transversal filter structure, although the tapped delay line was soon superceded by the use of CCDs and later by the use of digital techniques.

Sondhi also suggested the use of tapped R-C lines to implement the $G_k(s)$ in a transversal adaptive filter. This was shown to be analagous to approximating the unknown system's impulse response by a set of Laguerre functions. Tattersall (1981), suggested the use of dispersive delay sections to replace the pure time delays used in transversal filters, avoiding the need for the pre and post-filtering associated with sampled-data techniques, and this type of network could be used to form an adaptive transversal filter. The above techniques however, all have the disadvantage of requiring very many taps to approximately synthesise a transfer function with a variable pole position.

4.2.3 All Pole Adaptive Filters

Synthesis of a transfer function containing a variable pole requires the introduction of feedback between the adaptive filter output and its input. Consider the adaptive filter structure shown in Figure 4.9, where the filter output is fed back to the input, via frequency selective elements and variable parameters, to form a recursive type filter. The transfer function of the filter is:-

$$Y(s)/X(s) = a_0/(1+b_1 s+\ldots b_N s^N) \qquad\qquad 4.26$$

and it can be seen to be capable of synthesising N poles, all of whose positions are variable. The error signal when this filter is used to model an unknown system H(s), with an input signal X(s) is:-

$$E(s) = X(s)\{H(s)-a_0/(1+b_1 s+\ldots b_N s^N)\} \qquad\qquad 4.27$$

The denominator terms in $E^2(\omega)$ ensure that the gradients of the error surface with respect to b_i contain powers of b_i other than unity, and thus that the error surface is non-quadratic. The denominator terms in $E^2(\omega)$ can be removed by considering the filtered error signal:-

$$E'(s) = (1+sc_1+\ldots s^N c_N)E(s) \qquad\qquad 4.28$$

as explained in Section 4.1.4. If $c_i = b_i$, for $i = 0,1,\ldots N$, then the filtered error surface contains at most powers of b_i of order 2, and the error surface gradients contain at most powers of b_i of order 1. Thus the filtered error surface has a single unique minimum.

In Section 4.1.4.1 it was shown that if the adaptive filter was sufficient, i.e. in this case the unknown system could be accurately modelled by an all pole filter, then the location of the minimum in the filtered error surface coincided with the location of the minimum in the non-filtered error surface.

4.2.3.1. Implementation of the Error Filtering Function

In equation 4.28 the required error filtering function is indicated as a separate transfer function $1+c_1s+c_2s^2+....+c_Ns^N$. For accurate implementation of the error filtering function, it is required that the c_i filter parameters accurately track the b_i parameters in the adaptive filter transfer function. As shown in Figure 4.10 however, the required error signal can be obtained by modifying the adaptive filter structure, i.e. the desired signal $D(s)$ rather than the output signal $Y(s)$, is fed back via the transfer function $b_1s+....b_Ns^N$. Thus the new error signal obtained in this fashion is $E'(s)$, i.e:-

$$E'(s) = D(s)\{1+\sum_{i=1}^{N}b_is^i\}-a_0X(s)$$

$$= \{1+\sum_{i=1}^{N}s^ib_i\}E(s)$$

$E'(s)$ is therefore the required filtered error signal. Figure 4.10 shows that the overall effect of this modification is that the filtered error signal is the result of subtracting a linear combination of network outputs from the desired signal $D(s)$, without feedback, i.e. the recursive adaptive filter has been transformed to the transversal type structure discussed in Section 4.2.2.

4.2.3.2 Calculation of the Filtered Error Gradients for the All Pole Filter

Using the gradient estimate of equation 4.17:-
$$\partial e'^2(t)/\partial a_0 = 2e'(t)\partial e'(t)/\partial a_0 = -2e'(t)x(t) \qquad 4.29$$

and

$$\partial e^2(t)/\partial b_i = 2e'(t)\partial e'(t)/\partial b_i = 2e'(t)g_i(t) \qquad 4.30$$

where $g_i(t)$ is the output of the ith differentiator in Figure 4.10. In the non-filtered case estimation of the error gradients requires the signal:-

$$f(t) = \frac{a_0 X(s)s^i}{(1+b_1 s+\ldots b_N s^N)^2}$$

In both filtered and unfiltered cases a multiplier and integrator is needed to adapt each filter parameter, however in the non-filtered case an additional system of a similar complexity to that of the basic filter structure is also required. Thus the use of error filtering, in addition to rendering the error surface quadratic, considerably simplifies estimation of the error gradients.

4.2.4 Pole-Zero Adaptive Filters

The all pole adaptive filter of Section 4.2.3 requires the use of perfect differentiator circuits, and it is incapable of synthesising zeros in its transfer function (equation 4.26). This drawback can be overcome by using the structure shown in Figure 4.11. The transfer function of the filter is:-

$$Y(s)/X(s) = (a_0 s^N + a_1 s^{N-1} + \ldots a_N)/(s^N + b_1 s^{N-1} + \ldots b_N) \qquad 4.31$$

Thus an adaptive filter of this form is capable of synthesising N poles and N zeros, all of whose positions are variable. The unfiltered error surface for this filter is non-quadratic in the b parameters, however the filtered error surface produced by the error filtering function:-

$$E'(s) = \{1+b_1 s^{-1} + \ldots b_N s^{-N}\}E(s) \qquad 4.32$$

is quadratic in both the b_i and the a_i parameters. This filtered error signal can be produced by modifying the filter as shown in Figure 4.12.

4.2.4.1 Filtered Error Gradients for the Pole-Zero Filter

The gradient estimates are:-

$$\partial e'^2(t)/\partial a_i = 2e'(t)\partial e'(t)/\partial a_i = -2e'(t)g_i(t) \qquad 4.33$$

and

$$\partial e'^2(t)/\partial b_i = 2e'(t)\partial e'(t)/\partial b_i = 2e'(t)f_i(t) \qquad 4.34$$

where the signals $f_i(t)$ and $g_i(t)$ are as shown in Figure 4.12. In Section 4.2 it was estimated that a filter with a single real pole and zero would provide adequate ERLE, and in the next section the behaviour of analog adaptive filters with a single real pole, and with a single real pole and zero, are studied.

4.3 Adaptive Filter Convergence

In the previous sections the filter parameters have been considered constant with time, i.e. as though the loop controlling the filter parameters were open. To investigate the transient behaviour of the adaptive filters, the filter parameters must be treated as functions of time, and the effect of the non-stationarity of the error signal on the gradient estimates cannot be neglected (see Section 4.1.6). In this section a technique for numerical analysis of the convergence of adaptive filters is presented. The technique is initially explained using the example of the adaptive gain circuit of Figure 4.13. The error signal $e(t)$ given by:-

$$e(t) = d(t)-a_0(t)x(t) \qquad 4.35$$

and the control algorithm (Section 4.2.1) is:-

$$a_0(t) = A_0\int_{-\infty}^{t} x(\tau)e(\tau)d\tau \qquad 4.36$$

where A_0 represents the control loop gain. If the initial conditions

are represented by the $a_0(0)$, then the error signal can be written as:-

$$e(t) = d(t) - x(t) \left\{ a_0(0) + A_0 \int_{0^+}^{t} x(\tau)e(\tau)d\tau \right\} \qquad 4.37$$

The value of the function $e(t)$ which is a solution to equation 4.37 fully determines the transient response of this adaptive filter for any given $d(t)$, $x(t)$ and initial condition $a_0(0)$.

Equation 4.37 is known as a Volterra integral equation of the second kind, and the solution can be obtained by using the Picard method of successive approximation (Kanwal,1971). The analytical solution is expressed in terms of an infinite series, known as the Neumann series, and the solution must be derived separately for each input signal or unknown system. Even for the simple adaptive gain filter, with a sinusoidal input signal, the derivation of an expression for the error signal is cumbersome. The successive approximation technique can however be readily implemented on a computer to provide a numerical solution for both $e(t)$ and $a_0(t)$, the adaptive gain parameter. Consider equation 4.37 , where the initial condition is $a_0(0) = 0$; if the error signal is initially estimated by $d(t)$, i.e. $e_0(t) = d(t)$, then an updated estimate for the error signal is given by:-

$$e_1(t) = d(t) - A_0 \int_0^t x(\tau)d(\tau)d\tau \qquad 4.38$$

A new estimate for $e(t)$ can now be formed using $e_1(t)$ in place of $e_0(t)$. This iteration can be repeated indefinitely, and provided that the technique converges, it will lead to an approximate solution for $e(t)$. Kanwal (1971), gives the condition for convergence as:-

$$|A_0| \sqrt{\int_0^t x^2(\tau)d\tau} < 1$$

This convergence criterion restricts the use of the iterative

technique in investigating the behaviour of adaptive filters, and it will be seen that it limits the minimum adaptive filter convergence time for which a solution for e(t) can be found, although this does not mean that no solution exists (Kanwal, 1971, p30).

To implement the numerical solution of equation 4.37, the continuous signals must be represented by their samples at discrete time intervals, and the integrals can then be represented by discrete summations.   Equation 4.37 then becomes:-

$$e(n\Delta t) = d(n\Delta t) - x(n\Delta t)\left\{a_0(0) + A_0\Delta t\sum_{i=1}^{N} x(i\Delta t)e(i\Delta t)\right\}$$

The Fortran program listing to solve this equation for $e(n\Delta t)$, and calculate the values of the samples $a_0(n\Delta t)$ is given in Appendix A.2. The input signal samples $x(i\Delta t)$ are specified as samples of a single sine wave or a sum of sine waves of random phases and specified frequencies.   The samples $d(i\Delta t)$ are calculated from $x(i\Delta t)$ by specifying an unknown system of the form:-

$$H(s) = g(1+sz)/(1+sp_1+sp_2) \tag{4.39}$$

where g, z, p_1 and p_2 are inputs to the program.   The loop gain A_0 is also an input to the program.   Iteration is terminated when the mean-square value of the difference between the k+1th approximate solution for the error and the kth solution is less than some threshold value.   Since the amplitude of the error is directly dependant on the amplitude of $d(t)$, the threshold is set at 10^{-6} times the mean-square value of $d(t)$.

The use of non-linearities in the control circuits of adaptive filters was mentioned in Section 4.1.6, however introduction of a non-linear function of the error signal or of the filtered error signal, transforms a linear equation such as equation 4.37 to a non-linear equation.   In these cases Picard iteration will not necessarily provide a solution for e(t), and indeed this is found to

be the case. Therefore the analysis of the effects of
non-linearities on the convergence of the filters is confined to
non-linear functions of the signal multiplying the error signal in
the control equations. In this section, for the adaptive gain
filter, and for the single pole and the pole-zero filters, the
effects of the following variables on the speed of filter convergence
are examined:-

1) input signal ($x(t)$) power

2) unknown signal ($d(t)$) power

3) control loop gains (A_i and B_i)

4) non-linear functions of the input signals

5) input signal band-width

6) interaction between filter parameters

7) adaptive filter insufficiency

In the results of this section no attempt is made to estimate the
convergence of the error signal, as for a multi-parameter filter the
error varies with time according to the variation of each of the
filter parameters, and is thus composed of a number of different time
constants. Attention is therefore concentrated on the time taken for
each filter parameter to converge to its optimum value.

4.3.1 Convergence of the Simple Gain Adaptive Filter

Using the linear adaption algorithm of equation 4.36, it
was found that a_0 converged exponentially to its optimum value when
the unknown system was represented by a variable gain. Figure 4.14
shows the dependence of the time constant of a_0 on the loop gain A_0
and the input signal power. It can be seen that the time constant is
linearly related to the loop gain; i.e. doubling the loop gain
decreases the time constant by a factor of 2. The time constant is

similarly dependent on the signal power, i.e. decreasing the signal power by a factor of 2 increases the time constant by a factor of 2. Figures 4.15a and b show an example of the convergence of a_0 and the error signal, for an unknown system given by $H(s) = 1$, where the input signal was a sum of sinusoids of random phases between 1 kHz and 2 kHz.

Figure 4.16 shows the dependence of the time constant of a_0 on the loop gain and the power of the input signal, when a non-linear function of the input signal is used in the adaption algorithm (equation 4.21). It can be seen that the time constant is dependent on the square root of the signal power, rather than on the power. The convergence of the circuit is therefore improved by the use of the non-linear function.

For values of A_0 and input signal power such that the time constant was less than approximately 20 mS, it was found that the Picard iteration failed to converge, and more sophisticated techniques of solution (e.g. Fredholm theory, as described in Kanwal, 1971, Ch. 4) are required.

The speed of convergence of the simple gain filter was found to be independent of the bandwidth of the input signal, and also of the power of the desired signal.

4.3.2 Convergence of the Single Pole Adaptive Filter

Figure 4.17 shows a block diagram of a first order all pole adaptive filter, with error filtering and circuitry to adapt the filter parameters a_0 and b_1, as explained in Section 4.2.3. The filtered error signal can be written as:-

$$e'(t) = d(t) + b_1(t)f(t) - a_0(t)x(t)$$

The parameter control equations, using the steepest descent

algorithm, are:-

$$a_0(t) = A_0 \int_{-\infty}^{t} x(\tau)e'(\tau)d\tau$$

$$b_1(t) = -B_1 \int_{-\infty}^{t} f(\tau)e'(\tau)d\tau$$

where A_0 represents the total a_0 control loop gain, and B_1 represents the total b_1 control loop gain. Convergence of a_0 and b_1 is broadly in accordance with the results of the previous section, i.e. the time constant of each filter parameter is dependent on the product of the power of the signal driving its control loop and the loop gain. This underlying relationship is however complicated by the fact that the unknown signal ($d(t)$), filtered by the differentiator transfer function, drives the b_1 control loop (Figure 4.17). Convergence of the b_1 parameter is therefore dependent both on the power of the unknown signal, and its frequency/bandwidth. A further complication is the interdependence of the parameter values, since the optimum value for one parameter is dependent on the value of the other, as shown by equations 4.11 and 4.12.

The dependence of the convergence of the b_1 parameter on the power and bandwidth of the $d(t)$ signal is verified by the results shown in Table 4.1. In the first 4 rows the input signal is a sum of sine waves of random phases between 500 Hz and 2.5 kHz, while in the 5th row the bandwidth is reduced to 500 Hz to 1.5 kHz. Comparing rows 1, 2 and 3, it can be seen that reducing the power of $d(t)$ by a factor of 4 (by introducing attenuation of 0.5 in the unknown system transfer function), has the same effect as reducing the loop gain B_1 by a factor of 4. Comparing rows 1 and 3 however, shows that the effect of reduced $d(t)$ power on the time constants of the parameters in not clear, since the a_0 time constant increases by a factor of

approximately 1.6, while the b_1 time constant increases by a factor of 2.7. Comparing rows 2 and 4, the effect of the reduction in $d(t)$ power is more predictable, since the b_1 time constant increases very approximately by a factor of 4. The fact that the expected relationship holds approximately only when the a_0 time constant is much shorter than the b_1 time constant, indicates that this anomalous behaviour is due to the interdependence of the parameters. This effect can be examined in more detail by plotting the paths of the filter parameter values as functions of time, on the error contour plot for the given input signal and unknown system. The plot corresponding to the conditions of rows 1 and 2 is shown in Figure 4.18. Curve 1 shows the behaviour of the parameters for loop gains $A_0 = 480$ and $B_1 = 10$. It can be seen that a_0 initially converges to a value which is optimum for a near zero value of b_1. Once this has occurred a_0 maintains an optimum value as b_1 converges slowly to the optimum in the error surface (at point $a_0 = 1$, $b_1 = 0.25$). Curve 2 shows the situation with $A_0 = 480$, $B_1 = 80$, and in this case a_0 and b_1 are always close to their optimum values, i.e. curve 2 tends to join the points on each error contour closest to the starting point. This occurs when the loop gains are in inverse proportion to the powers of the signals driving the control loops, i.e:-

$$\frac{A_0}{B_1} = \frac{\overline{f(t)^2}}{\overline{x(t)^2}}$$

Curve 3 shows the behaviour of a_0 and b_1 for loop gains $a_0 = 120$, $B_1 = 80$. In this case, for given values of b_1, the values of a_0 are non-optimal.

By allowing a_0 to adapt much more quickly than b_1, as in curve 1, the convergence of b_1 is essentially independent of a_0, and in this case b_1 convergence is directly dependent on the power of the signal driving its control loop, i.e. the filter parameters have been

uncoupled, allowing the factors governing the speed of convergence of b_1 to be investigated.

Figure 4.19 shows the effect of reducing the input signal bandwidth to 500 Hz to 1.5 kHz, and it can be seen that the orientation of the error surface has changed, i.e. the semi-major axis of the elliptical contours is inclined closer towards the horizontal. This has the effect that the value of ERLE is less sensitive to the value of b_1, and this reduces the interdependence between the parameters. Reduction in coupling between the parameters is desirable, since ideally each parameter adapts directly towards the global minimum, without adapting to minimise the error due to a temporary non-ideal value of another parameter. The reduction in coupling between the parameters evident in Figure 4.19 can be simply explained by the observation that the lower the frequency, the smaller the amplitude of the differentiator output, and the less critical the value of b_1. Thus although in row 5 of Table 4.3 the power in the signal driving the b_1 control loop is increased slightly above that of row 2, the time constant of the a_0 parameter is shortened, while that of b_1 remains approximately the same.

The effect of using the non-linear algorithm with the single pole adaptive filter is to make the convergence time of each parameter dependent on the square-root of the power of the signal driving its control loop, as was found in the case of the simple gain adaptive filter.

The effect of insufficiency on the single pole adaptive filter can be examined by using a non-zero value of p_2 in the transfer function of the unknown system. In this case the unknown system is of the 2nd order, and by gradually increasing p_2, its response changes from overdamped towards underdamped, and the resonant frequency decreases. Thus if p_2 is near zero, the unknown

uncoupled, allowing the factors governing the speed of convergence of b_1 to be investigated.

Figure 4.19 shows the effect of reducing the input signal bandwidth to 500 Hz to 1.5 kHz, and it can be seen that the orientation of the error surface has changed, i.e. the semi-major axis of the elliptical contours is inclined closer towards the horizontal. This has the effect that the value of ERLE is less sensitive to the value of b_1, and this reduces the interdependence between the parameters. Reduction in coupling between the parameters is desirable, since ideally each parameter adapts directly towards the global minimum, without adapting to minimise the error due to a temporary non-ideal value of another parameter. The reduction in coupling between the parameters evident in Figure 4.19 can be simply explained by the observation that the lower the frequency, the smaller the amplitude of the differentiator output, and the less critical the value of b_1. Thus although in row 5 of Table 4.3 the power in the signal driving the b_1 control loop is increased slightly above that of row 2, the time constant of the a_0 parameter is shortened, while that of b_1 remains approximately the same.

The effect of using the non-linear algorithm with the single pole adaptive filter is to make the convergence time of each parameter dependent on the square-root of the power of the signal driving its control loop, as was found in the case of the simple gain adaptive filter.

The effect of insufficiency on the single pole adaptive filter can be examined by using a non-zero value of p_2 in the transfer function of the unknown system. In this case the unknown system is of the 2nd order, and by gradually increasing p_2, its response changes from overdamped towards underdamped, and the resonant frequency decreases. Thus if p_2 is near zero, the unknown

system can be approximately matched by a single real pole, and increasing p_2 increases the degree of insufficiency of the adaptive filter.

Figure 4.20a shows the adaptive filter adapting against an unknown system given by $g = 1$, $z = 0$, $p_1 = 10^{-4}$ and $p_2 = 10^{-9}$, while in Figure 4.21 p_2 is increased to $5*10^{-9}$. These correspond to 2nd order systems given by $f_0 = 5.0$ kHz and $\zeta = 1.6$ and $f_0 = 2.3$ kHz, $\zeta = 0.707$ (Figure 4.21). In both cases the input signal consists of 10 sine waves of random phases evenly spaced between 500 Hz and 2.5 kHz. Figure 4.20a shows both the filtered error contours (solid lines), and the non-filtered contours (dashed lines), and it is evident that the optimum parameter values are the same in both cases ($a_0 = 1$, $b_1 = 0.25$). The path of the values of a_0 and b_1 on the error surface, for loop gains $A_0 = 480$, $B_1 = 80$ are also shown, where the '*'s on the path represent 16 mS intervals. Greater than 15 dB ERLE is achieved within 64 mS and Figures 4.20b and c show the values of a_0 and b_1 against time. In Figure 4.21a the depth of the minimum in the filtered error surface is less than 9 dB, whereas in the non-filtered case at least 12 dB ERLE is possible. The path of a_0 and b_1 on the error surface is also shown, and it can be seen that the adaption algorithm performs considerably worse than in Figure 4.20a. The values of a_0 and b_1 against time are shown in Figures 4.21b and c respectively. In this case it is not clear whether the algorithm converges slowly to the shallow minimum in the filtered surface, or whether it has failed to locate even this minimum.

In other experiments with insufficient single pole adaptive filters it has been found that the effect of error filtering is first to decrease the depth of the minimum in the filtered error surface, and that as the amount of insufficiency is increased, the location of the minimum in the non-filtered surface moves away from that in the

filtered error surface.

4.3.3 Convergence of the Pole-Zero Adaptive Filter

In Figure 4.22 a first order pole-zero adaptive filter, with error filtering and adaption circuitry is shown. The equation for the filtered error signal is:-

$$e'(t) = d(t) + b_1 f(t) - a_0 x(t) - a_1 g(t)$$

and the parameter control equations, using the steepest descent algorithm to minimise the mean square filtered error, are:-

$$a_0(t) = A_0 \int_{-\infty}^{t} x(\tau) e'(\tau) d\tau$$

$$a_1(t) = A_1 \int_{-\infty}^{t} g(\tau) e'(\tau) d\tau$$

$$b_0(t) = -B_0 \int_{-\infty}^{t} f(\tau) e'(\tau) d\tau$$

These equations are solved as in the previous sections.

In investigating the convergence of the pole-zero adaptive filter, it was first verified that convergence of each parameter is dependent on the product of the loop gain and the power of the signal driving the control loop. As a consequence of the use of integrators as the frequency selective elements in the filter, the convergence times of a_1 and b_1 are frequency dependent. Investigation of the convergence of the pole-zero filter then concentrated on the properties particular to this type of filter.

Since the first order pole-zero adaptive filter has 3 adaptive parameters, the error surface cannot easily be visualised, and the reduced error contours described in Section 4.1.3. must be used. This presents problems in plotting the paths of the filter

parameters, since each contour plot assumes that one parameter is optimised, whereas the parameter values are calculated assuming only that all initial conditions are zero. This problem can be alleviated to some extent in the case of the filter adapting against simple gain circuits by setting the loop gains A_1 and B_1 to zero, thus ensuring that a_1 and b_1 are always zero. Although this gives an unrealistic impression of the behaviour of the filter, it ensures that the parameter path is consistent with the contour values, and allows some insight into the performance of the filter to be gained.

Figures 4.23a and b show the reduced error contour plots $ES(a_0,b_1)$ evaluated at $a_1 = a_{1optimum}$ and $ES(a_1,b_1)$ at $a_0 = a_{0optimum}$ respectively, when the pole-zero filter of Figure 4.22 adapts against an unknown system consisting of a gain of 0.5, where the input is a sum of sine waves between 500 Hz and 2.5 kHz. Both the filtered (solid lines) and the unfiltered (dashed lines) error surfaces have a distributed minimum given by; $a_0 = 0.5$ and $a_1 = 0.5*b_1$. Convergence of a_0 to its optimum value is shown in Figure 4.23a, where each '*' indicates an 8 mS interval in time. This speed of convergence is however unrealistic, since in a real situation a_1 and b_1 would not initially be optimum.

Figures 4.24a and b show the reduced error contour plots when the filter is attempting to match a system given by $g = 1$, $z = 0$, $p_1 = 10^{-4}$ and $p_2 = 0$, with the same input as that of Figure 4.23. In this case the error surfaces, both filtered and unfiltered, have single unique minima at $a_0 = 0$, $a_1 = b_1 = 1$. In both Figures 4.24a and b the semi-major axis of the contours is not horizontal, and thus the optimum values of the parameters are all interdependent. A consequence of this is shown by plotting the path of the a_1 and b_1 parameters (with $A_0 = 0$, and thus $a_0 = 0$) on Figure 4.24a, where it is evident that the slow convergence of either parameter retards the

convergence of the other.

Figures 4.25a and b show the effect of increasing the bandwidth of the input to the band 2 kHz to 3 kHz. In this case the minimum in the surface has become more like a distributed minimum, i.e. the error, both filtered and unfiltered, is relatively insensitive to the absolute value of b_1, as long as the ratio between b_1 and a_1 remains the same. This occurs because the power in the d(t) signal is reduced as the frequency of the input is increased above the cutoff frequency of the unknown system. The filter posesses sufficient "degrees of freedom" in this case, so that using only a_0 and a_1, with $b_1 = 0$, over 15 dB ERLE can be achieved.

The effect of changing the input signal to a single 500 Hz sine wave is shown in Figures 4.26a and b. In this case the filter again possesses sufficient degrees of freedom, because it is unnecessary to match exactly the unknown system, instead the error can be reduced by merely matching the signal d(t) in amplitude and phase. Thus the minimum has become distributed in nature, requiring only the correct ratios between parameters rather than correct absolute values. This condition has been termed "insufficient input richness" (Johnson and Larimore, 1977)

The effect of insufficiency on the pole-zero adaptive filter is shown in Figures 4.27 to 4.29. In each case the unknown system is specified as a second order system, and in Figure 4.27 the resonant frequency (f_0) is 5 kHz, decreasing in steps for Figures 4.28 and 4.29. The damping factor for Figure 4.27 is 1.6, and this also decreases for the other figures. The input signal consists of a sum of sine waves with random phases, evenly spaced between 500 Hz and 2.5 kHz. If p_2 were zero, the position of the minimum in both the filtered and the unfiltered error surfaces would be; $a_0 = 0$, $a_1 = 1$ and $b_1 = 1$. Thus Figures 4.27a and b show that the minimum in both

filtered and unfiltered surfaces has moved in the direction of increasing b_1 and decreasing a_0, but the depth of the minimum does not appear to be substantially decreased. While the pole-zero filter is unable to introduce a second pole to match the unknown system, it can keep the error small by increasing b_1 and decreasing a_0 below 0, so that a transmission zero is introduced into the left-hand half s-plane. The values of a_1 and b_1 with $a_0 = 0$, for loop gains $A_0 = 0$, $A_1 = 250$ and $B_1 = 250$, are shown in Figure 4.27, however the parameter values are not consistent with the contours, since the optimum value for a_0 is not zero for the insufficient case. In Figures 4.28a and b the amount of insufficiency is further increased, since $f_0 = 2.25$ kHz and $\zeta = 0.707$. In this case the depth of the filtered error minimum has begun to decrease, although both the filtered and unfiltered surfaces have the same minimum. The position of this minimum has moved further in the direction of increasing b_1 and decreasing a_0, and also begun to move in the direction of increasing a_1. The minimum in both surfaces is approximately given by; $a_0 = -0.4$, $a_1 = 1.25$ and $b_1 = 1.15$. Figures 4.29a and b show an example of extreme insufficiency, where $f_0 = 1.6$ kHz and $\zeta = 0.5$. The minimum in the unfiltered error surface now occurs at; $a_0 = -0.4$, $a_1 = 0.9$ and $b_1 = 0.75$, while for the unfiltered error surface the value of b_1 is somewhat higher. The maximum ERLE attainable in the filtered case is less than 9 dB, while for the unfiltered error at least 11 dB is possible.

The performance of the first order pole-zero adaptive filter against systems of order higher than 1 is substantially better than that of the single pole adaptive filter. This is due to the additional degree of freedom introduced by the third filter parameter, which can compensate to some extent for the insufficient order of the filter.

4.4 State Variable Description of Adaptive Filters

In the previous section a method of analysing the convergence of analog adaptive filters was developed. This method was seen to fail when the filters converged at high speed. In this section an alternative method of analysis is discussed, initially with reference to the example of the adaptive gain circuit of Figure 4.13.

The response of an adaptive filter can be uniquely described by the values of its filter parameters at any time. It would thus seem apt to consider the filter parameters as state variables, and use the techniques of state variable analysis to investigate the convergence of the filters. The rate of change of a_0 can be derived from equation 4.36 as:-

$$da_0/dt = A_0 x(t)e(t)$$

and substituting for $e(t)$ gives:-

$$da_0/dt + A_0 a_0(t)x^2(t) - A_0 x(t)d(t) = 0 \qquad\qquad 4.40$$

Equation 4.40 is a first order linear differential equation describing the transient behaviour of the parameter a_0 (the state variable) for any input signal, unknown system output and loop gain. The general solution to equation 4.40 can be obtained by the integrating factor technique (Kreyszig, 1967), however if $d(t) = \alpha x(t)$, the equation is separable and the solution is:-

$$a_0(t) = \alpha\{1-\text{Exp}(-A_0\int_0^t x^2(\tau)d\tau)\} + a_0(0)\text{Exp}(-A_0\int_0^t x^2(\tau)d\tau)$$

where $a_0(0)$ is the initial condition.

Since the function $\int x^2(\tau)d\tau$ is positive, it can be seen that the filter parameter $a_0(t)$ converges to the optimum value α, and that the speed of convergence is proportional to the product of the loop gain and the power in the input signal. This result confirms those of Section 4.3, and in particular shows that the non-convergence of

the iterative technique described earlier does not indicate a
theoretical limit on the speed of convergence of the filter.

For the single pole adaptive filter the equations governing
the behaviour of the a_0 and b_1 parameters can be derived in a similar
manner:-

$$da_0(t)/dt + a_0(t)A_0x^2(t) - b_1(t)A_0x(t)f(t) - A_0x(t)d(t) = 0 \qquad 4.41$$

$$db_1(t)/dt + b_1(t)B_1f^2(t) - a_0(t)B_1f(t)x(t) + B_1f(t)d(t) = 0 \qquad 4.42$$

Equations 4.41 and 4.42 are simultaneous (or coupled) first order
linear differential equations, and they can be written in
state-variable notation as:-

$$\dot{X}(t) = A(t)X(t) + D(t)M(t) \qquad 4.43$$

where:-

$$X(t) = \begin{bmatrix} a_0(t) \\ b_1(t) \end{bmatrix} ; \text{ the state variable matrix}$$

$$A(t) = \begin{bmatrix} A_0x^2(t) & -A_0x(t)f(t) \\ -B_1f(t)x(t) & B_1f^2(t) \end{bmatrix} ; \text{the coefficient matrix}$$

$$D(t) = \begin{bmatrix} -A_0x(t) \\ B_1f(t) \end{bmatrix} ; \text{ the transfer matrix}$$

and

$M(t) = d(t)$; the input matrix, in this case a scalar
The input-output equation for the system is:-

$$e'(t) = BX + HM \qquad 4.44$$

where:-

$$B = \begin{bmatrix} -x(t) & f(t) \end{bmatrix} ; \text{ the output matrix}$$

$H = I$; the identity matrix

Similarly the pole zero adaptive filter can be described by
equations 4.43 and 4.44, where:-

$$X(t) = \begin{bmatrix} a_0(t) \\ a_1(t) \\ -b_1(t) \end{bmatrix}$$

$$A(t) = \begin{bmatrix} A_0 x^2(t) & A_0 x(t)g(t) & -A_0 x(t)f(t) \\ A_1 g(t)x(t) & A_1 g^2(t) & -A_1 g(t)x(t) \\ -B_1 f(t)x(t) & -B_1 g(t)f(t) & B_1 f^2(t) \end{bmatrix}$$

$$D(t) = \begin{bmatrix} -A_0 x(t) \\ -A_1 g(t) \\ B_1 f(t) \end{bmatrix}$$

$$B = \begin{bmatrix} -x(t) & -g(t) & f(t) \end{bmatrix}$$

$$H = I$$

$$M = d(t)$$

Thus in general the investigation of the convergence of adaptive filters using state variable techniques, involves the solution of equations of the form of equation 4.43.

The theory of state variables deals mainly with systems where $A(t)$ and $D(t)$ are constant matrices, and in these cases the solutions for $X(t)$ can be found by solving a transformed set of simultaneous algebraic equations in the s-domain. This is not possible where the system being described has a time varying response, however Tou (1964) gives the general solution for equation 4.43 as:-

$$X(t) = \phi(t,t_0)X(t_0) + \int_t^{t_0} \phi(t,\tau)\{D(\tau)M(\tau)\}d\tau$$

where $\phi(t,t_0)$ is the state transition matrix. The author adds that in general, however, no closed form expression for $\phi(t,t_0)$ exists.

A possible approach to the solution of equations of the form of equation 4.43, for particular input signals, would be to

diagonalise the matrix A by a suitable linear transformation, and thus produce a set of independent first order differential equations which could be solved by conventional methods. This type of technique was used by Widrow (1966) in a comprehensive analysis of the convergence of adaptive transversal sampled data filters. It is felt however, that the iterative technique described in Section 4.3 has the advantage of being considerably simpler and more general, although its convergence is not guaranteed.

Unknown System		Optimum		Power of d(t)	Loop Gains		Time Const	
G	P_1	a_0	b_1		A_0	B_1	t_{a0}	t_{b1}
1.0	10^{-4}	1.0	0.25	.117	480	80	26.2	32.1
1.0	10^{-4}	1.0	0.25	.117	480	20	43.5	88.9
0.5	10^{-4}	0.5	0.25	.03	480	80	43.5	88.9
0.5	10^{-4}	0.5	0.25	.03	480	20	60.7	325.5
1.0	10^{-4}	1.0	0.25	.15	480	20	35.4	87.7

Table 4.1 Convergence of the Single Pole Adaptive Filter using the

Linear Adaption Algorithm

Figure 4.1: An Adaptive Hybrid Using an N-Parameter Adaptive Filter
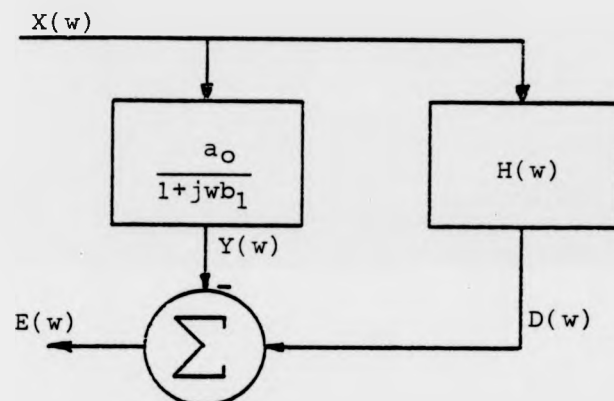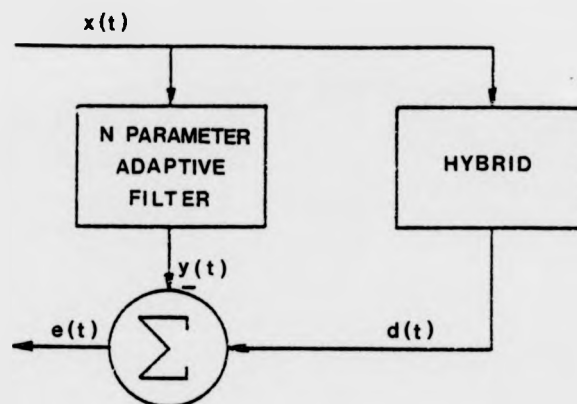
Figure 4.2: A Simple Adaptive Filter
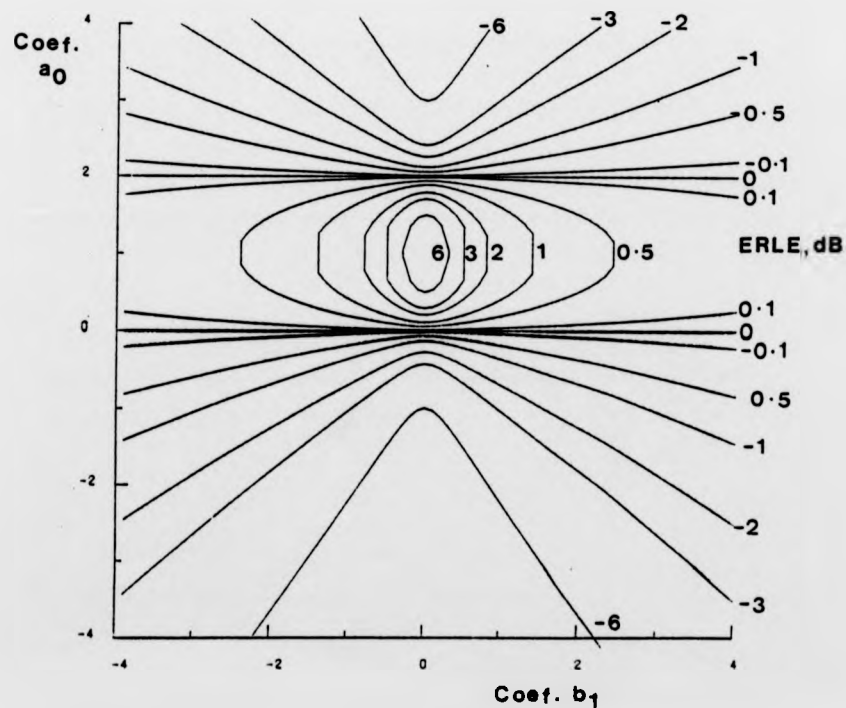
Figure 4.3: An Error Contour Plot for the Simple Adaptive Filter
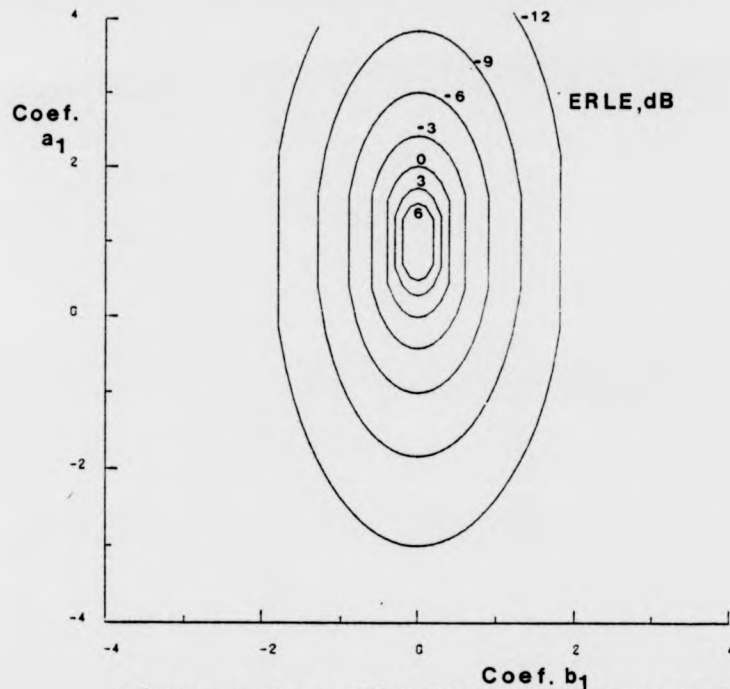
Figure 4.4: A Filtered Error Contour Plot for the Simple Adaptive Filter
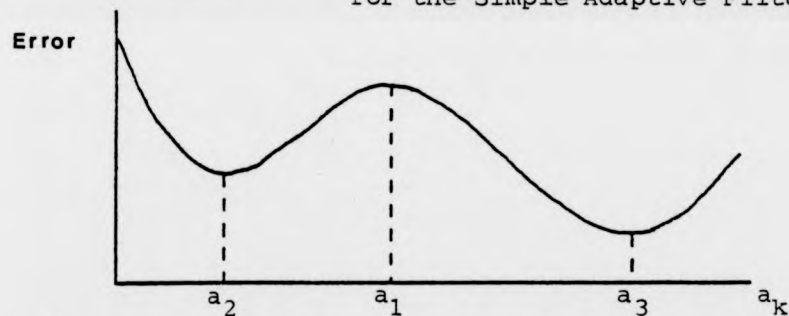
Figure 4.5: An Example of a Curve with Multiple Minima
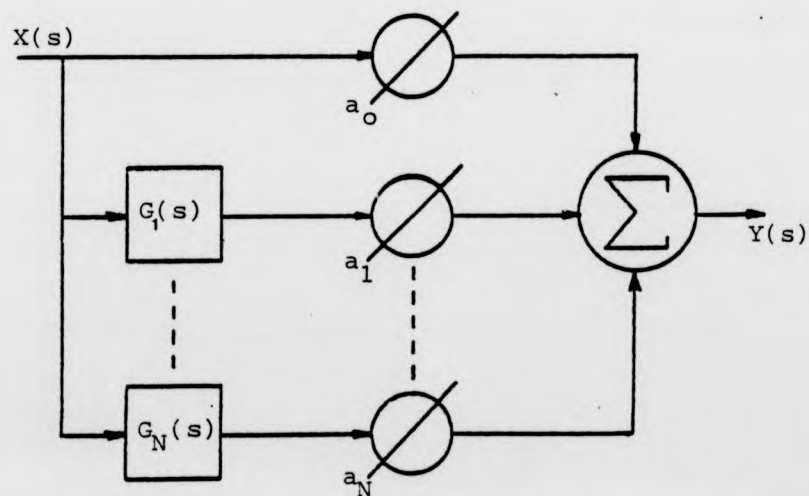
Figure 4.6: The Parallel Form Adaptive Filter
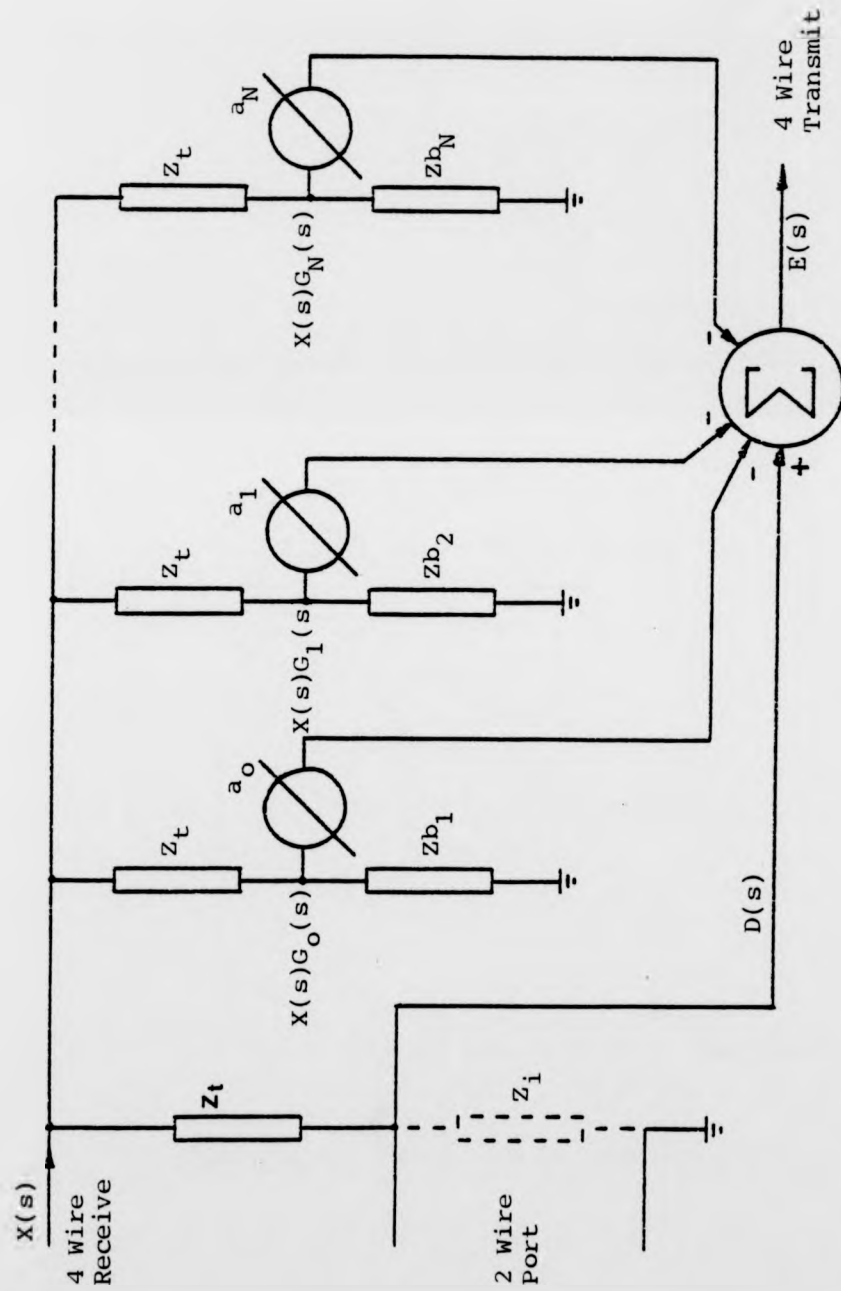
Figure 4.7: Adaptive Balancing Hybrid Using the Parallel Form Adaptive Filter
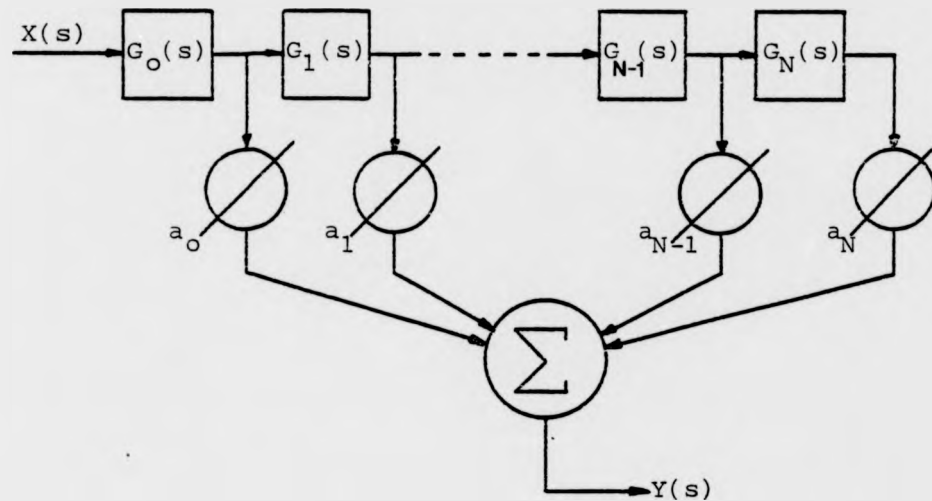
Figure 4.8: Series Form or Transversal Adaptive Filter
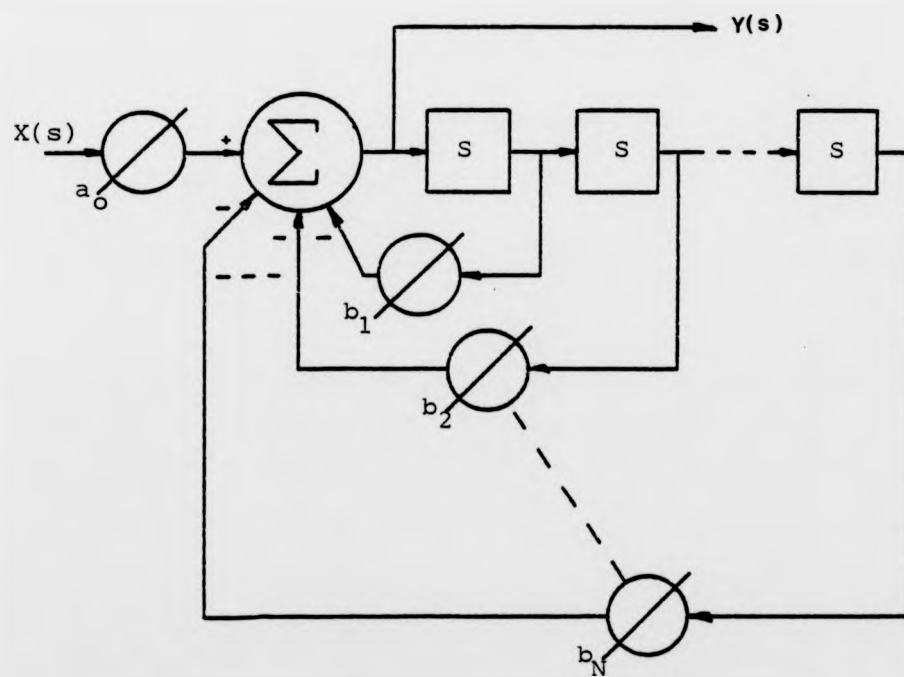
Figure 4.9: The All-Pole Adaptive Filter
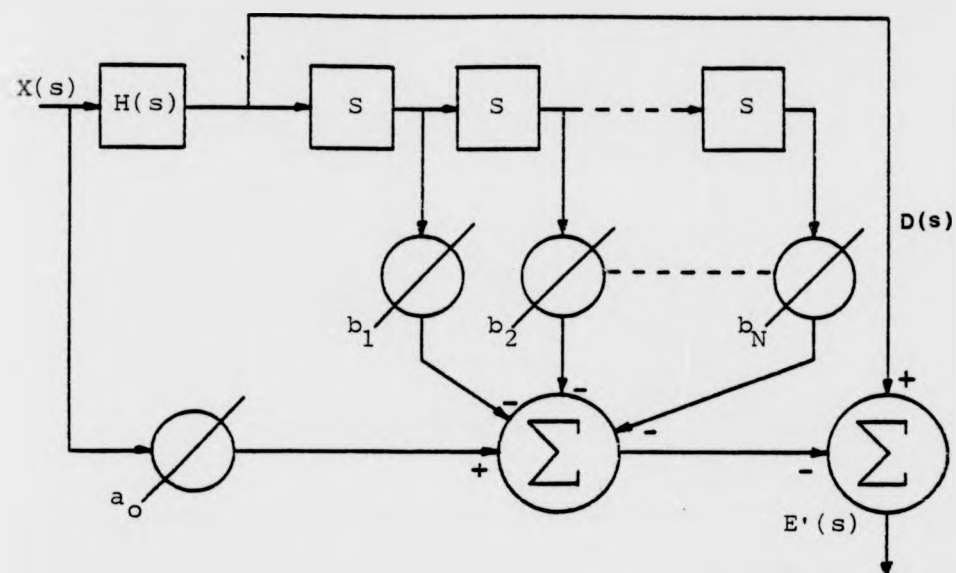
Figure 4.10: The All-Pole Adaptive Filter with Error Filtering
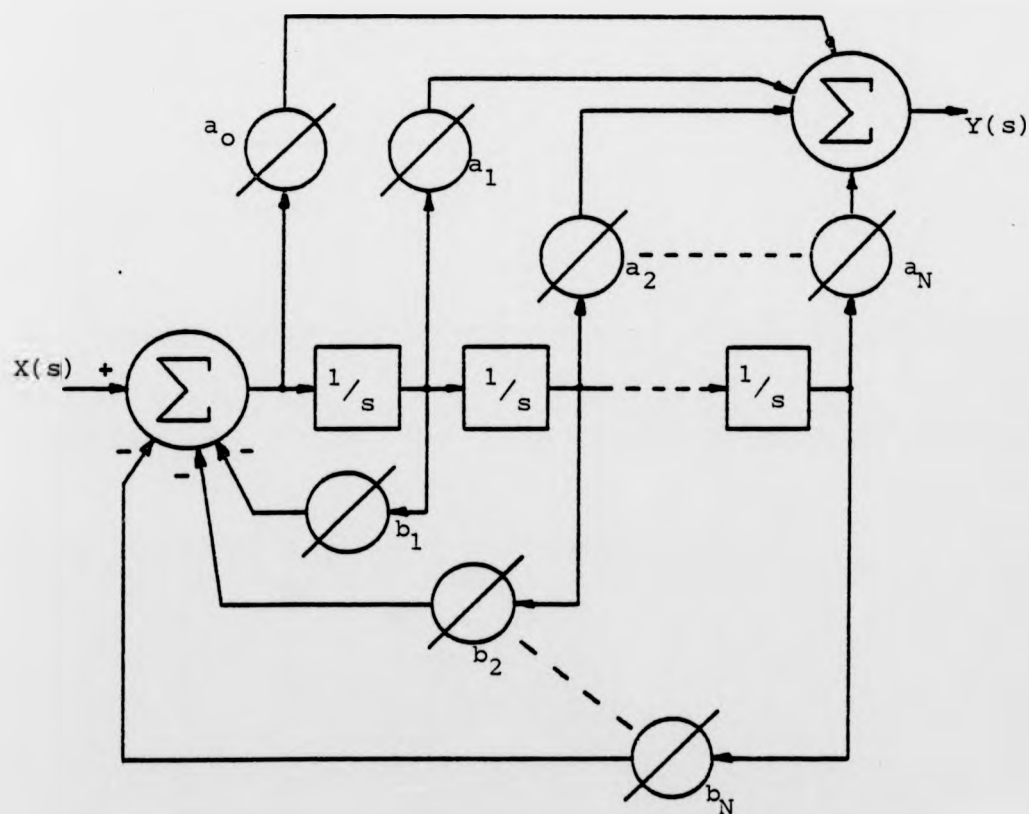
Figure 4.11: The Pole-Zero Adaptive Filter
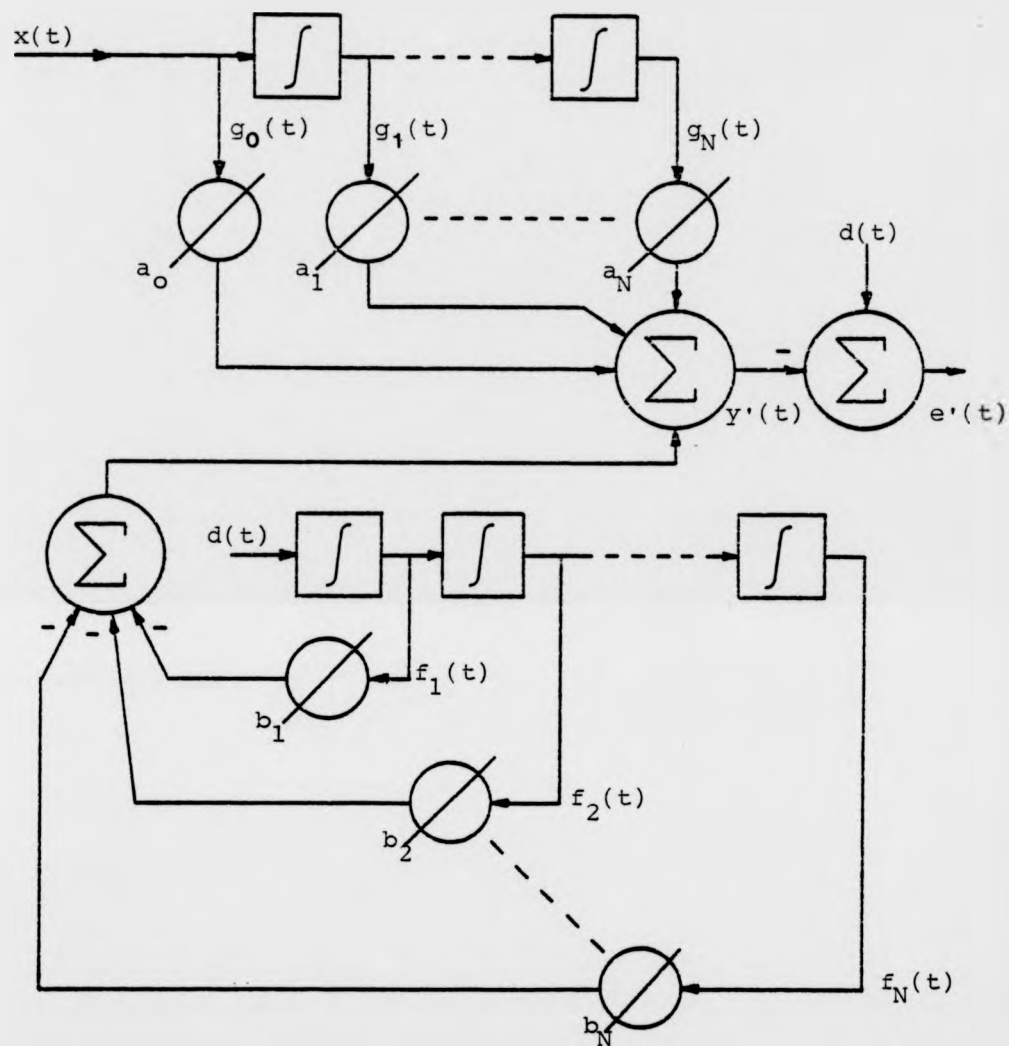
Figure 4.12:   The Pole-Zero Adaptive Filter with Error Filtering
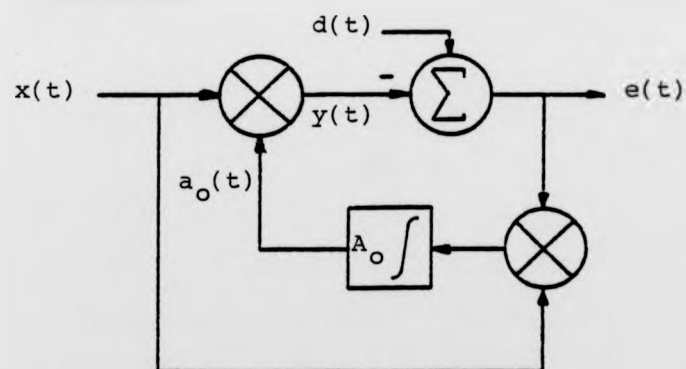
Figure 4.13:   A Simple Adaptive Gain Filter
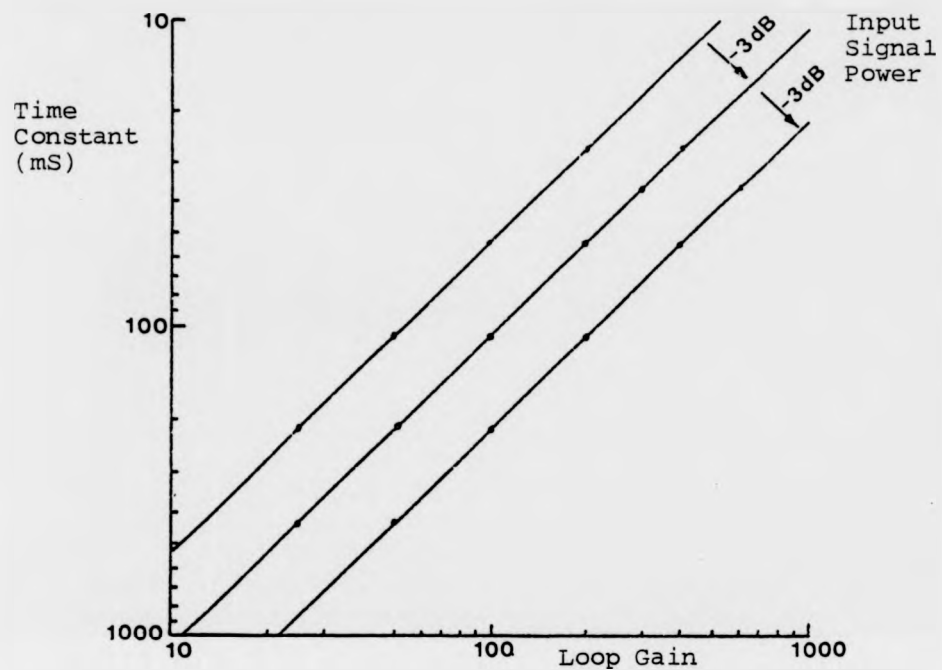
Figure 4.14: Dependence of the Time Constant of a_0 on the Loop Gain and the Input Signal Power, Using the Linear Adaption Algorithm
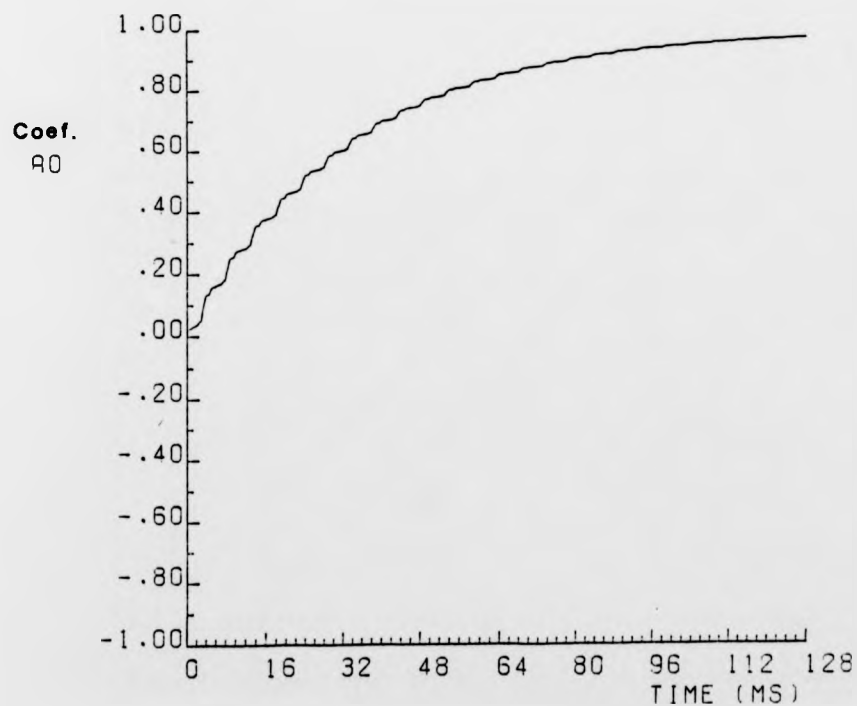
Figure 4.15a: Convergence of a_0 Using the Linear Adaption Algorithm
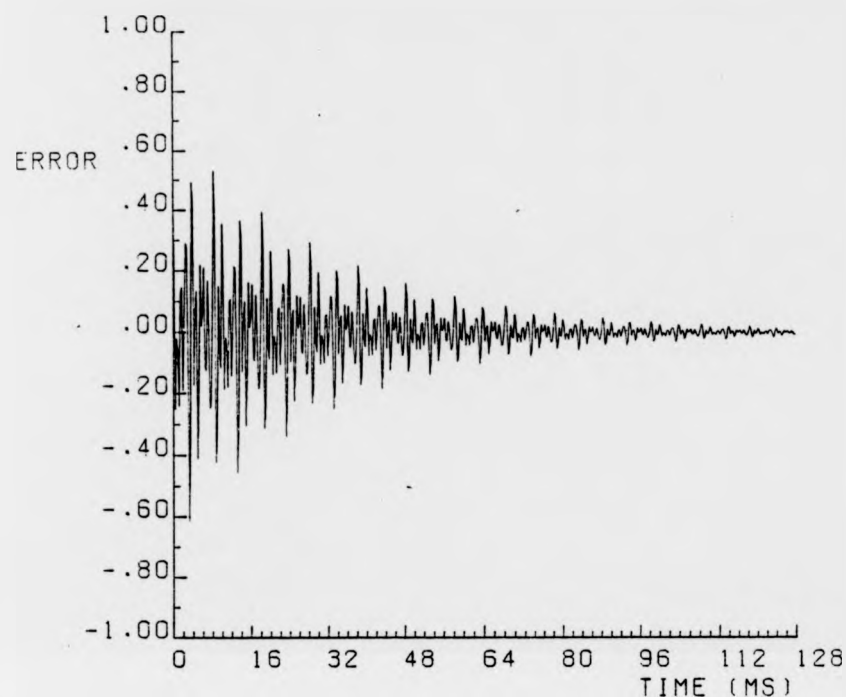
Figure 4.15b: Convergence of the Error Signal
Using the Linear Adaption Algorithm
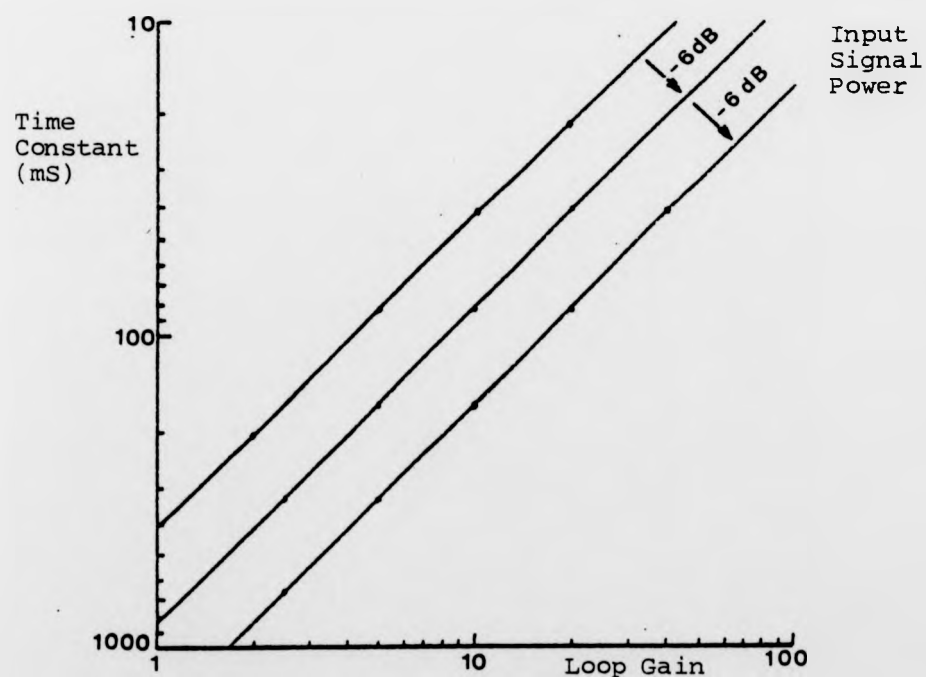
Figure 4.16: Dependence of the Time Constant of a_O on
the Loop Gain and the Input Signal Power,
Using the Non-Linear Adaption Algorithm
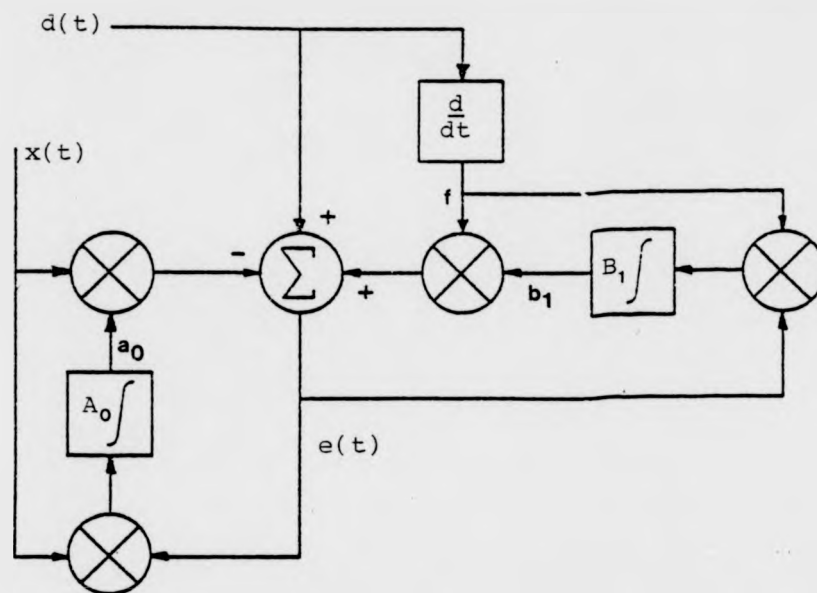
Figure 4.17: Block Diagram of the First
Order All-Pole Adaptive Filter
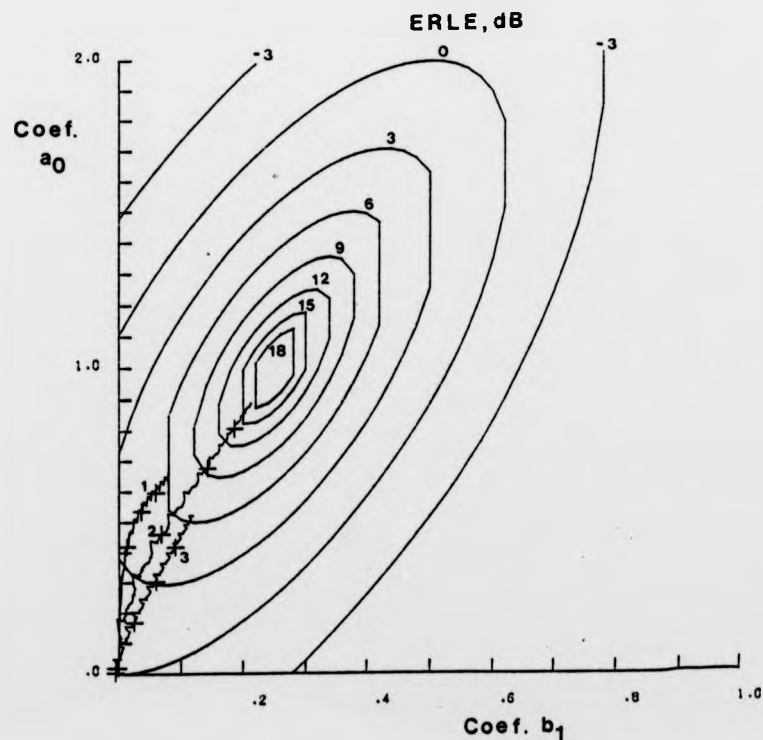
Figure 4.18: Convergence of the Single Pole Filter
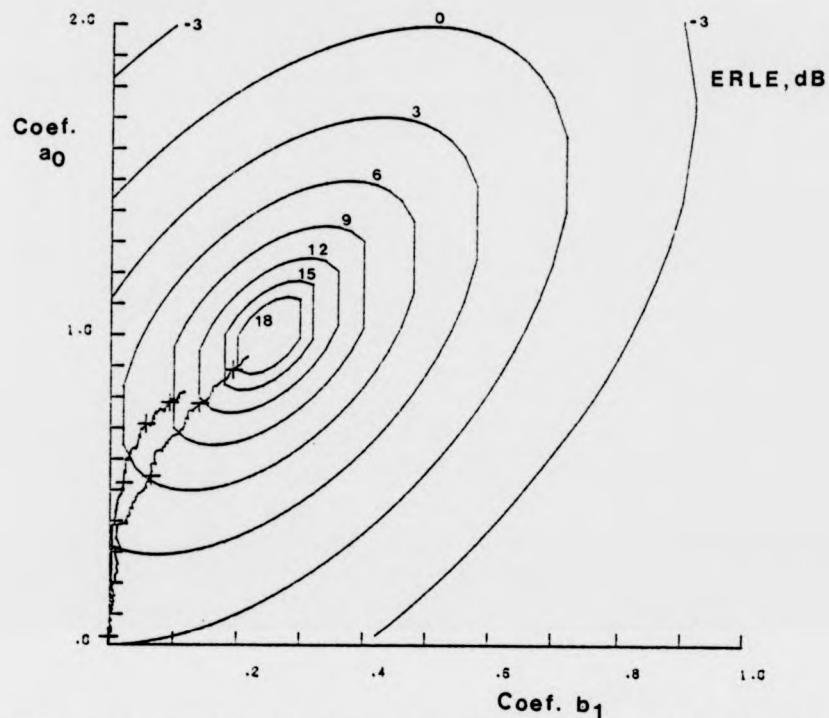
Figure 4.19: The Effect of a Reduction in the Bandwidth
of the Input Signal on the Single Pole Filter
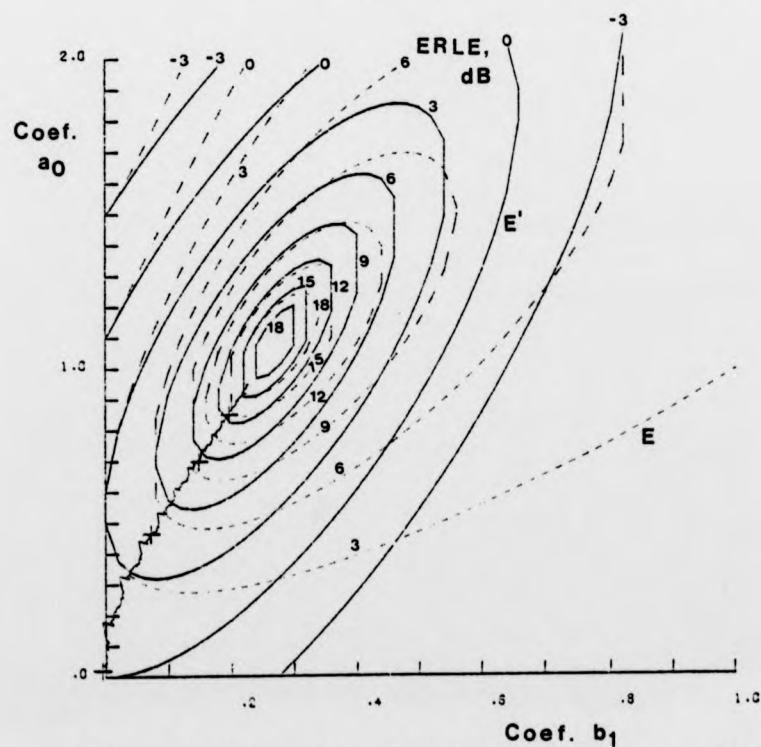
Figure 4.20a: The Effect of Slight Insufficiency
on the Single Pole Filter
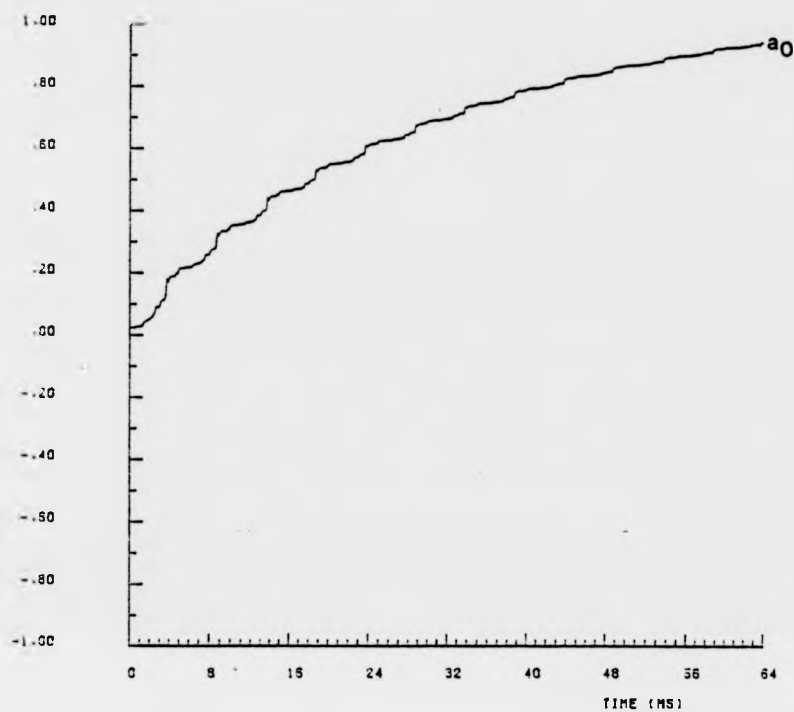
Figure 4.20b: The Effect of Slight Insufficiency
on the Convergence of a_0
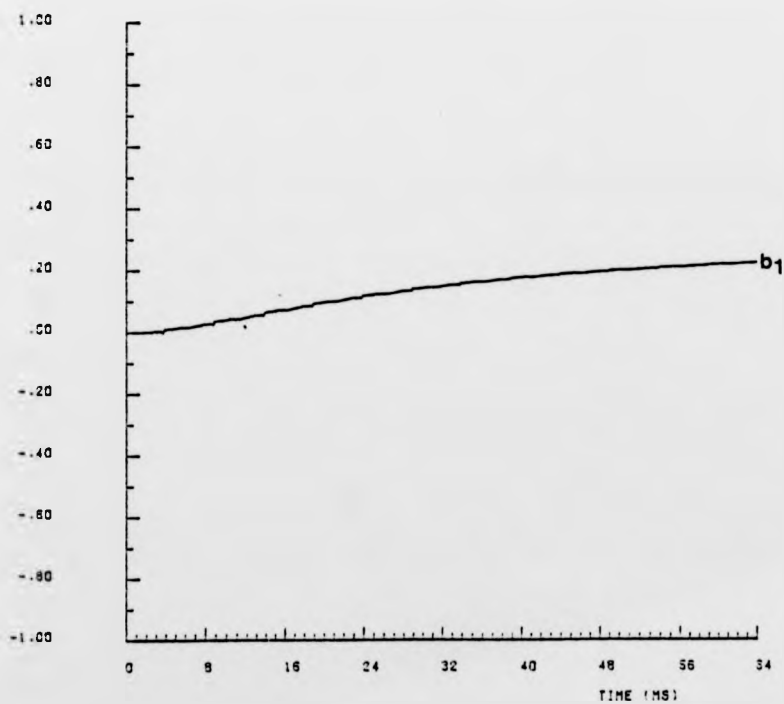
Figure 4.20c: The Effect of Slight Insufficiency
on the Convergence of b_1
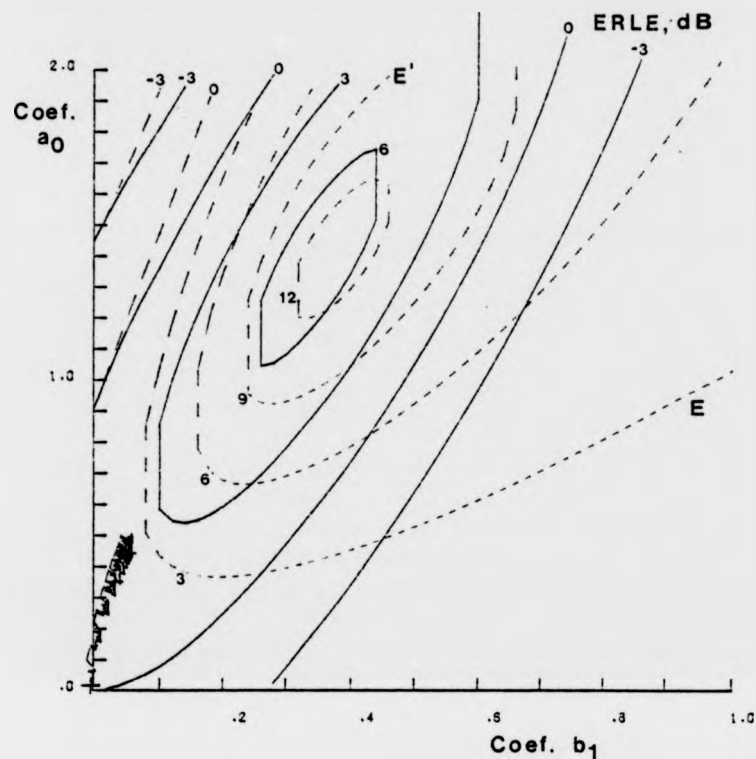
Figure 4.21a: The Effect of Moderate Insufficiency on the Single Pole Filter
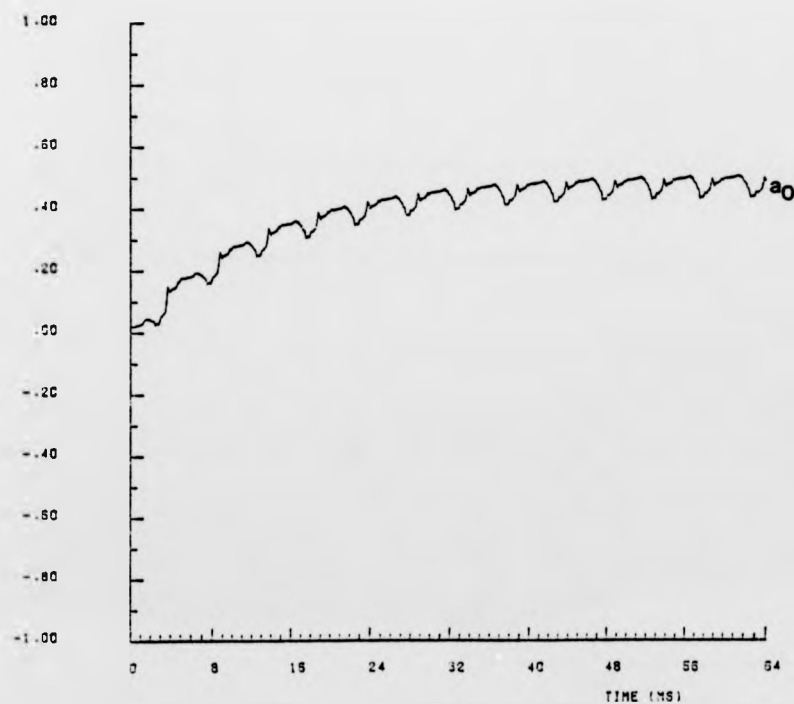
Figure 4.21b: The Effect of Moderate Insufficiency on the Convergence of a_0
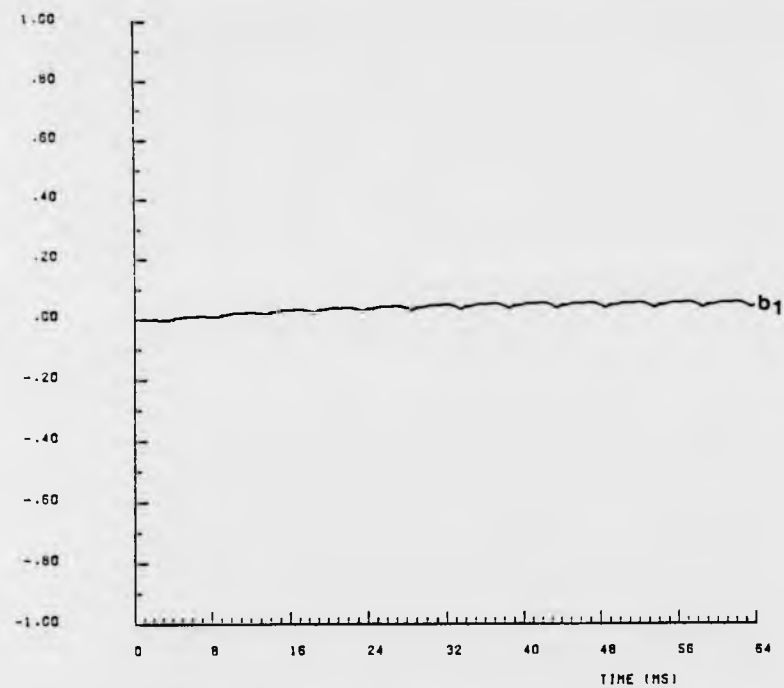
Figure 4.21c: The Effect of Moderate Insufficiency on the Convergence of b_1
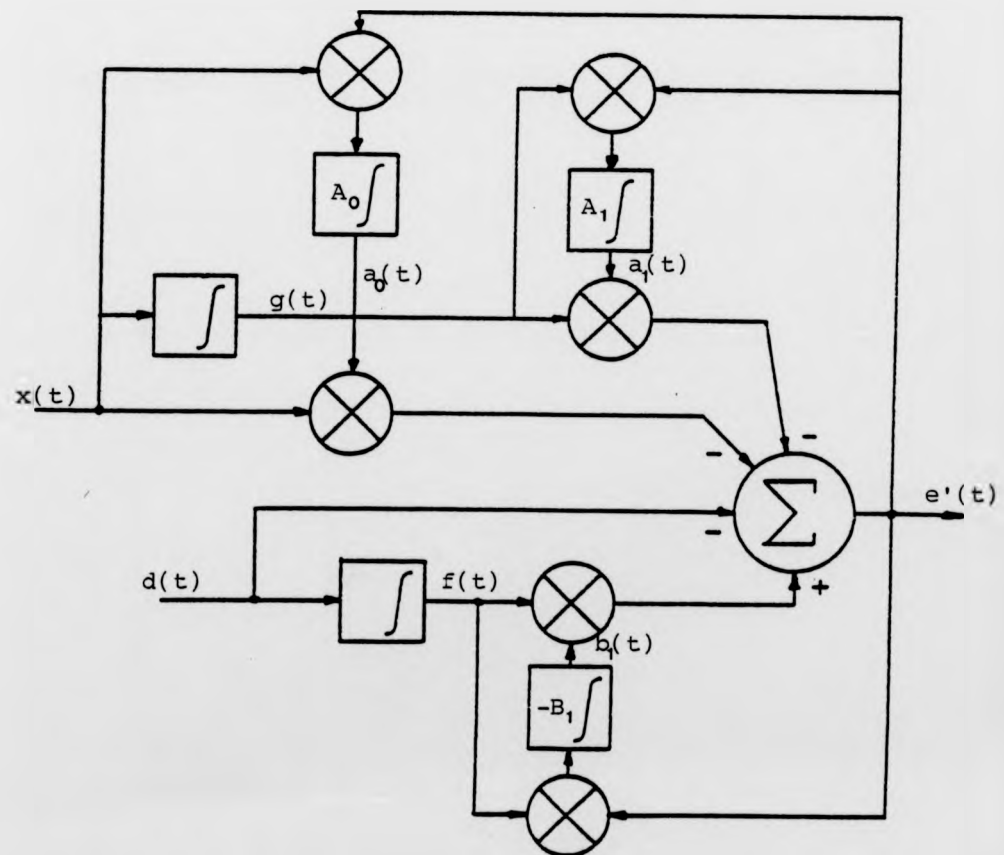
Figure 4.22: A Block Diagram of the First Order Pole-Zero Filter
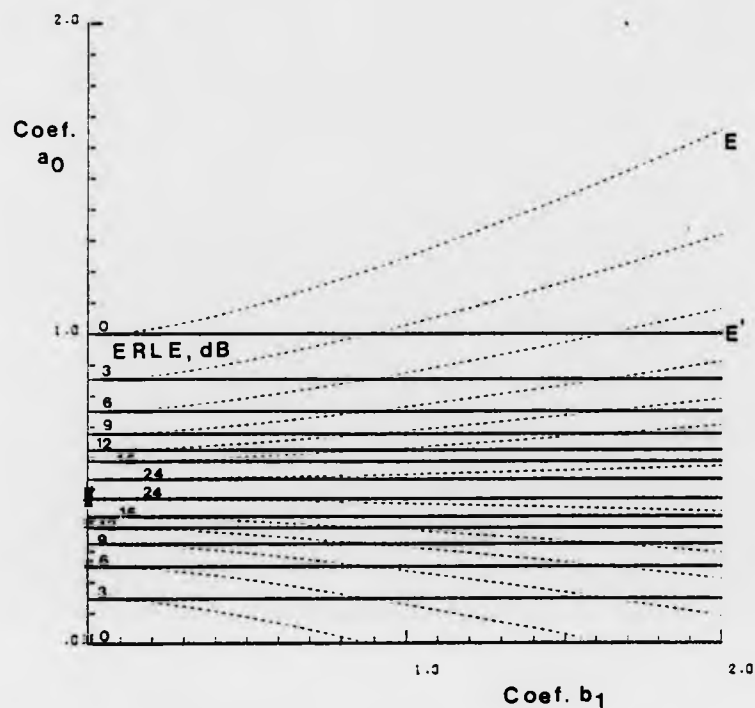
Figure 4.23a: Reduced Error Contour Plot $E(a_0, b_1)$ for the Pole-Zero Filter Adapting Against a Unity Gain
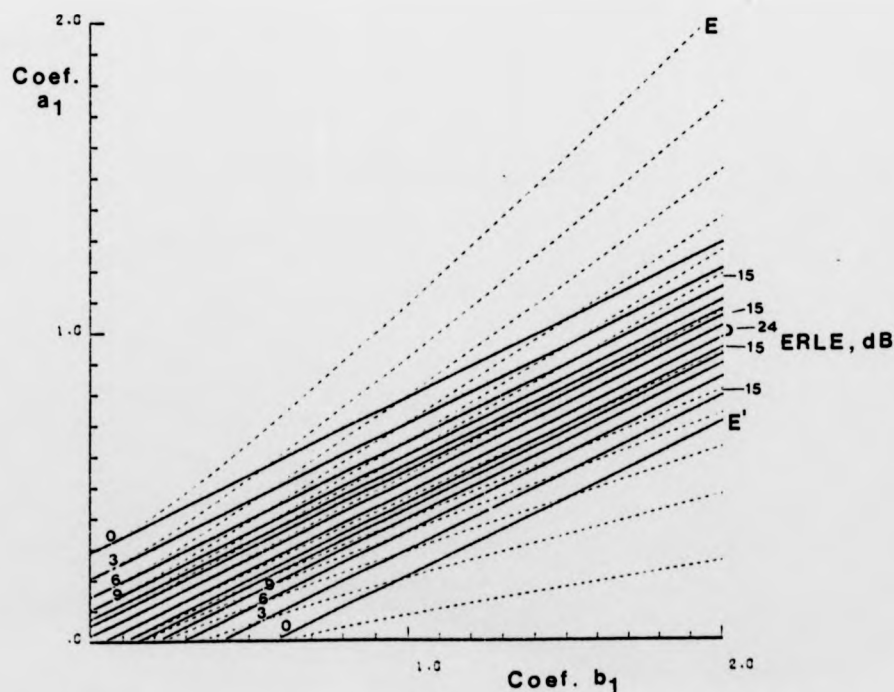
Figure 4.23b: Reduced Error Contour Plot $E(a_1, b_1)$ for the Pole-Zero Filter Adapting Against a Unity Gain
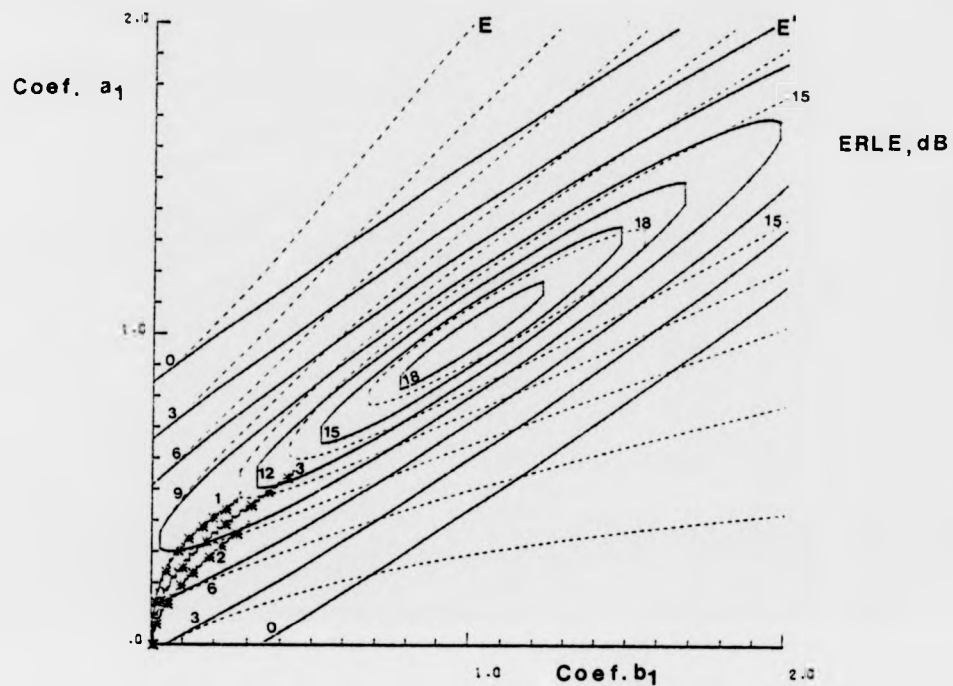
Figure 4.24a: Reduced Error Contours $E(a_1, b_1)$
for a Single Pole Unknown System
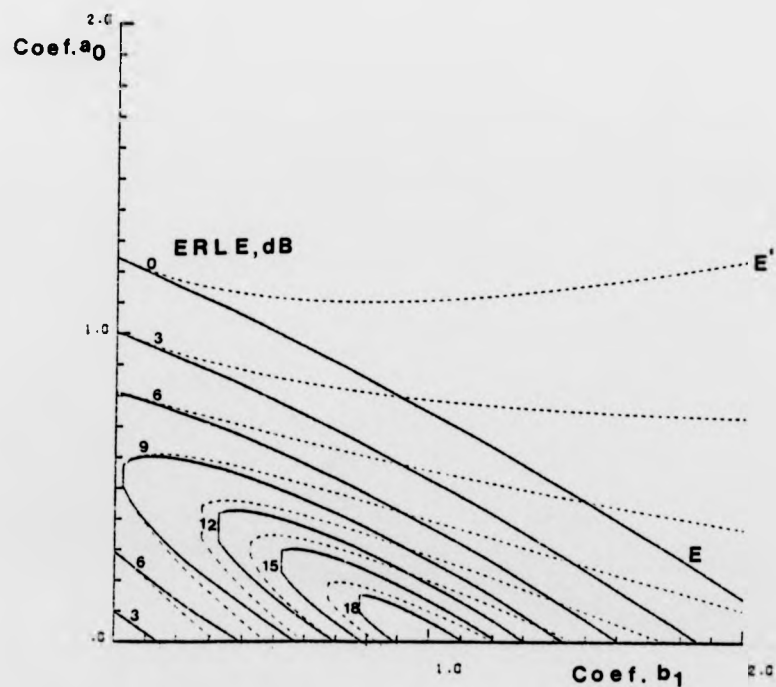
Figure 4.24b: Reduced Error Contours $E(a_0, b_1)$
for a Single Pole Unknown System
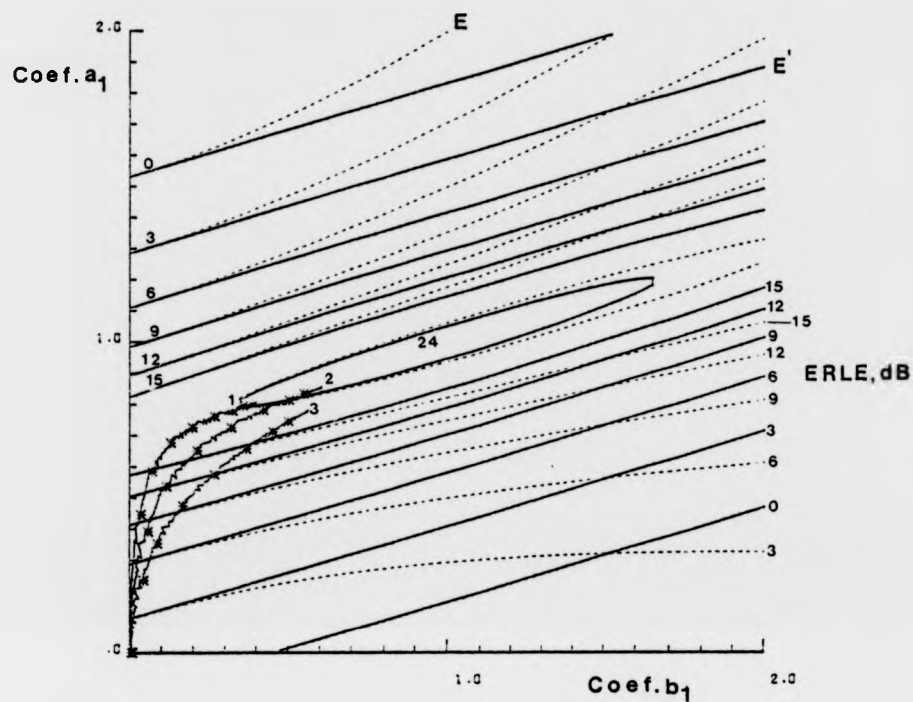
Figure 4.25a: The Effect of Increasing the Frequency of the Input Signal on $E(a_1, b_1)$
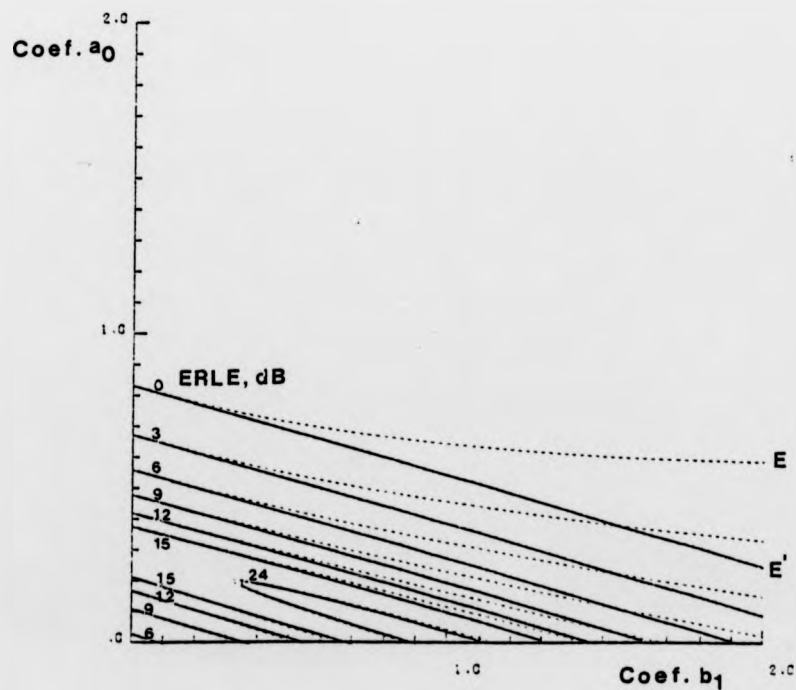
Figure 4.25b: The Effect of Increasing the Frequency of the Input Signal on $E(a_0, b_1)$
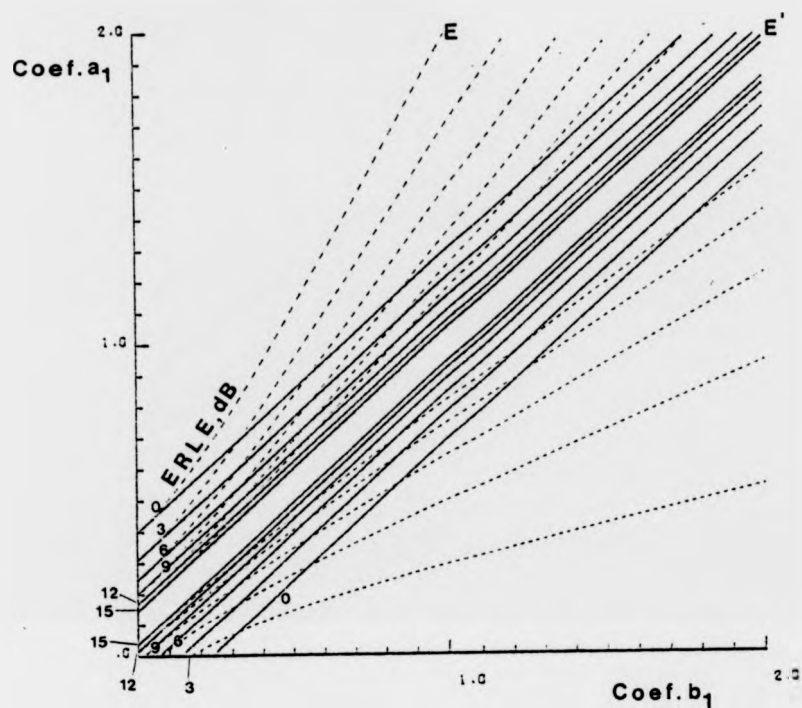
Figure 4.26a: $E(a_1,b_1)$ with a Sinusoidal Input Signal
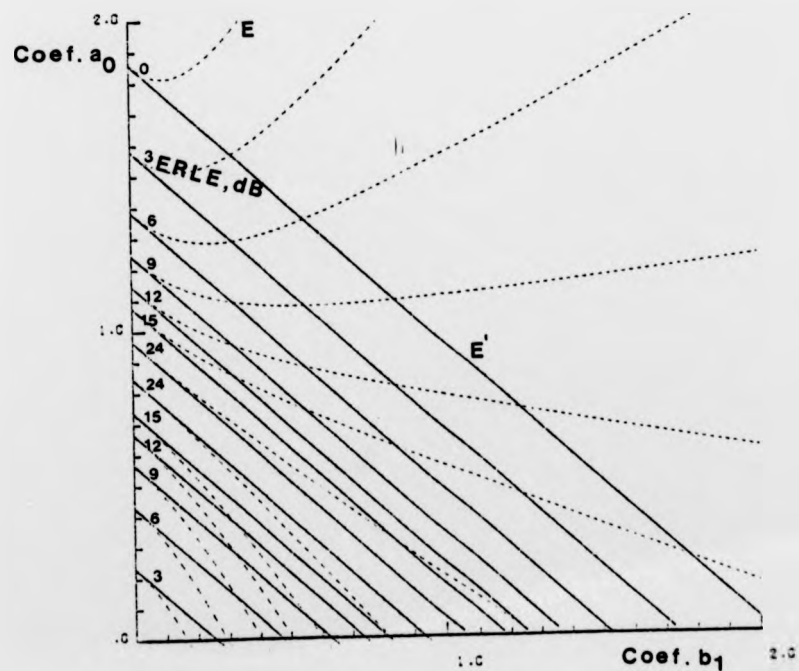
Figure 4.26b: $E(a_0,b_1)$ with a Sinusoidal Input Signal
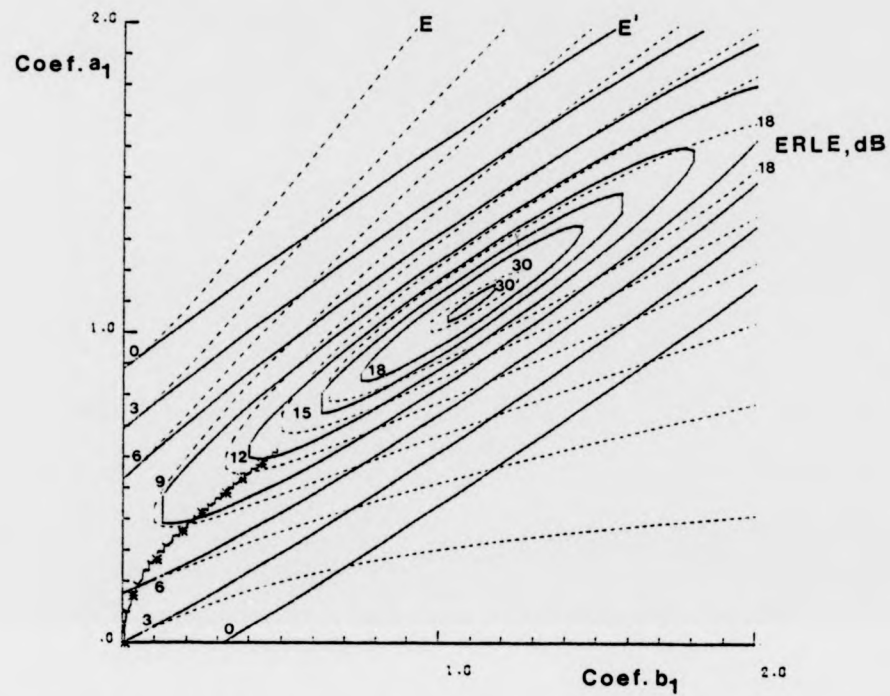
Figure 4.27a: The Effect of Slight Insufficiency on $E(a_1, b_1)$
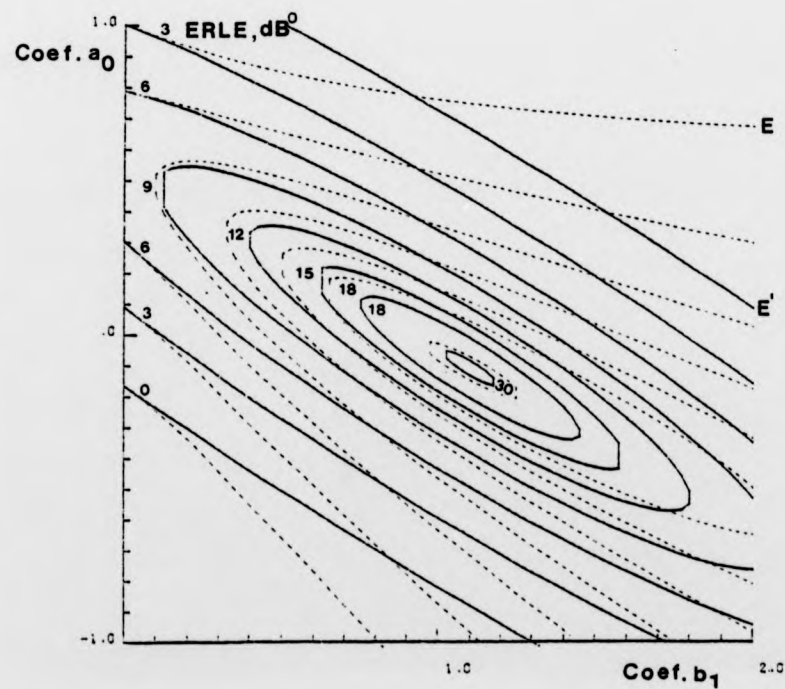
Figure 4.27b: The Effect of Slight Insufficiency on $E(a_0, b_1)$
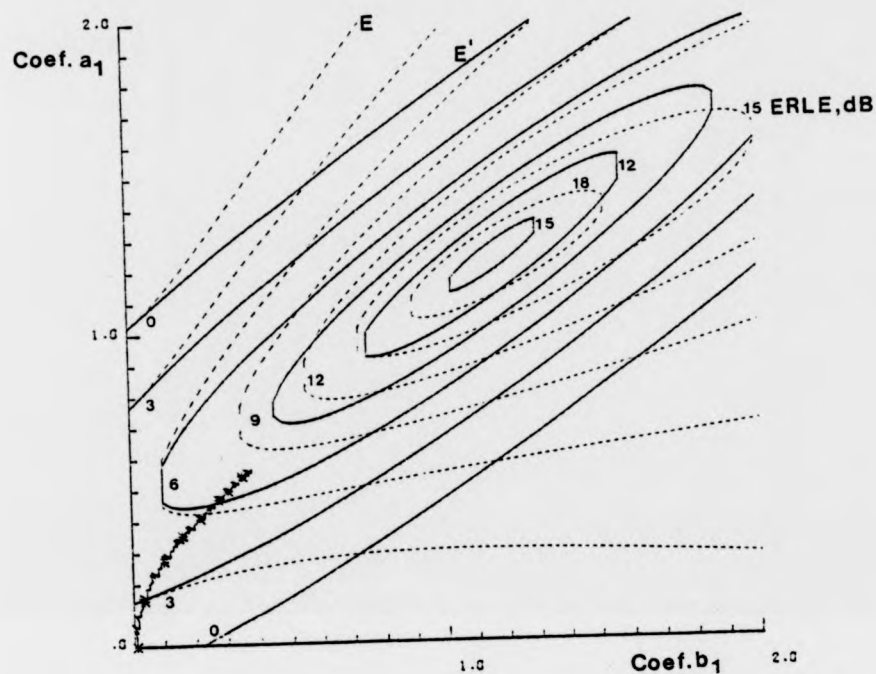
Figure 4.28a: The Effect of Moderate Insufficiency on $E(a_1, b_1)$
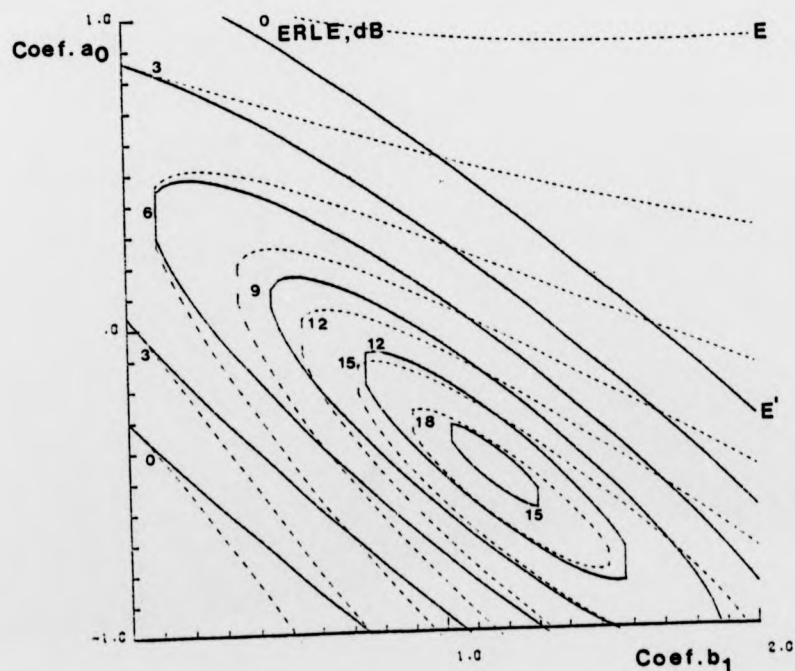
Figure 4.28b: The Effect of Moderate Insufficiency on $E(a_0, b_1)$
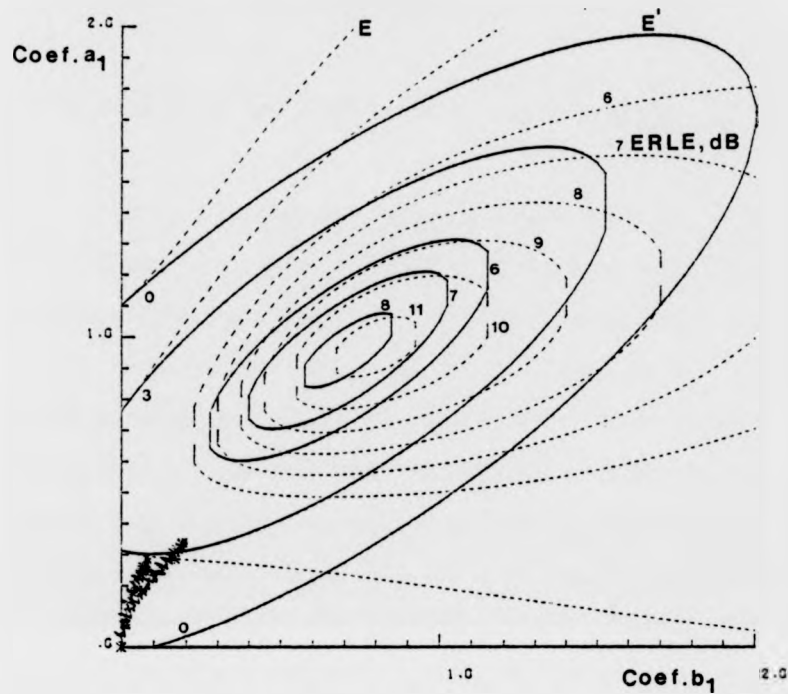
Figure 4.29a: The Effect of Severe Insufficiency on $E(a_1, b_1)$
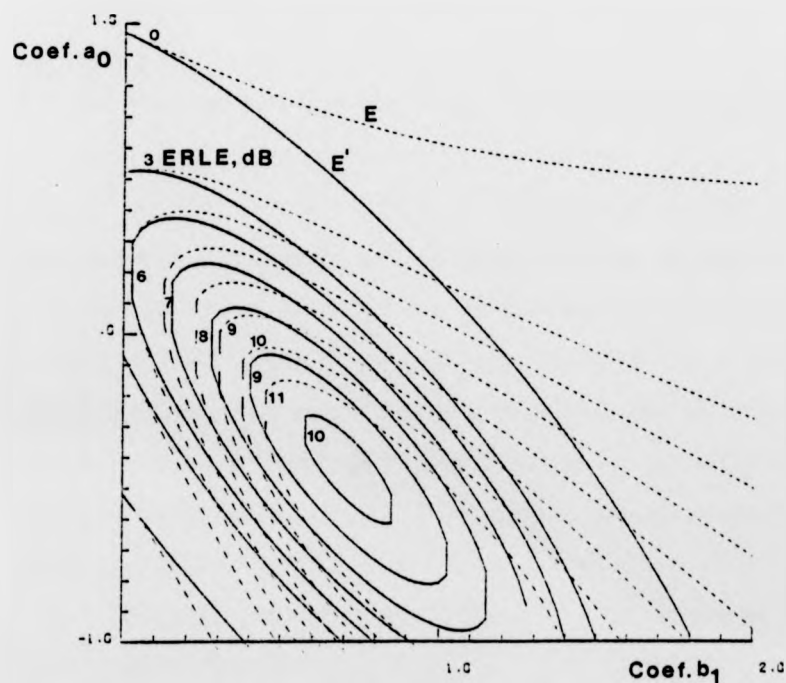
Figure 4.29b: The Effect of Severe Insufficiency on $E(a_0, b_1)$

CHAPTER 5

IMPLEMENTATION AND PERFORMANCE OF THE ANALOG ADAPTIVE FILTERS

In this chapter the implementations of the adaptive gain circuit, the first order all pole adaptive filter and the first order pole-zero adaptive filters are described. The effects of non-ideal circuit components are analysed, and the factors which limit the performance of the filters are quantified. These performance limitations are explored experimentally by testing the filters against simple unknown systems. Neither the adaptive gain circuit, nor the single pole filter were found to converge against simulated transhybrid responses. The pole-zero filter, however, performed well against simulated transhybrid responses, and the results of its performance are included in this chapter. In the final section of this chapter the problems of implementing an adaptive hybrid, using the pole-zero filter, are discussed.

5.1 The Adaptive Gain and the Single Pole Adaptive Filters

The single pole adaptive filter discussed in Chapter 4 can be considered as an adaptive gain circuit which has an additional recursive parameter b_1. Thus a prototype adaptive filter, which is capable of functioning as a simple adaptive gain, or as a single pole adaptive filter, can be constructed. A block diagram of such a filter is shown in Figure 5.1, where the switch Sw1 effectively zeros the b_1 parameter, thus switching the filter between the above two types.

The filter consists of signal path elements (shown in heavy lines), whose responses are controlled by the remaining elements of

the filter (control path elements). The multipliers M_1 and M_2 implement the variable parameters a_0 and b_1 respectively, and their outputs are combined in the adder S_1 to form the adaptive filter output $y(t)$. The error signal is formed by the subtractor S_2 and amplified by amplifier Ae for use in controlling the filter parameters. Similarly the input signal $x(t)$ and the differentiator output $g(t)$ are amplified to ensure high speed convergence. a_0 is controlled by the amplifier Aa_0, the multiplier Ma_0, and the integrator Ia_0, as described in Section 4.2.3.2. b_1 is controlled by Ab_1, Mb_1, and Ib_1, as described in Section 4.2.3.2 also.

A complete circuit diagram of the prototype adaptive filter is given in Appendix A3, and in Section 5.1.1 the design of the adaptive gain elements is described. Experimental results for the performance of the adaptive gain circuit are described in Section 5.1.2. Section 5.1.3 describes the design of the additional circuit elements needed to implement the single pole adaptive filter, and in Section 5.1.4 results for the performance of the single pole adaptive filter are given.

5.1.1.1 The Bandwidth of the Signal Path Elements

The theoretical transfer function of the adaptive gain circuit is given by:-

$$Y(s)/X(s) = a_0, \quad \text{and} \quad E(s) = D(s) - a_0 X(s) \qquad 5.1$$

assuming that M_1, S_1 and S_2 have infinite bandwidth. In practice these elements have limited bandwidth, and the resulting phase shift interferes with the correct operation of the filter. This effect can be quantified by considering the error signal which results when the filter is attempting to cancel the output of an unknown system whose transfer function is α. Assuming that the filter has N elements in

the signal path, each of first order with a pole frequency of ω_p rads/sec, and that the filter converges correctly, then $a_0 = \alpha$, and the error signal is:-

$$E(\omega) = \alpha X(\omega) \left[1 - \frac{1}{1 + j\,\omega/\omega_p}\right]^n \qquad\qquad 5.2$$

as shown in Figure 5.2. The return loss enhancement is:-

$$RLE(\omega) = D(\omega)/E(\omega) = \frac{(1 + j\,\omega/\omega_p)^n}{(1 + j\,\omega/\omega_p)^n - 1} \qquad\qquad 5.3$$

A plot of this function, evaluated in dB at the speech band edge (3.4KHz), for $n = 1, 2, 3$ and 4, is shown in Figure 5.3. It can be seen from the figure that the bandwidth of the individual circuit elements imposes an upper bound on the value of the return loss enhancement which can be achieved at the band edge.

5.1.1.2 The Effect of D.C. Offsets on the Adaptive Gain Circuit

In general the d.c. offsets possible in the adaptive gain circuit can be represented as shown in Figure 5.4. These offsets are detailed below, where some offsets have been lumped together, e.g. O_3 represents the output offset of Ma_0 and the input offset of Ia_0. O_7 and O_8 are not lumped with O_4 and O_5 respectively, because the amplifiers Aa_0 and Ae can not be assumed to operate linearly, due to their high gains. O_1 and O_6 are removed from the input of Ae by a.c. coupling (indicated by π), and their effects are ignored.

O_1 and O_2 : The input offsets of the signal multiplier M_1

O_3 : The output offset of the control multiplier Ma_0 and the input offset of the control integrator Ia_0

O_4 and O_5 : The input offsets of the control multiplier Ma_0

O_6 : The output offset of the signal multiplier M_1 and the input offset of the adders S_1 and S_2

O_7 and O_8 : The input offsets of the control amplifiers Aa_0

the signal path, each of first order with a pole frequency of ω_p rads/sec, and that the filter converges correctly, then $a_0 = \alpha$, and the error signal is:-

$$E(\omega) = \alpha X(\omega)\left[1 - \frac{1}{1+j\,\omega/\omega_p}\right]^n \qquad\qquad 5.2$$

as shown in Figure 5.2.   The return loss enhancement is:-

$$RLE(\omega) = D(\omega)/E(\omega) = \frac{(1+j\omega/\omega_p)^n}{(1+j\omega/\omega_p)^n - 1} \qquad\qquad 5.3$$

A plot of this function, evaluated in dB at the speech band edge (3.4KHz), for $n = 1, 2, 3$ and 4, is shown in Figure 5.3.   It can be seen from the figure that the bandwidth of the individual circuit elements imposes an upper bound on the value of the return loss enhancement which can be achieved at the band edge.

5.1.1.2 The Effect of D.C. Offsets on the Adaptive Gain Circuit

In general the d.c. offsets possible in the adaptive gain circuit can be represented as shown in Figure 5.4.   These offsets are detailed below, where some offsets have been lumped together, e.g. O_3 represents the output offset of Ma_0 and the input offset of Ia_0. O_7 and O_8 are not lumped with O_4 and O_5 respectively, because the amplifiers Aa_0 and Ae can not be assumed to operate linearly, due to their high gains. O_1 and O_6 are removed from the input of Ae by a.c. coupling (indicated by ∥), and their effects are ignored.

O_1 and O_2 : The input offsets of the signal multiplier M_1

O_3 : The output offset of the control multiplier Ma_0 and the input offset of the control integrator Ia_0

O_4 and O_5 : The input offsets of the control multiplier Ma_0

O_6 : The output offset of the signal multiplier M_1 and the input offset of the adders S_1 and S_2

O_7 and O_8 : The input offsets of the control amplifiers Aa_0

and Ae respectively.

The effect of O_2 is merely to add a fixed voltage to the paramater voltage Va_0, and this can be neglected by considering the actual filter parameter to be; $a'_0 = a_0 + O_2$. The offset O_3, since it is followed by the integrator Ia_0, causes Va_0 to ramp towards its maximum positive or negative value. In the steady state O_3 must be balanced by an equivalent d.c. voltage from the multiplier. The effect of O_3 is shown in the following analysis:-

Suppose that the filter is adapting against an unknown system consisting of a variable loss (α), and that the input signal is a sine wave ($Vsin(\omega t)$). Then $P(t)$, the output signal of the control multiplier is:-

$$P(t) = AeAa_0V^2[\alpha-a_0(t)] - AeAa_0V^2[\alpha-a_0(t)]Cos^2(\omega t) \quad 5.4$$

where it is assumed that Ae and Aa_0 are operating linearly. The second term in equation 5.4 is an a.c. signal at twice the frequency of the input signal, and should be considerably attenuated by Ia_0. Thus in the steady state a_0 tends towards its final value a_{0f}, and:-

$$\alpha-a_{0f} = \frac{O_3}{AeAa_0V^2}$$

The final value of return loss achieved is:-

$$X(\omega)/E(\omega) = 1/(\alpha-a_{0f}) = \frac{AeAa_0V^2}{O_3} \quad 5.5$$

If O_3 is zero, then perfect cancellation of $d(t)$ is possible, however if O_3 is large, then the gains Ae and Aa_0 must be high to achieve good steady state cancellation. Thus the level of the offset O_3 imposes a fundamental restriction on the ultimate value of return loss which can be achieved using the analog adaptive filters.

The operation of the adaption algorithm can be explained intuitively from equation 5.4, since any mismatch between α and $a_0(t)$ produces a d.c. signal at the control multiplier output which is

integrated by Ia_0, driving $a_0(t)$ towards α. O_3 either adds to this d.c. voltage, increasing the rate of convergence of $a_0(t)$, or subtracts from it, decreasing the rate of convergence.

The offset O_5 adds an a.c. component to the signal at the multiplier output, and a d.c. component given by O_4O_5. A further a.c. component is added by O_4, although this component decreases as the filter converges.

5.1.1.3 The Signal and Control Multipliers

In general a distinction can be made between the multipliers required for the signal paths of the adaptive filters, and those required for the control paths. The signal path multipliers should have good linearity, while the linearity of the control multipliers is not critical, since any harmonic distortion products are attenuated by the associated integrators. In the case of the non-linear adaption algorithm, the control multipliers are required to perform only sign multiplication (Section 4.1.6). In all cases the control multipliers should be 4-quadrant, whereas the b_1 signal multiplier need only be 2-quadrant, since negative b_1 would produce an unstable filter.

The approach adopted in implementing the prototype adaptive filters is to use linear 4-quadrant multipliers for maximum flexibility, and possible simplifications are discussed where appropriate. Since the multipliers are required to have high bandwidth, the MC1495 variable transconductance multiplier was chosen. These multipliers produce a differential output current which is proportional to the product of the input voltages. For the signal path multipliers this current is converted to a single-ended output voltage using an operational amplifier. The output current of

the control multipliers is integrated directly by an operational amplifier circuit as described in the next section.

5.1.1.4 Design of the Control Integrators

The differential output currents of the control multipliers are applied to the inputs of the control integrators, whose outputs form the filter parameters. The value of the integration capacitor should be chosen such that a.c. signals at the output of the integrator are sufficiently rejected, since these would cause harmonic distortion in the error signal. In Appendix A4 the design of the integrator is described in detail, and a value of 10 μF is chosen for the integration capacitor. This ensures at least 50 dB ERL, assuming that the filter adapts correctly. The requirement for high integration capacitor values means that these components would have to be external to an integrated version of the adaptive filters. The number of capacitors required per filter parameter could be halved by using a differential to single-ended converter at the multiplier outputs. Similarly the values of the capacitors required could be reduced by following the integrators by low-pass filters.

5.1.1.5 The Amplifiers Aa_0 and Ae.

In Section 5.1.1.2 it was shown that amplifiers Aa_0 and Ae should have high gains to overcome the effects of O_3. The fact that these amplifiers have finite gain-bandwidth products may therefore effect the performance of the filter. By a similar analysis to that of Section 5.1.1.2, it can be shown that the d.c. output voltage of the control multiplier is:-

$$P_{dc}(t) = \frac{AeAa_0V^2\{\alpha-a_0(t)\}\cos(\phi_e-\phi_{a0})}{2\sqrt{1+\omega^2a_e^2}\ \sqrt{1+\omega^2a_{a0}^2}} \qquad 5.6$$

where amplifiers Ae and Aa_0 have open loop gains Ae and Aa_0, and pole frequencies a_e and a_{a0} respectively, $\phi_e = \tan^{-1}(\omega a_e)$, $\phi_{a0} = \tan^{-1}(\omega a_0)$, the input voltage is $V\sin(\omega t)$, the unknown system has transfer function α, and both Ae and Aa_0 are assumed to operate linearly. Thus the voltage which drives $a_0(t)$ towards α is dependent on the gain of the amplifiers, and also affected by a difference in the phase shift introduced by each amplifier. This result shows that the phase response of any of the control path elements leading up to the integrators can be neglected, provided that no differential phase shift is introduced between the input signals of the control multiplier.

Since in the prototype adaptive filters the loop gains are approximately 4000, the d.c. output voltage of the multiplier is severely limited by clipping, and this can be expected to slow the convergence of the filter parameters.

5.1.2 Performance of the Adaptive Gain Filter

In this section results are presented for the performance of the adaptive gain filter adapting against various unknown systems, and the effects of non-ideal circuit components are measured. Section 5.1.2.1 gives the results when the filter adapts against unknown systems represented by a simple gain, for sine wave inputs of various frequencies. In Section 5.1.2.2 the results for the performance of the filter with a wideband noise input signal are presented. In both of these sections the results are for the steady state performance of the filter, i.e. a_0 is allowed to converge and the final value of return loss is measured.

The adaptive gain filter was found to be incapable of

accurately modelling the transhybrid responses due to most subscribers' lines, and attention was therefore concentrated on the remaining two types of adaptive filter.

5.1.2.1 The Adaptive Gain with Sinusoidal Input Signals

Figure 5.5 shows the return loss enhancement (RLE) achieved by the filter, as a function of the input signal level, for input signal frequencies of 200 Hz, 1 kHz and 4 kHz, where the unknown system was represented by a short circuit. It can be seen that the RLE falls linearly with decreasing input signal level over most of the range of input signal amplitudes. This occurs because the error signal contains noise introduced by the circuit, and the 'noise floor' is approximately 55 dB below the 0 dB input signal level (1 V RMS).

At high input signal levels the value of RLE is frequency dependant. This occurs because at these levels, and high input frequencies, the RLE is limited by the phase shift of the signal path elements, rather than by the circuit noise. At very high input signal levels (above 5 dB), the signal path multiplier M_1 begins to introduce distortion, thus limiting the degree of cancellation. The signal level at which this occurs is also frequency dependant, since if the RLE is limited to say 40 dB by phase shift, then distortion products below this level are unrecorded.

At very low input signal levels (below -50 dB), the frequency of the input signal again affects the degree of cancellation which can be obtained. This effect is probably due to differential phase shift in the control path of the filter, which reduces the maximum available d.c. voltage at the multiplier output. When this occurs the offset O_3 causes a_0 to drift from its optimum value of 1.

Figure 5.6 shows the performance of the circuit for the same input signal conditions, when the unknown system is represented by a unity gain inverting amplifier. In this case the performance of the circuit is virtually identical to that of Figure 5.5, with the exception that the limitation of the RLE due to phase shift is less severe, e.g. 55 dB RLE is obtainable at 1 kHz, whereas in the previous case the corresponding value was 50 dB. This improvement is due to the phase shift introduced by the inverting amplifier which forms the unknown system. This phase shift compensates for a similar phase shift in the signal path of the adaptive filter.

When the unknown system is represented by an open circuit, the return loss is as shown in Figure 5.7, for a 1 kHz input signal. The curve shown deviates from a straight line at very high input signal levels, when some distortion is produced by M_1. At lower input signal levels the value of a_0 is zero, and phase shifts have no effect. Thus there is no observable difference in performance at 200 Hz or at 4 kHz.

Figure 5.8 shows the behaviour of the voltage representing a_0, as a function of the unknown system's gain, where the input signal was a 1 kHz sine wave at level 0 dB. It can be seen from the figure that the relationship between the parameter voltage and the gain of the unknown system is linear, and that offset O_2 is approximately -0.14 V. Since much higher parameter voltages are possible, it is clear that the adaptive gain circuit as constructed can match unknown systems having gains greater than 1. The usefulness of this is explained in Section 5.1.3.2.

5.1.2.2 The Adaptive Gain with Wideband Input Signals

The ERL when the adaptive gain filter adapts against unknown systems represented by an open circuit, a short circuit, and a unity gain inverter, for an input signal consisting of white noise, bandlimited to 500 Hz to 2.5 kHz, is shown in Figure 5.9. When the unknown system is an open circuit, the relationship between ERL and input signal level is almost exactly linear, as is the case for sinusoidal excitation. For unknown systems whose transfer functions are +1 or -1, the ERL values are approximately equal, i.e. the effect of phase shift in the inverting amplifier of the unknown system is unnoticed. This occurs because the ERL is averaged over low frequencies (where the phase shift is negligable), and because components in the input signal with frequencies above 2.5 kHz are attenuated. At very low input signal levels (below -45 dB) the performance differs slightly for the 3 types of unknown system. The explanation for this is that the offset O_3, in the absence of an input signal, drives a_0 towards the negative supply voltage. Thus at low input signal levels, the offset causes a_0 to drift from its optimum value at higher signal levels for a positive parameter, than the signal levels at which drift occurs for a negative parameter. Thus the offset in this case favours unknown systems with 180° phase shift.

5.1.3 Design of the Differentiator for the Single Pole Filter

The components required by the single pole adaptive filter are those of the adaptive gain filter, with the addition of the differentiator D_1, the signal path multiplier M_2, and the b_1 control elements Ab_1, Mb_1 and Ib_1 (Figure 5.1). The design of the

differentiator is central to the correct functioning of the single pole filter, and in this section the factors affecting the design are briefly summarised. The details of the design are included in Appendix A4.

In the block diagram of Figure 5.1, the differentiator is indicated as having an ideal response. In practice, to guarantee the stability of the differentiator, it is necessary to introduce compensation poles into its closed loop transfer function (CLTF). These compensation poles however, could produce instability in the loop consisting of components S_1, D_1 and M_2 (Figure 5.1) if the error filtering were removed, i.e. if the loop were closed via Sw2. This loop will be referred to as the b_1 feedback loop. The stability of this loop determines the frequency by which the compensation poles should have reduced the gain of the differentiator to unity. This frequency in turn determines the maximum time constant to which the adaptive filter can adapt.

In the prototype single pole adaptive filter it was found that an upper unity gain frequency of 2 MHz guaranteed the stability of the b_1 feedback loop, using an externally compensated operational amplifier. By placing the differentiator compensation poles at 19.5 kHz and 21.9 kHz, the maximum time constant to which the filter can adapt is 264 μS. This is reduced to 120 μS by attenuation around the b_1 feedback loop. In the next section the effect of the differentiator compensation poles on the performance of the adaptive filter is examined.

5.1.3.1 The Effect of Non-Ideal Differentiation

In the previous section it was seen that it is necessary to introduce two compensation poles into the CLTF of the differentiator.

This compensation results in inaccurate differentiation at high frequencies. To examine the effect of this inaccuracy on the degree of cancellation which can be achieved by the filter, consider an unknown system given by:-

$$H(s) = \alpha/(1+\beta s)$$

where the adaptive filter transfer function is:-

$$G(s) = \frac{a_0}{1 + b_1 ps/(1+sq)^2}$$

with $a_0 = \alpha$ and $b_1 p = \beta$

i.e. the unknown system is a first order system, it is assumed that the adaptive filter has adapted correctly, and the differentiator in the adaptive filter has two compensating poles at $1/q$ rads/sec. Assuming that the amplitude of the input signal's spectral density is unity, i.e:-

$$X(\omega) = 1$$

then the filtered error power can be written as:-

$$|E'(\omega)|^2 = \frac{\alpha^2 \omega^2 \beta^2}{1+\beta^2 \omega^2} \left[\frac{\omega^2 q^2 (4+\omega^2 q^2)}{(1+\omega^2 q^2)^2} \right]$$

The power of the unknown signal can be written as:-

$$|D(\omega)|^2 = \frac{\alpha^2}{1+\beta^2 \omega^2}$$

Thus the maximum filtered ERLE which can be achieved against a time constant β, is given by:-

$$ERLE = \frac{\displaystyle\int_{\omega_1}^{\omega_2} 1/(1+\omega^2 \beta^2)\ d\omega}{\displaystyle\int_{\omega_1}^{\omega_2} \frac{(4+\omega^2 q^2)\,\omega^2 \beta^2 \omega^2 q^2}{(1+\omega^2 \beta^2)(1+q^2 \omega^2)}\ d\omega} \qquad 5.7$$

where $\omega_1 = 2\pi.500$ rads/sec and $\omega_2 = 2\pi.2500$ rads/sec

Figure 5.10 shows a plot of this function in dB for various values of compensating pole frequency and unknown system time constant. This figure shows that the differentiator inaccuracy imposes a severe restriction on the degree of cancellation possible against an unknown system with a given time constant. For the prototype single pole adaptive filter the predicted ERLE against the maximum time constant to which the filter can adapt (120 μS) is 6 dB. The stability return loss enhancement will be lower than this, since the differentiator inaccuracy is worst at the upper band edge.

In the above analysis it has been assumed that the adaptive filter parameters a_0 and b_1 have values which are optimal for the ideal differentiator case. This assumption neglects the possibility that more accurate cancellation can be achieved using alternative values of a_0 and b_1, such that the filter compensates for the differentiator inaccuracy. Using the error contour plotting technique described in Section 4.1.2, it can be shown that such compensation is possible.

Figure 5.11 shows error contour plots for a single pole adaptive filter at various input signal frequencies, where the unknown system is a single pole of time constant 1 mS. At low frequencies the effect of the differentiator inaccuracy is small, and the optimum parameter values are close to their theoretical values (0.65,1.0). As the input signal frequency is increased however, the differentiator becomes less accurate, and the effect of this is seen to be a movement of the optimum parameter values, both of which increase.

5.1.4 Performance of the Single Pole Adaptive Filter

In this section results are presented for the performance of the single pole adaptive filter adapting against unknown systems represented by:-

$$H(s) = 1/(1+sa)$$

for various input signals. Section 5.1.4.1 gives the performance of the filter for sinusoidal input signals between 200 Hz and 4 kHz, while in Section 5.1.4.2 the results for wideband noise input signals are presented. It is seen that the inaccuracy of the differentiator imposes a severe limitation on the performance of the filter.

As is the case for the adaptive gain circuit, the single pole filter was found to be incapable of modelling the transhybrid responses of most subscribers' lines. For this reason its characteristics were not further investigated.

5.1.4.1 Performance of the Single Pole Filter with Sinusoidal Excitation

Figure 5.12a shows the filtered RLE achieved by the filter as a function of the time constant of the unknown system, for a range of input signal frequencies. The corresponding values of the filter parameter voltages Va_0 and Vb_1 are shown in Figures 5.12b and 5.12c respectively.

From Figure 5.12a it can be seen that at all input signal frequencies, the filter achieves good cancellation for unknown systems with small time constants (< 40 µS). As the time constant increases above this value, the performance of the filter drops sharply, and the value of the time constant at which this drop occurs is frequency dependent. From Figure 5.12c it is clear that this

sudden drop in cancellation occurs because b_1 reaches its maximum value. Figure 5.12b shows that the frequency dependence of this 'parameter saturation point' is due to the differentiator inaccuracy, as explained in Section 5.1.3.2. Thus as the frequency of the input signal is increased, the optimum parameter values increase until eventually b_1 saturates, and the cancellation suddenly drops. At the lowest input frequency (200 Hz), the value of time constant at the saturation point is 100 μS. This value is close to the theoretical maximum time constant of 120 μS, the difference being within the range possible for the low tolerance components used in the prototype filter.

For small time constants, and at high input signal frequencies, the performance of the single pole filter is better than that of the adaptive gain circuit, adapting against a short circuit (Figure 5.5). This is because it is able to compensate for the phase shift introduced in the a_0 signal path. The degree of cancellation achieved by the single pole filter at low unknown system time constants is frequency dependent, and is probably due to non-ideal control loop amplifiers.

5.1.4.2 Performance of the Single Pole Filter with Wideband Input Signals

Figure 5.13a shows the filtered ERLE achieved by the filter after convergence, as a function of the time constant of the unknown system. The values of the parameter voltages are shown in Figure 5.13b. The use of a wideband input signal means that full compensation for the differentiator inaccuracy is not possible, although the increase in the value of a_0 shown in Figure 5.13b indicates that some compensation takes place. The graph of Figure

5.13a falls linearly with increasing time constant, because b_1 increases with increasing time constant. Any inaccuracy in the differentiator response thus becomes more important, and the degree of cancellation achieved falls as a result.

When the time constant becomes greater than approximately 80 μS, b_1 reaches its maximum value, and the cancellation drops rapidly thereafter. The value of a_0 decreases gradually for time constants above 80 μS, indicating that the filter adopts a value of a_0 which minimises the error signal, although b_1 holds its maximum value.

5.2 The First Order Pole-Zero Adaptive Filter

In Section 5.1.3.1 it was shown that stability problems resulted from the use of a differentiator in the single pole adaptive filter. The stability constraints imposed on the design of the differentiator severely restrict the maximum time constant to which the single pole filter can adapt. Furthermore it was found that neither the adaptive gain circuit, nor the single pole filter could provide sufficient ERLE against most subscribers' lines.

In the first order pole-zero adaptive filter, as described in Chapter 4, the frequency selective element is an integrator. This avoids the stability problems associated with the use of a differentiator, and it will be shown that in theory a pole-zero filter can synthesise infinite time constants. In Section 5.3 it is shown that the ability of the first order pole-zero filter to synthesise a zero in addition to a pole, allows it to achieve considerable ERLE against simulated subscribers' lines.

In the following sections the aspects of the design of the first order pole-zero filter which differ significantly from those of Section 5.1 are discussed. Results for the performance of the filter

are described in Section 5.3

5.2.1 Design of the Signal Integrators

Figure 5.14 shows a block diagram of a first order pole-zero adaptive filter, with error filtering and adaption circuitry, as described in Section 4.2.4.   A circuit diagram of the filter is given in Appendix A3.   The circuit consists of signal multipliers, adders and integrators, and control multipliers and integrators, as described for the previous filters, with the exception of the signal integrators Ix and Id.   In Section 4.2.4 it was assumed that these integrators both had transfer functions given by:-

$$I(s) = -1/sp$$

i.e. ideal integrators with time constant p. This ideal transfer function has infinite gain at d.c., and in practice small d.c. offsets would cause such an integrator to 'ramp' towards the positive or negative supply rail.   To control this effect the d.c. gain of the integrator can be reduced by using the 'leaky integrator' circuit shown in Figure 5.15 whose transfer function is:-

$$I(s) = -1/(q+sp)$$

where $p = C_2 R_1$, $q = R_1/R_2$ and it is assumed that the operational amplifier is ideal.   In the following sections it is assumed that the integrators Ix and Id are identical, i.e.   only first order effects of leaky integration are examined.

5.2.1.1 The Effect of the Leaky Integrator on the Error Surface

The filtered error signal, using the leaky integrators, is:-

$$E'(s) = D(s)\left[1+\frac{b_1}{q+sp}\right] - X(s)\left[a_0+\frac{a_1}{q+sp}\right] \qquad 5.8$$

while the unfiltered error signal is:-

$$E(s) = D(s) - \frac{X(s)\{a_0+a_1/(q+sp)\}}{1+b_1/(q+sp)} \qquad 5.9$$

Thus the effect of the leaky integration is to change the error filtering function from $1+b_1/sp$ to $1+b_1/(q+sp)$. This alters the frequency weighting effect of the error filtering, although the filtered error surface remains quadratic in a_0, a_1 and b_1.

The effect of the leaky integration on the unfiltered error surface can be seen by considering a case where the filter adapts against an unknown system given by:-

$$H(s) = \alpha(1+\gamma s)/(1+\beta s)$$

i.e. in this example the filter is sufficient. The optimum values of the filter parameters can be simply shown to be:-

$$a_0 = \alpha\gamma/\beta, \quad a_1 = (p-q\gamma)\alpha/\beta \text{ and } b_1 = (p/\beta)-q$$

Since $q = 0$ for the ideal integrator, it can be seen that the effect of the non-ideal integration is a movement in the position of the minimum in the error surface. The depth of the minimum is unaltered for this sufficient example, i.e. perfect matching of the adaptive filter and the unknown system responses is still possible.

5.2.1.2 Choice of the Integrator Time Constant

In this section it is shown that the pole-zero adaptive filter can accurately model large time constants, but that it is incapable of modelling a range of small time constants. The signal integrators are designed so as to minimise this effect.

In the example of the previous section, if the unknown system can be represented by a gain and a pole, i.e. if $\gamma = 0$, then the optimum filter parameters are:-

$$a_0 = 0, \ a_1 = p\alpha/\beta \text{ and } b_1 = (p/\beta)-q$$

If the time constant of the unknown system is very large, i.e. $\beta \to \infty$, then $b_1 \to -q$ and $a_1 \to 0$ to keep the error zero. Thus in theory the filter can model an unknown system with an infinite time constant.

For small time constants, i.e. $\beta \to 0$, the values of the filter parameters required tend to infinity. Thus the minimum time constant which the filter can accurately model is given by:-

$$\beta > p\alpha/a_{1max} \text{ and } \beta > p/(b_{1max}+q) \qquad\qquad 5.10$$

Assuming $a_{1max} = b_{1max} = 1$, then the worst case is given by $\beta_{min} = p$. Furthermore, since $q < 1$, then when $\alpha = 1$ this restriction is not significantly eased. For time constants smaller than p the error thus begins to rise from zero, if wideband excitation is assumed. Very small time constants can however be modelled, to varying degrees of accuracy, by a_0 alone (over a restricted bandwidth), with $a_1 = b_1 = 0$. The error therefore decreases again for time constants less than some value.

Choosing small values of p results in an integrator having high gain at low frequencies, and this gain must be such that the signal handling capacity of the signal multipliers is not exceeded. For very low values of p this requirement is difficult to achieve if integration is to be accurate over the bandwidth 300 Hz to 3.4 kHz. Thus the time constant of the integrator should be as large as possible, while providing an acceptable minimum error in the region where the filter is unable to accurately model a short time constant.

To quantify this effect, it is necessary to make some assumptions about the behaviour of the filter when it is unable to accurately model the unknown system. In particular, if it is assumed that very small time constants are modelled by a variable gain (a_0 alone), while long time constants are modelled by a single pole (using a_1 and b_1, with $a_0 = 0$), and that these two states are mutually exclusive, then the analysis is greatly facilitated.

Figure 5.16 shows a variable gain a_0 attempting to model a single pole unknown system with a time constant β. Writing the equation for $|E(\omega)|^2$, and differentiating with respect to a_0, gives the optimum value for a_0 as:-

$$a^*_0 = \frac{\tan^{-1}(\omega_2\beta) - \tan^{-1}(\omega_1\beta)}{\beta(\omega_2 - \omega_1)} \qquad 5.11$$

where the input signal is assumed to be bandlimited white noise of bandwidth $\omega_2 - \omega_1$. The amount of attenuation achieved as a function of frequency can be written as:-

$$D(\omega)/E'(\omega) = 1/\{(1-a^*_0)^2 + a^*_0\beta^2\omega^2\} \qquad 5.12$$

If $\omega = \omega_2$, the maximum frequency of the input signal, then this quantity represents the maximum SRL enhancement which the adaptive gain circuit can achieve. Since error fltering is used in the pole-zero filter, then equation 5.12 becomes:-

$$D(\omega)/E(\omega) = \frac{\{1+(b_1/\omega p)^2\}}{(1-a^*_0)^2 + a^*_0\beta^2\omega^2} \qquad 5.13$$

This equation represents the portion of the time constant range for which the filtered error decreases with decreasing time constant.

When the filter is correctly modelling the pole, then the error signal can be written as:-

$$E'(s) = X(s)(1 - \beta/\beta_{min})/(1+\beta s)$$

When $\beta < \beta_{min}$ (equation 5.10), and assuming that the filter models β by a larger time constant β_{min}, then the filtered RLE can be shown to be:-

$$|D(\omega)/E'(\omega)|^2 = 1/(1 - \beta/\beta_{min})^2 \qquad 5.14$$

Equation 5.14 represents the SRL enhancement achievable over the portion of the time constant range $\beta < \beta_{min}$, where the filtered error increases with desreasing time constant.

Finally, to allow choice of the integrator time constant p, it is necessary to assign a value to b_1 in equation 5.13. Since in

this case it was assumed that the filter was operating as a variable gain, then the value of b_1 is irrelevant if $a_0 b_1 = a_1$. For compatibility with equation 5.14 it should be assumed that $b_1 = b_{1max}$. The SRL enhancement due to equations 5.13 and 5.14 can now be plotted as a function of β for various values of p. This allows p to be chosen so as to achieve a given value of SRL enhancement in the transition between modelling by a variable gain and by a single pole. Such a plot is shown in Figure 5.17, and it can be seen that a value of p = 100 μS guarantees 6 dB SRL enhancement for any value of unknown system time constant. Thus 100 μS is the value of integrator time constant chosen for the signal integrators. Assuming perfect integration, this gives a gain of 14.5 dB at 300 Hz.

In this analysis it has been assumed that the adaptive filter models very small time consants by a variable gain, that as the time constant increases a_0 abruptly goes to zero, and that the filter then begins to model the time constant by a larger one. In practice the transition can be expected to be more gradual, however in Section 5.3.2 the above analysis will be seen to provide a reasonable model for the behaviour of the pole-zero adaptive filter.

5.2.1.3 The Effect of Leaky Integration on the Adaption Algorithm

In the analysis of the previous sections, it was assumed that the pole-zero filter correctly optimises its parameters, and the effect of leaky integration on the error surface was examined. In this section it is shown that the use of a leaky integrator has a significant effect on the performance of the adaption circuitry.

When the adaptive filter attempts to model a single pole system, the adaption circuitry calculates the cross-powers between the integrator outputs and the error signal, and adjusts the filter

parameters so as to minimise the respective cross-powers (Figure 5.14). Consider for example the cross-power between two sinusoidal signals which are displaced in phase by an angle ψ:-

$$P = \frac{1}{2\pi} \int_0^{2\pi} \cos(\omega t)\cos(\omega t+\psi)dt = (\cos\psi)/2$$

This fuction is plotted in Figure 5.18, and it can be seen that if ψ = $\pi/2$, then the cross-power is zero.

Thus if β = 0 and the integrators are perfect (i.e. they provide 90° phase shift), then there is no cross-power between either of the integrator outputs and the input signal. If the sum of the a_1 and b_1 signal multiplier outputs is zero, then a_0 alone controls the error signal, which is in phase with the input signal. The cross-powers driving the a_1 and b_1 parameters are therefore zero, i.e. the absolute values of a_1 and b_1 are irrelevant, provided that $a_1 = b_1 a_0$

If the signal integrators are leaky, they provide less than $\pi/2$ phase shift, and depending on the magnitude of the integrator inaccuracy, there are small positive cross-powers between the error signal and the integrator outputs, even when $a_1 = b_1 a_0$ This drives a_1 and b_1 towards their maximum values, and in effect the filter models a simple gain by the combination of a_0 and a superimposed pole-zero pair at the highest possible frequency. This effect is useful in that it "biases" the circuit towards poles and zeros at infinity. The transition between modelling a short time constant by an adaptive gain and by a single pole is thus eased. It also helps to ensure the stability of the filter, as will be seen in the next section.

Assuming imperfect integrators, then as the unknown system's time constant increases, the total phase shift between the b_1 integrator's output and the error signal (which is assumed in-phase with the input signal) tends towards $\pi/2$, and eventually exceeds $\pi/2$.

Parameter b_1 then begins to be driven in the opposite direction to that previously described, i.e. towards $b_1 = 0$. The filter thus begins to converge, but this does not occur until a certain minimum time constant, which depends on the extent of the integrator inaccuracy and the bandwidth of the input signal. This contrasts with the case of perfect integrators, where any small phase shift due to the unknown system causes a small negative cross-power to drive the filter's parameters to convergence.

5.2.1.4 The Effect of D.C. Offsets

In Section 5.1.1.2 it was seen that the most significant d.c. offsets were the parameter control multiplier output offsets and the parameter control integrator input offsets. These offsets were seen to limit the precision with which the adaptive filter could approach its optimum parameters, i.e. a minimum level of error was requred to produce a d.c. signal at each multiplier output to balance the offset voltages. This is also true of the pole-zero filter, and the control amplifiers Ae, Aa_0, Aa_1 and Ab_1 are used to ensure that very small error signals can produce sufficient d.c. signals at the multiplier outputs to balance the offsets.

The pole-zero filter however, because of the existence in some cases of a distributed minimum, is particurlarly susceptable to the effect of d.c. offsets. Thus if the d.c. offset at the input to the b_1 integrator tended to drive b_1 negative, then the resulting adaptive filter would be unstable without error filtering. In the previous section it was seen that the use of a leaky integrator biases the filter towards poles at infinity ($b_1 = b_{1max}$), rather than at zero, and this helps to ensure the stability of the filter. Similarly, the effect of the leaky integrator is that b_1 must become

less than -q, rather than 0, before the filter becomes unstable. In the experimental filter, it was found that the value of b_1 never became negative.

In the previous section it was seen that the use of a leaky integrator can cause the adaption algorithm not to converge until a certain minimum phase shift is provided by the unknown system. This effect can be accentuated by the d.c. offsets at the inputs to the a_1 and b_1 control integrators, since these must be balanced before a_1 and b_1 begin to converge. Alternatively, the d.c. offsets may be of such a polarity as to add to, rather than subtract from, the cross-powers driving a_1 and b_1. Further discussion of the effects of d.c. offsets is included in Section 5.3.

5.3 Results for the Pole-Zero Adaptive Filter

In this section results are presented for the performance of the pole-zero filter, adapting against a variety of unknown systems, with both sinusoidal and wideband excitation. This allows the effect of non-ideal integration and d.c. offsets to be quantified. Section 5.3.4 gives the results for the steady state performance of the filter against simulated subscriber's lines, and in Section 5.3.5 the results for the dynamic performance are presented.

5.3.1 Unknown Systems Consisting of a Simple Gain

Figure 5.19 shows the filtered RLE achieved by the pole-zero filter, adapting against a short circuit, for various input signal levels and at frequencies of 300 Hz, 1 kHz, and 3.4 kHz, where the filtered error signal was used for the measurements. It can be seen

that the performance of the filter in general falls linearly with decreasing input signal level. This is due to the constant noise floor of the filter (Section 5.1.2.1). At high input signal levels the RLE decreases with decreasing input signal frequency. This effect occurs because the signal integrators (Ix and Id in Figure 5.14) have a low frequency gain of 10, and performance is limited by the distortion produced by the a_1 and b_1 signal multipliers. This distortion was found to consist mostly of the 2nd harmonic of the input signal frequency.

At low input signal levels the performance of the filter again drops with increasing input signal frequency. This occurs because the roll-off of the responses of the control amplifiers Aa_0, Aa_1 and Ab_1 reduces the cross-powers driving the filter parameters, which begin to drift under the influence of d.c. offsets.

Figure 5.20 shows the filtered RL achieved by the filter as a function of the input signal frequency, for unknown systems whose transfer functions are +1, 0, and -1, where the input signal level is 0 dB. In the open circuit case the value of b_1 is irrelevant, since $d(t) = 0$. Under these circumstances the optimum values for a_0 and a_1 are zero. This minimises the effects of low frequency distortion in the a_1 signal multiplier, and results in performance superior to the +1 and -1 cases.

When the transfer function of the unknown system is ± 1, all three signal multipliers produce output signals (due to the distributed minimum). This results in harmonic distortion at low frequencies, causing the observed drop in return loss. The differing results for +1 and -1 are due to asymmetry in the a_1 multiplier's overload characteristic, caused by the a_1 offset voltage.

5.3.2 Complex Unknown Systems

For sinusoidal input signals and complex unknown systems, the pole-zero filter is not necessarily required to match the transfer function of the unknown system, since the error signal can be made zero by matching the desired signal in amplitude and phase. In this case the behaviour of the filter is determined by non-idealities, e.g. d.c. offsets, leaky integration, etc. In this section attention is concentrated on the behaviour of the filter with wideband input signals, since this represents the worst case, although some results for sinusoidal excitation are included at the end of this section.

Some understanding of the operation of the pole-zero filter can be gained by investigation of its performance against unknown systems consisting of a simple variable pole. Figure 5.21d shows the filtered ERLE for such a system, where the excitation is white noise, bandlimited to 500 Hz to 2.5 KHz, at level -6 dB (Figure 5.19). The values of the filter parameters are shown in Figures 5.21a, b and c .

For time constants less than 60 μS the values of a_1 and b_1 are constant, while a_0 decreases with increasing time constant. This corresponds to the filter modelling the unknown system by a variable gain (a_0), a variable zero ($-a_1/a_0 p$ rads/sec), and a fixed pole ($-b_1/p$ rads/sec). As the time constant increases the position of the zero also increases, and its effect on the error signal becomes negligable. Furthermore, if the fixed pole frequency is also high, the filter effectively models the unknown system by a variable gain. Thus for $\beta < 44$ μS, the filter behaves approximately as explained in Section 5.2.1.2.

Since a_1 and b_1 have effective maximum values of approximately 2.3, due to the gain of the summing amplifier S_1 in Figure 5.14, the value of the fixed pole is $100/2.3 \approx 43$ μS. Thus

when the unknown system time constant is 43 μS a large peak is
observed in the ERLE. As the time constant increases above this
value the ERLE falls again, until at approximately 70 μS a_1 and b_1
converge and the ERLE suddenly increases. The discrepancy between
the minimum time constant which the filter can model and the time
constant at convergence, is due to the effects of leaky integration
and d.c. offsets on the adaption algorithm, as explained in Section
5.2.1.3.

When the time constant becomes greater than 2 mS the power in
$d(t)$ becomes small, and b_1 begins to diverge.

Figure 5.22 shows the performance of the pole-zero filter
with sine wave inputs of various frequencies, adapting against a
single pole unknown system. It can be seen that at high input
frequencies the filter achieves large values of filtered RLE over a
wide range of unknown system time constants. At low frequencies
however, a sharp drop in RLE is observed due to a_0 reaching its
maximum negative voltage, although the filter reconverges for higher
unknown system time constants. This effect appears to be due to
inaccurate integration at low frequencies.

5.3.3. The Pole-Zero Filter Adapting against an Artificial Line

An initial test of the performance of the filter was
conducted by allowing it to adapt against subscriber's lines which
were simulated by the artificial line and hybrid of Chapter 3. The
adaptive filter was first calibrated so that its gain, pole frequency
and zero frequency could be calculated from the measured values of
a_0, a_1 and b_1. The calibration is achieved by allowing the filter to
adapt against an unknown system whose gain and the positions of its
poles and zeros are known. The filter can then be used for system

identification, and the value of ERLE serves as a guide to the
accuracy of the identification. This facility is useful because when
the filter adapts against simulated lines, the spread of poles and
zeros of the transhybrid responses can be ascertained, and it also
allows investigation of a possible interdependence of the pole and
zero positions, or dependence of either on the line length, etc.

Figures 5.23a, b and c show the results obtained when the
filter adapts against the hybrid and artificial line, with Zb = Zl =
600 Ω, and Zt = 370 Ω, 620 Ω, 0.31 μF. (This value of terminating
impedance was chosen because it ensures proper control of sidetone,
as explained in Section 1.3.) For comparison the results obtained
using the same transhybrid responses, simulated on the line and
hybrid simulator (LHS) are also shown.

Figure 5.23a shows the estimated positions of the poles and
zeros which lie in the left-hand s-plane. Poles or zeros at
positions outside the range shown are recorded at the extremes of the
range. Figure 5.23b shows the equivalent range in the right-hand
s-plane. Figure 5.23c shows the measured values of the original ERL
and cancelled ERL, where the original simulated and artificial ERLs
were approximately equal.

For all line lengths above 0.1 mile the transhybrid response
is modelled by zeros in the right-hand s-plane, and the filtered
cancelled ERL is always greater than 24 dB. Both the pole and the
zero frequencies initially decrease with increasing line length,
although for line lengths above 3.5 miles they are approximately
constant. Similarly the original ERL and filtered cancelled ERL
decrease with increasing line length. For very short line lengths
there is a large discrepancy between the estimated simulated response
and the estimated artificial response. This is probably due to small
differences between the actual hybrid and the simulated hybrid, or

between the actual line characteristics and the simulated line characteristics, since the original ERL is greater than 30 dB and these effects could be signficant.

5.3.4 The Pole-Zero Filter Adapting against Simulated Lines

To obtain an estimate of the echo performance which could be obtained by using the pole-zero filter in an adaptive hybrid, the filter was allowed to converge against simulated subscribers' lines. These lines were chosen from the 1845 line survey described in Chapter 2, and simulated as described in Chapter 3, with the hybrid given by; $Zb = 600\ \Omega$, and $Zt = 370\ \Omega$, $620\ \Omega$, $0.31\ \mu F$, and the load impedance as that of the measured 706-type telephone. Since measurement of the filter's performance against all 1845 lines would be impractical, a subset of lines was selected. To facilitate this selection the lines were first sorted in order of increasing original ERL, and every 25th line was selected for inclusion in the subset. The total number of lines in the subset was then increased to 100 by selecting further lines from those at the extremes of original ERL. The filter was allowed to adapt against these lines with input excitation of white noise, bandlimited to 500 Hz to 2.5 KHz, at level -2.5 dB.

The results presented in the following sections are based on measurements of the unfiltered error. This signal is obtained by passing the filtered error through the the system shown in Figure 5.24, whose response is:-

$$\frac{E(s)}{E'(s)} = \frac{1}{1 + b'_1/(q'+sp')}$$

5.15

Thus if $q'=q$, $p'=p$ and $b'_1=b_1$, then $E(s)$ is the unfiltered error signal. In the experimental pole-zero filter the response of the

circuit was adjusted, using two potentiometers, so that with $a_0 = a_1$ = 0, E(s) matched D(s) to within 0.25 dB over the range 300 Hz - 3.4 kHz. In an implementation of an adaptive hybrid using the pole-zero filter, it would be necessary to achieve this matching without adjustment.

Figure 5.25 shows a scatter plot of the results obtained from the measurements of original ERL and cancelled ERL, where the relevant statistics are given in Table 5.1. In these and in the following figures the x-axis indicates the number of the line in the subset of lines chosen from the 1845 line sample. The original ERL of the lines increases from left to right, as shown in Figure 5.25. The values of cancelled ERL bear no relationship to the original ERL values. The scatter plot of the lengths of the chosen lines is shown in Figure 5.26, and the correlation between the value of the original ERL and the length of the line is evident.

The scatter plots of the positions of the estimated poles and zeros of the transhybrid response are shown in Figures 5.27 and 5.28 respectively. Poles and zeros above the maximum frequency are plotted at the maximum frequency, since the adaptive filter is inaccurate for very high frequency poles and zeros with the given excitation bandwidth. Both plots show a correlation between the line length (Figure 5.26) and the position of the pole or zero, the longer lines having the lower pole and zero positions. The majority of lines have zeros in the right-hand s-plane, although some short lines appear to produce both a pole and a zero in the left hand s-plane. These lines were found to be modellable by a variable gain and zero, or in some cases by a variable gain.

5.3.5 Results for the Convergence of the Pole-Zero Filter

The results of the previous sections describe the steady
state performance of the pole-zero filter. The dynamic response of
the filter is also important, since in practice it is required to
converge quickly when subscribers' lines are connected. Moreover,
when near-end speech is present, the adaption circuitry may need to
be disabled, and the filter may be required to reconverge when
near-end speech ceases. This section reports results obtained for
the convergence of the pole-zero filter against simulated
subscribers' lines.

5.3.5.1 Dynamic Measurement of the Error Signal

Figure 5.29 shows a simplified block diagram of the system
used to measure the dynamic performance of the pole-zero filter. The
error signal is half-wave rectified and low-pass filtered by an RC
filter. Thus the d.c. output of the filter is proportional to the
power of the error signal. The time constant of the RC filter is 44
mS. This gives adequate rejection of signal components in the
rectifier output, but allows the system to respond quickly (relative
to the adaptive filter response) to transients due to the convergence
of the filter. The combination of rectifier and filter therefore
functions as an envelope detector, and the output of the detector is
displayed on a digital storage oscilloscope (DSO). Switch Sw2 is
used to prevent the system from responding to transients due to
loading transhybrid responses into the LHS, while switch Sw1 is used
to examine the convergence of the adaptive filter from initial
application of the input signal.

5.3.5.2 Convergence from Zero Input Signal

Between the time when two subscribers are connected, and before speech has begun, the parameters of the adaptive filter used in an adaptive hybrid drift under the control of d.c. offsets. The final value of the filter parameters (and thus the time taken for the filter to converge) depends on the response being adapted to. Figures 5.28 and 5.29 show the spread of responses to which the filter must adapt, and to obtain a realistic spread of convergence times, 21 equally spaced lines were therefore selected from those of Figures 5.28 and 5.29. For each of these lines the filter was first allowed to drift by setting the LHS output to zero and opening Sw1. Sw2 was then opened and the transhybrid response of the line was loaded into the LHS. Sw1 and Sw2 were then closed and the dynamic performance of the filter was measured on the oscilloscope.

Figure 5.30 shows a typical oscilloscope trace obtained by following this procedure. The initial steep rising edge is due to the rise time of the RC filter. The maximum value of the trace is used as a measure of the initial ERL due to the combination of the adaptive filter and the subscriber's line. The error then decreases slowly as the adaptive filter converges. By measuring the power of the LHS output signal, the time taken to achieve any given value of ERLE can be calculated from a trace such as Figure 5.30.

The values of initial ERL measured for each of the selected lines are shown in Figure 5.31. For the best case line only 1.6 dB initial ERL is achieved, while for most of the lines the initial ERL is negative. It is therefore clear that the pole-zero filter cannot be allowed to begin convergence from a condition controlled by d.c. offsets, and some initial conditions must be imposed on the filter parameters. Table 5.2 records the mean and standard

deviations of the times required to achieve 0, 6 and 10 dB ERLE, averaged over the 21 lines. The table shows that even if the initial gain across the combination of adaptive filter and hybrid were acceptable, no improvement in ERL is achieved by the filter until 2.4 S after the input signal is applied. Ideally the filter should provide some improvement in ERL within a few syllables of speech.

5.3.5.3 The Rate of Convergence

As shown in Figure 5.30, the power in the error signal decreases linearly with time as the filter converges. Thus the rate of convergence of the filter can be expressed as:-

$$R = \{20\log_{10}(v_1/v_2)\}/(t_2-t_1) \text{ dB/Sec}$$

where v_1 is the envelope detector output at time t_1, and v_2 is the output at time t_2. The dependence of the rate of convergence on the input signal level is shown in Figure 5.32. In this case the filter was allowed to adapt, from zero input signal, against the line whose poles and zeros lay approximately half way between the extremes shown in Figures 5.27 and 5.28. The rate of convergence decreases with decreasing signal level, although the change is small over the first 10 dB of the dynamic range of the filter.

5.3.5.4 Convergence with Imposed Initial Conditions

If some initial conditions are imposed on the parameters of the adaptive filter before the input signal is applied to it, then by a suitable choice of the conditions it should be possible to considerably improve the dynamic performance of the filter. Suitable initial conditions would be an estimate of the parameter values required to model the mean transhybrid response.

Initial conditions can be imposed on the parameters of the experimental pole-zero filter by allowing it to adapt against a chosen initial transhybrid response. The transhybrid response is then altered to that of the required subscriber's line, and convergence of the error signal can be observed. The initial transhybrid response chosen was that whose pole and zero lay half way between the extreme pole and zero positions. Table 5.3 shows the longest times taken to achieve 0, 6 and 10 dB ERLE for the lines whose responses lay at either extreme. The high frequency pole and zero case (short lines) gives the worst performance, indicating that a slight improvement could be gained by altering the choice of initial conditions. Nonetheless, 6 dB ERLE was provided within 460 mS in the worst case, and the initial ERL was always greater than 9 dB.

5.4 Discussion

In this chapter it has been seen that neither the simple gain nor the single pole adaptive filter can accurately model most subscriber's lines. The pole-zero adaptive filter was shown to be capable of modelling large time constants, but incapable of accurately modelling a range of small time constants. To control this problem a method of designing the integrator in the filter was proposed.

The static performance of the pole-zero filter, adapting against simulated transhybrid responses, is more than adequate for use in an adaptive hybrid. The dynamic performance of the filter is inadequate however, and it was shown that some method of storing a set of initial conditions for the filter parameters is essential. These initial conditions could be common to the adaptive hybrids of

all subscribers' lines, and could be imposed at the parameter control integrators, as is commonly done in analog computing.

A major problem in the implementation of an adaptive hybrid using the pole-zero filter, is the need to accurately compensate for the effects of error filtering on near-end speech signals. This compensation should be such that the passband ripple specification for the near-end channel is not breached. This may require the use of high accuracy components in certain sections of the filter, and strict control of the b_1 offset voltage. The stability of the pole-zero filter can be guaranteed by allowing only positive values of b_1, provided that the b_1 offset voltage can be sufficiently reduced.

Simple polarity multiplication could be used for the control multipliers, and if the output offset of the multipliers can be kept small, then improvements in both the static and dynamic performance of the adaptive hybrid will result.

The problem of divergence of the filter parameters during near-end speech has not been examined, but since the filter uses an instantaneous error criterion, some form of near-end speech detection is necessary. Thus the parameter control integrators could be disconnected from the control multipliers on detection of near-end speech, and the filter parameters held until near-end speech ceases. If large values of integration capacitor are used, and the integrator operational amplifiers have low input offset currents, then the rate of drift of the filter parameters should be low.

Although the pole-zero filter can perform well in an adaptive hybrid, the conclusion to this chapter must be that sufficient problems of implementation remain to warrant the investigation of digital adaptive filters.

	Mean	Std Dev	Min	Max
Cancelled ERL (dB)	35.3	2.4	28.4	39.7
ERLE (dB)	26.7	3.2	20.0	31.7

Table 5.1   Performance of the Pole-Zero Adaptive Filter against 100 Simulated Subscribers' Lines.

	t_0	t_6	t_{10}
Mean	2.4	2.7	2.9
Std Dev	0.12	0.16	0.19

Table 5.2   Mean and Standard Deviations of Times (in Seconds) to achieve 0, 6 and 10 dB ERLE.

	t_0	t_6	t_{10}
Short Lines	.38	.46	.52
Long Lines	0	.22	.40

Table 5.3   Worst Case Times (in Seconds) to achieve 0, 6 and 10 dB ERLE with Initial Conditions.
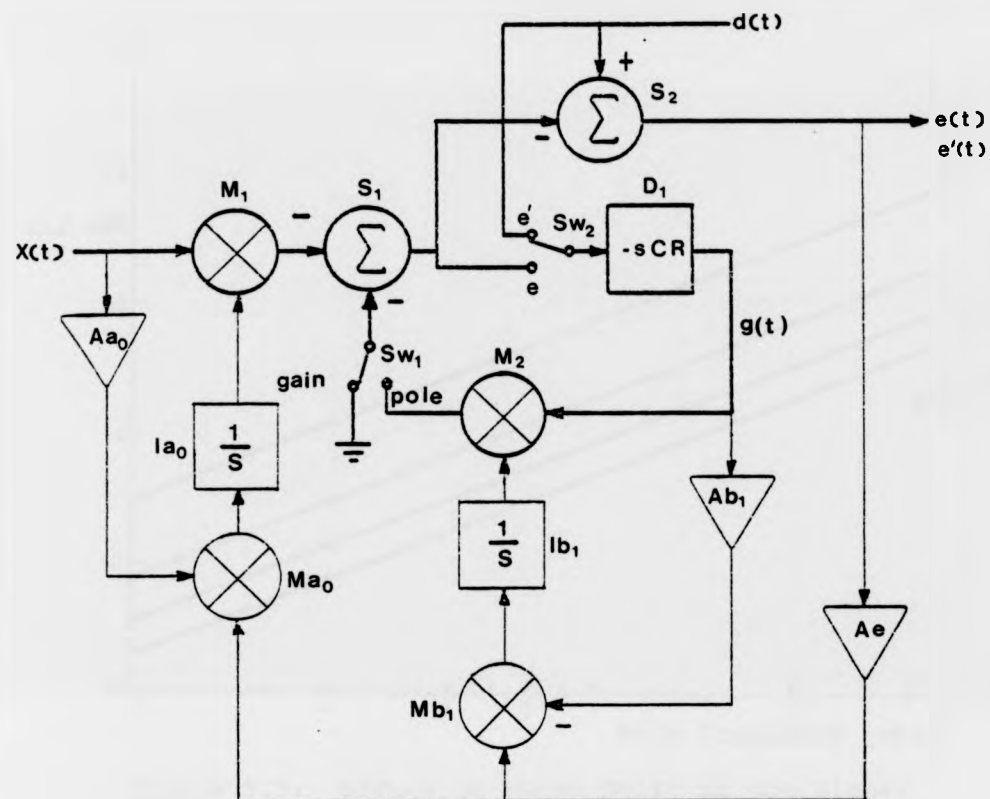
Figure 5.1: A Block Diagram of the
Single Pole Adaptive Filter
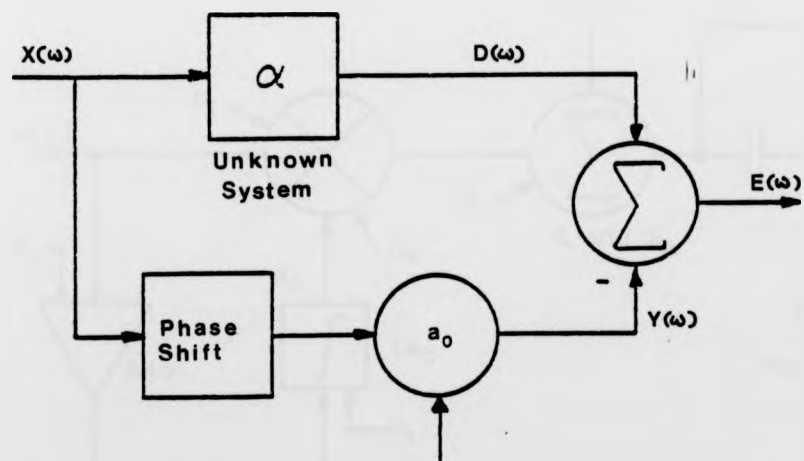
Figure 5.2: The Adaptive Gain Filter with
Phase Shift in the Signal Path
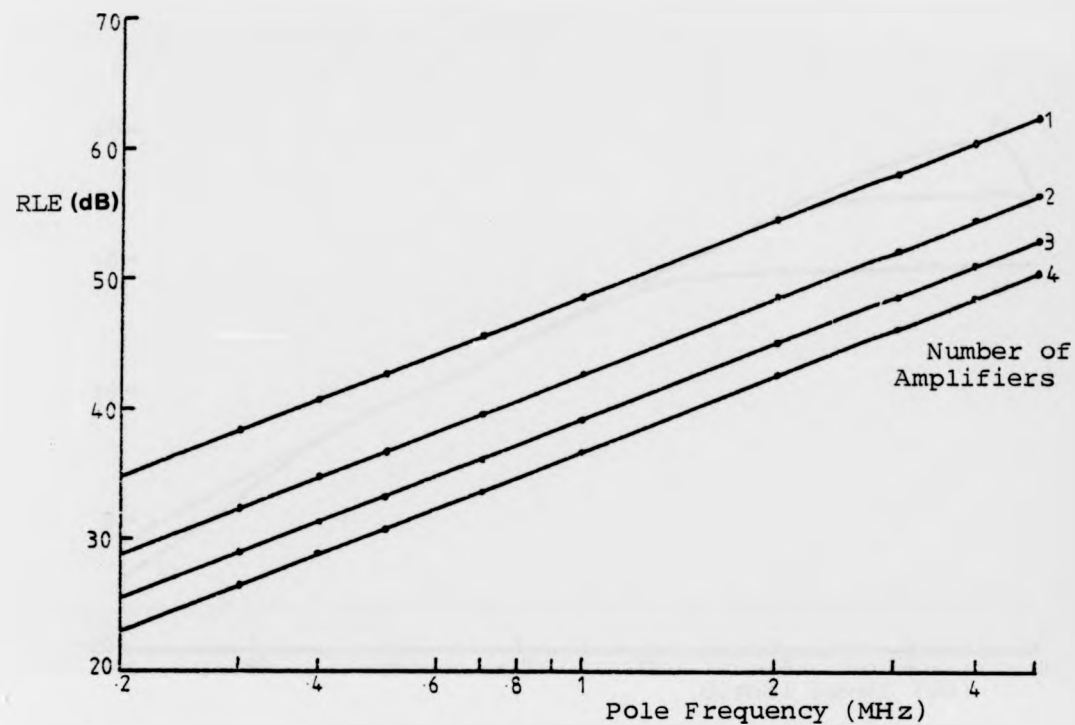
Figure 5.3: Effect of Phase Shift in the Signal
Path on the Possible RLE at 3.4 kHz
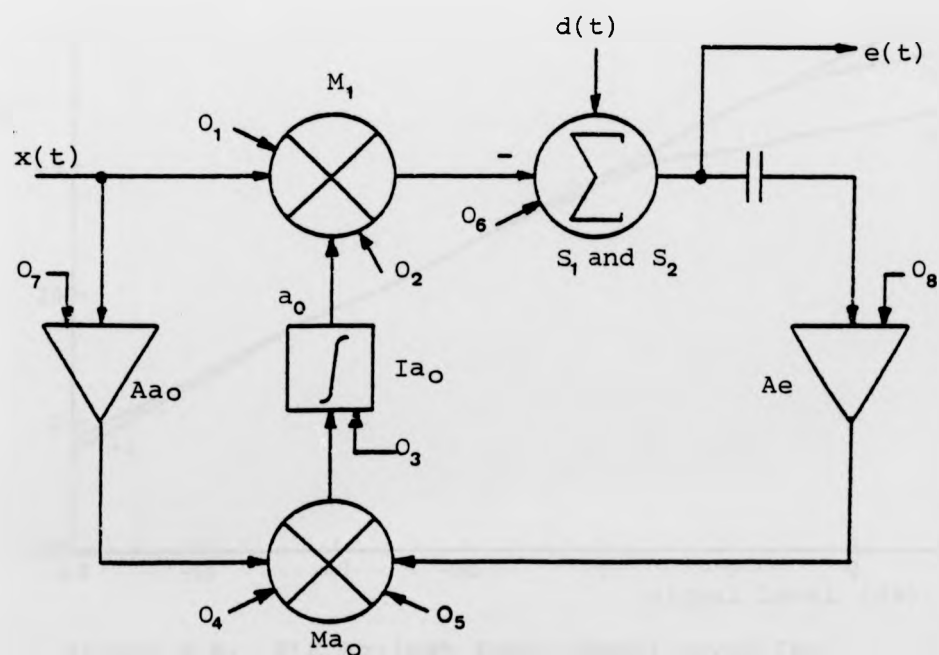
Figure 5.4: D.C. Offsets in the Adaptive Gain Circuit
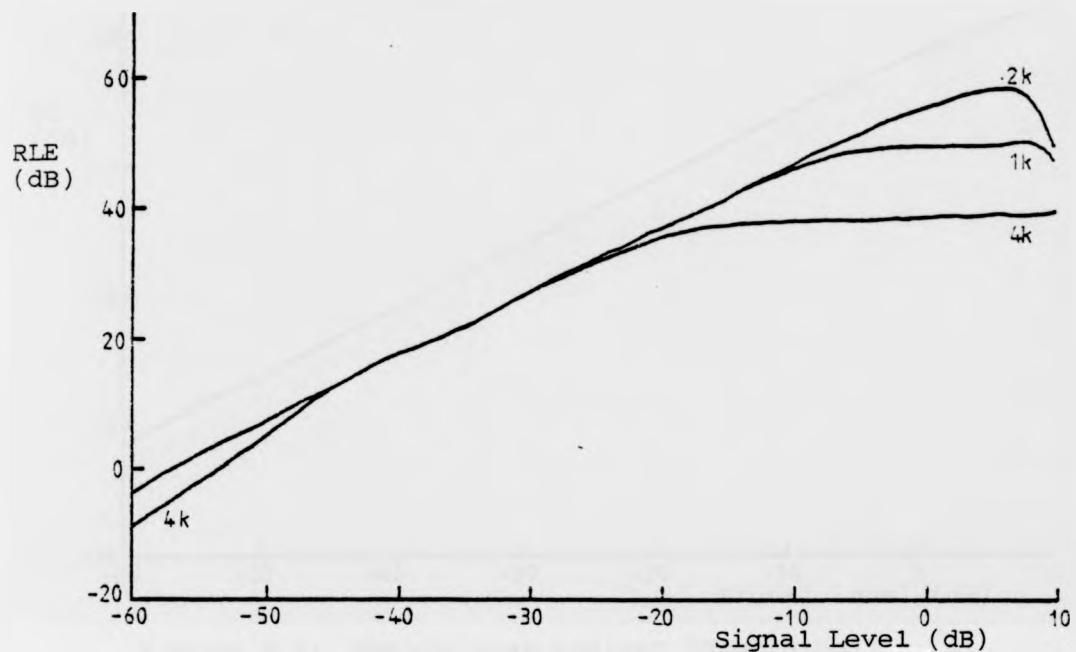
Figure 5.5: RLE Against Input Signal Level for
Various Frequencies; H(s) = 1
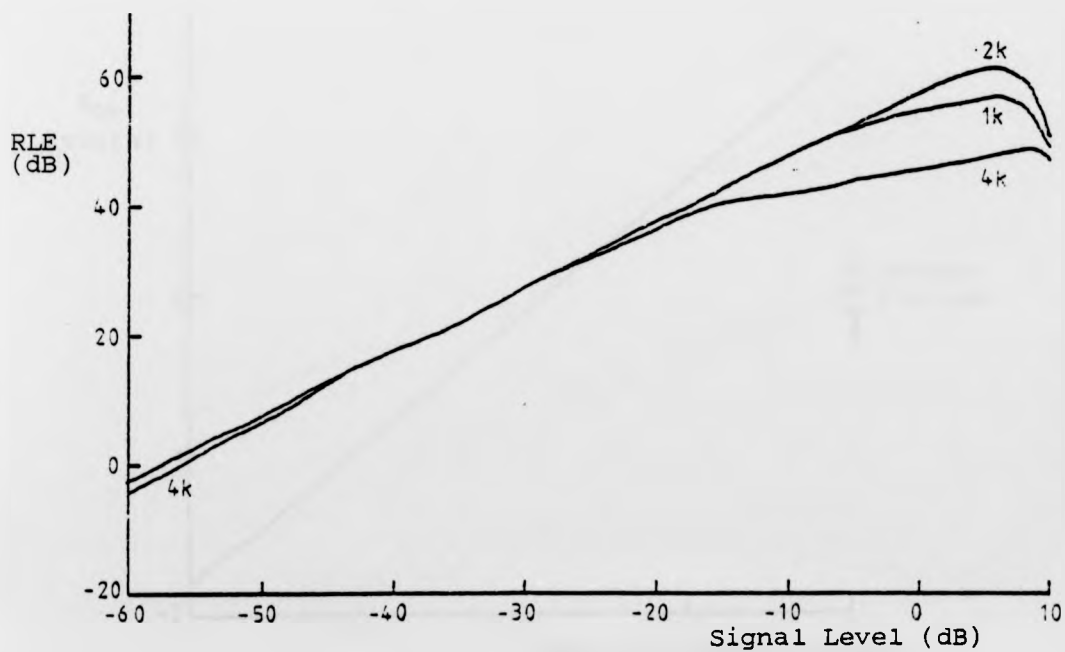
Figure 5.6: RLE Against Input Signal Level for
Various Frequencies; H(s) = -1
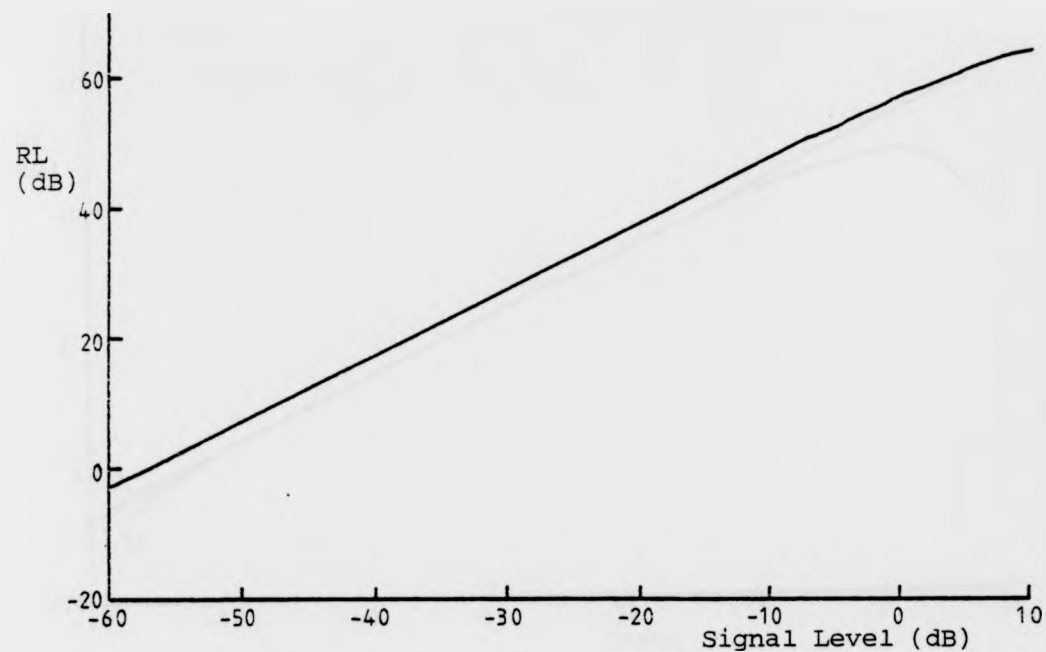
Figure 5.7:   Return Loss Against Input Signal
Level at 1 kHz; H(s) = 0
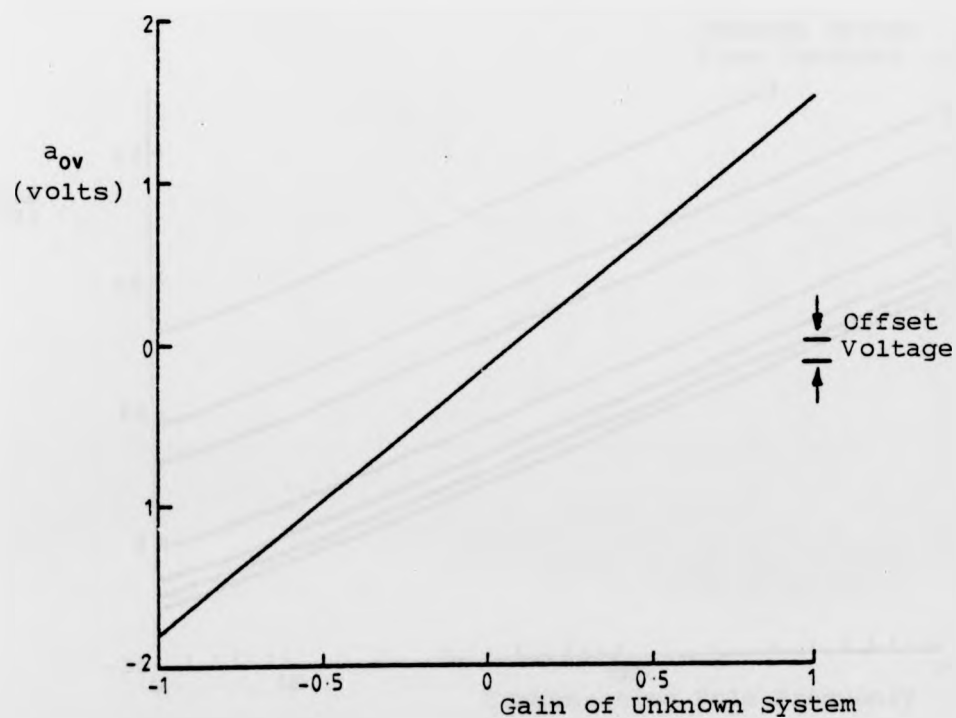
Figure 5.8:   Coefficient Voltage Versus Gain
of the Unknown System, at 1 kHz
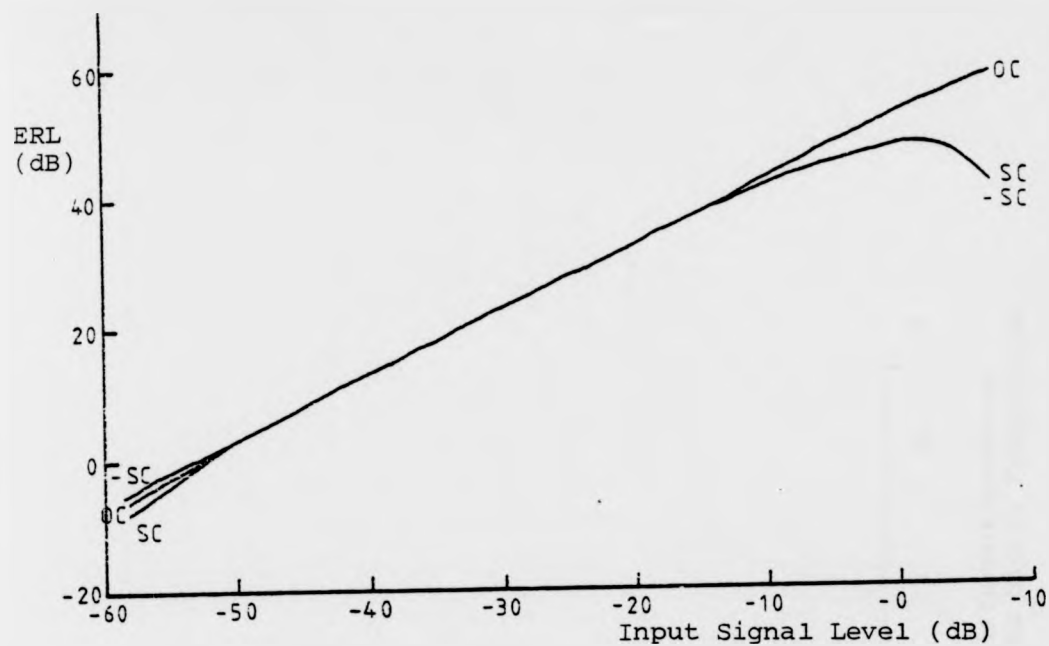
Figure 5.9: ERL Versus Input Signal Level
for Various Unknown Systems
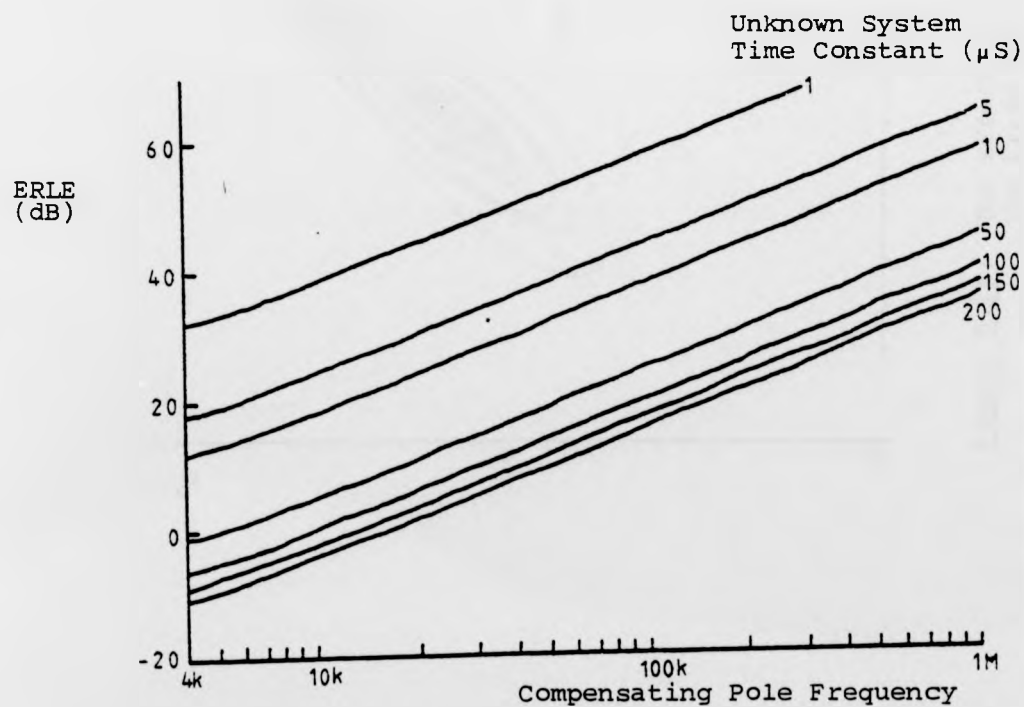
Figure 5.10: The Effect of Non-Ideal Differentiation
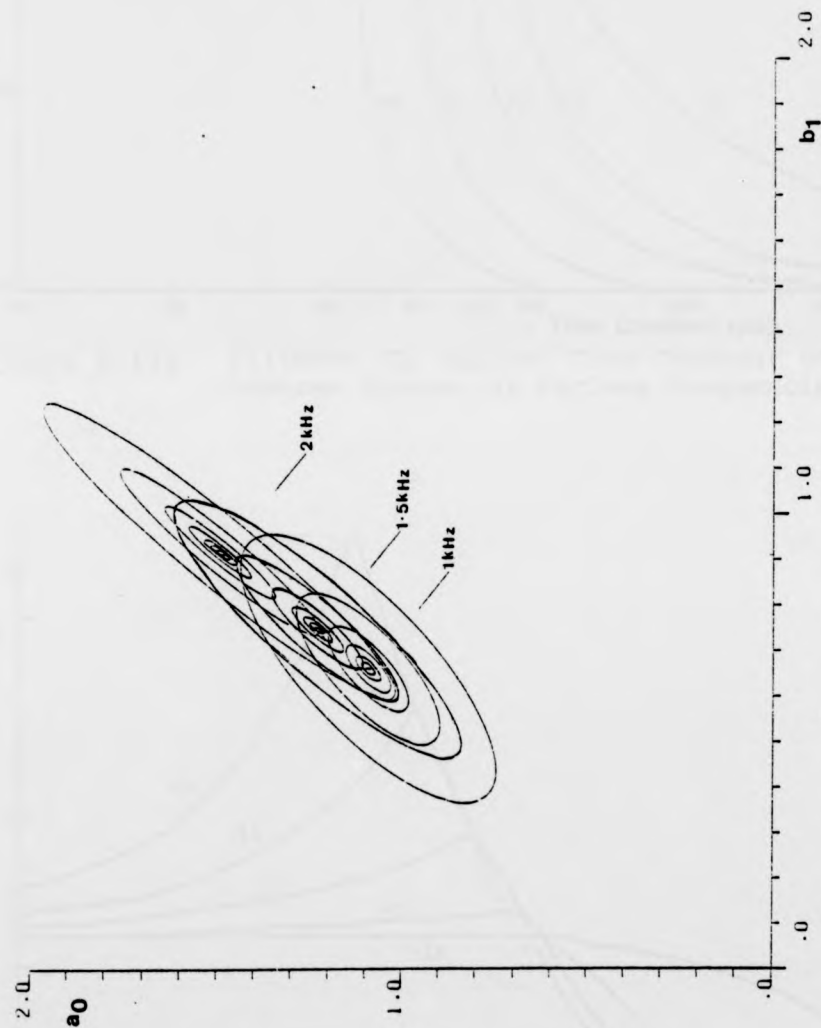
Figure 5.11: The Effect of Inaccurate Differentiation on the Error Surface at Various Signal Frequencies
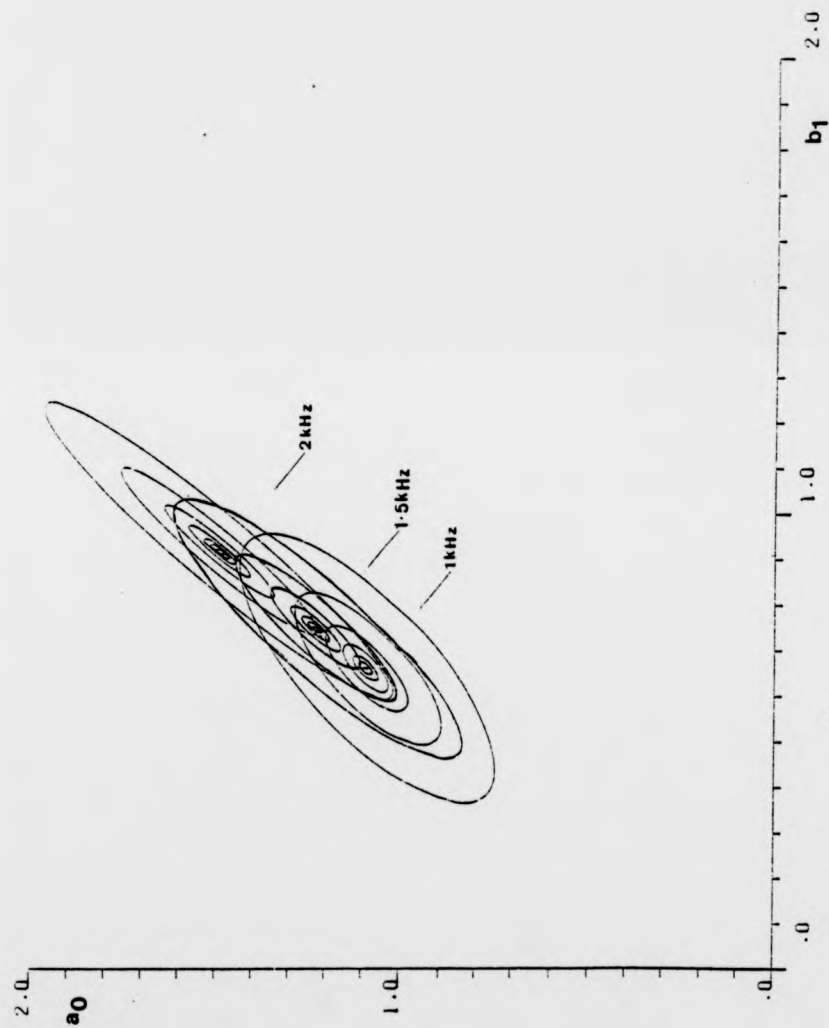
Figure 5.11: The Effect of Inaccurate Differentiation on the Error Surface at Various Signal Frequencies
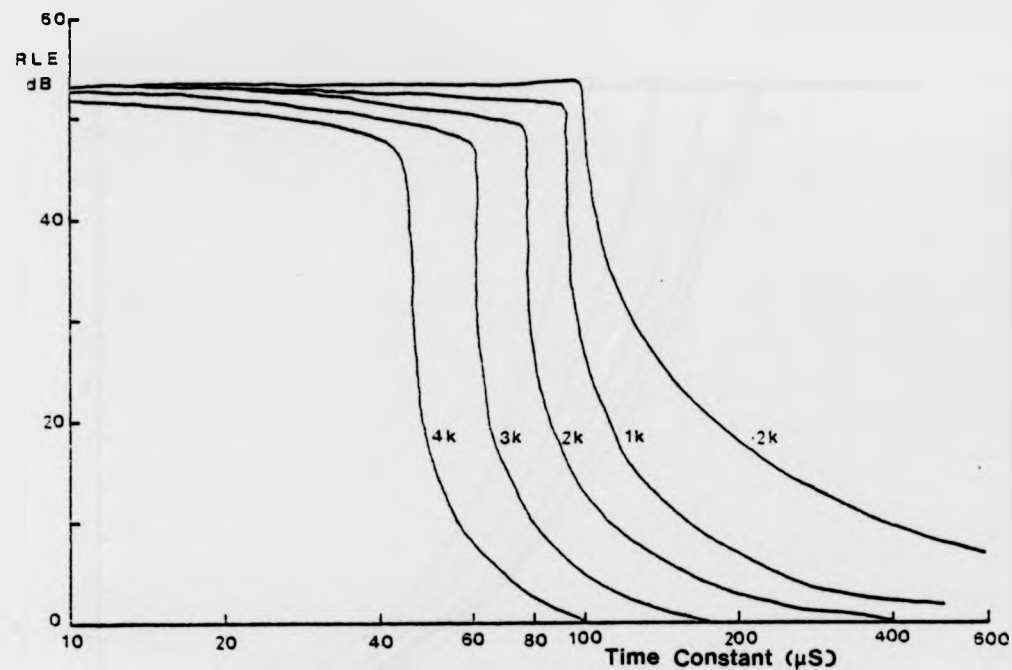
Figure 5.12a: Filtered RLE Against Time Constant of Unknown System, at Various Frequencies
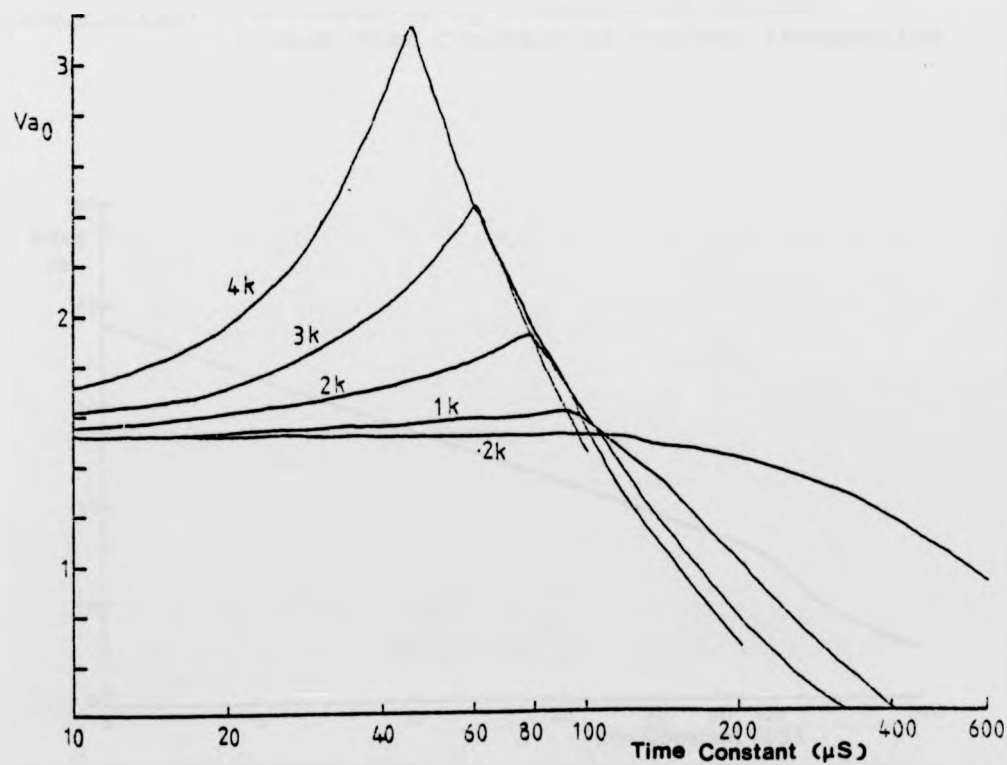
Figure 5.12b: Variation of a_0 Voltage with Time Constant of Unknown System at Various Frequencies
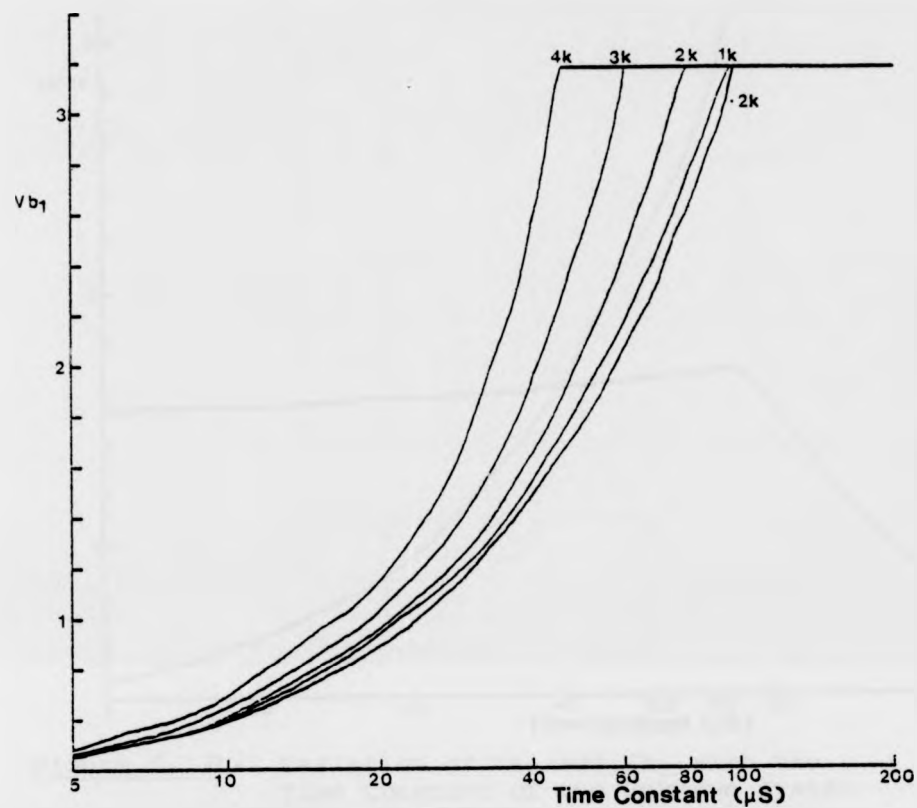
Figure 5.12c: Variation of b_1 Voltage with Unknown System Time Constant at Various Frequencies
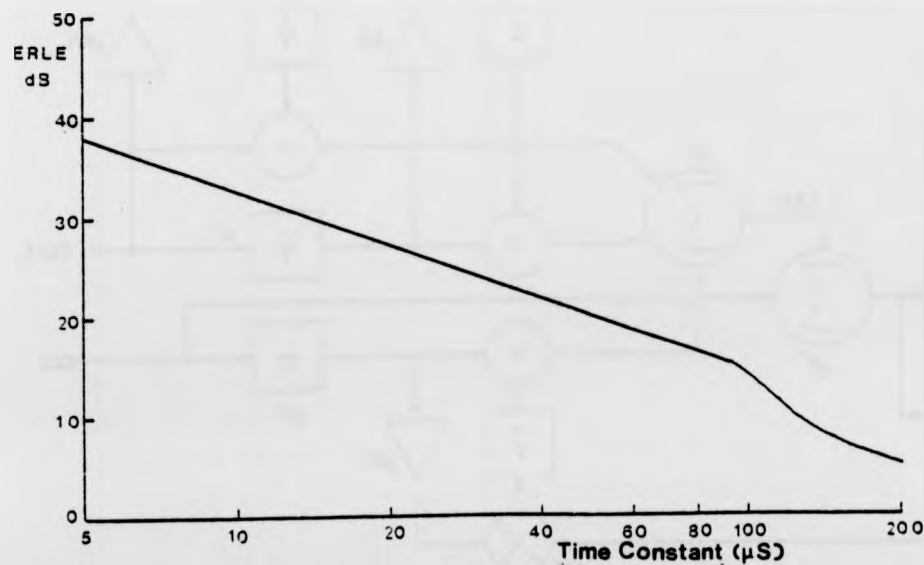
Figure 5.13a: Variation of ERLE with the Time Constant of the Unknown System
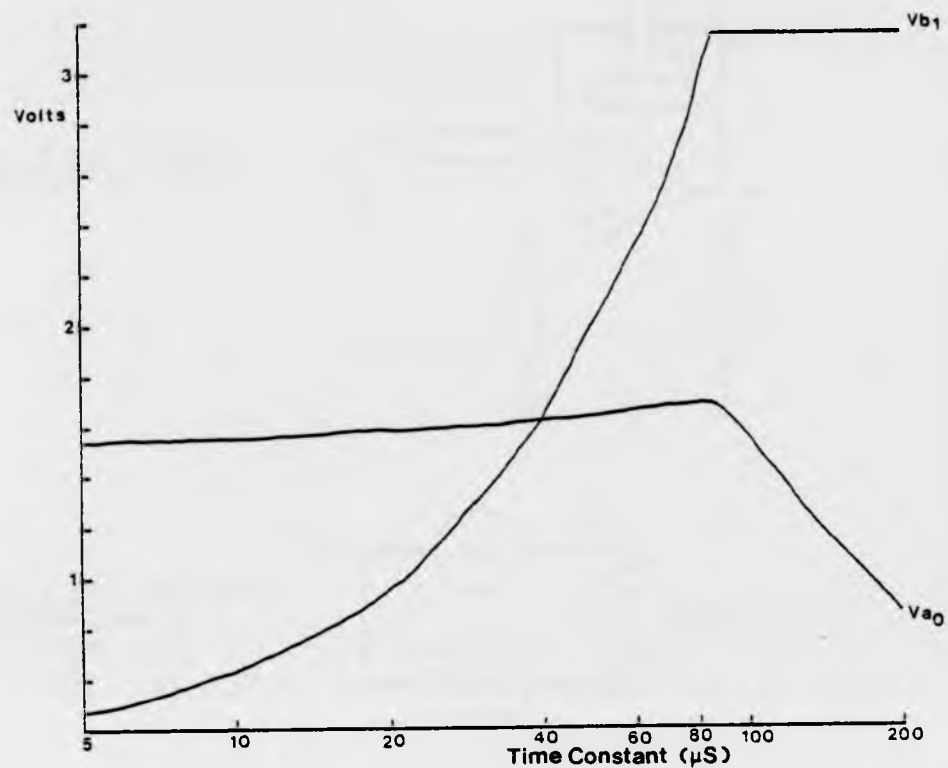
Figure 5.13b: Variation of Va_0 and Vb_1 with the Time Constant of the Unknown System
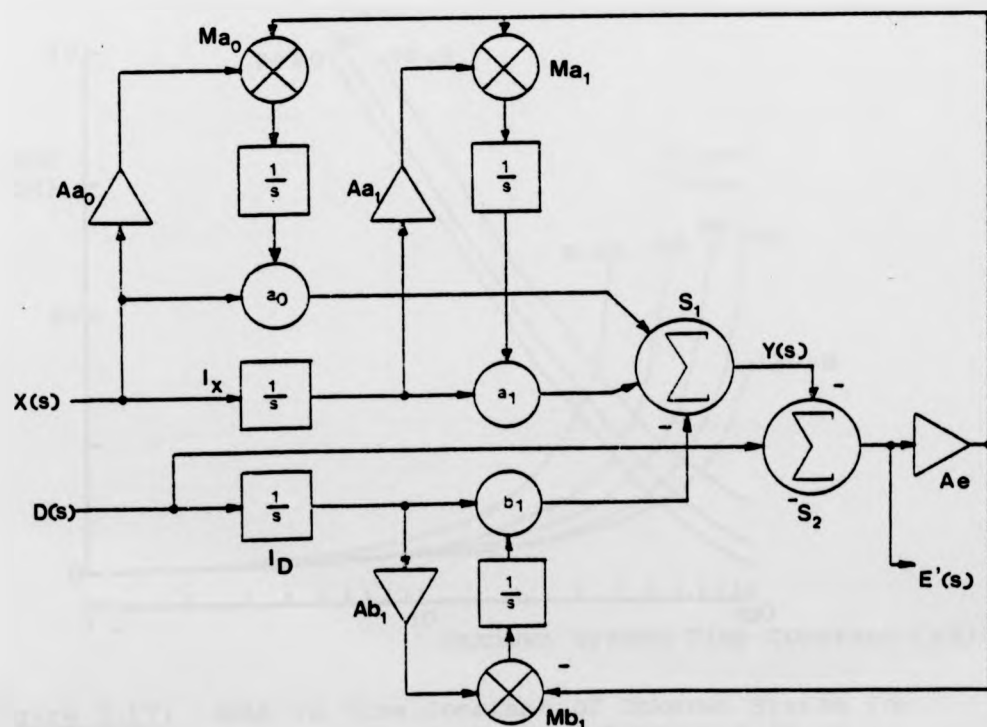
Figure 5.14: Block Diagram of a First Order Pole-Zero Filter

Figure 5.15: Leaky
Integrator Circuit
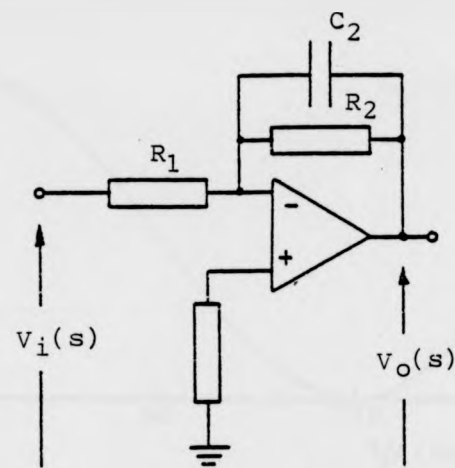
Figure 5.16: Adaptive
Gain Modelling a
Single Pole
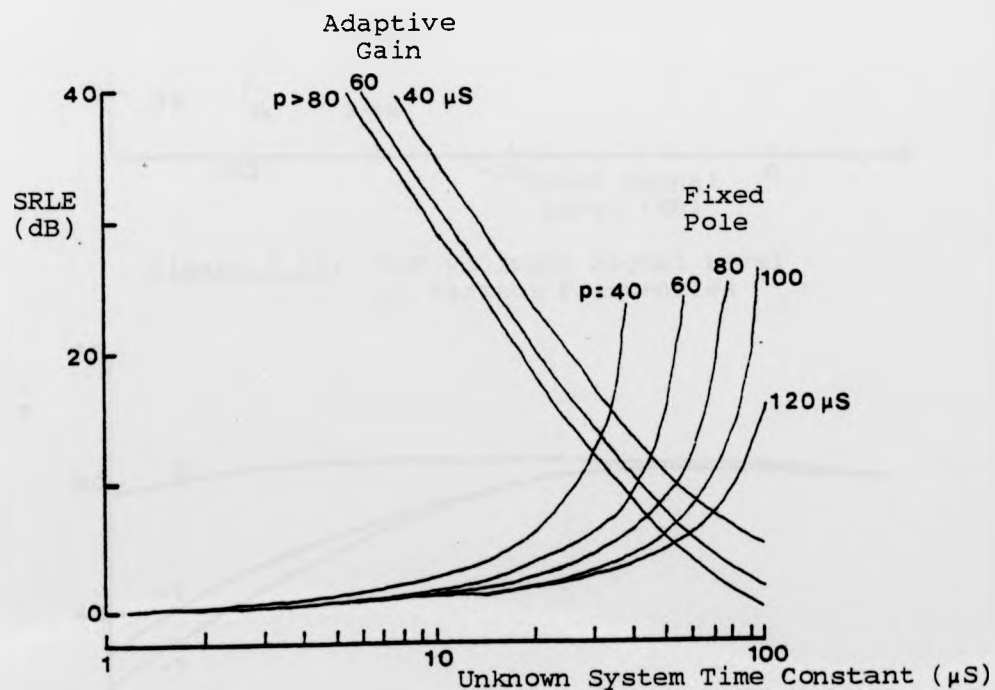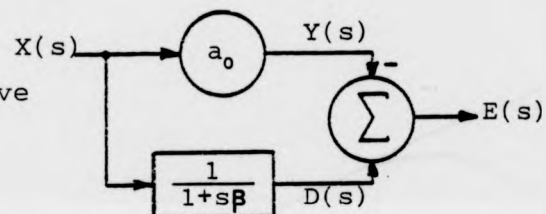
Figure 5.17: SRLE vs Time Constant of Unknown System for
Various Integrator Time Constants in μS
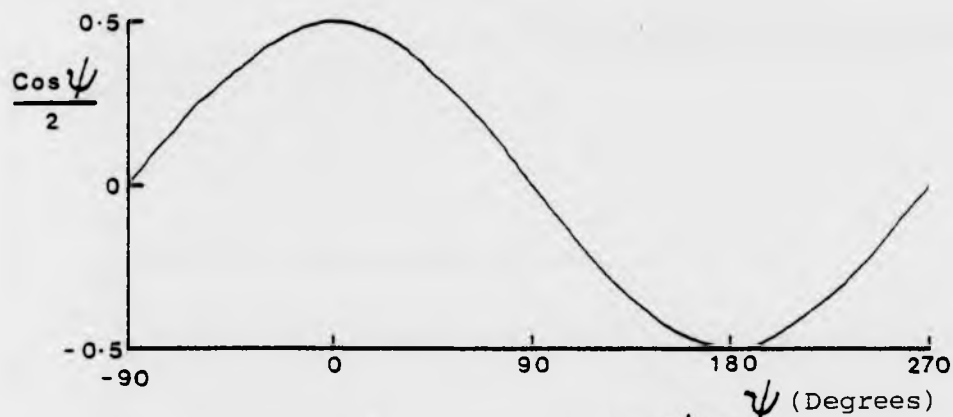
Figure 5.18: Plot of $\frac{\cos \psi}{2}$
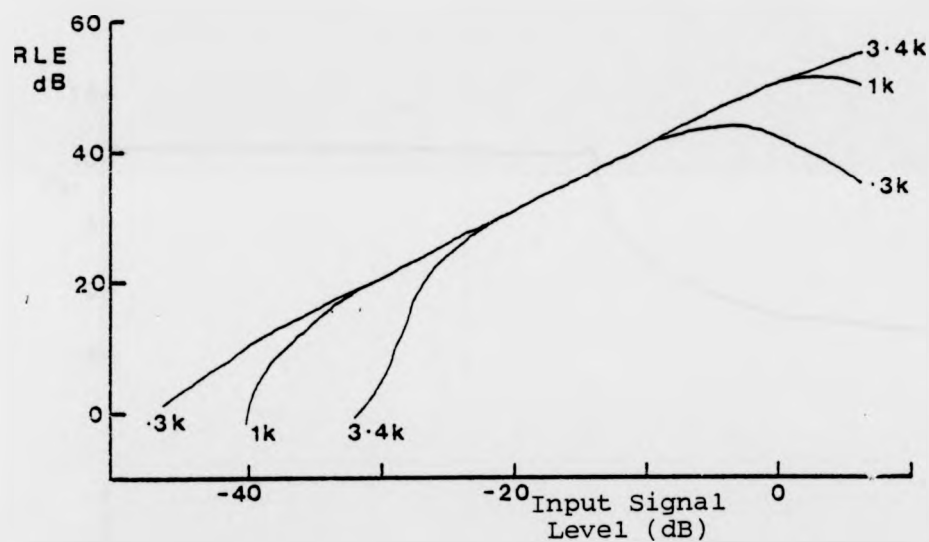
Figure 5.19: RLE vs Input Signal Level at Various Frequencies
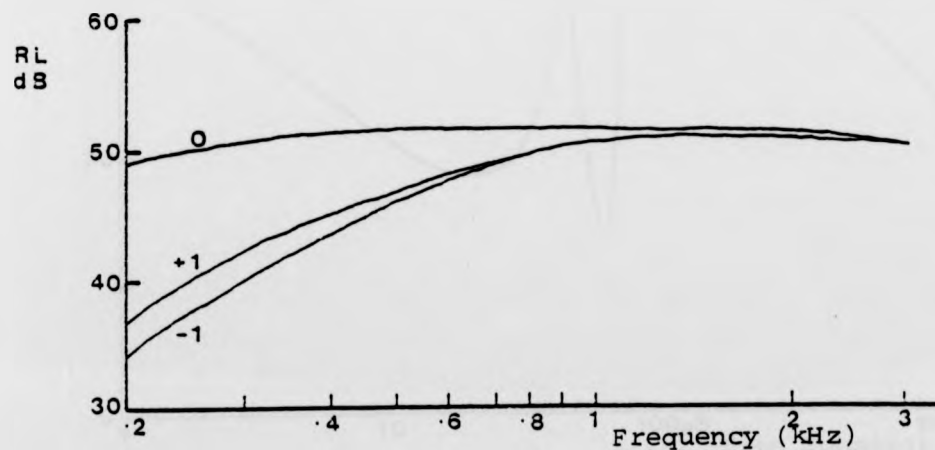
Figure 5.20: RL vs Frequency for Various Unknown Systems
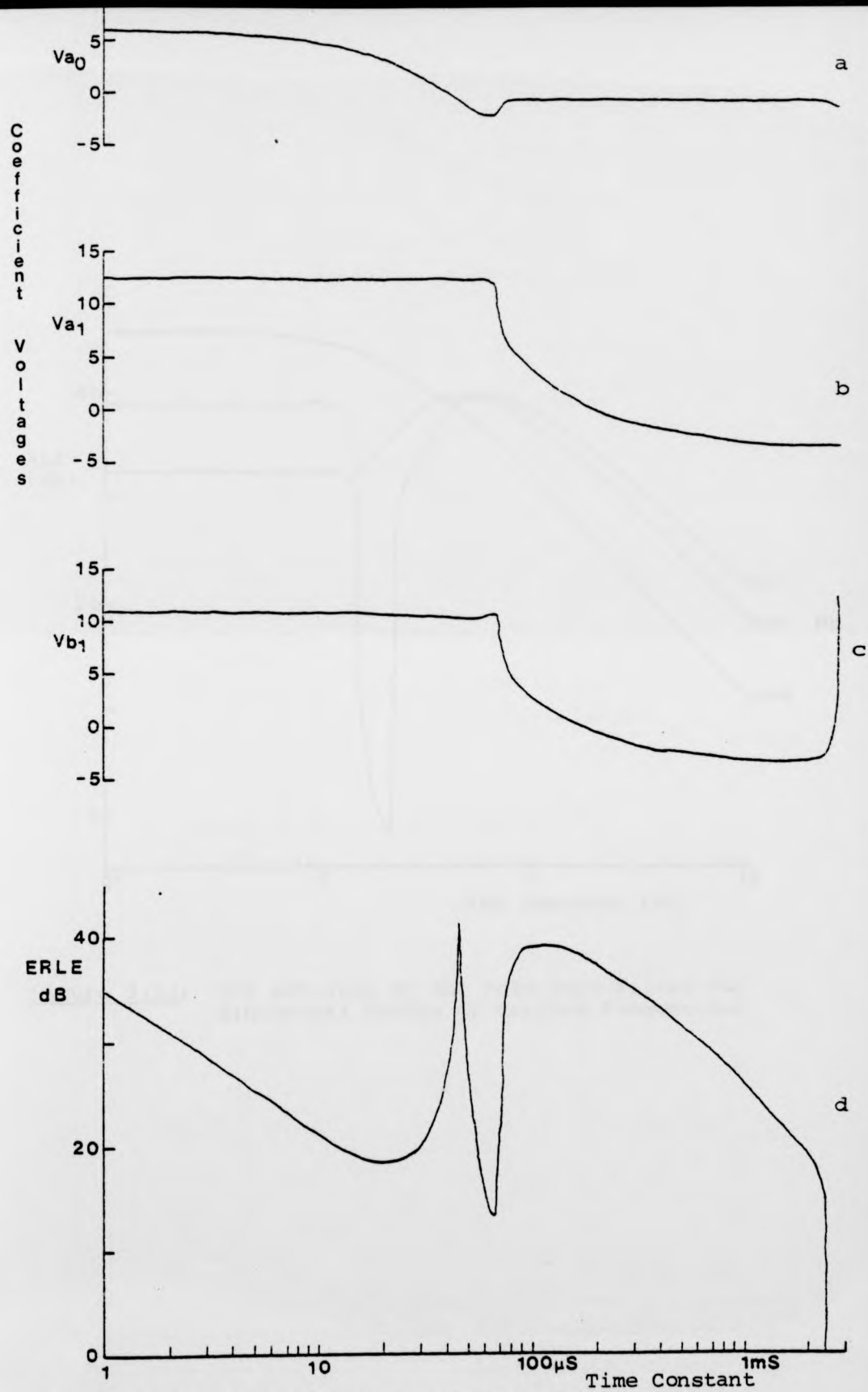
Figure 5.21: Filtered ERLE vs Unknown Time Constant
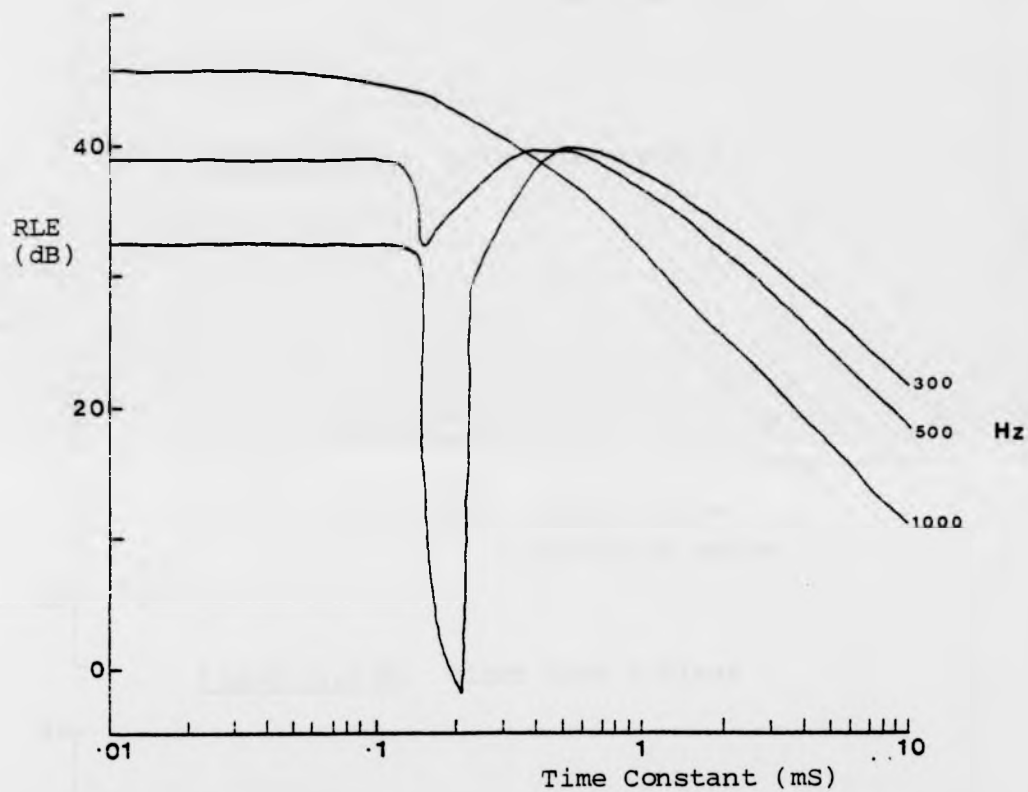
Figure 5.22: RLE Achieved by the Pole-Zero Filter for Sinusoidal Inputs of Various Frequencies

a

krads
per
sec

solid line : actual poles

x   : simulator poles
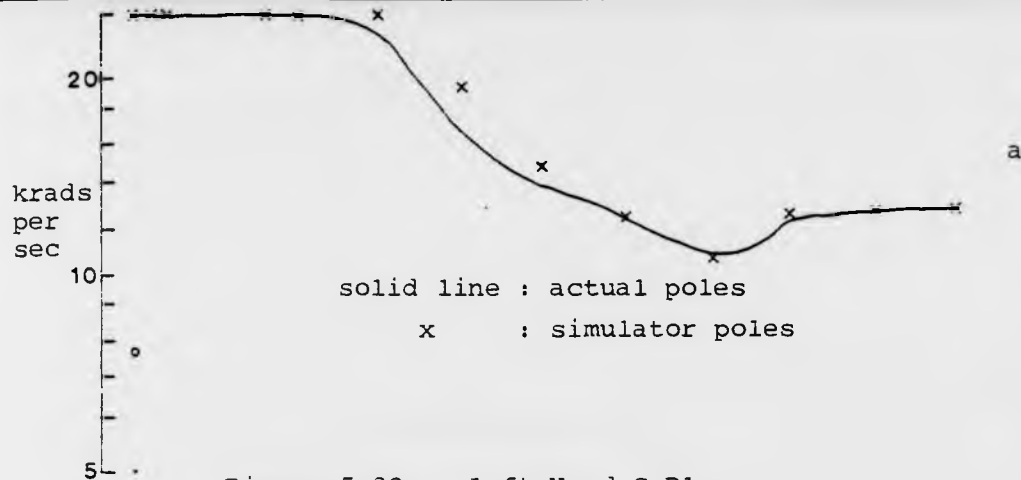
Figure 5.23a: Left Hand S-Plane

krads
per
sec

solid line : actual zeros

o   : simulator zeros
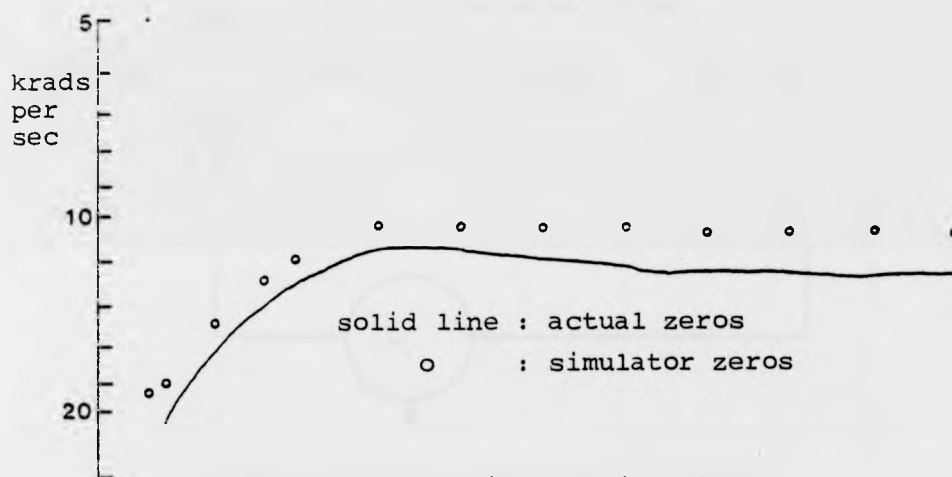
Figure 5.23b: Right Hand S-Plane

ERLE
(dB)

Cancelled ERL

$\triangle$: simulated

Original ERL

Line Length (Miles)
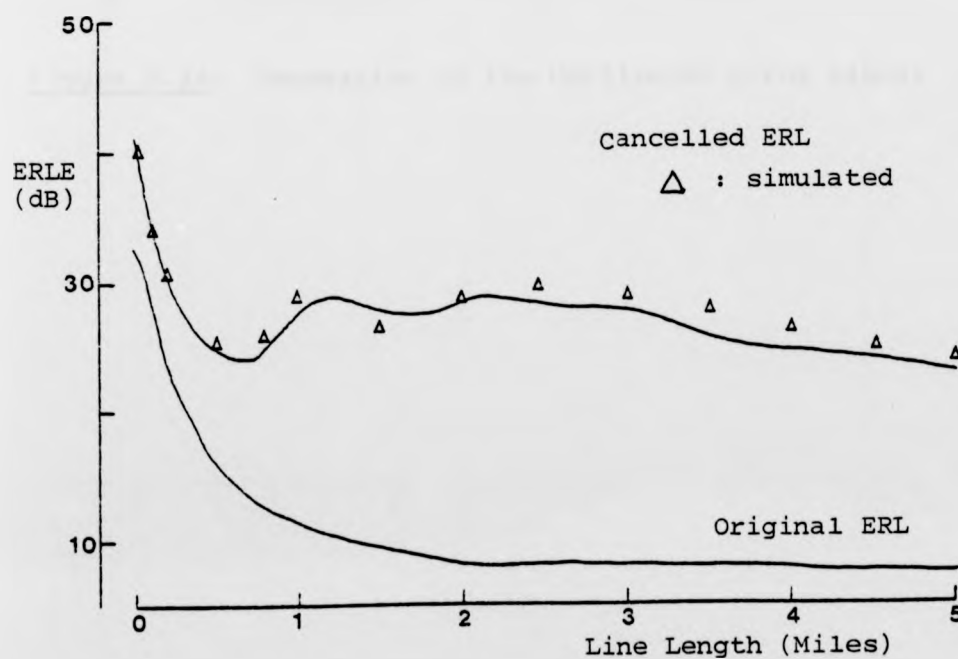
Figure 5.23: Performance of the Pole-Zero
              Filter Against an Artificial Line
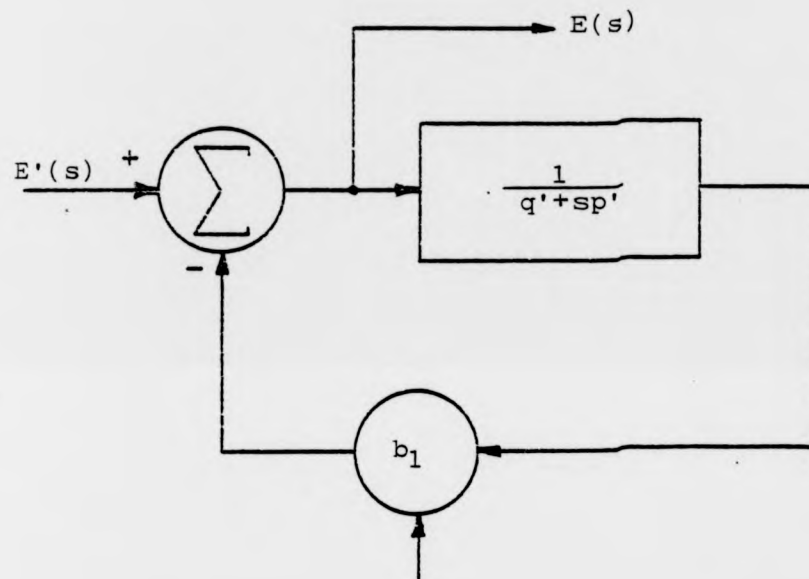
Figure 5.24: Generation of the Unfiltered Error Signal

Figure 5.25: Scatter Plot of Original ERL and Cancelled ERL of 100 Subscribers' Lines
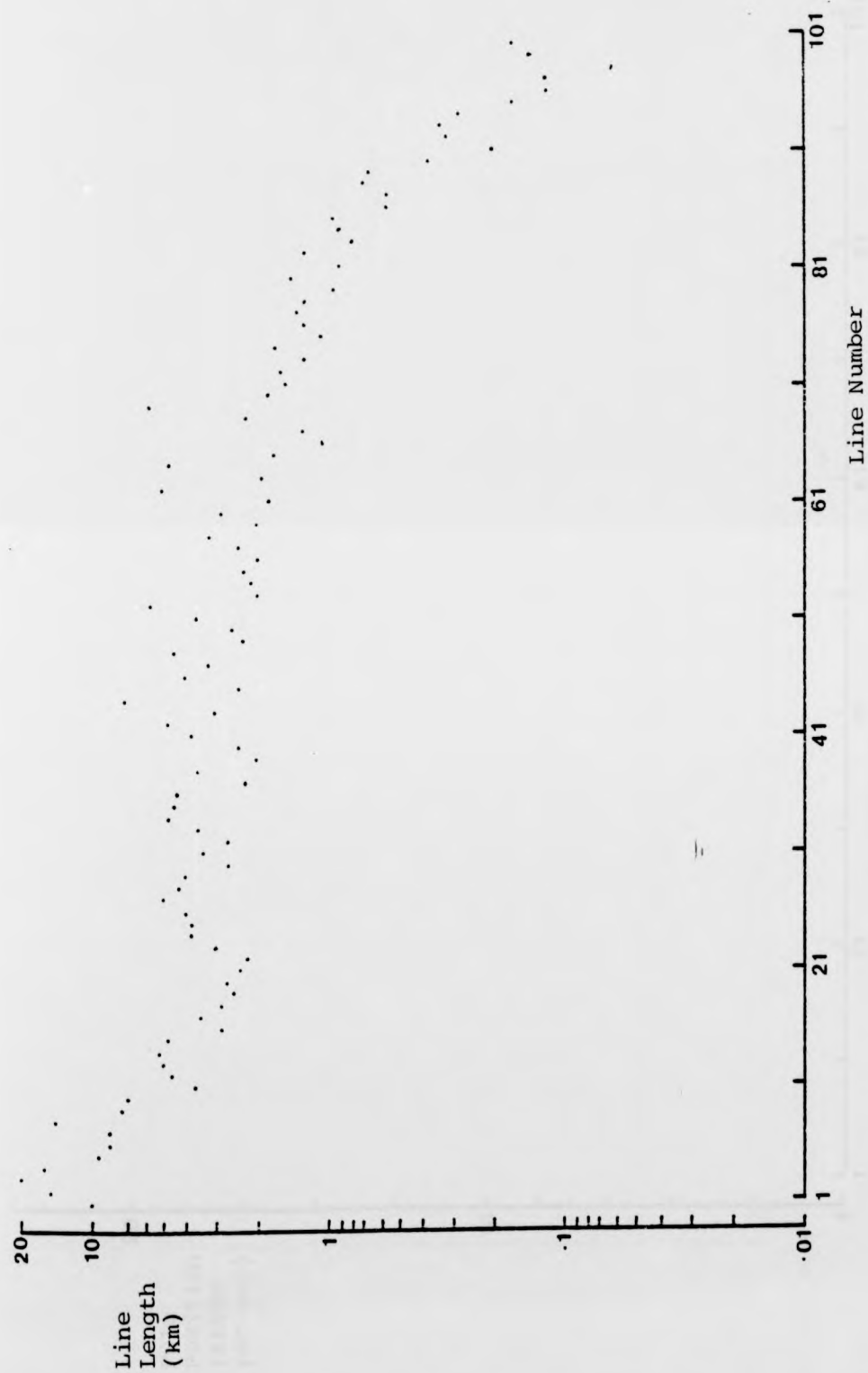
Figure 5.26: Scatter Plot of Line Lengths

Pole
Position
(krads
per sec)

Line Number
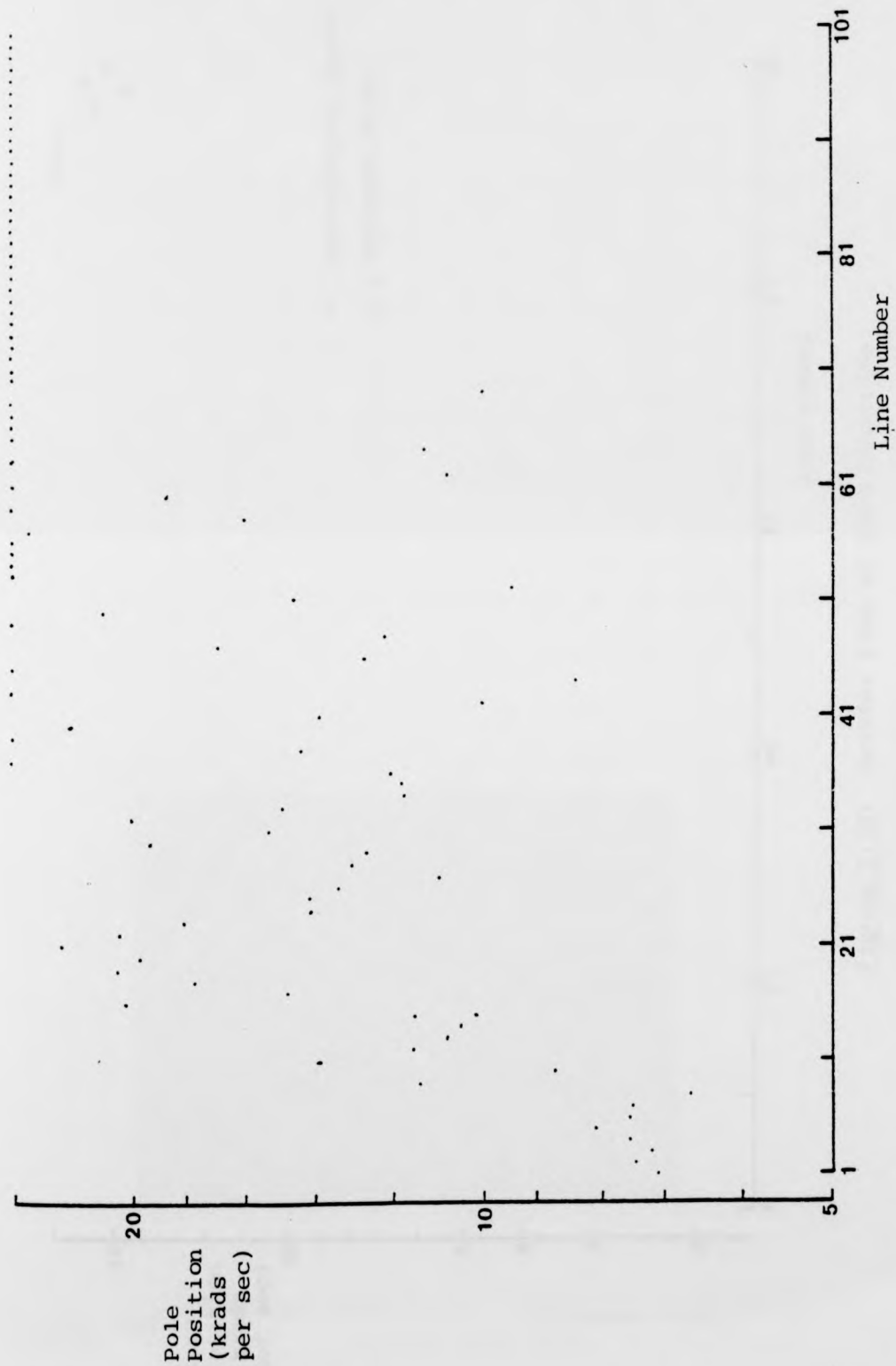
Figure 5.27: Scatter Plot of Pole Positions
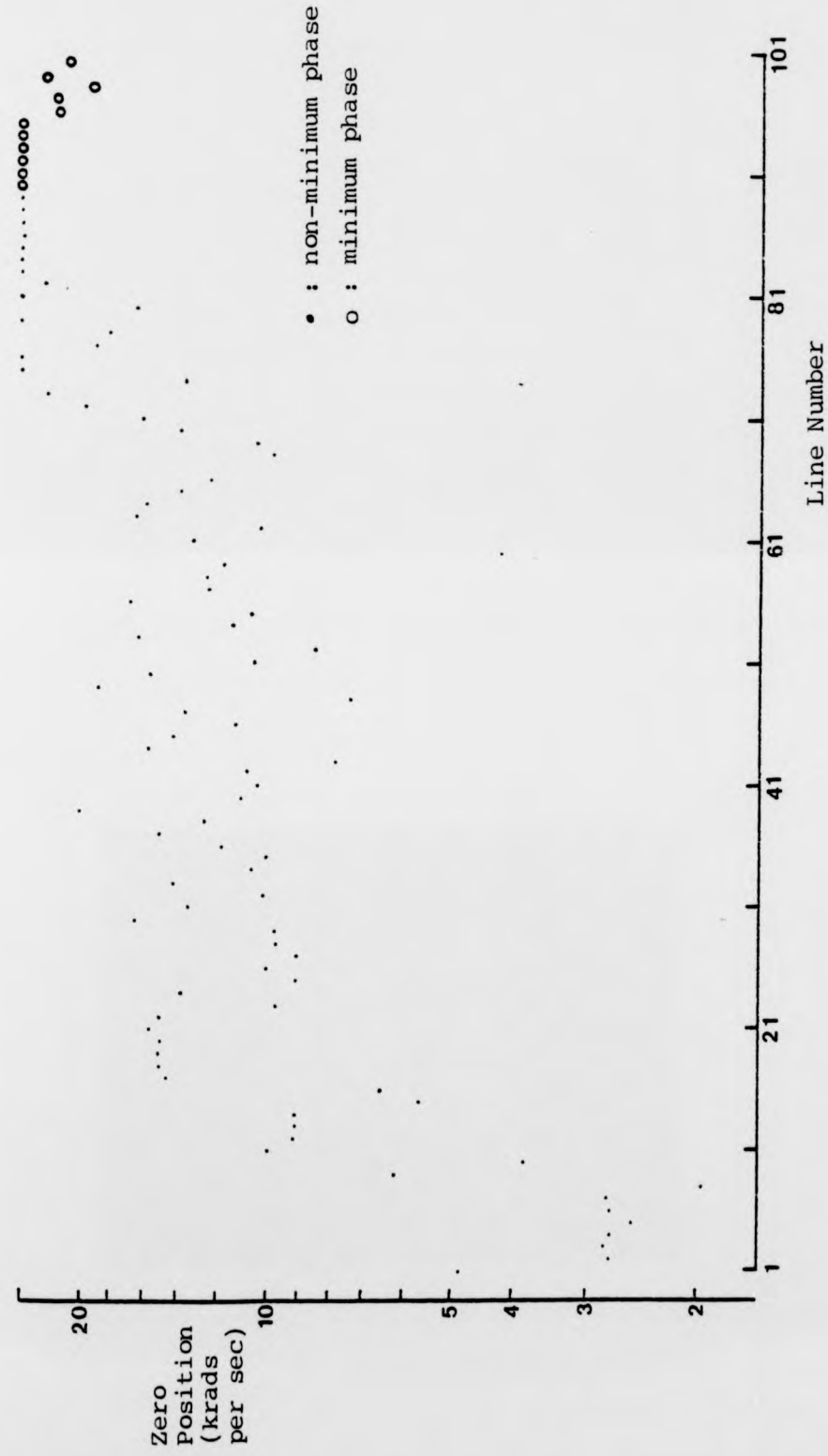
Figure 5.28: Scatter Plot of Zero Positions
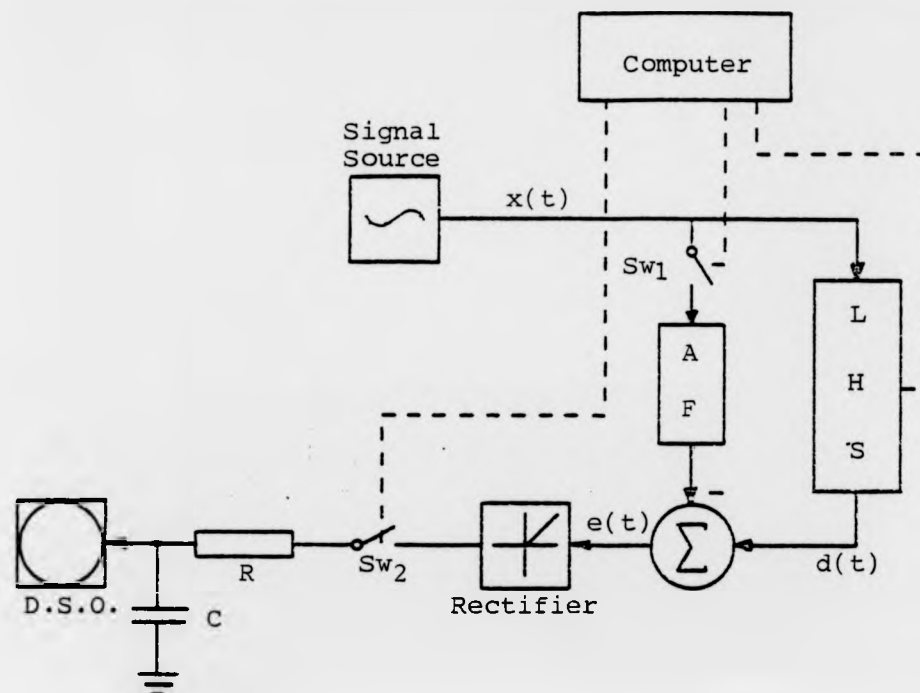
Figure 5.29: Dynamic Measurement of the Error Signal
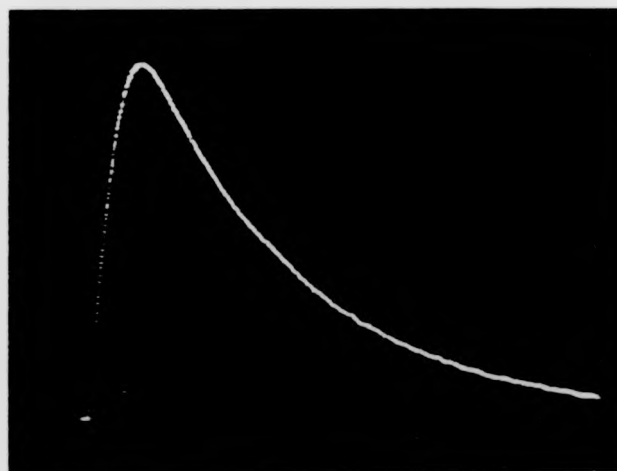
Figure 5.30: A Typical Oscilloscope Trace
Showing Convergence of the Filter
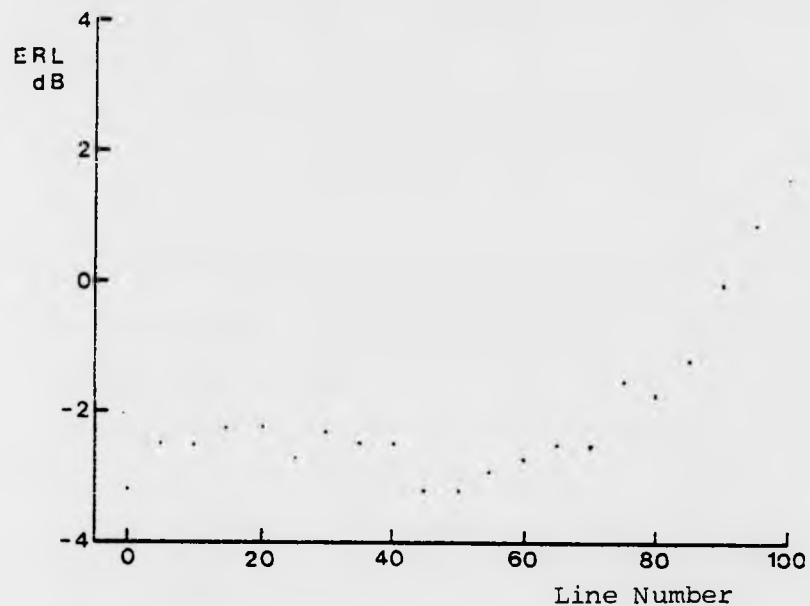
Figure 5.31: Values of Initial ERL
for 21 Selected Lines
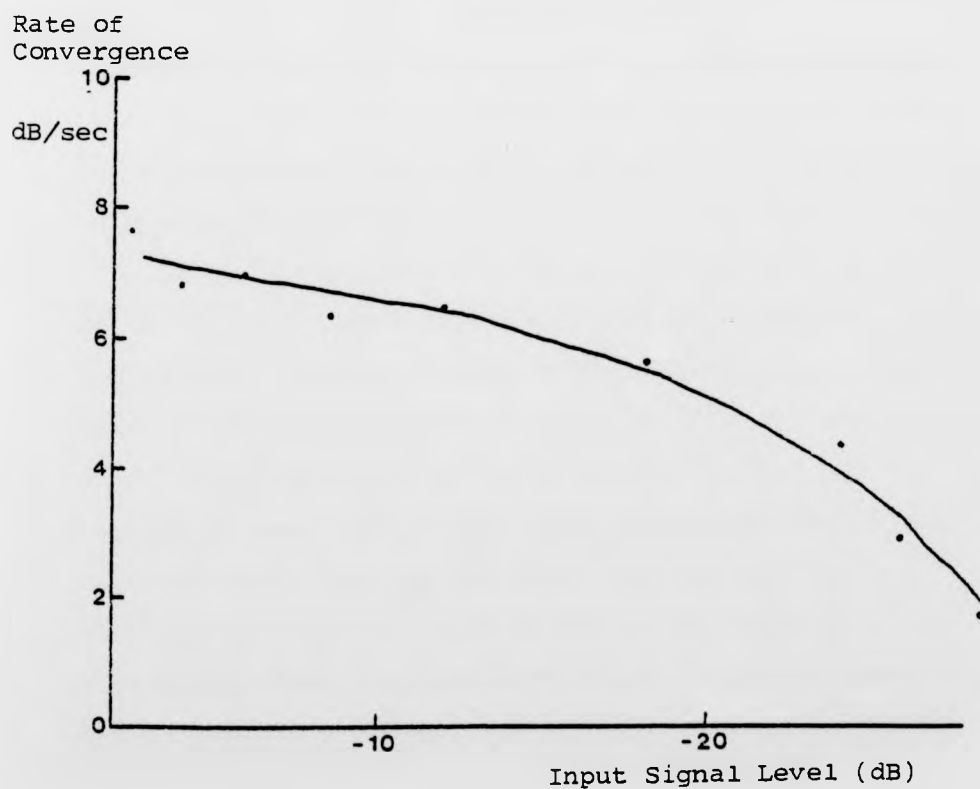
Figure 5.32: Rate of Convergence of
the Pole-Zero Filter

CHAPTER 6

THE FILTERING AND SAMPLING RATE REQUIREMENTS
OF THE DIGITAL ADAPTIVE HYBRID

In Chapter 5 it was shown that an analog adaptive filter
having a transfer function with a real pole and zero can provide
ample ERLE against subscribers' lines. The problems of implementing
the analog adaptive hybrid were discussed in Section 5.4, and the use
of a digital adaptive filter would avoid almost all of these
problems. In Section 1.7 however it was shown that the use of a
digital adaptive filter increases the complexity of the response
which the filter must model.

In this chapter the effects of the intermediate sampling
rate, the A/D and D/A converters and the analog filters on the
performance of the digital adaptive hybrid are analysed. The aim of
this analysis is to achieve an optimum combination of analog filters,
with digital compensation for their responses, for each value of
intermediate sampling rate.

Figure 6.1 shows a block diagram of the digital adaptive
hybrid, where the adaptive filter operates at an intermediate
sampling rate. The transfer function which the digital adaptive
filter must be capable of synthesising is the combined responses of
the D/A and A/D converters and the bandlimiting filters. The
responses of these elements depend on the intermediate sampling rate
used in the codec. Low sampling rates dictate the use of sharp
cutoff analog filters whose responses can only be matched by a high
order digital filter in the cancellation path. Section 6.1 therefore
examines the relationship between the intermediate sampling rate and
the required complexity of the analog bandlimiting filters.

The analog filters and the converters introduce additional complexity into the response to be matched by the adaptive filter. In Section 6.2 the effect of this additional complexity on the ERL and SRL which can be achieved is investigated. The responses of the filters and converters can be compensated by a fixed digital filter in the cancellation path. However, since the responses of the analog filters are imprecisely known, due to component tolerances and ageing, this technique can not be completely effective. Section 6.2 therefore also examines the effect of deviations in the responses of the filters, assuming that the nominal responses of the filters are perfectly compensated.

The results of the previous two sections are used in Section 6.3 to deduce optimum filters for each sampling rate. The filters chosen are optimal in that they allow the largest deviations in the filters' responses, while still meeting return loss and filtering specifications.

In Section 6.4 the return loss which can be achieved by using simple digital filters to compensate for the effects of the converters and analog filters is investigated. Section 6.5 presents conclusions about the optimum combinations of filtering, sampling and compensation.

6.1 Choice of Analog Filter Order and Cutoff Frequency

The complexity of the bandlimiting filters must be such that both the response between the D/A input and the 4 wire receive port, and the response between the 4 wire transmit port and the A/D output, are within the template shown in Figure 6.2. In general this response is provided by the analog bandlimiting filters in conjunction with the filtering inherent in the D/A and A/D

converters.   In particular, if delta-sigma modulation (Everard, 1979)
is used for A/D and D/A conversion, the A/D converter will contain a
digital quantisation noise filter having a $Sinc^2(x)$ response.
Similarly, the output of the D/A converter is effectively sampled and
held at the intermediate sampling frequency, thereby producing
$Sinc(x)$ frequency shaping.   This filtering in the converter reduces
the complexity of the required analog bandlimiting filters.

To determine the optimum cutoff frequency for the analog
filters at different sampling rates, the maximum and minimum cutoff
frequencies which can be allowed without infringing the specification
of Figure 6.2 are calculated for Butterworth and Tchebichef filters
of orders 1 to 5. This calculation is done for intermediate sampling
rates of 8, 16, 32, 64 and 128 kHz.   The maximum cutoff frequencies
differ for the encode and decode directions because of the different
internal filtering in the converters.

In cases where the minimum cutoff frequency is greater than
the maximum cutoff frequency for a particular sampling rate, the
filter cannot meet the specifications at that sampling rate.   In the
remaining cases the mean of the minimum and maximum cutoff
frequencies is calculated and chosen as the nominal cutoff frequency.
The filter types and nominal cutoff frequencies are recorded in Table
6.1 for the decode direction, and Table 6.2 for the encode direction.
The percentage deviation in cutoff frequency allowed for each viable
filter type, at each sampling frequency, is then calculated.   This is
important because it affects the component tolerances required in the
analog filter.   The results of this calculation are shown in Figure
6.3 for the decode direction, and Figure 6.4 for the encode
direction.

Both Figures 6.3 and 6.4 show that increasing the sampling
rate increases the allowed deviation in cutoff frequency for a given

filter order, although for the encode direction no filter is necessary for sampling rates of 32 kHz and above. Similarly, increasing the filter order for a given sampling rate allows larger deviations in cutoff frequency, although the advantage gained decreases with increasing filter order. This effect must be weighed against the higher individual component accuracies which are required to ensure the same deviation in cutoff frequency for a higher filter order. In all cases the Tchebichef filters allow higher deviations than the Butterworth filters. This occurs because they have narrower transition bands (and hence larger allowed deviations) than the corresponding Butterworth filters.

6.2 The Effect of the Filters and Converters on the ERL and SRL

The results of the previous section show that in some cases large deviations in the cutoff frequency of the analog filters are tolerable without infringing the filtering specifications. This property may be useful, since it allows the filters to be constructed from low precision components. If the necessary compensation for the responses of the D/A and A/D converters and the filters is provided by a fixed digital filter, then the deviations in the responses of the filters may unacceptably degrade the resulting return loss of the system. The responses for which the fixed filter must compensate consist of two parts:-

1) the $Sinc(x)$ response due to the sample and hold of the D/A converter and the $Sinc^2(x)$ response due to the quantisation noise filter in the A/D converter

and

2) the combined responses of the analog encode and decode filters.

The responses due to the converters are fixed and will be considered first.

6.2.1 Compensation for the Responses of the Converters

The sample and hold and the quantisation noise filter introduce phase and amplitude distortion. Since both responses have constant group delays, the phase responses can be simply compensated by a pure time delay in the fixed digital filter. If it is assumed that the transhybrid response is unity, then the return loss which can be achieved without compensating for the amplitude response of the sample and hold or the quantisation noise filter, at frequency f is:-

$$RL(f) = \frac{1}{1-Sinc^3(\pi f/f_s)}$$

where f_s is the intermediate sampling frequency. The SRL at 3.4 kHz, and the ERL, for various sampling rates, are tabulated in Table 6.3.

The table shows that no compensation for the amplitude response of the converters is necessary at sampling frequencies of 128, 64 and 32 kHz, and that without compensation at 16 kHz, 14 dB SRL at the band edge is still possible.

6.2.2 Compensation for the Responses of the Analog Filters

To examine the effect of component inaccuracies in the analog filters, it is initially assumed that only the delay effects due to the converters are compensated for. The transhybrid response is assumed to be unity, as is the response of the digital adaptive filter. This allows the ERL and SRL due to any analog filter, or combination of analog filters, to be calculated. The sensitivity of

a particurlar filtering/sampling strategy to variations in component
values is characterised by the sensitivity of the return loss to
shifts in the cutoff frequency of the filters, since such shifts
affect both the phase response and the amplitude response in the
passband.   This avoids restricting the analysis to a particular
filter structure and simplifies the calculation, since Monte Carlo or
similar analyses are not required.

1) ERL and SRL with no compensation for the analog filter's response

The results of the analysis of the effect of a shift in the
analog filter's cutoff frequency, with compensation only for the
delay due to the converters, are shown in Figures 6.5 and 6.6 for the
various filtering/sampling options of Table 6.1.   The figures show
that the higher the sampling frequency, the less sensitive is the
return loss to variations in cutoff frequency.   At sampling rates of
16 kHz and below, even with no deviation in the filter's cutoff
frequency, compensation is necessary to achieve return loss greater
than 0 dB.   The figures also show that increasing the filter order
increases the sensitivity of the the return loss to deviations in
cutoff frequency.

If values of 20 dB and 10 dB are assigned to the minimum
allowed ERL and SRL respectively, then at 64 kHz the maximum allowed
negative deviations in cutoff frequency are as given in Table 6.4.
Positive deviations have a lesser effect, since they have a lesser
effect in the passband.   The maximum allowed deviations in cutoff
frequency are termed the return loss sensitivities of each filter.

At 32 kHz sampling rate, even with no downward shift in the
filter's cutoff frequency, the 10 dB and 20 dB SRL and ERL
specifications cannot be met without some compensation for the

responses of the filters.

2) ERL and SRL with perfect compensation for the nominal analog
filter's response

Assuming that the responses of the filters are perfectly
compensated, then the various filter types can be expected to have
different return loss sensitivities. Analysis of these sensitivities
allows choice of the optimum filters.

The return loss sensitivities of the various
filtering/sampling options, assuming perfect compensation for the
analog filter's response, are shown in Figures 6.7 and 6.8. These
figures show the return loss sensitivities decreasing with increasing
filter order, and in most cases the Butterworth filters have higher
return loss sensitivities than the equivalent Tchebichef filters.
For sampling frequencies of 32 kHz and above, no analog filters are
required in the encode path, and the return loss sensitivity of the
decode filter is the overall return loss sensitivity for the
subscriber's line unit. However, at 16 kHz, the overall return loss
sensitivity is due to the return loss sensitivities of both the
encode and decode filters. In Section 6.3 a method of estimating
this overall return loss sensitivity is proposed.

6.3 The Optimal Analog Filters

By superimposing Figures 6.3 and 6.4 on Figures 6.7 and 6.8
respectively, the implications of the various sampling frequency and
filtering options can be more clearly seen. This is shown in Figures
6.9 (decode direction) and 6.10 (encode direction). The following
conclusions can be drawn from these figures:-

1) 64 kHz sampling frequency

At 64 kHz sampling frequency the optimum filter is the first order Tchebichef (nominal cutoff frequency = 6.7 kHz). The maximum allowed deviation in cutoff frequency is ±64% without infringing the filtering specification. Chosing the Butterworth type filter (nominal cutoff frequency = 25.74 kHz) reduces the allowed deviation to ± 62%, and for convenience the use of this filter is assumed for the remainder of this chapter.

2) 32 kHz sampling frequency

At 32 kHz sampling frequency the optimum filter is a second order Butterworth (nominal cutoff frequency = 10.19 kHz). The maximum allowed deviation is -37% without infringing the return loss specification. The filtering specification allows a deviation of ±49%, indicating that the performance could be improved by increasing the cutoff frequency by a small amount.

3) 16 kHz sampling frequency

At 16 kHz sampling frequency the optimum decode filter is a 3rd order Butterworth (nominal cufoff frequency = 5.34 kHz). A deviation of -15% in cutoff frequency is allowed without infringing the return loss specification, whereas ±19% deviation is allowable by the filtering specification.

In the encode path at 16 kHz sampling frequency, a second order Butterworth filter (nominal cutoff frequency = 7.428 kHz) allows -28% deviation while meeting the return loss specification, and ± 29.5% while still meeting the filtering specification. Use of a 2nd order Tchebichef filter (nominal cutoff frequency = 4.54 kHz) allows ± 38% deviation without infringing the filtering specification, and if the nominal cutoff frequency is increased, the deviation allowed while meeting the return loss specification can probably be increased above the -28% allowable for the Butterworth

filter.

The filters described above are chosen as optimal for the various sampling frequencies, and in the next section the effects of imperfect compensation are discussed. Before this can de done however, it is necessary to make some assumptions about the combined effects of component tolerances in the encode and decode filters at 16 kHz.

In Figure 6.11 the return loss sensitivity of the combination of encode and decode filters at 16 kHz sampling frequency is shown for deviations in the cutoff frequencies of both filters. It has been assumed that the responses of the nominal filters are perfectly compensated, but that the magnitude responses due to the converters are uncompensated. The figure shows that the overall return loss sensitivity is worst when both filters have cutoff frequencies lower than nominal, the maximum deviation in this case being approximately -10%. Figure 6.11 also shows that if both filters deviate in opposite directions, then large deviations are allowed, but that the allowed deviation is always lower for the decode filter than for the encode filter. For reference, the deviations allowed while meeting the filtering specifications are also shown in Figure 6.11. To obtain a realistic estimate of the performance of the filters at 16 kHz, the probability distributions of the deviations in cutoff frequency for each filter should be superimposed on Figure 6.11, however in the following section the worst case is assumed, i.e. it is assumed that both filters have equal negative deviations in cutoff frequency.

6.4 Digital Compensation for the Analog Filters

In the previous section it was assumed that the responses of the nominal analog bandlimiting filters could be perfectly matched, in both amplitude and phase, by a digital compensating filter. In practice this is impossible. In this section the effect on the ERL and SRL of modelling the analog filters by the following practical digital systems are examined:-

1) a mapped equivalent of the analog filters

2) a first order digital all-pass section

3) a pure time delay

4) a single pole digital filter

6.4.1 Mapping the Analog Filters to Equivalent Digital Filters

There are many techniques for mapping analog filter responses into the digital domain (Rabiner and Gold, 1975), however most of these techniques do not preserve the phase response of the filter in the passband. A technique which is suitable for all pole type analog responses (e.g. Butterworth and Tchebichef filters), is the invariant impulse response method. This technique produces a recursive digital filter whose impulse reponse is a sampled version of the analog filter's impulse response. However, for the method to be successful, the analog filter's response must be sufficiently bandlimited to prevent aliasing in the design process. This problem is particularly acute when attempting to design compensating filters which match the analog filters used for the higher sampling frequencies, since these filters have responses with significant values at more than half the sampling frequency. For example, at 32 kHz sampling frequency, the 2nd order Butterworth filter only attenuates the first image band by

18 dB. Figure 6.12 shows the passband responses of the analog filter and a digital equivalent designed using the impulse invariant method. It can be seen that gross aliasing has occurred.

At the 16 kHz sampling rate the required analog filters have higher values of stopband attenuation, and the invariant impulse response technique is capable of yielding a reasonably accurate digital compensation filter. This filter is however of 5th order. Attempts to map the analog filters to equivalent digital filters were abandoned for these reasons.

6.4.2 Compensation with a First Order Digital All-Pass Section

The requirement that all of the analog filters have a maximum ripple of 0.25 dB in the passband indicates that they can be matched to 30 dB return loss by all-pass sections, if the phase response of the sections can be matched to that of the filters. The response of a first order all-pass section is given by:-

$$H(z) = (z^{-1}-a)/(1-az^{-1}) \qquad\qquad 6.1$$

and the coefficient 'a' can be used to vary the phase response of the section. As in Section 6.2.2, the return loss for each of the filtering/sampling options is calculated, assuming that the all-pass network is used to compensate for the responses of the filters, and that the magnitude responses of the converters are uncompensated.

At 64 kHz and 32 kHz sampling rates, even with 'a' = 0, good compensation is achieved only for cutoff frequencies much lower than nominal.

At 16 kHz the optimum value for 'a' allows only ± 3% deviation in the cutoff frequencies of the filters, assuming that both deviate together, and the values of ERL and SRL achieved when both filters have their nominal cutoff frequencies are only slightly

in excess of 20 dB and 10 dB respectively. To achieve adequate compensation at 16 kHz at least one further all-pass section is required.

6.4.3 Compensation with a Pure Time Delay

If 'a' = 0 in equation 6.1, the all-pass section becomes equivalent to a pure time delay of 1 sample period. It has been seen that this provides good compensation at 64 and 32 kHz sampling rates, only if the cutoff frequency of the analog filter is much lower than nominal. Large deviations in cutoff frequency are allowed at these sampling rates however, and the nominal cutoff frequency can thus be decreased to ease the compensation problem.

Figure 6.13 shows the ERL and SRL achieved, as a function of the nominal cutoff frequency, if the analog filter in the decode path is compensated by a pure time delay of 1 sample period. The sampling frequency is 64 kHz, the filter is a first order Butterworth, and it is assumed that the magnitude responses of the converters are uncompensated. Also shown in Figure 6.13 are the maximum allowed negative deviations from the nominal cutoff frequency without breaching the filtering or the return loss specifications. The maximum positive deviations allowed while meeting both specifications are greater than 80% for nominal cutoff frequencies between 6 kHz and 20 kHz, and are not shown in Figure 6.13.

Figure 6.13 shows that the nominal cutoff frequency should be 10.3 kHz to maximise the return loss, but this allows a negative deviation of only -4% without breaching the return loss specification. The deviation allowed can be increased to -20%, while still giving 33 dB ERL and 22 dB SRL (assuming no deviation), if the nominal cutoff frequency of the filter is increased to 12.3 kHz.

At 32 kHz sampling rate, using the second order Butterworth filter in the decode path, compensated with a delay of 1 sample period, and assuming the filter has the nominal cutoff frequency, the ERL and SRL achieved are as shown in Figure 6.14. The maximum deviations allowed are also shown in Figure 6.14. In this case it can be seen that choosing a nominal cutoff frequency of 7.2 kHz gives 46 dB nominal ERL, and 21 dB nominal SRL. The maximum deviations allowed while meeting the return loss specification are +80% and -26%. The nominal cutoff frequency of the filter can be increased to allow larger negative deviations, but only at the expense of the return loss and the allowed positive deviation.

6.4.4 Compensation with a Single Pole Digital Filter

The pure time delay of the previous section provides poor compensation for the nominal analog filters at 32 kHz and 64 kHz sampling rates because it over-compensates for the phase shift due to the filters. Reducing the nominal cutoff frequency of the filters allows better compensation to be achieved, but at the expense of the maximum allowed negative deviation. A system which provides less phase shift than the pure time delay is the single pole digital filter, whose response is given by:-

$$H(z) = 1/(1-az^{-1})$$

The ERL and SRL as a function of the percentage deviation in cutoff frequency, for the first order Butterworth filter and various values of filter coefficient ('a'), at a sampling rate of 64 kHz, are shown in Figures 6.15 and 6.16.

It can be seen from the figures that the optimum value of 'a' is slightly less than 0.3, and that the digital filter provides excellent compensation. The maximum deviation allowed without

infringing the return loss specification is -70%.

At 32 kHz sampling rate the performance of the single pole compensation is as shown in Figures 6.17 and 6.18. In this case the filter provides good average compensation, however Figure 6.18 indicates that the compensation at the band edge is poor. Compensation at the nominal cutoff frequency, and the average compensation, can be traded off for increased allowed negative frequency deviation. The optimum value for 'a' is thus between 0.4 and 0.5.

6.5 The Optimum Filtering/Compensation Strategy

For the various sampling rates, the following conclusions can be drawn from the data presented in this chapter:-

1) At 128 kHz sampling rate no analog bandlimiting filters are required. If the phase responses of the A/D and D/A converters are compensated by a pure time delay, the maximum possible ERL and SRL are 62 dB and 49 dB, as given in Section 6.2.1.

2) At 64 kHz sampling rate a first order analog filter is required in the decode direction. If a Butterworth filter is chosen, its optimum cutoff frequency is 25.7 kHz, and ±62% deviation from this nominal cutoff frequency is allowed without breaching the filtering specification.

If the phase responses due to the A/D and D/A converters are compensated by a time delay, but no other compensation is used, then 26 dB ERL and 18 dB SRL are possible, assuming that the filter's cutoff frequency does not deviate from its nominal value. The maximum allowed deviation is -52% while still guaranteeing 20 dB ERL and 10 dB SRL.

The optimum compensation for the response of the analog filter is a single pole digital filter, with coefficient 'a' = 0.3. This compensation gives approximately 60 dB ERL and 40 dB SRL, assuming the filter does not deviate from its nominal response. The maximum deviation allowed is -70% while guaranteeing 20 dB ERL and 10 dB SRL, although a lesser deviation is allowed by the filtering specification.

If the nominal cutoff frequency of the analog filter is reduced, then a pure time delay of 1 sample period provides reasonable compensation for the filter's response. Reducing the cutoff frequency to 12.3 kHz still allows a negative deviation of -20% while meeting the filtering specification. The nominal ERL and SRL for this compensation are 33 dB and 22 dB respectively. These conclusions are summarised in Table 6.5.

3) at 32 kHz sampling rate a 2nd order Butterworth filter is required in the decode direction. The optimum cutoff frequency for the filter is 10.2 kHz, and the maximum allowed deviation in cutoff frequency is ±49% without breaching the filtering specification.

The response of the filter, in addition to the phase responses of the converters, must be compensated to achieve greater than 13 dB ERL or 6 dB SRL.

If compensation with a single pole digital filter is used, the optimum filter coefficient is between 0.4 and 0.5. This compensation achieves between 33 dB and 23 dB ERL, and between 15 dB and 14 dB SRL, depending on the value of the filter coefficient, and assuming that the analog filter has the nominal cutoff frequency. The maximum allowed deviation in cutoff frequency is between -27% and -36%.

Reducing the nominal cutoff frequency of the filter to 7.2 kHz still allows a negative frequency deviation of -26%, with a

single period pure time delay as compensation. The nominal ERL and SRL for this compensation are 46 dB and 21 dB respectively. These conclusions are summarised in Table 6.6.

4) At 16 kHz sampling rate a 2nd order Butterworth filter is required in the encode direction, and a 3rd order Butterworth filter is required in the decode direction. The allowed deviations in cutoff frequency, while meeting the filtering requirements, are ±19% for the decode filter, and ±30% for the encode filter.

Compensation for the filter responses is necessary, and the required compensation is a digital filter of at least 2nd, and possibly as high as 5th, order. If perfect compensation for the filter responses is possible, then the maximum deviations allowed in the cutoff frequencies of both filters, while guaranteeing 20 dB ERL and 10 dB SRL, is -10%, assuming that worst case deviations occur.

5) At 8 kHz sampling frequency, both the encode and the decode directions require analog filters of order higher than 5th. Compensation for the responses of the filters would require a high order digital filter, and only very small deviations in the cutoff frequencies of the filters would be allowed.

SAMPLING FREQUENCY IN kHz	FILTER TYPE	NOMINAL CUTOFF FREQUENCY IN kHz	PERCENTAGE VARIATION ALLOWED (+ OR -)
128	NO FILTERS REQUIRED	-	-
64	B1	25.74	61.7
	B2	27.7	81
	B3	28.9	84.9
	B4	29.6	86.2
	B5	30.07	86.9
	T1	6.17	64.18
	T2	17.61	84.16
	T3	23.83	86.9
	T4	26.91	88.0
	T5	28.54	88.48
32	B2	10.19	48.8
	B3	11.5	62.3
	B4	12.46	67.2
	B5	13.06	69.9
	T2	6.51	57.18
	T3	9.95	68.8
	T4	12.0	73.1
	T5	13.21	75.11
16	B3	5.341	18.7
	B4	5.8	29.6
	B5	6.137	35.9
	T2	2.94	5.12
	T3	4.512	31.2
	T4	5.57	42.0
	T5	6.25	47.38
8	GREATER THAN 5th ORDER, B OR T	-	-

TABLE 6.1: Decode path filtering/sampling options

SAMPLING FREQUENCY IN kHz	FILTER TYPE	NOMINAL CUTOFF FREQUENCY IN kHz	PERCENTAGE VARIATION ALLOWED (+ OR -)
128 64 32	NO FILTERS REQUIRED	-	-
16	B2 B3 B4 B5 T2 T3 T4 T5	7.428 7.44 7.55 7.62 4.54 6.01 6.75 7.16	29.74 41.63 45.9 48.45 38.57 48.38 52.2 54.07
8	B, GREATER THAN 5th ORDER T5	- 3.2915	- .106

TABLE 6.2: Encode path filtering/sampling options

SAMPLING RATE (kHz)	ERL (dB)	SRL (dB)
128	62.1	49.2
64	50.0	37.2
32	38.1	25.3
16	26.2	13.9
8	15.0	4.2

TABLE 6.3: ERL and SRL if the magnitude responses of the converters are uncompensated

FILTER TYPE	MAXIMUM DEVIATION IN CUTOFF FREQUENCY
B1,T1	- 52%
T2	- 40%
B2	- 38%

TABLE 6.4: Maximum allowed negative deviations in cutoff frequency while meeting the return loss specification, for a sampling rate of 64 kHz

	NO COMPENSATION	SINGLE POLE	PURE TIME DELAY
MAXIMUM + ALLOWED DEVIATION -	62%	62%	> 80%
	52%	62%	20%
NOMINAL ERL	26.4	60	33
NOMINAL SRL	17.6	40	22

TABLE 6.5: Performance of digital compensation at 64 kHz sampling frequency

	SINGLE POLE	PURE TIME DELAY
MAXIMUM + ALLOWED DEVIATION -	49%	80%
	> 27%, < 36.5%	26%
NOMINAL ERL	> 23.5, < 33	46
NOMINAL SRL	> 13.6, < 15.4	21

TABLE 6.6: Performance of digital compensation at 32 kHz sampling frequency
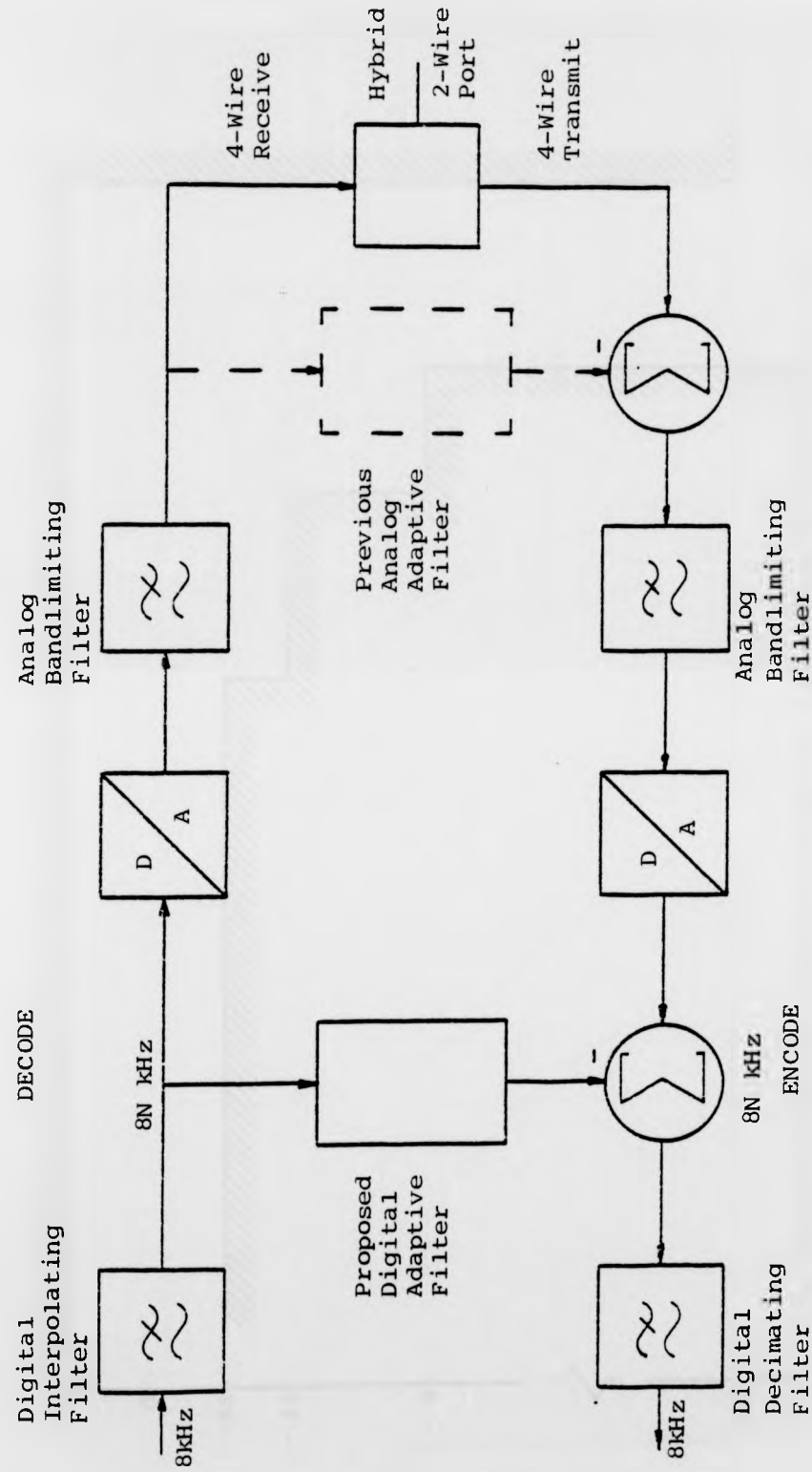
Figure 6.1: The Digital Adaptive 2 to 4 Wire Converter
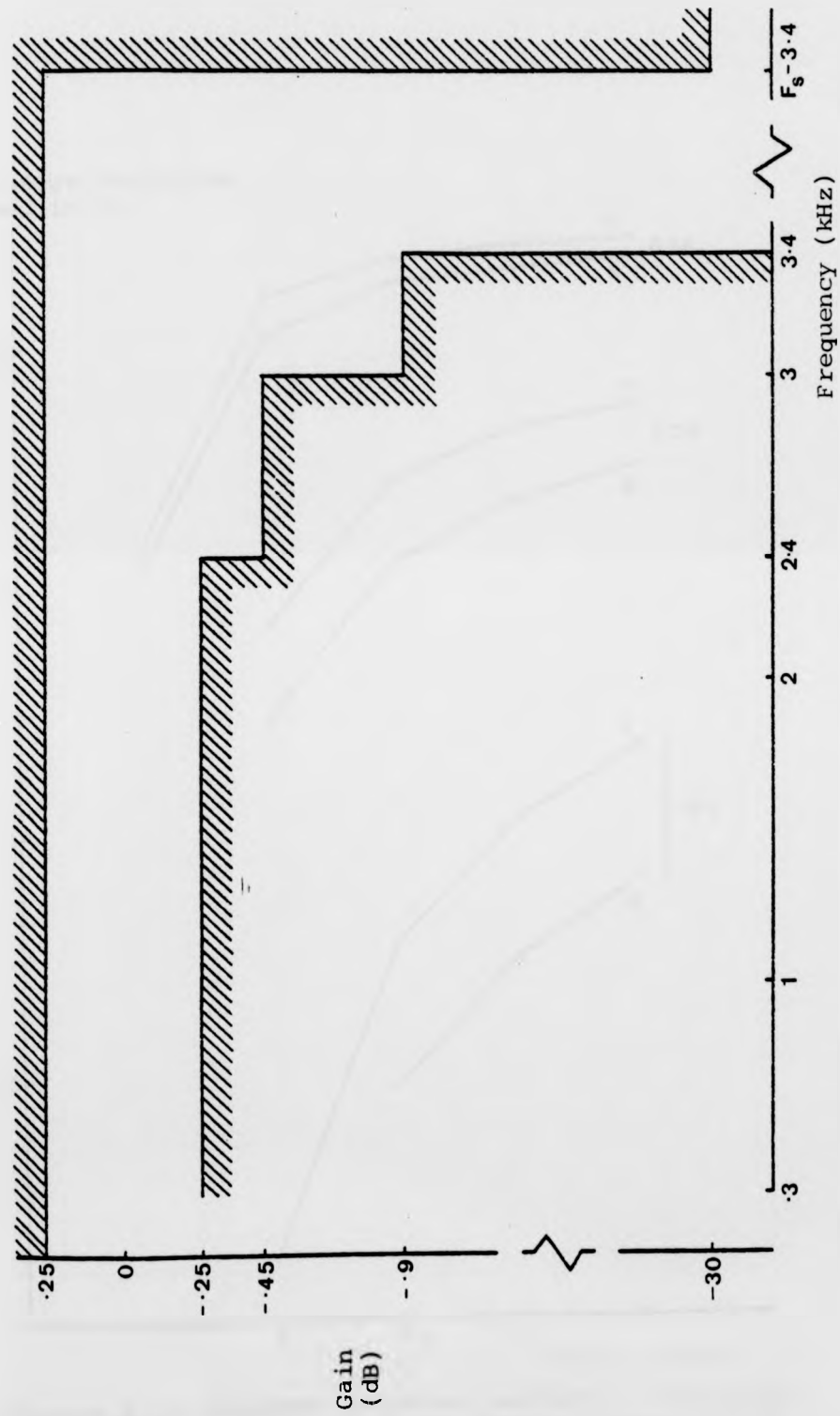
Figure 6.2: The Filtering Specification

Percentage Variation
Allowed in Fc
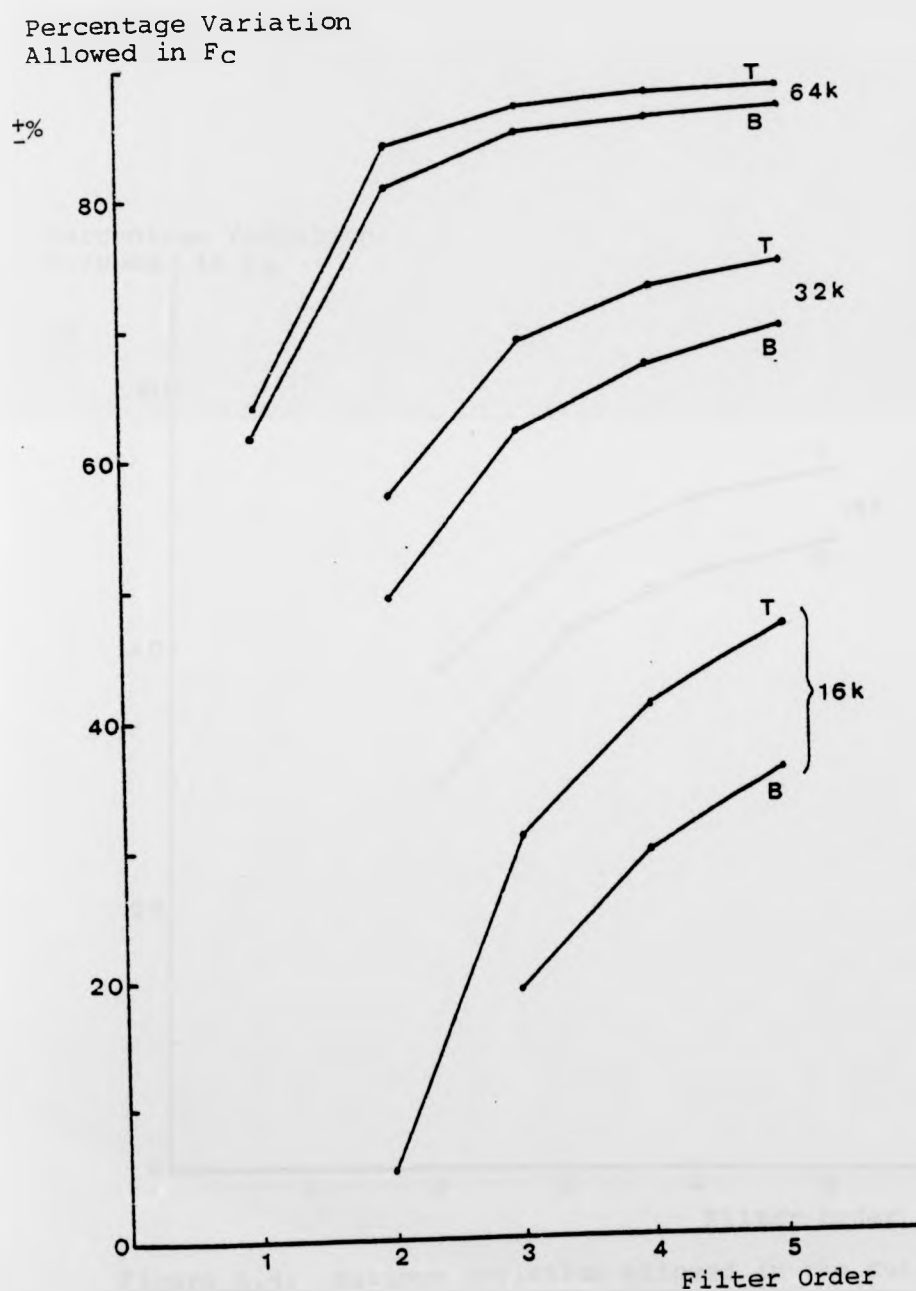
Figure 6.3: Maximum Deviation Allowed in the Cutoff
Frequency of the Decode Filter Without
Breaching the Filtering Specification
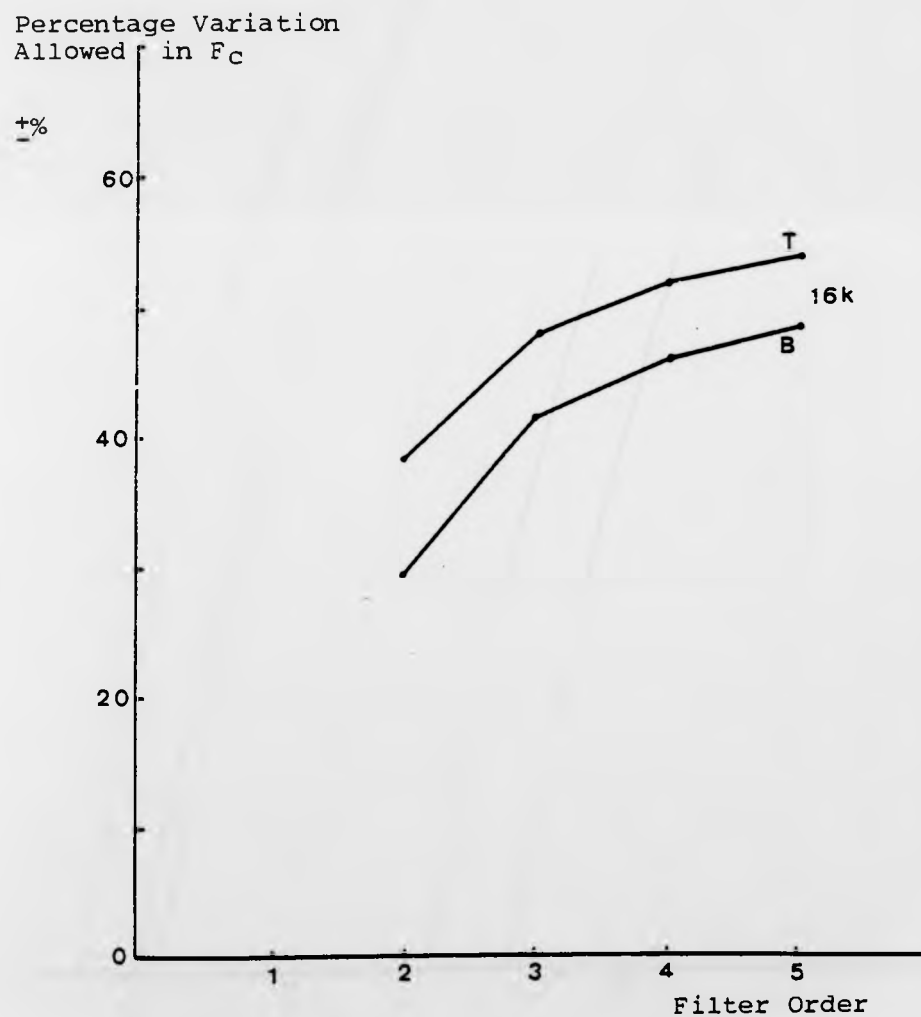
Figure 6.4: Maximum Deviation Allowed in the Cutoff
Frequency of the Encode Filter Without
Breaching the Filtering Specification
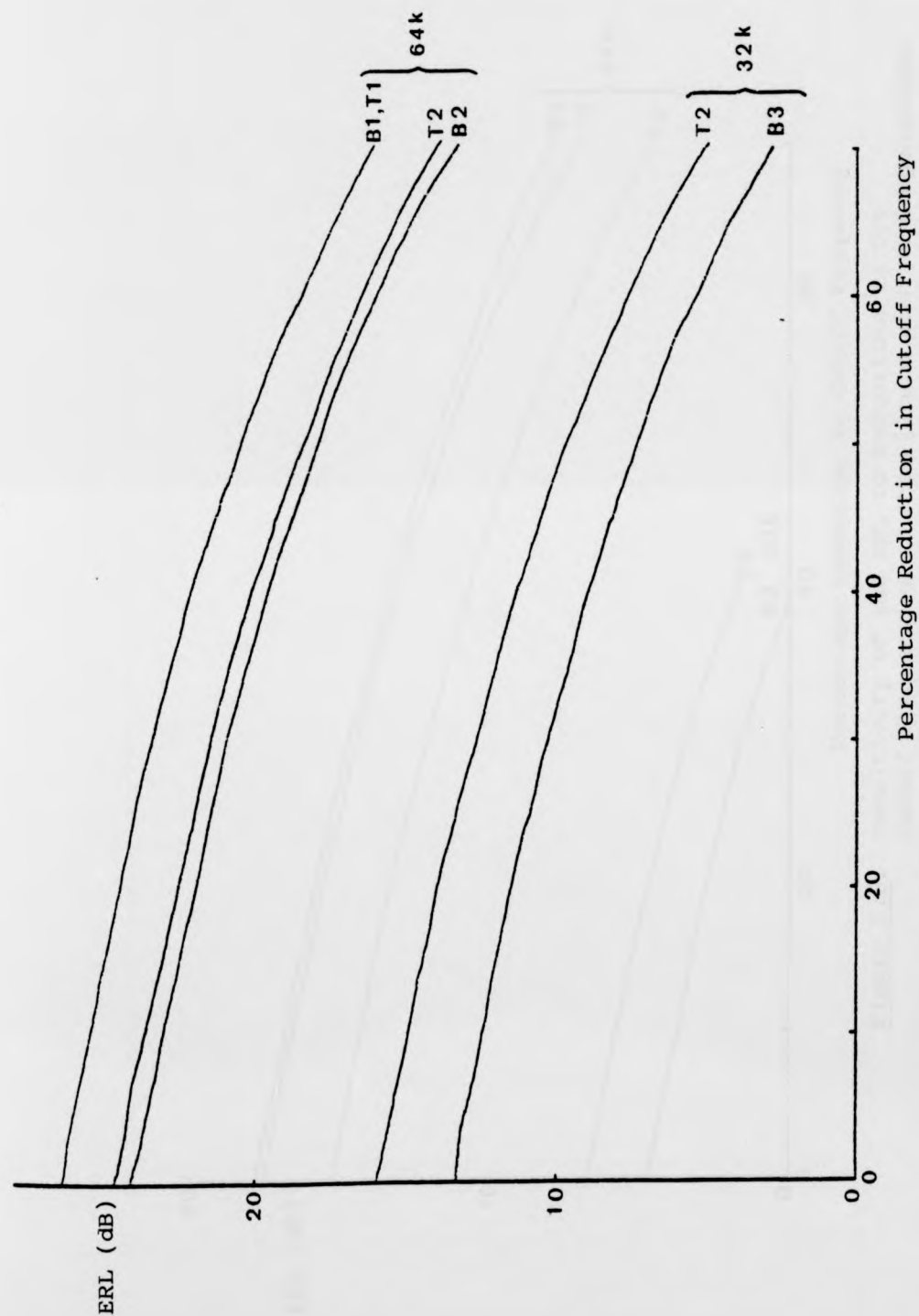
Figure 6.5: Sensitivity of the ERL to Reductions in the Cutoff Frequencies of the Filters with no Compensation
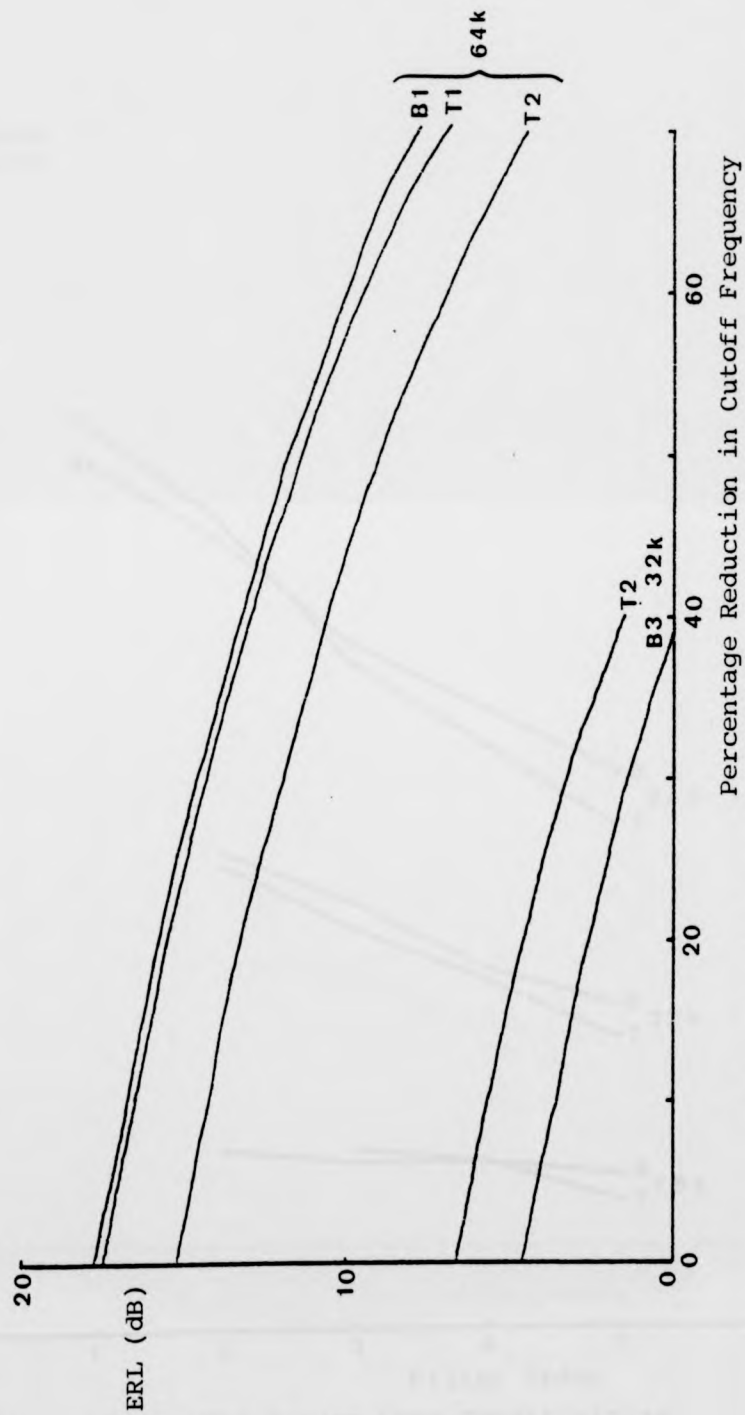
Figure 6.6: Sensitivity of the SRL to Reductions in the Cutoff Frequencies of the Filters with no Compensation
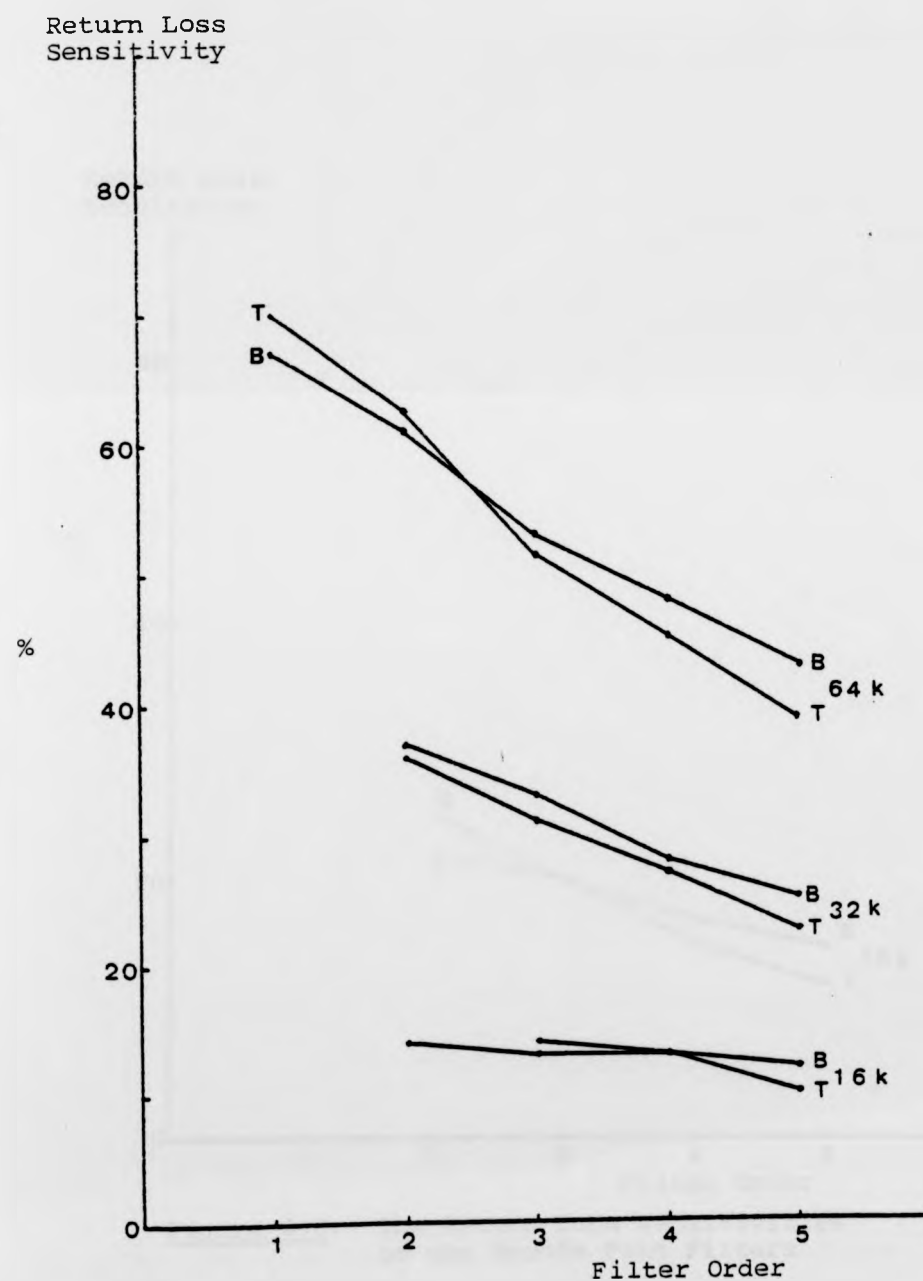
Figure 6.7: The Return Loss Sensitivities
of the Decode Path Filters
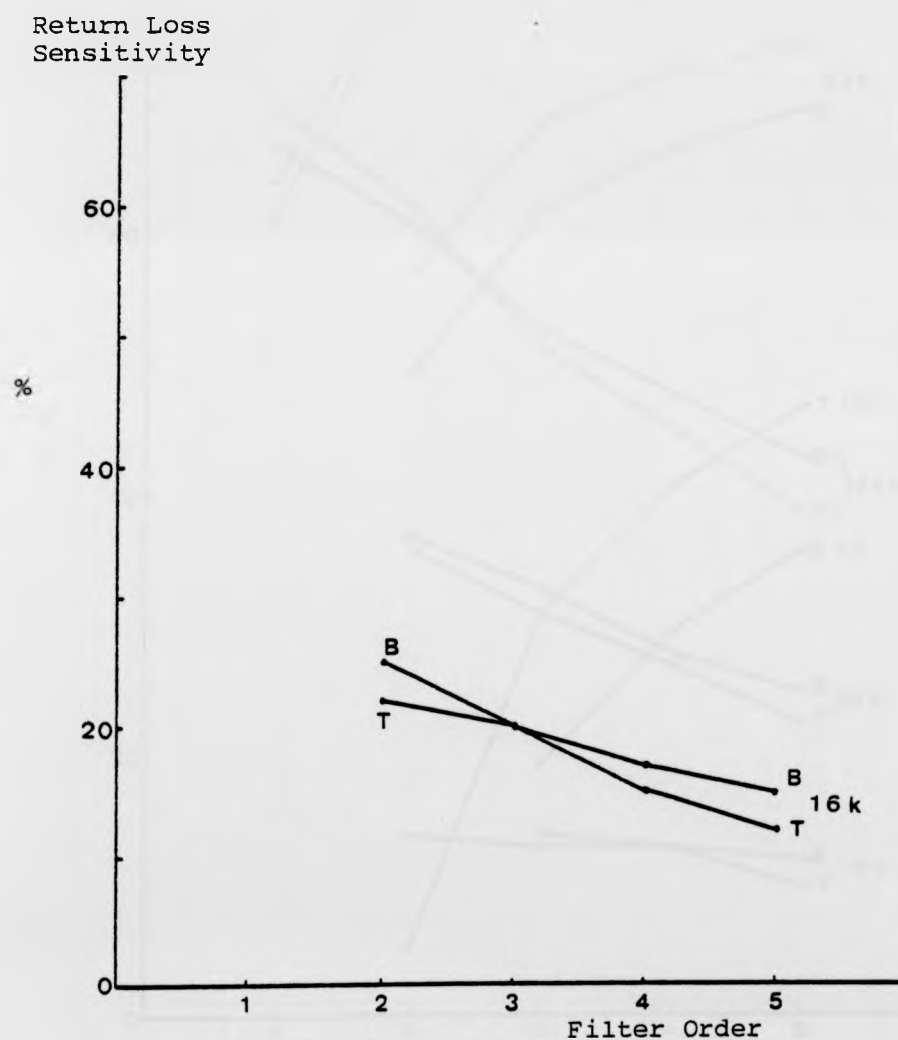
Figure 6.8: The Return Loss Sensitivities of the Encode Path Filters

Figure 6.9: Choice of the Optimal Decode Path Filter

Percentage Variation
in Cutoff Frequency
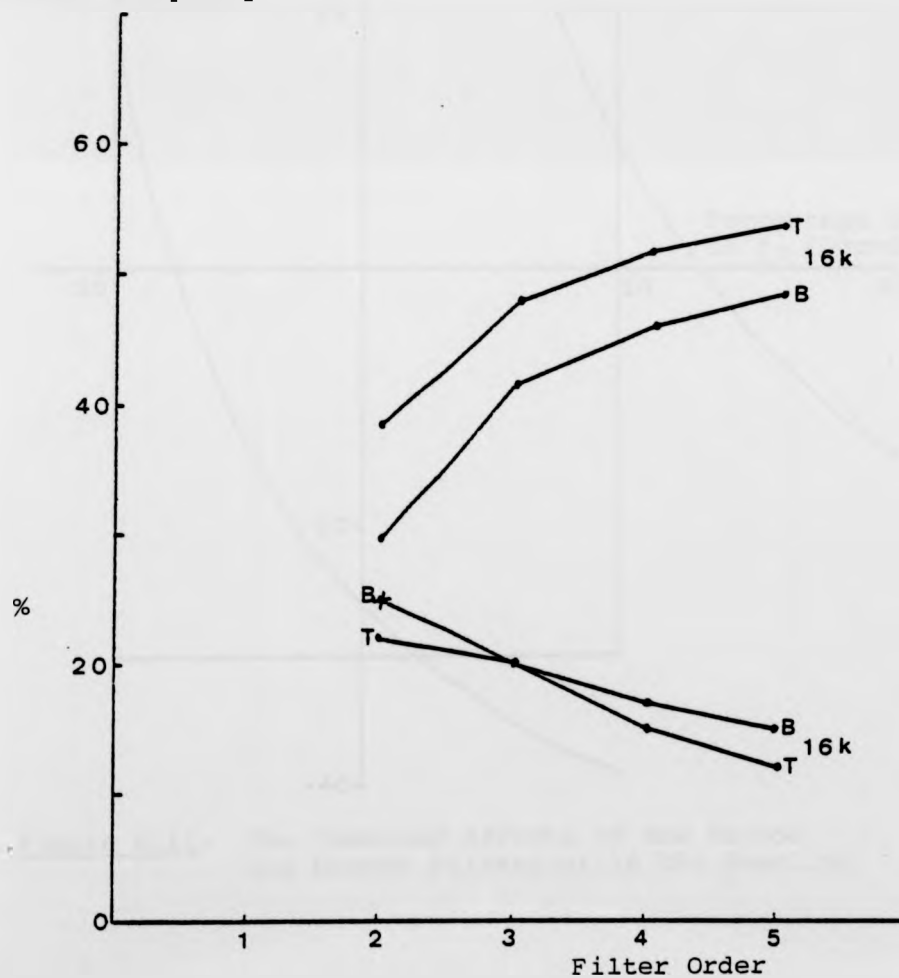
Figure 6.10: Choice of the Optimal Encode Path Filter
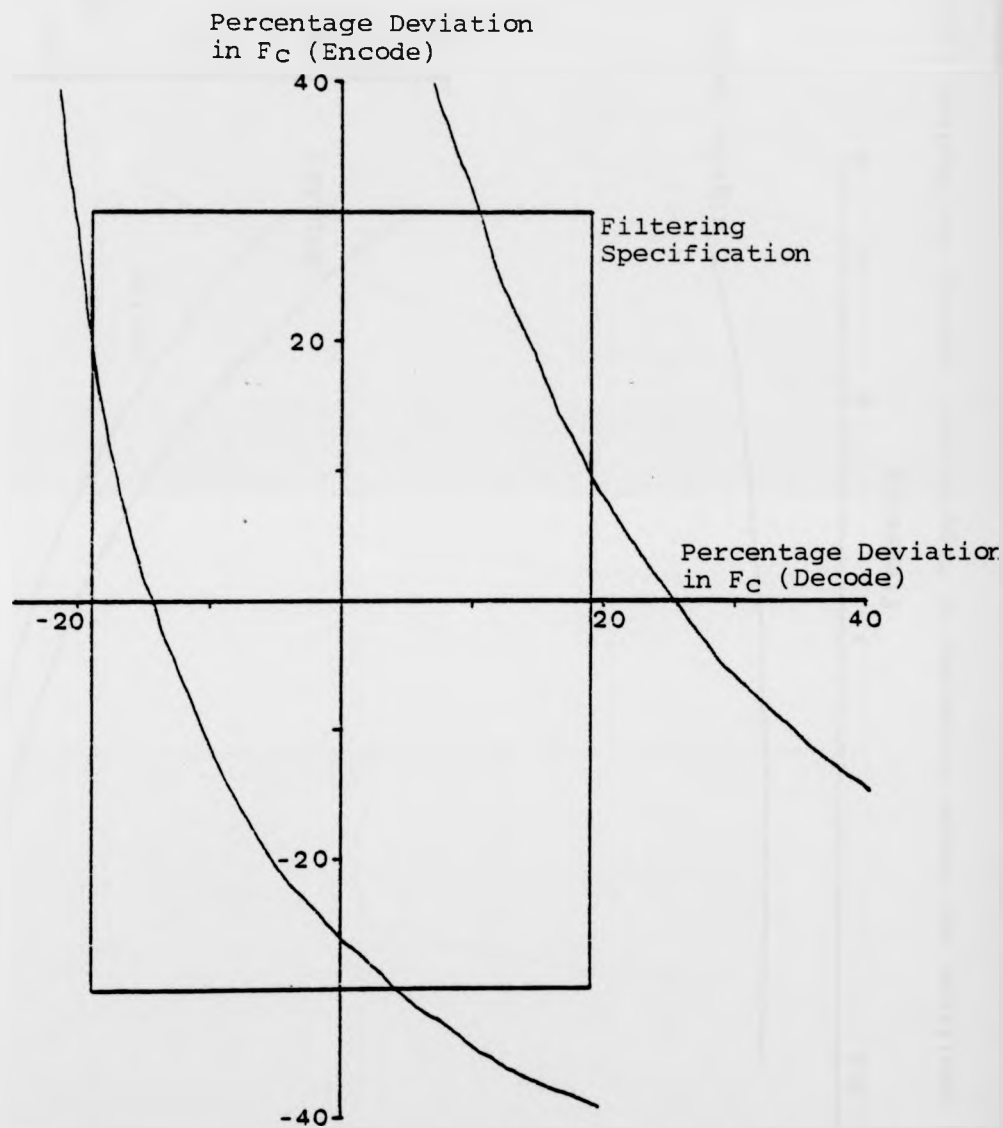
Figure 6.11: The Combined Effects of the Encode and Decode Filters at 16 kHz Sampling
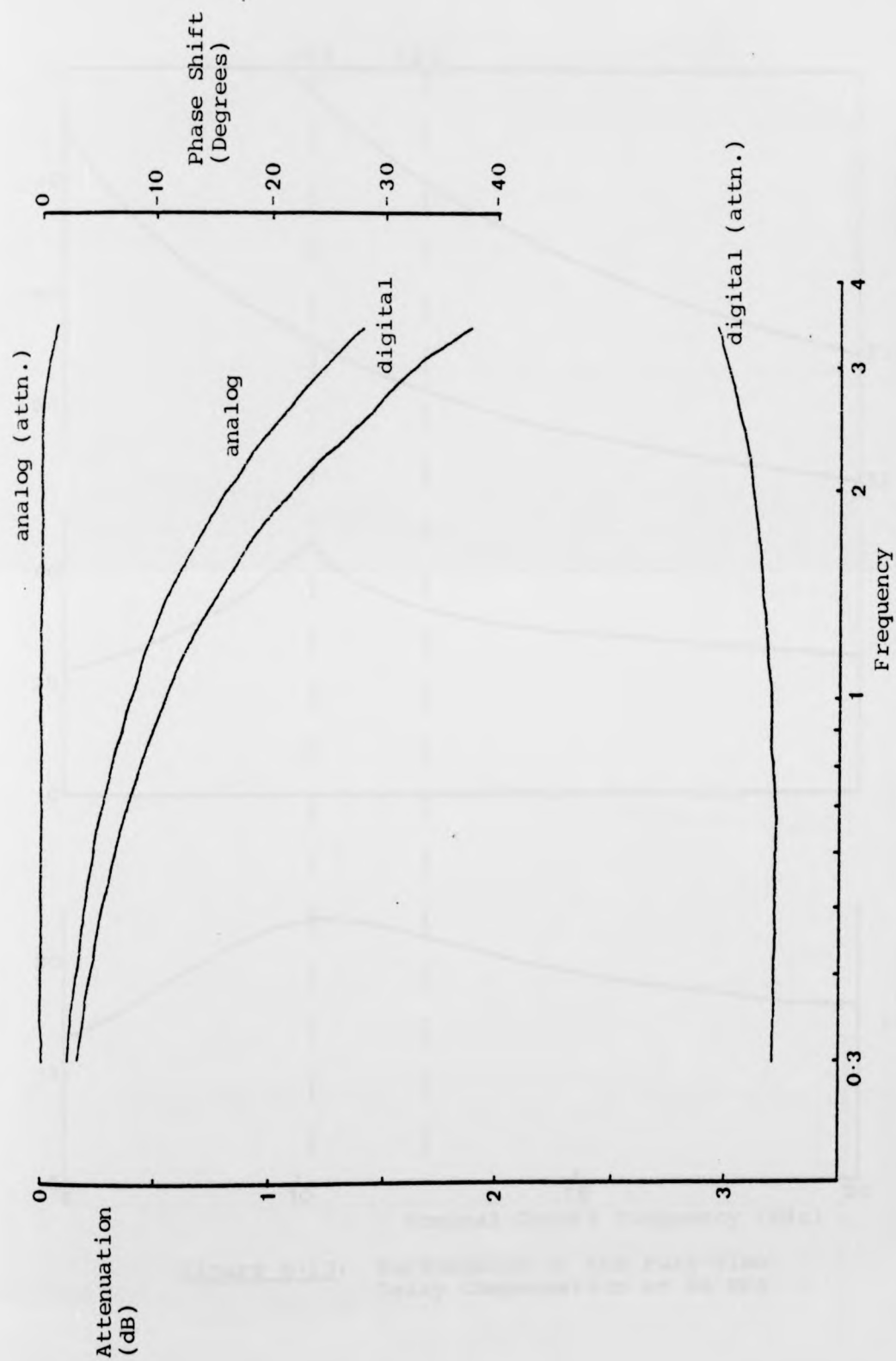
Figure 6.12: Amplitude and Phase Responses of "Equivalent" Analog and Digital Filters
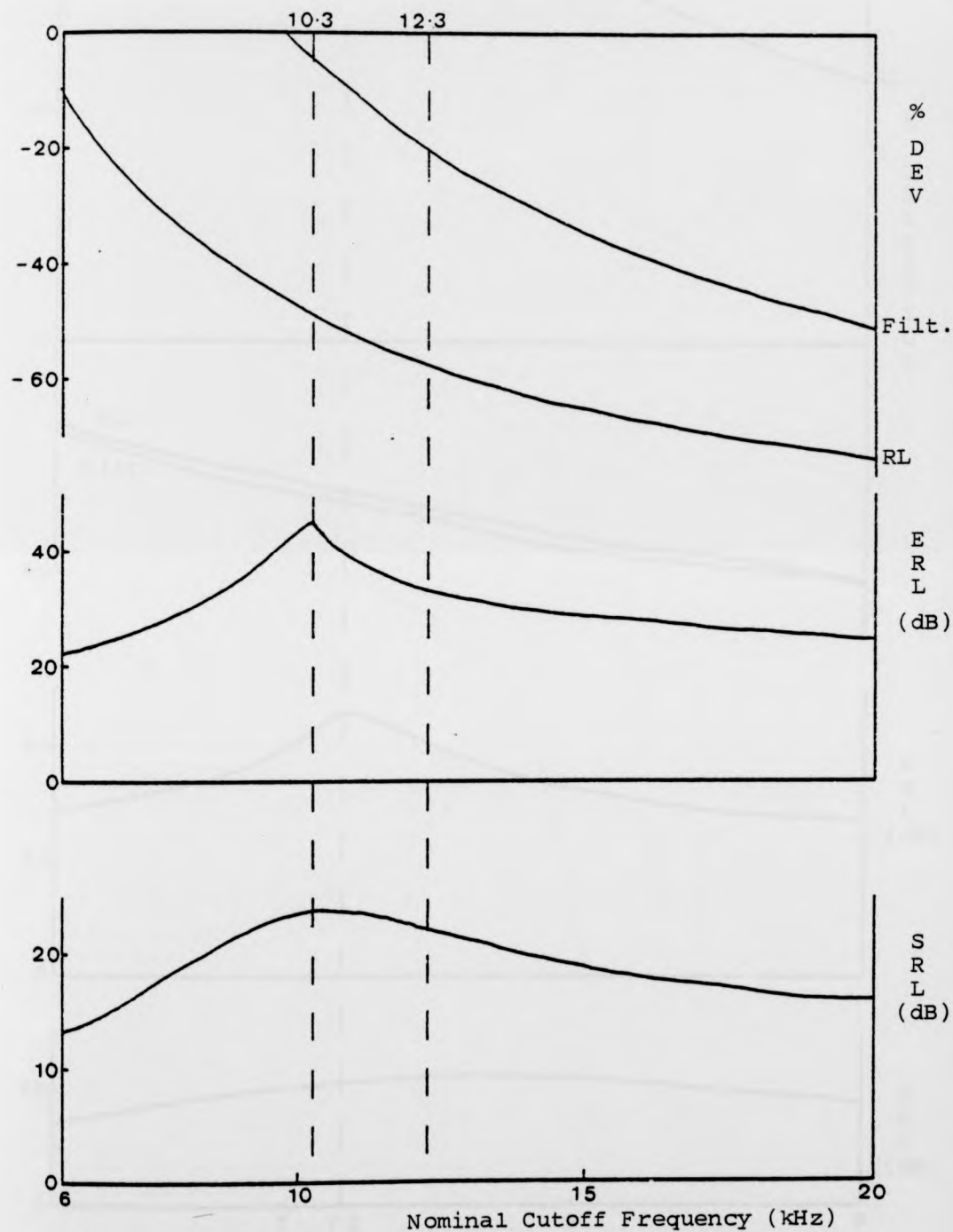
Figure 6.13: Performance of the Pure Time Delay Compensation at 64 kHz
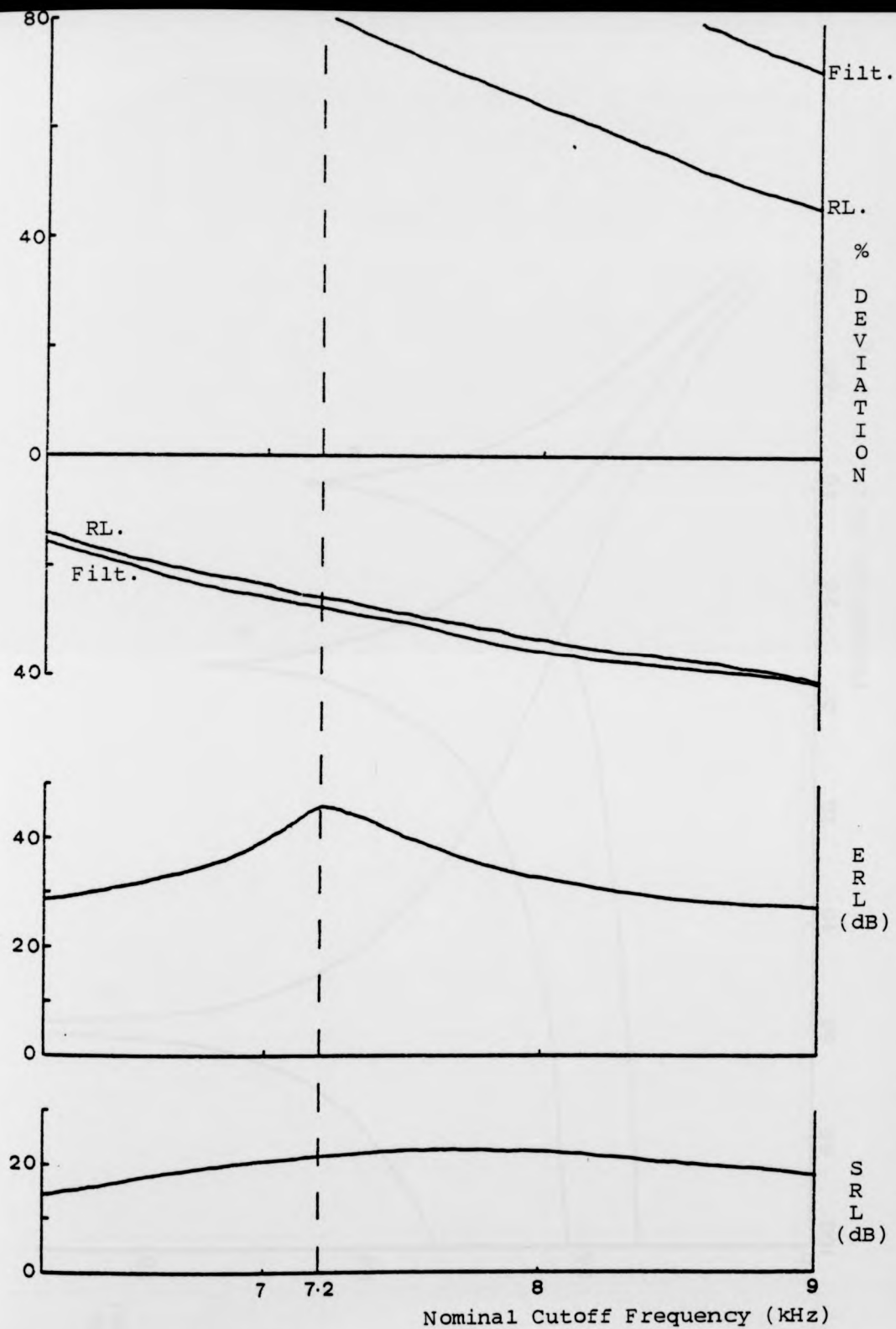
Figure 6.14: Performance of the Pure Time
Delay Compensation at 32 kHz
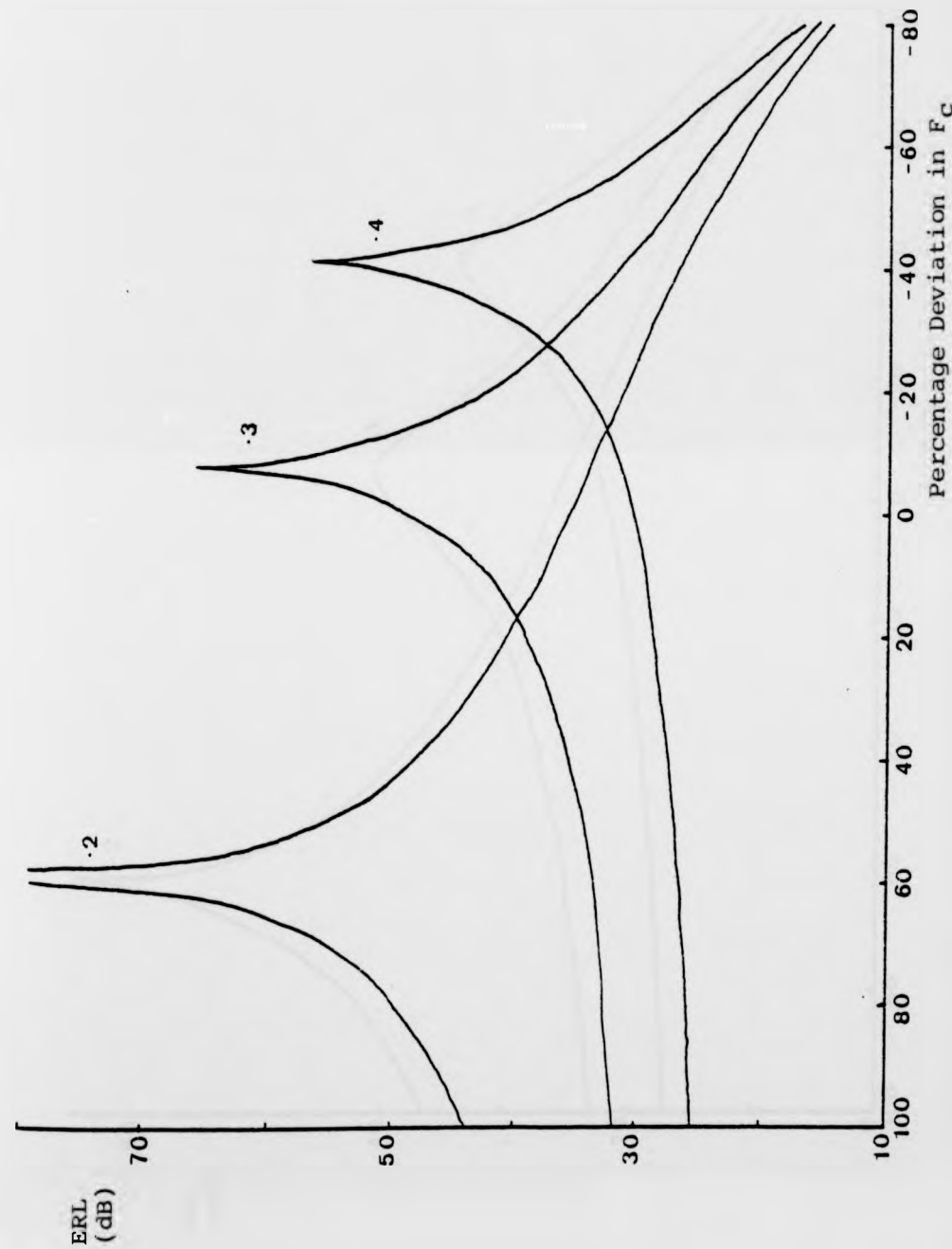
Figure 6.15: ERL Achievable with Single Pole Compensation at 64 kHz Sampling Frequency
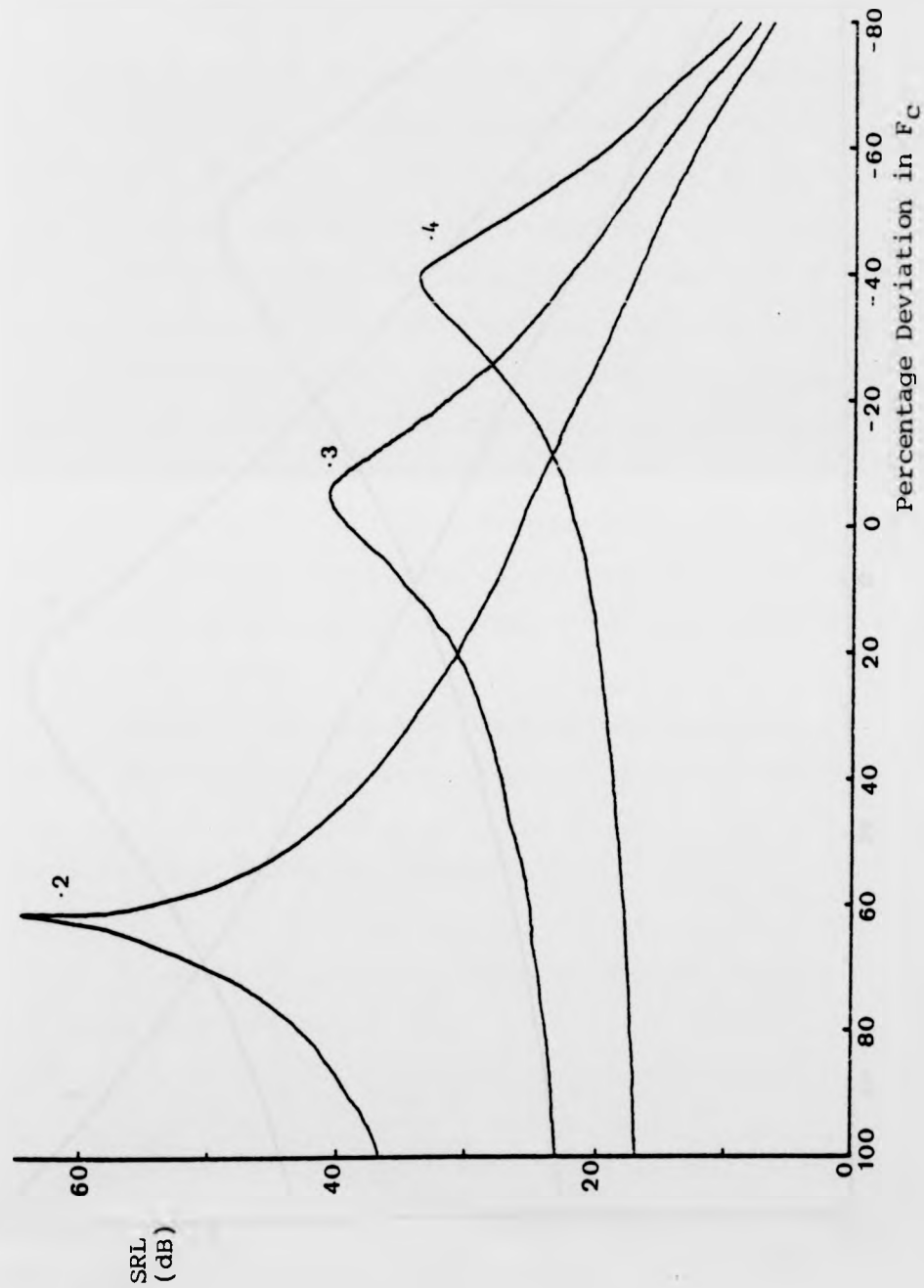
Figure 6.16:   SRL Achievable with Single Pole Compensation at 64 kHz Sampling Frequency
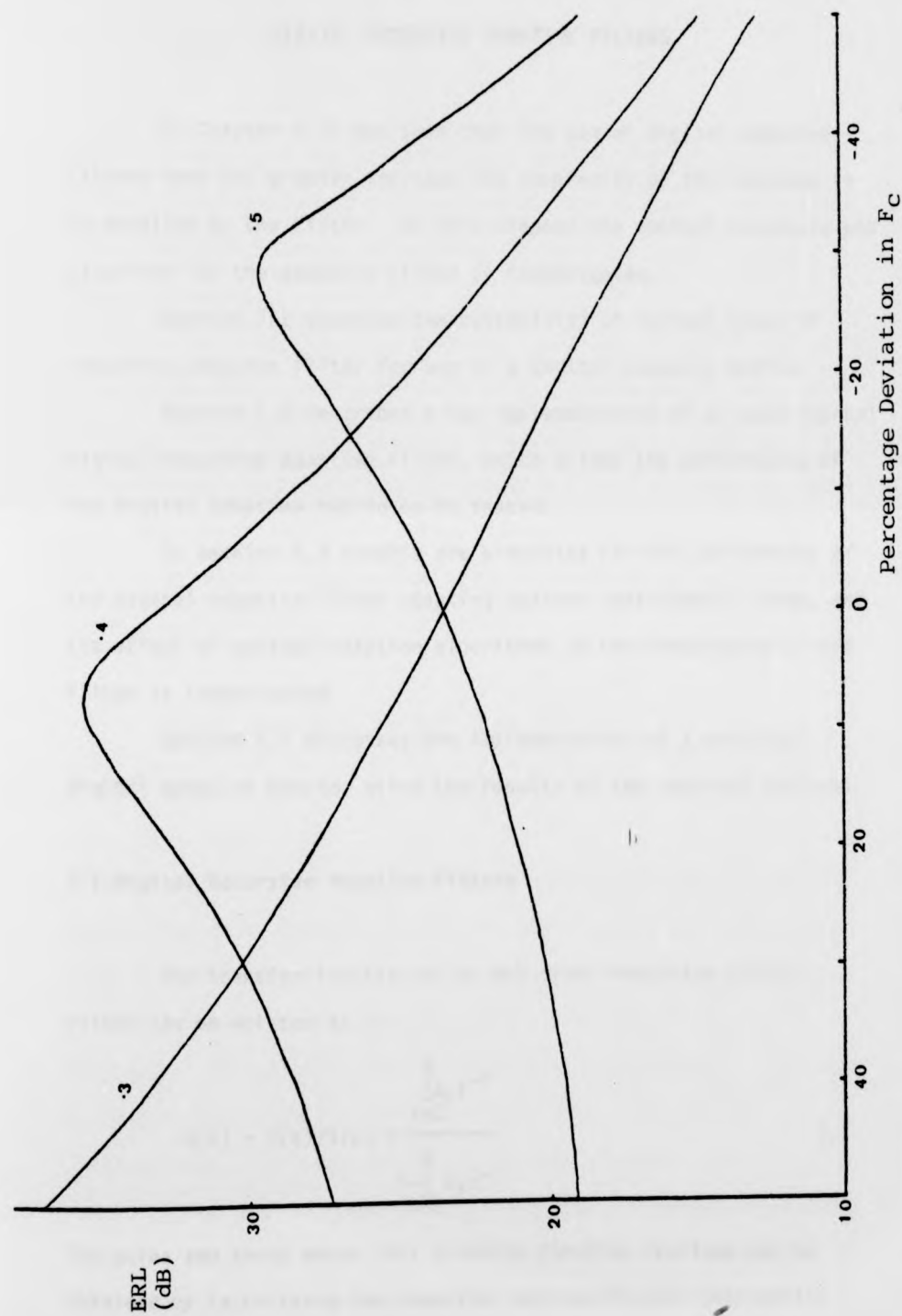
ERL
(dB)

30

20

10

.3

.4

.5

-40   -20   0   20   40

Percentage Deviation in F_c

Figure 6.17: ERL Achievable with Single Pole Compensation at 32 kHz Sampling Frequency
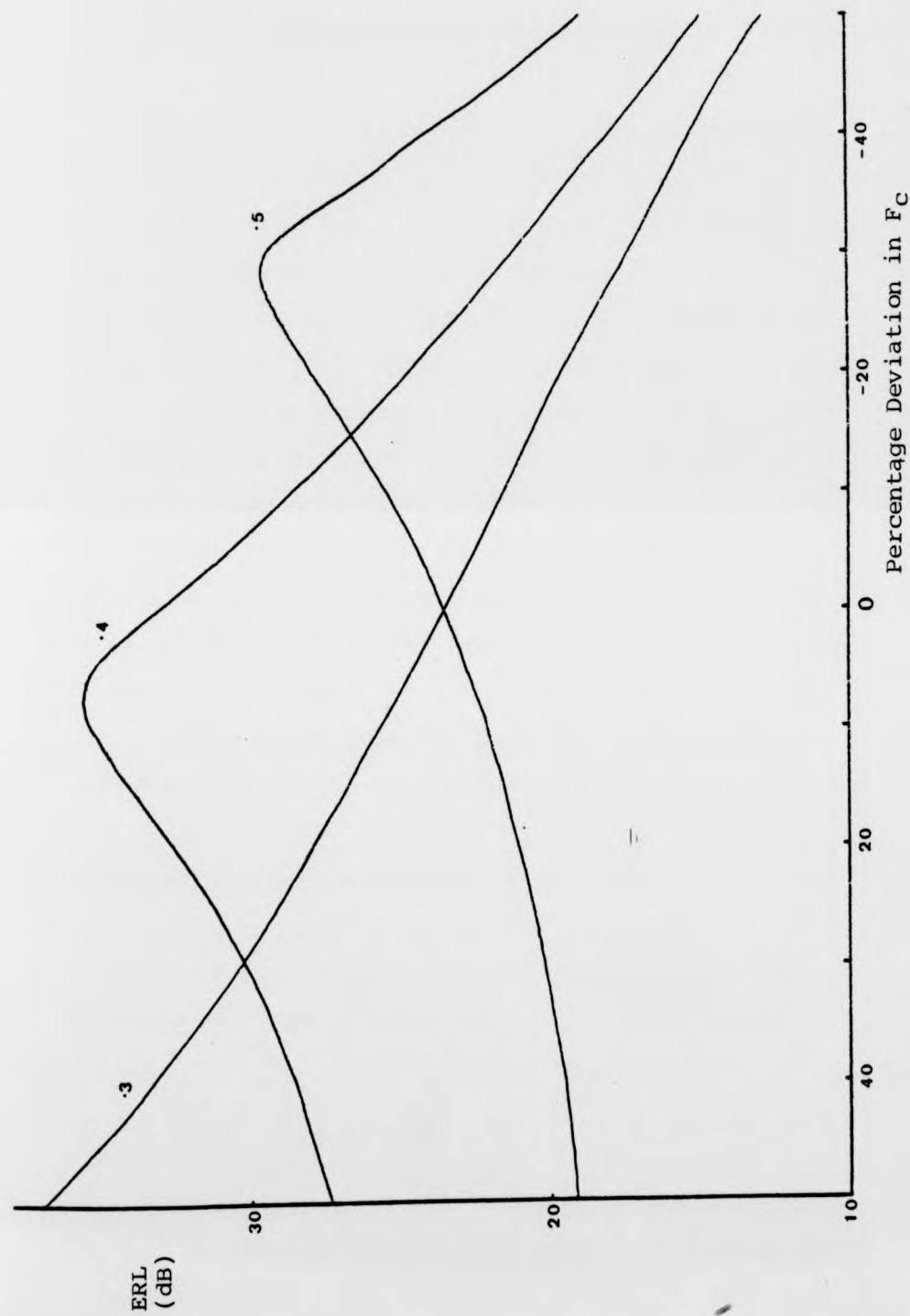
Figure 6.17: ERL Achievable with Single Pole Compensation at 32 kHz Sampling Frequency

CHAPTER 7

DIGITAL RECURSIVE ADAPTIVE FILTERS

In Chapter 6 it was seen that the use of digital adaptive filters need not greatly increase the complexity of the response to be modelled by the filter. In this chapter the optimal structure and algorithm for the adaptive filter is investigated.

Section 7.1 assesses the suitability of various types of recursive adaptive filter for use in a digital adaptive hybrid.

Section 7.2 describes a new implementation of an experimental digital recursive adaptive filter, which allows the performance of the digital adaptive hybrid to be tested.

In Section 7.3 results are presented for the performance of the digital adaptive filter adapting against subscribers' lines, and the effect of various adaption algorithms on the convergence of the filter is investigated.

Section 7.4 discusses the implementation of a practical digital adaptive hybrid, using the results of the previous sections.

7.1 Digital Recursive Adaptive Filters

The transfer function of an Nth order recursive digital filter can be written as :-

$$G(z) = Y(z)/X(z) = \frac{\sum_{i=0}^{N} a_i z^{-i}}{1 + \sum_{i=1}^{N} b_i z^{-i}} \qquad 7.1$$

The poles and zeros which this transfer function realises can be obtained by factorising the numerator and denominator polynomials

CHAPTER 7

DIGITAL RECURSIVE ADAPTIVE FILTERS

In Chapter 6 it was seen that the use of digital adaptive filters need not greatly increase the complexity of the response to be modelled by the filter. In this chapter the optimal structure and algorithm for the adaptive filter is investigated.

Section 7.1 assesses the suitability of various types of recursive adaptive filter for use in a digital adaptive hybrid.

Section 7.2 describes a new implementation of an experimental digital recursive adaptive filter, which allows the performance of the digital adaptive hybrid to be tested.

In Section 7.3 results are presented for the performance of the digital adaptive filter adapting against subscribers' lines, and the effect of various adaption algorithms on the convergence of the filter is investigated.

Section 7.4 discusses the implementation of a practical digital adaptive hybrid, using the results of the previous sections.

7.1 Digital Recursive Adaptive Filters

The transfer function of an Nth order recursive digital filter can be written as :-

$$G(z) = Y(z)/X(z) = \frac{\sum_{i=0}^{N} a_i z^{-i}}{1 + \sum_{i=1}^{N} b_i z^{-i}} \qquad 7.1$$

The poles and zeros which this transfer function realises can be obtained by factorising the numerator and denominator polynomials

into the form:-

$$\frac{Y(z)}{X(z)} = \frac{\prod_{i=1}^{N}(z-\alpha_i)}{\prod_{i=1}^{N}(z-\beta_i)}$$

where α_i and β_i are the locations of the zeros and poles in the z plane. Thus the Nth order filter can realise at most N poles and N zeros, and these can be situated on the real axis, or in complex conjugate pairs.

A realisation of the transfer function of equation 7.1 can be obtained by writing it in the form of a difference equation, i.e:-

$$y_n = a_0 x_n + a_1 x_{n-1} + \ldots a_n x_{n-N} - b_1 y_{n-1} - b_2 y_{n-2} - \ldots b_N y_{n-N} \qquad 7.2$$

This equation can be realised in the direct form as shown in Figure 7.1. When this filter is used as an adaptive filter, adapting against an unknown system whose transfer function is H(z), then the error signal is:-

$$E(z) = D(z) - Y(z) = X(z) \, H(z) - \frac{\sum_{i=0}^{N} a_i z^{-i}}{1 + \sum_{i=1}^{N} b_i z^{-i}} \qquad 7.3$$

or $e_n = d_{n\cdot} - y_{n\cdot}$ \qquad 7.4

As was seen in Chapter 4, the mean square value of the error signal can be considered to be a surface, in this case in 2N+1 dimensions. To derive the value of the mean square error for a given X(z), H(z) and G(z), the inverse Z transform of equation 7.3 can be taken, giving e_n. This procedure is equivalent to substituting values for x_n, d_n, a_i and b_i into equations 7.2 and 7.4, for $n = 0, 1, 2, \ldots$. Alternatively, $E(\omega T)$ can be calculated from equation 7.3 by integration around the unit circle, i.e. $z = e^{j\omega T}$, where $1/T = F_s$, the sampling frequency.

In the following subsections the major developments in

digital recursive adaptive filters are reviewed, and the suitability of the various techniques for use in a digital adaptive hybrid are assessed.

7.1.1 Mantey (1964)

Mantey has shown that the error surface resulting from equation 7.3 is not quadratic, and that it can have multiple minima, even when the adatptive filter is sufficient. For the case when the filter is of lower order than the unknown system, an example has been reported more recently by Larimore and Johnson (1977), in which the error surface has two minima. To overcome the problem of multiple minima, Mantey proposed the use of a modified or filtererd error criterion. This was achieved by filtering the error signal by the denominator polynomial of equation 7.1 to produce the filtered error signal $E'(z)$, i.e:-

$$E'(z) = \left(1 + \sum_{i=1}^{N} b_i z^{-i}\right) E(z) \qquad 7.5$$

Mantey showed that the filtered error signal is quadratic in both the a_i and the b_i coefficients, and that when the filter is sufficient, the minimisation of the mean square filtered error also minimises the mean square unfiltered error.

In addition to producing a quadratic filtered error surface, Mantey's proposal greatly simplifies the coefficient adaption algorithm. This can be seen by writing the equation for the Nth filtered error sample:-

$$e'_n = d_n + b_1 d_{n-1} + \ldots b_N d_{n-N} - a_0 x_n - \ldots a_N x_{n-N} \qquad 7.6$$

Thus e'_n can be considered as the subtracted outputs of two distinct transversal filters, one operating on samples of $d(t)$ and the other operating on samples of $x(t)$. The gradients of the instantaneous

squared filtered error can therefore be written as:-

$$\partial e_n'^2/\partial a_i = 2e_n'\,\partial e_n'/\partial a_i = -2e_n' x_{n-i} \qquad 7.7$$

The steepest descent algorithm (Widrow, 1966) for adapting the a and b coefficients is:-

$$a_{i,n+1} = a_{i,n} + \mu_a e_n' x_{n-i} \qquad 7.8$$

and

$$b_{i,n+1} = b_{i,n} - \mu_b e_n' d_{n-i} \qquad 7.9$$

where the subscripts $i,n+1$ denote the ith coefficient at time t = $(n+1)T$, and the parameters μ_a and μ_b are the a and b step sizes. This algorithm is relatively simple to implement by comparison with those for the other types of recursive adaptive filter, considered in the remainder of this section. Further simplifications are possible by using non-linear functions of the signal samples, as widely reported for transversal adaptive filters

The alteration in the filter structure guarantees the stability of the filtered error signal, as was seen for the analog recursive adaptive filters. Since error filtering in the digital case also affects the near-end signal, it is necessary to form the unfiltered error signal. This is done by passing the filtered error through a system with transfer function:-

$$F(z) = \frac{1}{1+\sum_{i=1}^{N} b_i z^{-i}} \qquad 7.10$$

and in this case stability problems may arise. The stability of the circuit which provides the compensation for the effects of error filtering can however be assured by checking the values of the b_i coefficients as they are calculated by the adaption algorithm, e.g:- for a first order filter the stability requirement is simply:-

$$b_i < 1$$

For higher order filters the check becomes more complex.

7.1.2 White (1975)

A recursive adaptive filter proposed by White used a recursive algorithm to compute the error gradients for the a_i and b_i coefficients. An example of the technique used can be obtained by calculating the gradient $\partial e_n/\partial b_i$ from equations 7.4 and 7.2, where N = 2, i.e:-

$$\frac{\partial e_n}{\partial b_i} = -\frac{\partial y_n}{\partial b_i} = y_{n-i} + b_1 \frac{\partial y_{n-1}}{\partial b_i} + b_2 \frac{\partial y_{n-2}}{\partial b_i}$$

Thus $\partial e_n/\partial b_i$ is the output of the recursive section shown in Figure 7.2. The gradient with respect to a_i can be calculated in a similar manner. The above algorithm has also been referred to as Stearn's algorithm (Stearns, Elliott and Ahmed, 1976).

To implement a second order recursive adaptive filter, using White's algorithm, requires 6 second order sections. In addition it is necessary to make some asumptions about the initial values of the error gradients, and the effect of these assumptions on the convergence of the filter is unknown.

7.1.3 Feintuch (1976)

Feintuch's controversial paper proposed to adjust the coefficients in the recursive filter whose output is given by equations 7.4 and 7.2, using the algorithms:-

$$a_{i,n+1} = a_{i,n} + \mu_a e_n x_{n-i}$$

and

$$b_{i,n+1} = b_{i,n} - \mu_b e_n y_{n-i}$$

In subsequent correspondence Johnson and Larimore (1977) pointed out that Feintuch's algorithm represents a truncation of White's algorithm after the first term, and that the basis on which it was

derived is invalid when the filter's coefficients are updated using the gradients. Two examples of the failure of Feintuch's algorithm were given by Johnson and Larimore, both of which involved insufficiency in the adaptive filter. In one case the error surface had two minima, neither of which were located by the adaption algorithm, while in the other case it failed to locate even a single minimum.

Feintuch and Bershad (1977) in reply to Johnson and Larimore, reported two examples in which Feintuch's algorithm showed correct convergence. In both of these cases the adaptive filter was sufficient. A further comment on Feintuch's algorithm was made by Widrow and Mc. Cool (1977).

7.1.4 Parikh and Ahmed (1978)

Parikh and Ahmed proposed a sequential regression algorithm (SER) for recursive adaptive filters, in which the error criterion to be minimised is :-

$$J(\alpha) = q\sum_i [d(i) - y(i)]^2 + \alpha^T\alpha \qquad 7.11$$

where the filter output is:-

$$y_i = \alpha^T\beta_i$$

and y_k is the desired signal sample, α is the vector of filter coefficients, β is the vector of input and output samples, and q is a weighting factor. The first term in equation 7.11 is a measure of the error, while the second term is added to control the filter coefficients when the input signal is zero. Using equation 7.11, the expression for the rth estimate of the coefficient vector is:-

$$\alpha_k = \alpha_{k-1} + qP_k^{-1}\lambda_k e_k \qquad k = 1,\ldots.r \qquad 7.12$$

where

$$P_k = I + \sum_{j=1}^{k} q \lambda_j \beta_j^T \qquad\qquad 7.13$$

and $\lambda_j = \nabla_\alpha(g_j)$, the gradient vector at time $t = jT$. If the second term is absent from equation 7.11 , then the identity matrix is absent from equation 7.13, and when the input signal is zero, P_i is a singular matrix. P_i^{-1} does not exist under these conditions, and Equation 7.12 then becomes meaningless (Ahmed, Hummels et al, 1979).

P_k and λ_j are computed recursively using the relationships:-

$$\lambda_j = \beta_j + \sum_{p=1}^{N} b_{p,j-1} \lambda_{j-p} \quad \text{(White's algorithm)} \qquad 7.14$$

and

$$P_k^{-1} = P_{k-1}^{-1} - P_{k-1}^{-1} \lambda_k \beta_k^T P_{k-1}^{-1} / \gamma \qquad\qquad 7.15$$

where

$$\gamma = \beta_k^T P_{k-1}^{-1} \lambda_k + 1/q \qquad\qquad 7.16$$

Parikh and Ahmed used an example of a first order adaptive filter converging against a second order system, to show the convergence of the SER algorithm to the global minimum. It was also shown that White's algorithm converged to the minimum which was nearest to its starting point.

Implementation of the SER algorithm in hardware would be extremely difficult because of the many operations involved in calculating equations 7.12 and 7.14 to 7.16. Furthermore, Parikh and Ahmed do not suggest a method of assigning initial values to the gradients of equation 7.14. It is indicative of the complexity of this approach that Ahmed, Hummels et al report an example of a modified SER algorithm operating at 8 samples/sec.

7.1.5 Treichler, Larimore and Johnson (1978)

Treichler, Larimore and Johnson applied analytical techniques developed by Ljung (1977) and Landau (1976) to the convergence of adaptive filters. In particular it was shown that if the adaptive filter whose transfer function is given by equation 7.1 models an unknown system with transfer function:-

$$H(z) = \frac{\sum\limits_{j=0}^{M} \alpha_j z^{-j}}{1 + \sum\limits_{i=1}^{N} \beta_i z^{-i}}$$

then the error signal can be considered to be generated by the system shown in Figure 7.3, where $W(z)$ is a function of the desired signal, the adaptive filter's output and of the mismatch between the coefficients of the adaptive filter and those of the unknown system. The transfer function of the forward path is:-

$$F(z) = \frac{1}{1 + \sum\limits_{i=1}^{N} \beta z^{-1}}$$

Thus assuming β_i is constant, then the time varying element of the adaption algorithm is isolated in the feedback path of Figure 7.3, and the hyperstability theory of non-linear systems (Popov, 1973 or Larimore, 1981) can be applied. Treichler, Larimore and Johnson reported that to guarantee the convergence of the error signal, it is sufficient that:-

1) the feedback path satisfy the constraint given by:-

$$-\sum_{k=0}^{\infty} w_k e_k < A$$

where A is a positive constant, i.e. the gain of the feedback path is positive on average, and

2) the system in the forward path has a strictly positive real part, i.e. the forward path always introduces less than 90° phase shift. The latter condition imposes restrictions on the type of unknown system against which an adaption algorithm will converge, and it was shown that the region of convergence does not include unknown systems of the second order with poles near $z = 1$.

Treichler Larimore and Johnson suggested that the adaption algorithm minimise a filtered error signal given by:-

$$E'(z) = E(z)[1 + \sum_{i=1}^{P} c_i z^{-i}]$$

In this case the forward path transfer function of Figure 7.3 becomes:-

$$F(z) = \frac{1 + \sum_{i=1}^{P} c_i z^{-i}}{1 + \sum_{i=1}^{N} \beta_i z^{-i}}$$

and the error filtering coefficients (c_i) can then be used to control the convergence of the filtered error signal, in accordance with the hyperstability conditions.

In an example in which the adaptive filter was sufficient, it was shown that the use of a single error filtering coefficient caused much faster convergence of Feintuch's algorithm. It was also found that the hyperstability condition was "sufficient but not necessary" to ensure convergence.

More recent work on hyperstable adaptive filters, for example Johnson, Larimore, Treichler and Anderson (1981), and Johnson, Landau, Taylor and Dugard (1981) has failed to arrive at a satisfactory technique for automatically selecting the error filtering coefficients. Nevertheless, the implementation of simple

error filtering functions does not greatly complicate the adaptive filter structure, and the technique may allow simple adaption algorithms to be used.

7.1.6 Parikh, Ahmed and Stearns (1980)

Parikh, Ahmed and Stearns introduced an algorithm for adapting the coefficients of a lattice type digital recursive adaptive filter. This lattice structure is a development of a technique used for the linear prediction of speech, and it has the advantage that each lattice coefficient can be adjusted independently of the other coefficients (Gibson and Haykin, 1980). This leads to fast convergence. A further advantage of the lattice filter is that a simple check on each coefficient is adequate to ensure the stability of the filter (Gray and Markel, 1973).

The scheme proposed by Parikh, Ahmed and Stearns used a highly complex recursive algorithm to adapt the coefficients of the lattice, in general 3 multiplications, 3 additions and an N-stage convolution being required for each new coefficient, where N is the order of the filter. A recent attempt to simplify this algorithm (Ayala, 1982) resulted in the lattice becoming unstable following convergence.

Due to the difficulty of implementing the lattice adaptive filter in hardware, it was not considered suitable for use in a digital adaptive hybrid.

7.2 The Experimental Digital Recursive Adaptive Filter

In the previous section it was seen that the filter structure proposed by Mantey is relatively simple, and is readily implemented

error filtering functions does not greatly complicate the adaptive
filter structure, and the technique may allow simple adaption
algorithms to be used.

7.1.6 Parikh, Ahmed and Stearns (1980)

Parikh, Ahmed and Stearns introduced an algorithm for
adapting the coefficients of a lattice type digital recursive
adaptive filter. This lattice structure is a development of a
technique used for the linear prediction of speech, and it has the
advantage that each lattice coefficient can be adjusted independently
of the other coefficients (Gibson and Haykin, 1980). This leads to
fast convergence. A further advantage of the lattice filter is that
a simple check on each coefficient is adequate to ensure the
stability of the filter (Gray and Markel, 1973).

The scheme proposed by Parikh, Ahmed and Stearns used a
highly complex recursive algorithm to adapt the coefficients of the
lattice, in general 3 multiplications, 3 additions and an N-stage
convolution being required for each new coefficient, where N is the
order of the filter. A recent attempt to simplify this algorithm
(Ayala, 1982) resulted in the lattice becoming unstable following
convergence.

Due to the difficulty of implementing the lattice adaptive
filter in hardware, it was not considered suitable for use in a
digital adaptive hybrid.

7.2 The Experimental Digital Recursive Adaptive Filter

In the previous section it was seen that the filter structure
proposed by Mantey is relatively simple, and is readily implemented

in hardware. The results of Chapter 5 show that an analog adaptive filter having a single pole and zero can achieve adequate ERLE against most subcsribers' lines. Furthermore, Chapter 6 showed that the process of A/D and D/A conversion need not introduce much further complexity into the required adaptive filter structure. For the above reasons it was decided to implement a low order digital recursive adaptive filter, based on that proposed by Mantey. To maintain maximum flexibility the adaption algorithm is resident on a computer, while for real-time operation with simulated transhybrid responses the actual filter is implemented in hardware. The following sections describe the implementation and operation of the experimental digital recursive adaptive filter.

7.2.1 Implementation of the Experimental Filter

Figure 7.4 shows a block diagram of the required filter structure. The filter consists of two transversal sections, each having 4 coefficients. The combined output from these sections is:-

$$E'(z) = D(z)\sum_{i=0}^{3} b_i z^{-i} - X(z)\sum_{i=0}^{3} a_i z^{-i} \qquad 7.17$$

$E'(z)$ is therefore the filtered error signal of Section 7.1.1. The remaining section of the filter implements the compensation for the effect of error filtering on near-end speech, i.e:-

$$E(z)/E'(z) = \frac{1}{1 + \sum_{i=1}^{3} c_i z^{-i}} \qquad 7.18$$

and assuming $c_i = b_i$, for $i = 1,2,3$, with $b_0 = 1$, then the non-filtered error signal is given by equation 7.3, with $N = 3$. Thus the structure of Figure 7.4 is capable of implementing recursive adaptive filters of up to third order, with compensation for error filtering.

in hardware. The results of Chapter 5 show that an analog adaptive
filter having a single pole and zero can achieve adequate ERLE
against most subcsribers' lines. Furthermore, Chapter 6 showed that
the process of A/D and D/A conversion need not introduce much further
complexity into the required adaptive filter structure. For the
above reasons it was decided to implement a low order digital
recursive adaptive filter, based on that proposed by Mantey. To
maintain maximum flexibility the adaption algorithm is resident on a
computer, while for real-time operation with simulated transhybrid
responses the actual filter is implemented in hardware. The
following sections describe the implementation and operation of the
experimental digital recursive adaptive filter.

7.2.1 Implementation of the Experimental Filter

Figure 7.4 shows a block diagram of the required filter
structure. The filter consists of two transversal sections, each
having 4 coefficients. The combined output from these sections is:-

$$E'(z) = D(z)\sum_{i=0}^{3} b_i z^{-i} - X(z)\sum_{i=0}^{3} a_i z^{-i} \qquad 7.17$$

$E'(z)$ is therefore the filtered error signal of Section 7.1.1. The
remaining section of the filter implements the compensation for the
effect of error filtering on near-end speech, i.e:-

$$E(z)/E'(z) = \frac{1}{1 + \sum_{i=1}^{3} c_i z^{-i}} \qquad 7.18$$

and assuming $c_i = b_i$, for $i = 1,2,3$, with $b_0 = 1$, then the
non-filtered error signal is given by equation 7.3, with $N = 3$. Thus
the structure of Figure 7.4 is capable of implementing recursive
adaptive filters of up to third order, with compensation for error
filtering.

Figure 7.5 shows a block diagram of the implementation of the filter, using only a single multiplier and accumulator (MAC) to perform all the required arithmetic operations. Both the signal samples and the coefficients are represented by 12 bit 2s complement numbers. This implementation is similar to that of the 128th order transversal filter described in Chapter 3, with the exception that the signal samples are held in a RAM rather than in a recirculating shift register. This allows the samples to be readily accessed by the adaption algorithm, but requires a complex RAM addressing scheme, as discussed in the next section.

The samples of $x(t)$ are obtained from the A/D, which also produces input samples for the line and hybrid simulator (LHS). The $d(t)$ samples are read from the output of the LHS, and the D/A can be used to examine the filtered error, the unfiltered error, or the LHS output, as shown in Figure 7.5. A delay of either 1 or 2 sample periods can be imposed on the x_n samples to compensate for the delays through the LHS.

The experimental filter is interfaced to the computer using techniques similar to those described in Chapter 3, and in the next section discussion is therefore restricted to the operation of the filter itself.

7.2.2 Operation of the Experimental Filter without Adaption

Figure 7.6a shows the contents of both the signal and the coefficient RAMs at some time $t = t_0$. Within the next sample period both RAMs are addressed in the sequence 0,1,....11, with the MAC first calculating e'_n according to equation 7.6, with $N = 3$. e'_n is then clocked into output register 2, and the MAC continues to calculate:-

$$e_n = e'_n - \sum_{i=1}^{3} c_i e_{n-i} \qquad\qquad 7.19$$

e_n is then clocked into output register 1, and a single cycle of operation has been performed.

Before the next such cycle can begin, the filter loads x_{n+1}, d_{n+1} and e_n into signal RAM locations 3, 7 and 11 respectively. Thus the contents of the RAMs are as shown in Figure 7.6b. To calculate e'_{n+1} and e_{n+1} the signal RAM is now addressed in the sequence 3,0,1,2, 7,4,5,6, 11,8,9,10. This completes the second cycle, and the filter now loads x_{n+2}, d_{n+2} and e_{n+1} into locations 2, 6 and 10 respectively. This leaves the RAM contents as shown in Figure 7.6c. To complete the 3rd cycle the signal RAM is addressed in the sequence 2,3,0,1, 6,7,4,5, 10,11,8,9, while e'_{n+2} and e_{n+2} are calculated. Signal RAM locations 1, 5 and 9 are now loaded with x_{n+3}, d_{n+3} and e_{n+2}, and the RAMs' contents are as shown in Figure 7.6d.

During the 4th cycle the signal RAM is addressed in the sequence 1,2,3,0, 5,6,7,4, 9,10,11,8 while e'_{n+4} and e_{n+4} are calculated. Finally locations 0, 4 and 8 are loaded with x_{n+4}, d_{n+4} and e_{n+3}, leaving the RAMs' contents as shown in Figure 7.6e. The filter has now completed 4 cycles, and the sequence repeats.

Figure 7.7 shows a simplified timing diagram of the operation of the filter during the second cycle, in which the error samples e'_{n+1} and e_{n+1} are calculated, new signal samples are loaded into the signal RAMs, and the accumulator is cleared preparatory to calculating e'_{n+2} and e_{n+2}.

7.2.3 Operation of the Experimental Filter during Adaption

The computer is interfaced to the filter via 4 input/output ports, in a manner similar to that described in Chapter 3. In order to load coefficients into the coefficient RAM, or to read signal

samples from the signal RAM, the computer halts the RAM address
counter via the control port. A handshaking system ensures that the
counter is always halted during the first cycle, when the contents of
the RAMs are as shown in Figure 7.6a. The computer can then address
either of the RAMs by first writing the address of the required
location to the address counter via the address port, and reading the
signal sample from the signal port, or writing the updated
coefficient to the coefficient port. The sample of the filtered
error signal is obtained by addressing output register 2 (via the
address counter), and reading the sample via the signal port. The
Macro-11 programs AFWRIT and AFREAD which allow the filter to be
controlled from a Fortran program are given in Appendix A2.

While the filter is in the halt state the previous error
signal samples are held at the output registers, and no new signal
samples are input to the signal RAM. Thus when the filter is
restarted with new coefficients, a transient is observed in the error
signals. When the transient response due to the recursive section of
the filter is long, then the transient in the unfiltered error signal
is slow to decay. Transients in the filtered error signal decay
after 4 input sample periods.

7.3 Performance of the Experimental Filter

In this section results for the performance of the
experimental digital recursive adaptive filter, adapting against
simulated transhybrid responses, are given. In Section 7.3.1 the
optimum order for the filter is investigated by measuring the values
of cancelled ERL which filters of various orders can achieve against
all 1845 lines in the line survey. The dynamic performance of the

optimal filter is investigated in Section 7.3.2.

Section 7.3.3 investigates the effect of the adaption algorithm on the speed of convergence of the adaptive filter, and an adaption algorithm with an adaptive loop gain is developed.

7.3.1 Filter Order

Measurement of the cancelled ERL achieved by adaptive filters of various orders against all 1845 lines in the line survey would be a time consuming task. However, since the adaptive filter is controlled by a computer, and the computer has access to samples of the input, desired input, and non-filtered error signals, then automated measurements of original ERL, cancelled ERL and ERLE are possible. This can be achieved by calculating the quantities:-

$$\text{original ERL} = 10\log_{10}\{\sigma^2_x/\sigma^2_d\}$$
$$\text{cancelled ERL} = 10\log_{10}\{\sigma^2_x/\sigma^2_e\}$$

and

$$\text{ERLE} = 10\log_{10}\{\sigma^2_d/\sigma^2_e\}$$

where σ^2_x, σ^2_d and σ^2_e are the variances of the samples of the input, desired input and error signals respectively. In the experimental digital recursive adaptive filter the samples are available in blocks of 4 consecutive samples (Section 7.2.2), and to ensure that no samples are used more than once it is necessary to introduce a delay between readings of data from the filter. To determine the number of blocks of 4 samples of each signal which are required for accurate calculation of the return losses, the following experiment was conducted.

The adaptive filter and the LHS were loaded with coefficients which gave a RLE of 6.02 dB at all frequencies. 100 calculations of ERLE were carried out for various numbers of blocks of 4 samples, and

the resulting mean and standard deviations of the ERLE calculations were computed. The value of the mean ERLE was found to be accurate to within 1% in all cases.

Using 100 blocks of samples it was found that the standard deviation of ERLE was 0.2 dB. If the values of ERLE are assumed to be normally distributed about the mean, then this number of blocks gives a probability of 99.75% that the ERLE is within ± 0.6 dB of the computed value. Thus in the remainder of this section 100 blocks of 4 consecutive samples are used to calculate the return losses, and the accuracy of the calculation is estimated to be ± 0.6 dB.

To investigate the performance which can be achieved by adaptive filters of various orders, the transhybrid response due to each subscriber's line in the line survey is calculated and loaded into the LHS, as described in Chapter 3. The adaptive filter is then allowed to adapt against this response using the linear adaption algorithm described in Section 7.1.1, with an input signal of white noise, bandlimited to 500 Hz to 2.5 kHz, at level -4 dB. The value of the step size is chosen so that the filter converges quickly at this level of input signal (see Section 7.3.3). After 500 iterations the value of the return losses are calculated as described previously, and the final values of the filter coefficients are also stored for subsequent analysis. The value of 500 iterations is chosen because it ensures that the filter has converged fully in all cases. A copy of the Fortran program ADHYB, used to carry out these measurements is given in Appendix A2.

Table 7.1 records the results obtained for 5 different adaptive filter orders, where NA is the number of transversal coefficients used in the adaptive filter, and NB is the number of feedback coefficients. The entries in the table are in order of decreasing mean cancelled ERL, the best performance being obtained by

the structure with NA = 2 and NB = 1 (a variable pole and zero). In
this case the mean cancelled ERL is 33.6 dB, and the minimum
cancelled ERL is 26 dB. Using 4 transversal coefficients alone, the
mean ERL is reduced by 4.3 dB, while the minimum cancelled ERL is
reduced by 10 dB. The remaining filter structues are simpler than
either of the previous two, but their performance is considerably
worse.

7.3.2 Dynamic Performance of the Experimental Filter

In the previous section it was seen that the filter having a
variable pole and zero gave the best performance of a range of simple
structures. In this section the number of iterations required for
this filter to achieve a given cancelled ERL is measured. This
measurement is performed with the step size close to the maximum step
size possible for the given input signal level, and using the linear
adaption algorithm. The effect of lower input signal levels, and
different step sizes and adaption algorithms, is considered in
Section 7.3.3.

As discussed in Section 5.3.5, the dynamic performance of the
filter is vital in determining the feasibility of an adaptive hybrid
In Section 5.3.5 it was also shown that the dynamic performance of an
adaptive hybrid can be considerably improved by allowing it to begin
convergence from a properly chosen set of initial coefficients.
Since the storage of a set of initial coefficients is a trivial
problem in the case of a digital adaptive filter, this method was
used in measuring the convergence of the filter. Figures 7.8a, b and
c show plots of the probability distributions of the coefficients a_0,
a_1 and b_1 for the single pole and zero filter, adapting against the
1845 subscribers' lines, where a coefficient value of 2048 represents

an actual coefficient value of 1. The mean values of the coefficients are:-

$$a_{0m} = 102, \ a_{1m} = -563 \text{ and } b_{1m} = 666$$

and these values were chosen as the initial coefficient set of the filter. The filter was then allowed to adapt against the 1845 subscribers' lines, and the initial cancelled ERL and the number of iterations required to achieve 20 dB cancelled ERL were measured. Figure 7.9 shows a plot of the resulting cumulative distribution of initial cancelled ERL, and it can be seen that all lines have initial cancelled ERL greater than 7 dB. This figure thus represents the guaranteed minimum initial ERL which can be achieved in the network using the single pole and zero filter, with the given initial coefficient set. Figure 7.9 also shows however, that 52% of lines have initial cancelled ERL values greater than 20 dB. Figure 7.10 shows the cumulative distribution of the number of iterations required to achieve 20 dB cancelled ERL. For all lines this value of ERL is achieved within 100 iterations. For 80% of lines however, 20 dB cancelled ERL is achieved within 20 iterations, while for all lines this value of cancelled ERL is obtained within 100 iterations.

Using the linear adaption algorithm, with the adaptive filter operating at 16 kHz, the rate of iteration of the experimental adaptive filter was found to be 400/Sec. Thus in the worst case, 20 dB canceled ERL was achieved within 250 mS. This slow iteration rate is due to the implementation of the adaption algorithm in Fortran, and it could be increased by an assembly language implementation. The fastest possible iteration rate for the experimental filter is once per 4 input samples.

7.3.3 Adaption Algorithms

In this section the effect of various adaption algorithms on the convergence of the adaptive filter is investigated experimentally, using an example of an adaptive transversal filter having a single coefficient. Widrow (1966) has shown that for a digital transversal adaptive filter, using the linear adaption algorithm, there is a maximum value of step size which can be allowed without causing the filter to diverge. Widrow also showed that this maximum step size is inversely proportional to the power of the input signal. To investigate these effects further, the 0th order transversal filter was allowed to adapt against an LHS response having a single 0th order coefficient of value 1024, for various values of step size and input signal power. An average value of the coefficient a_0 was calculated after each iteration of the algorithm, over N_{adpt} adaptions from an initial value of 0. This allows an averaged convergence curve for the coefficient to be plotted, with the variations in the speed of convergence due to statistical fluctuations in the input signal removed. In each case N_{adpt} was chosen so that a smooth curve was obtained for a_0. The standard deviations of the a_0 values after each iteration were also calculated, since this gives a measure of the speed with which the spread in the values of a_0 is reduced to zero. A typical convergence curve, obtained as described above, for the case when the input signal level is -4 dB and the step size is 1/1024, is shown in Figure 7.11. It can be seen that $\overline{a_0}$ converges exponentially to its optimum value, and that the spread of coefficient values rapidly reaches its maximum value and then drops to zero, indicating that in all cases the filter converges. Figure 7.12a and b shows the values of the time constants of $\overline{a_0}$ and σ_{a0} (in iterations), as a function of the

step size, for various levels of input signal (white noise, bandlimited to 500 Hz to 2.5 kHz). Using the linear adaption algorithm. The figure shows that for each level of input signal there is a value of step size which gives optimal convergence, and increasing the step size above this level causes the filter to "hunt". An example of this is shown in the results of a single adaption of a_0 with step size = 1/96 and input level = -4 dB, recorded in Figure 7.13. This hunting causes the sharp increase in the time constant of σ_{a0} shown in Figure 7.12b. As the value of the step size is further increased the hunting becomes worse and the filter eventually becomes unstable.

The dependence of the speed of convergence of the filter on the power of the input signal is undesirable, and it can be reduced by using only the sign of the input signal in the adaption algorithm (Sondhi and Presti, 1966, see Chapter 1). Thus if the adaption algorithm is :-

$$a_{0,i+1} = a_{0,i} + \mu_a e_i' Sgn[x_i]$$

then the dependence of the speed of convergence of the filter on the step size μ_a and the input signal level is shown in Figure 7.14a and b. In this case the optimum step size is inversely proportional to the square root of the signal power, i.e:- a reduction in the signal power by a factor of 4 allows a doubling of the optimum step size.

These results show that to achieve optimum convergence of the filter it is necessary to estimate the power of the input signal, and adjust the step size accordingly. Such a scheme was proposed for use in an echo canceller by Hoge (1975).

In the experimental adaptive filter the power of the input signal can be simply obtained by calculating the variance of the input signal samples over a suitable number of blocks of 4 samples. This process takes time however, and during this time the filter must

adapt using a default step size. This default step size should be
optimum for the maximum input signal power, to avoid the possibility
of instability. Thus if the input signal power is low, the initial
convergence will be far from optimal. To minimise this effect the
number of blocks used to compute σ^2_x should be small. Use of too few
blocks to compute σ^2_x however, could result in too high a value of
step size for a given input signal power, and the filter could become
unstable. To allow a choice between these conflicting requirements,
100 calculations of the input signal power were performed over
various numbers of iterations, and the mean and standard deviations
of the signal powers were calculated. The input signal was
bandlimited white noise at level -4 dB. If it is assumed that the
calculated values of the signal power are normally distributed about
the mean, then the σ, 2σ and 3σ values can be used to assign limits
to the errors in the calculations with probabilities of 66.6%, 95%
and 99.75% respectively. This is shown in Figure 7.15, from which it
can be seen that choosing 32 iterations over which to calculate σ^2_x
gives a 99.7% probability that the actual σ^2_x value is within ± 50%
of the calculated value.

If the non-linear adaption algorithm were used, the required
step size would be inversly proportional to the square root of σ^2_x.
Since extraction of the square root would be difficult in an
all-hardware implementation of the adaptive filter, the linear
adaption algorithm should be used with the adaptive step size. A
value of 1/512 was chosen as the required step size at the -4 dB
signal level. This is sufficiently far from the optimum step size to
ensure no danger of instability, even with an error of ± 50% in σ^2_x.
The mean calculated value of σ^2_x for the -4 dB input signal level was
$0.23*10^{+6}$, and thus the equation for the step size is:-

$$\mu_a = \frac{0.23*10^{+6}}{512*\sigma^2_x}$$

Figure 7.16 shows the convergence of the mean and standard deviations of a_0, using the adaptive step size, when the input signal level is -34 dB. The figure shows that with the initial value of step size no adjustement in the initial value of a_0 is observed, however after 32 iterations the step size is increased and the filter converges rapidly. Using this algorithm the maximum time required for the filter to converge is 32 iterations, followed by a time constant of approximately 4 iterations.

When the adptive filter has a feedback path in addition to the feedforward path, then the feedback path can be considered to be a transversal filter if error filtering is used. Thus the optimum step size used in calculating the feedback coefficient is related to the power in the desired input signal. Estimation of this power, in adition to that of the input signal, would add greatly to the complexity of the filter, although it could perhaps be assumed that power of $d(t)$ is a constant proportion of the power of $x(t)$. For the results of Sections 7.3.1 and 7.3.2, the step sizes were the same for both the feedback and the feedforward coefficients, and thus it can be deduced that the times taken for the filter to converge to 20 dB cancelled ERL, with any input signal level, are those of Section 7.3.2 plus 32 iterations. This assumes that an adaption algorithm with an adaptive step size is used, and that the number of iterations over which the step size is measured is 32.

7.4 Discussion

It has been shown that a digital adaptive filter using error filtering, with a single feedback coefficient and a pair of feedforward coefficients, provides a minimum cancelled ERL of 26 dB

for all 1845 lines in the survey. Using a set of stored initial coefficients, the filter ensures 7 dB initial cancelled ERL for all lines. The filter guarantees 20 dB cancelled ERL for all lines within 100 iterations at high signal levels. If an adaptive step size is used, this figure is increased by only 32 iterations, even for very low signal levels.

A block diagram of the proposed first order digital adaptive filter, for use in a digital adaptive hybrid, is shown in Figure 7.17. The filter includes compensation for effects of error filtering, and a means of measuring the input signal power for use in adapting the step size. The multiplications indicated by multipliers a_0, a_1 and the two b_1 multipliers, and the additions indicated by S_1 and S_2 can be easily performed by a single time-shared multiplier/accumulator (MAC), as in the experimental adaptive filter. Similarly the multipliers M_{a0}, M_{a1} and M_{b1}, and the accumulators following them, could consist of another time-shared MAC. Estimation of the signal power would require a third MAC. The scalers in the circuit can be designed to scale by powers of 2, and are therefore simply implemented.

A suggested implementation of the circuit is shown in Figure 7.18. For a 32 kHz sampling rate, MAC1 should be capable of performing a single multiply/accumulate in 7.8 µS, while MAC2 should be capable of performing a single multiply/accumulate in 10.4 µS. This assumes that the coefficients are updated as fast as possible, i.e; at the sampling frequency. MAC3 is required to perform a single multiply/accumulate in 31.25 µS. Thus the main arithmetic requirement of the filter could be performed by a single MAC, capable of performing a multiply/accumulate in 3.9 µS. In addition to the MACs, the filter requires only 9 words of data storage (assuming N bits are used to represent both the coefficients and the signal

samples), 2 multiplexers and 2 scalers. This level of complexity is well within the possibilities of current technology (for example Adams, Harbridge and Macmillan, 1981), however the use of a single time-shared MAC would require complicated control and timing circuitry. Use of separate MACs allows greater flexibility in the choice of the number of bits required to represent the various signals, and this could lead to considerable reductions in the required speed of the MACs.

	Mean	Std. Dev	Minimum	Maximum
Original ERL	10.14	1.95	6.0	17.5
Na=2, Nb=1 Cancelled ERL	33.65	3.06	26.0	41.5
ERLE	23.5	2.11	11.5	30.5
Na=4, Nb=0 Cancelled ERL	29.3	5.97	16.0	44.5
ERLE	19.16	4.46	9.5	31.5
Na=2, Nb=1, a_0=0 Cancelled ERL	28.2	5.15	14.5	38.0
ERLE	18.1	5.35	2.5	28.5
Na=2, Nb=0 Cancelled ERL	24.4	6.75	12.0	39.5
ERLE	14.3	5.07	6.0	25.0
Na=1, Nb=1 Cancelled ERL	19.5	5.65	9.0	36.0
ERLE	9.4	3.87	2.5	9.0

Note: All Return Losses are expressed in dB.

Table 7.1   Performance of the Experimental Digital Recursive Adaptive Filter against Subscribers' Lines.
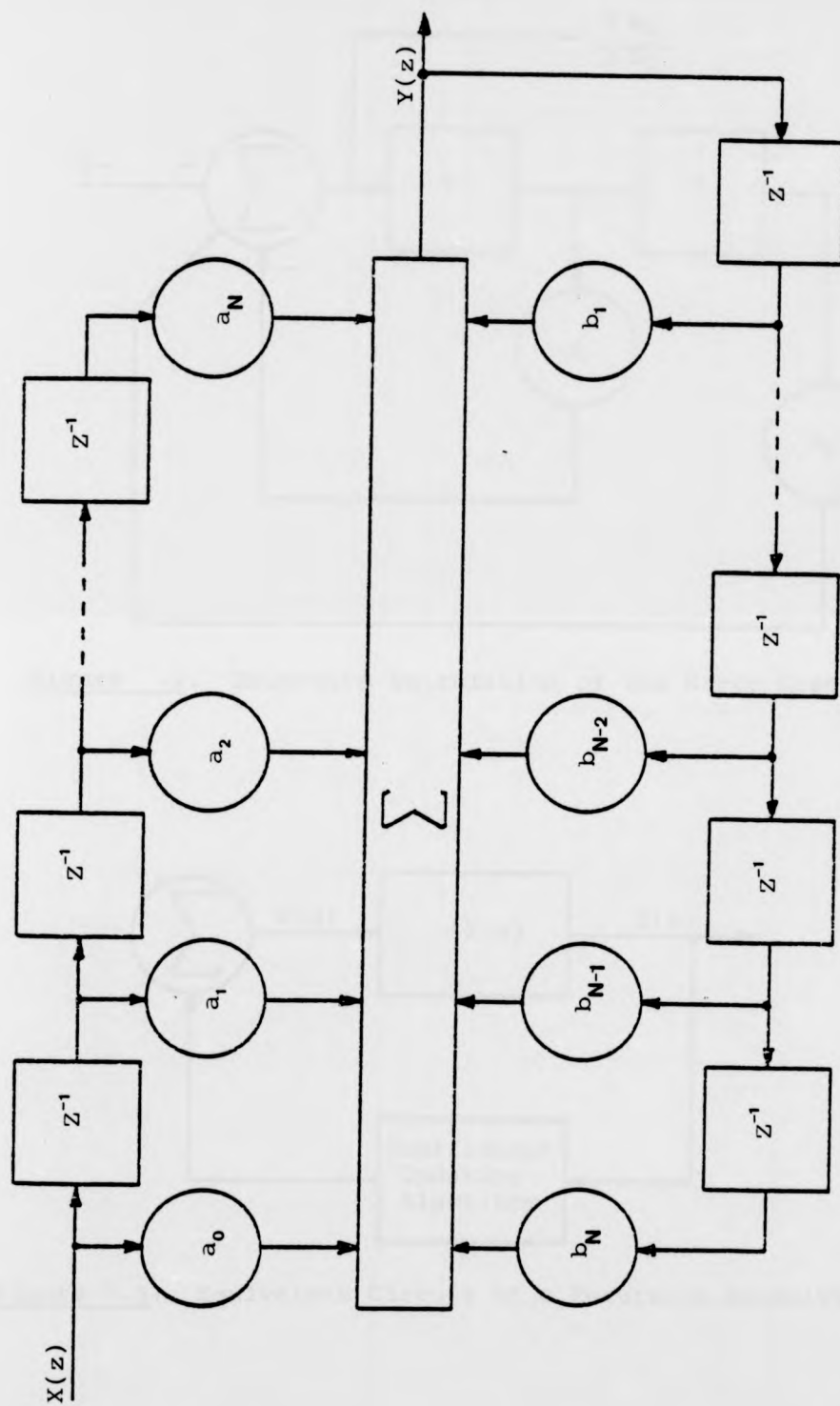
Figure 7.1: Direct Form Realization of an Nth Order Recursive Digital Filter

$$\frac{\partial e_n}{\partial b_i}$$

Y_{n-i}

Σ

T

T

b_1

b_2
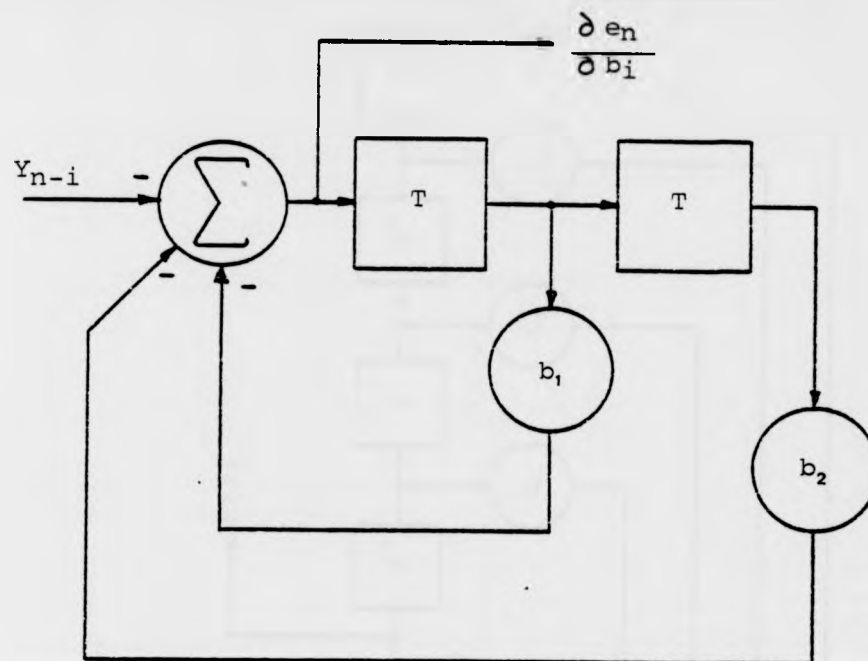
Figure 7.2: Recursive Calculation of the Error Gradients

Σ

W(z)

F(z)

E(z)

Coefficient
Updating
Algorithm
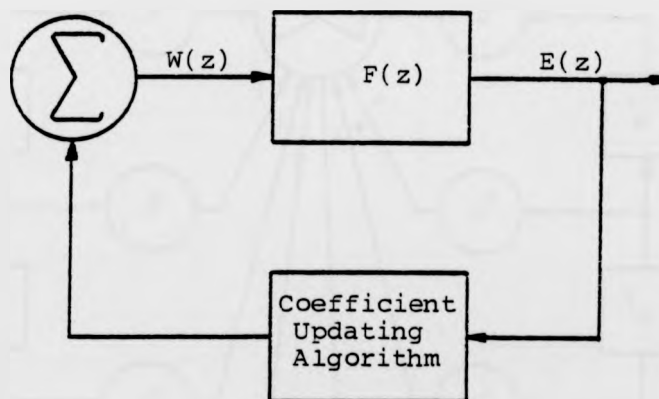
Figure 7.3: Equivalent Circuit of a Recursive Adaptive Filter
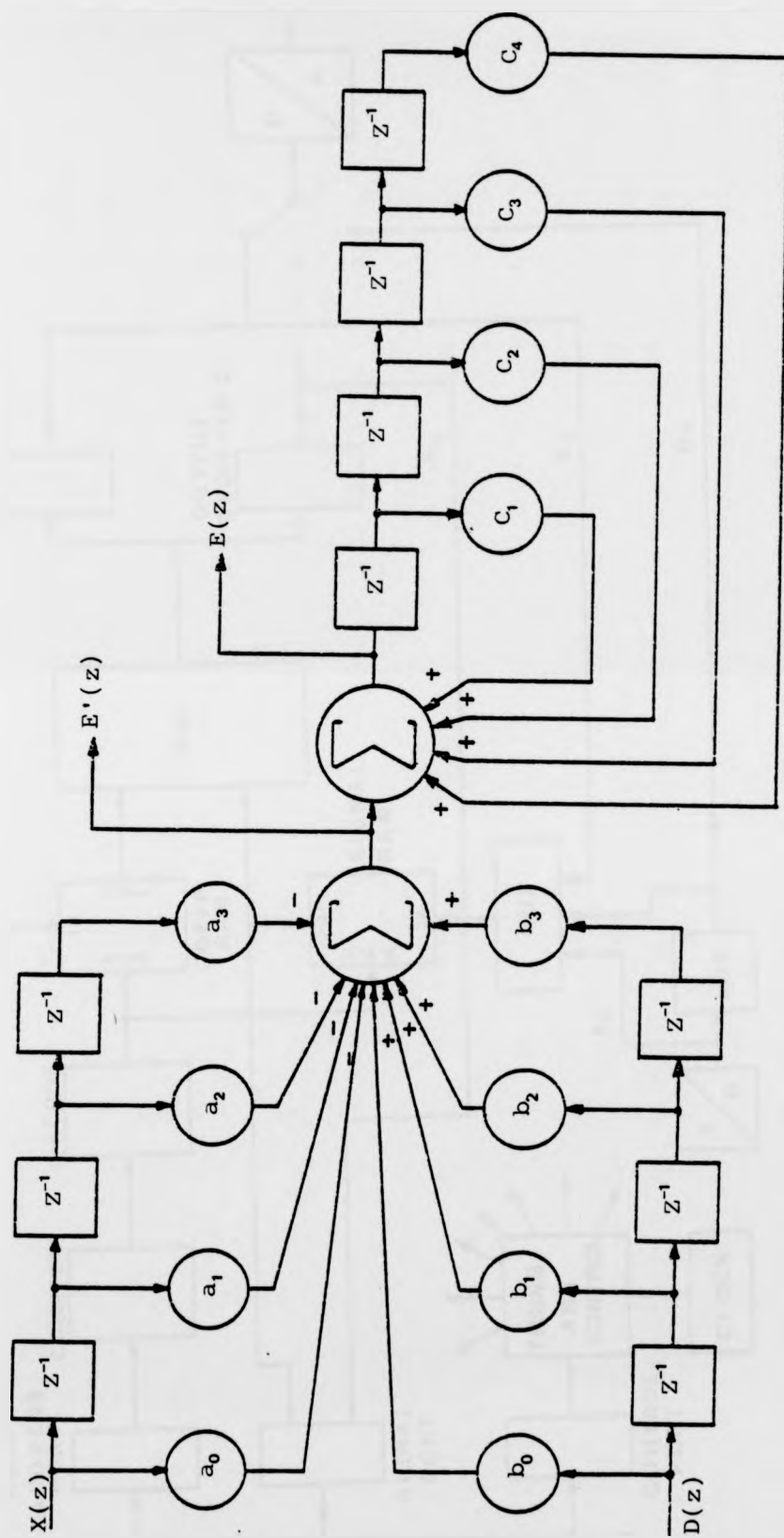
Figure 7.4: Experimental Recursive Adaptive Filter Structure
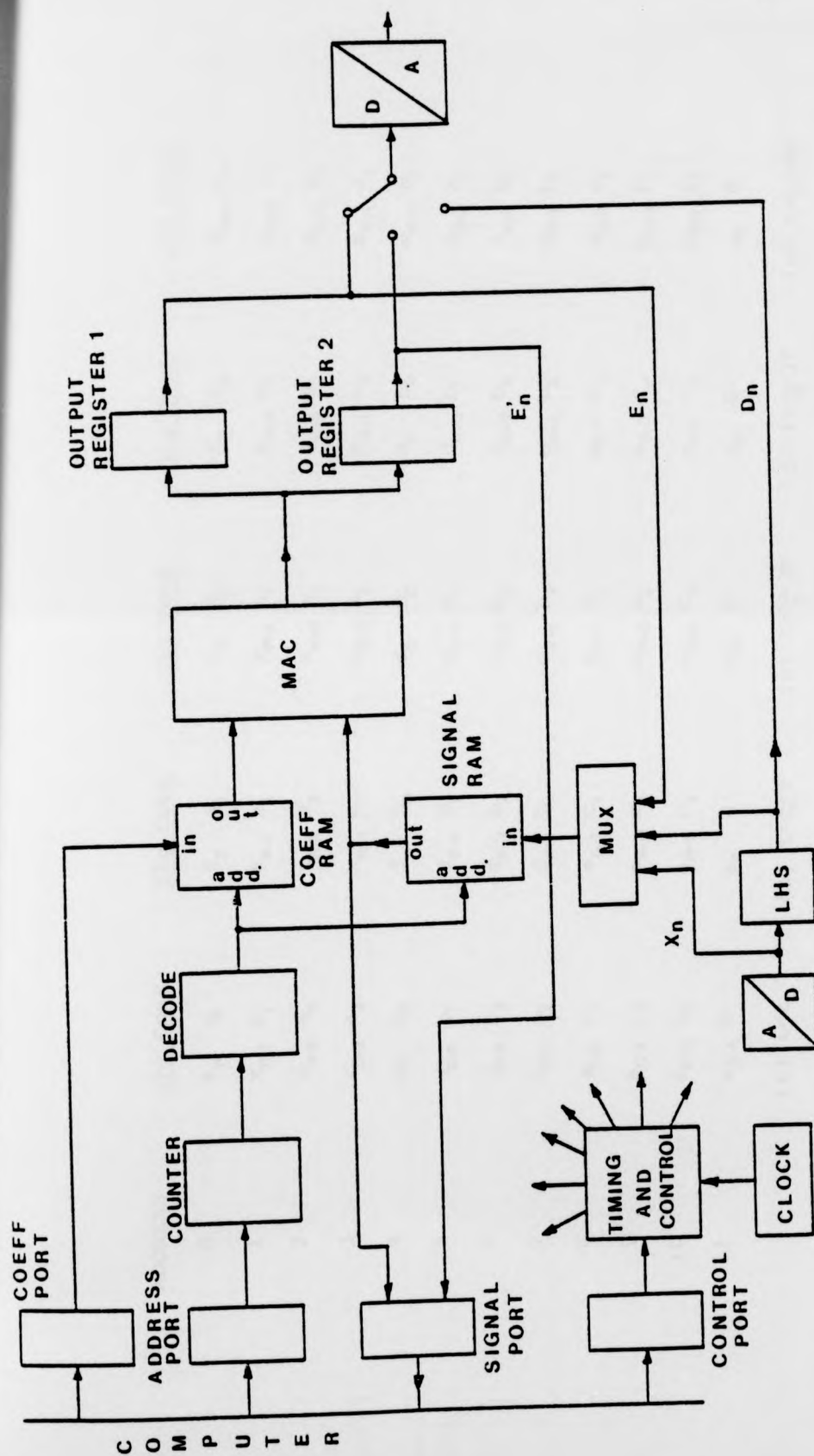
Figure 7.5: Implementation of the Experimental Digital Adaptive Filter

ADDRESS	(a) $t=t_0$ Sig.	Coef.	(b) $t=t_0+T$ Sig.	Coef.	(c) $t=t_0+2T$ Sig.	Coef.	(d) $t=t_0+3T$ Sig.	Coef.	(e) $t=t_0+4T$ Sig.	Coef.
0	x_n	a_0	x_n	a_0	x_n	a_0	x_n	a_0	x_{n+4}	a_0
1	x_{n-1}	a_1	x_{n-1}	a_1	x_{n-1}	a_1	x_{n-3}	a_1	x_{n+3}	a_1
2	x_{n-2}	a_2	x_{n-2}	a_2	x_{n+2}	a_2	x_{n+2}	a_2	x_{n+2}	a_2
3	x_{n-3}	a_3	x_{n+1}	a_3	x_{n+1}	a_3	x_{n+1}	a_3	x_{n+1}	a_3
4	d_n	b_0	d_n	b_0	d_n	b_0	d_n	b_0	d_{n+4}	b_0
5	d_{n-1}	b_1	d_{n-1}	b_1	d_{n-1}	b_1	d_{n+3}	b_1	d_{n+3}	b_1
6	d_{n-2}	b_2	d_{n-2}	b_2	d_{n+2}	b_2	d_{n+2}	b_2	d_{n+2}	b_2
7	d_{n-3}	b_3	d_{n+1}	b_3	d_{n+1}	b_3	d_{n+1}	b_3	d_{n+1}	b_3
8	e_{n-1}	c_1	e_{n-1}	c_1	e_{n-1}	c_1	e_{n-1}	c_1	e_{n-3}	c_1
9	e_{n-2}	c_2	e_{n-2}	c_2	e_{n-2}	c_2	e_{n+2}	c_2	e_{n+2}	c_2
10	e_{n-3}	c_3	e_{n-3}	c_3	e_{n+1}	c_3	e_{n+1}	c_3	e_{n+1}	c_3
11	e_{n-4}	0	e_n	0	e_n	0	e_n	0	e_n	0

Figure 7.6: Contents of the Signal and Coefficient RAMs of the Experimental Digital Adaptive Filter
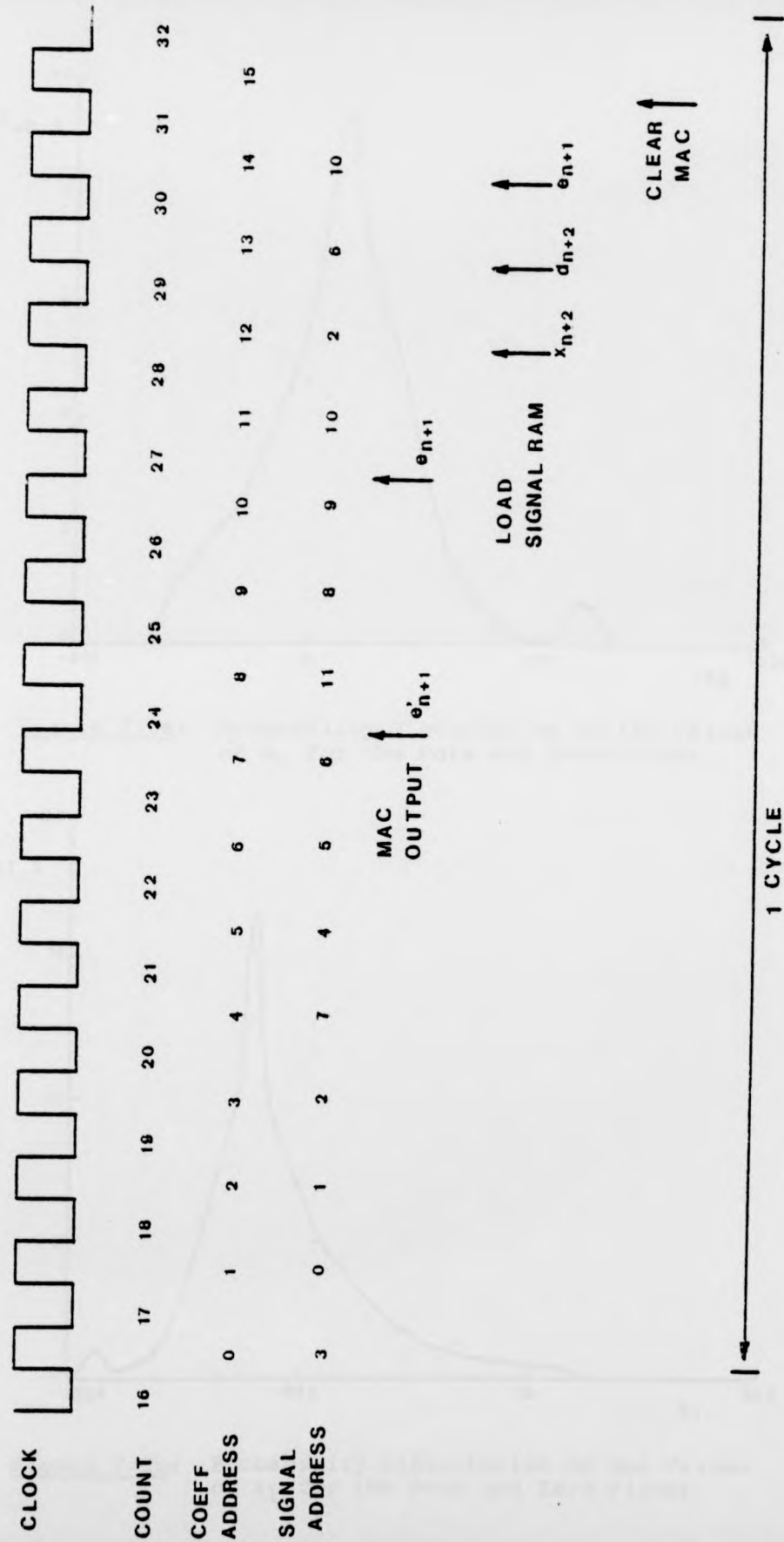
Figure 7.7: Simplified Timing Diagram of the Operation of the Experimental Digital Adaptive Filter
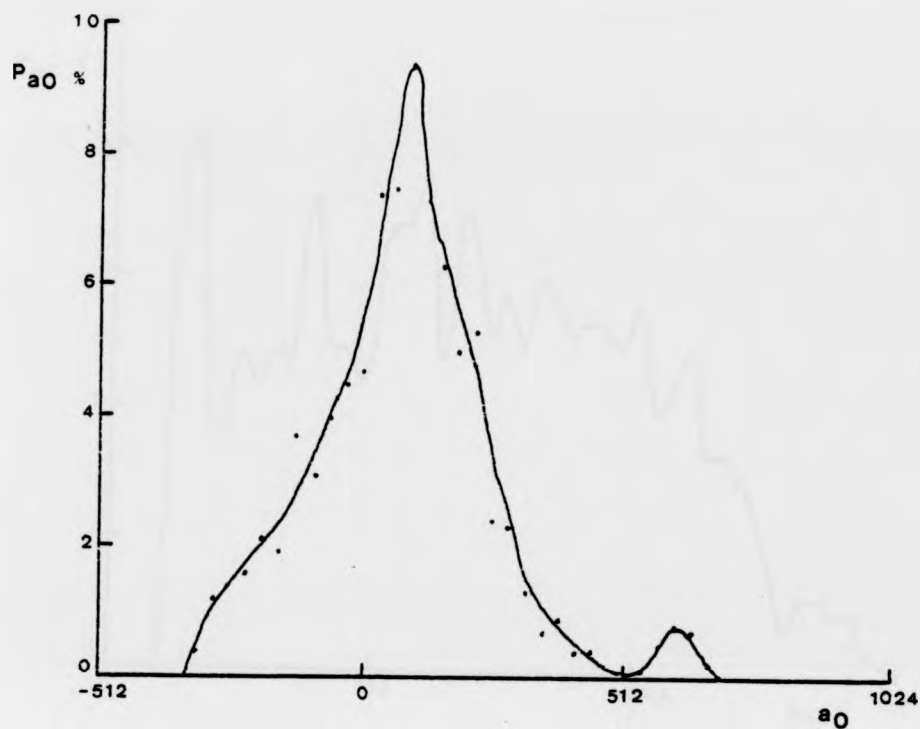
Figure 7.8a: Probability Distribution of the Values of a_0 for the Pole and Zero Filter
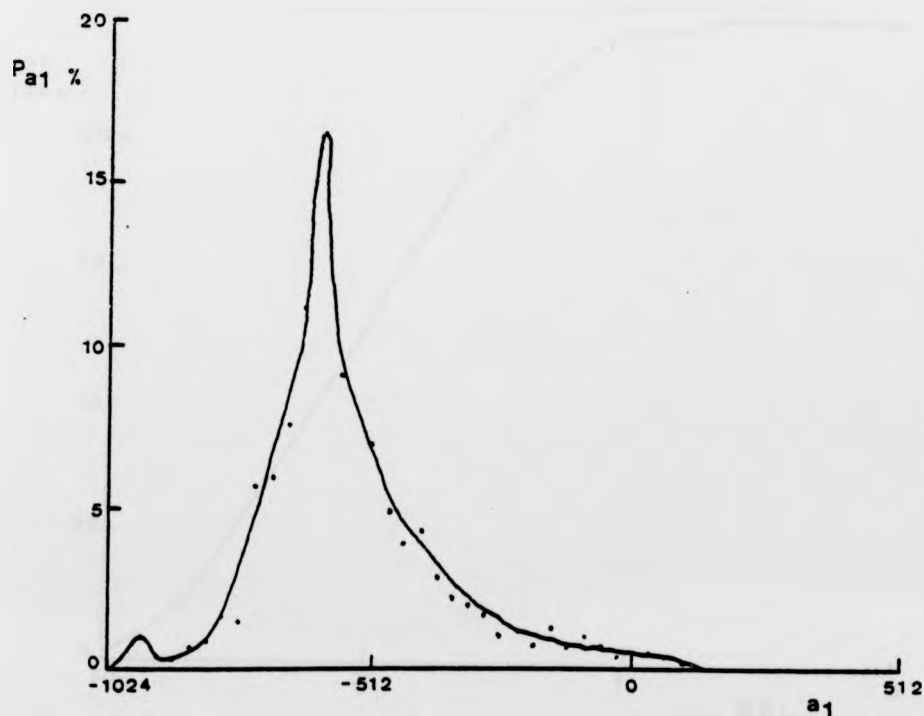
Figure 7.8b: Probability Distribution of the Values of a_1 for the Pole and Zero Filter
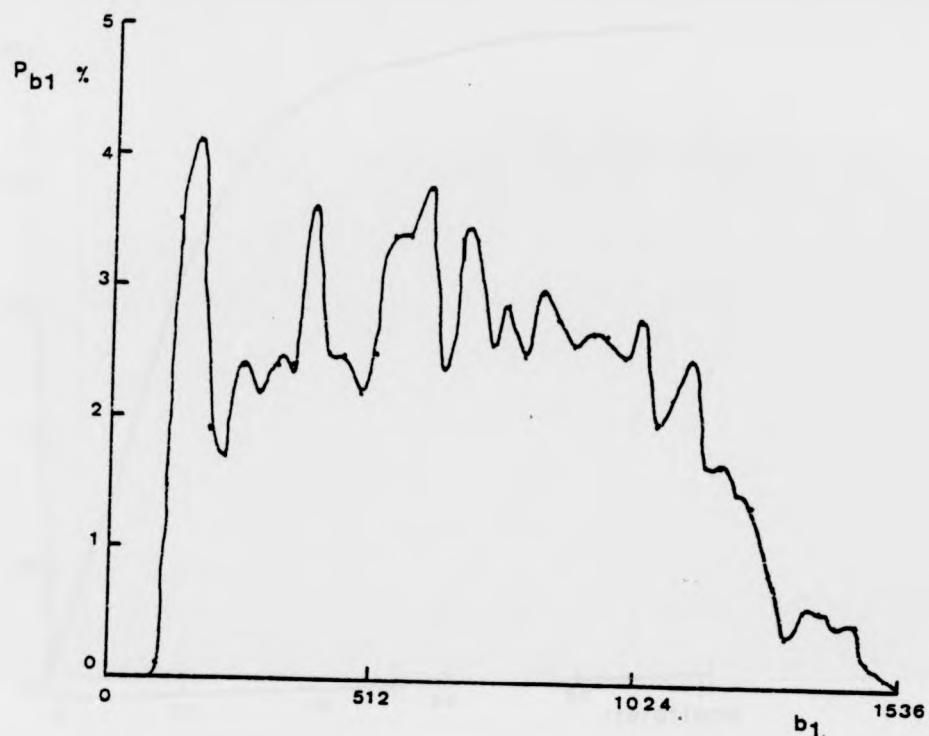
Figure 7.8c: Probability Distribution of the Values
of b_1 for the Pole and Zero Filter
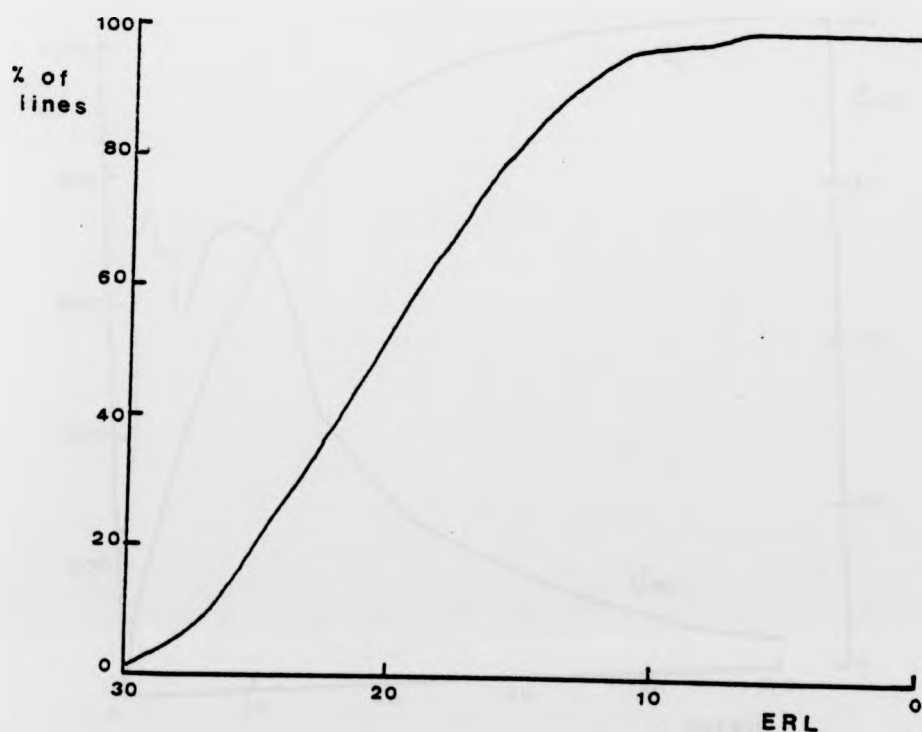
Figure 7.9: Cumulative Distribution
of Initial Cancelled ERL
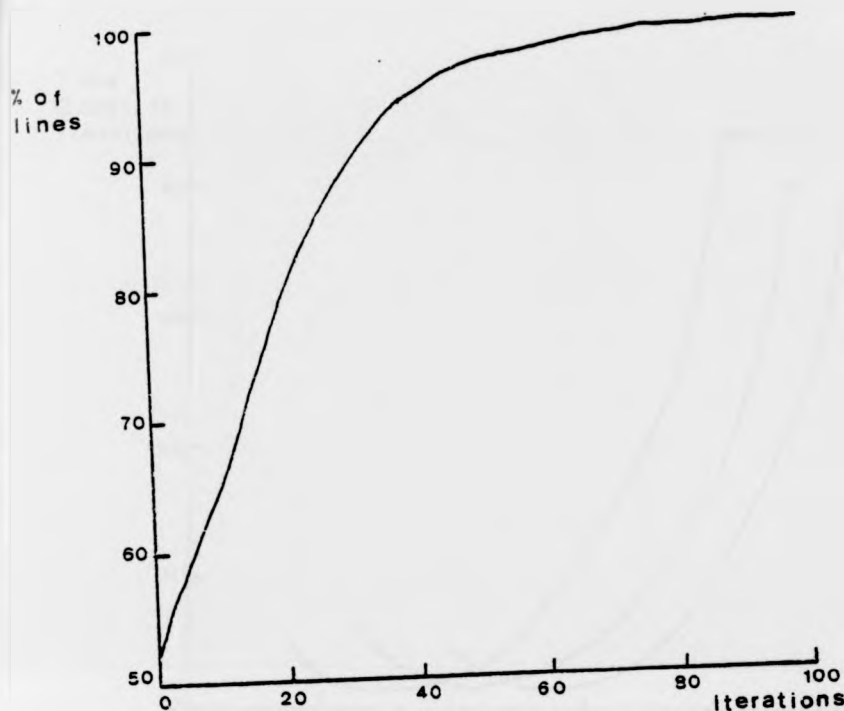
Figure 7.10: Cumulative Distribution of Number of Iterations Required to Achieve 20 dB ERL
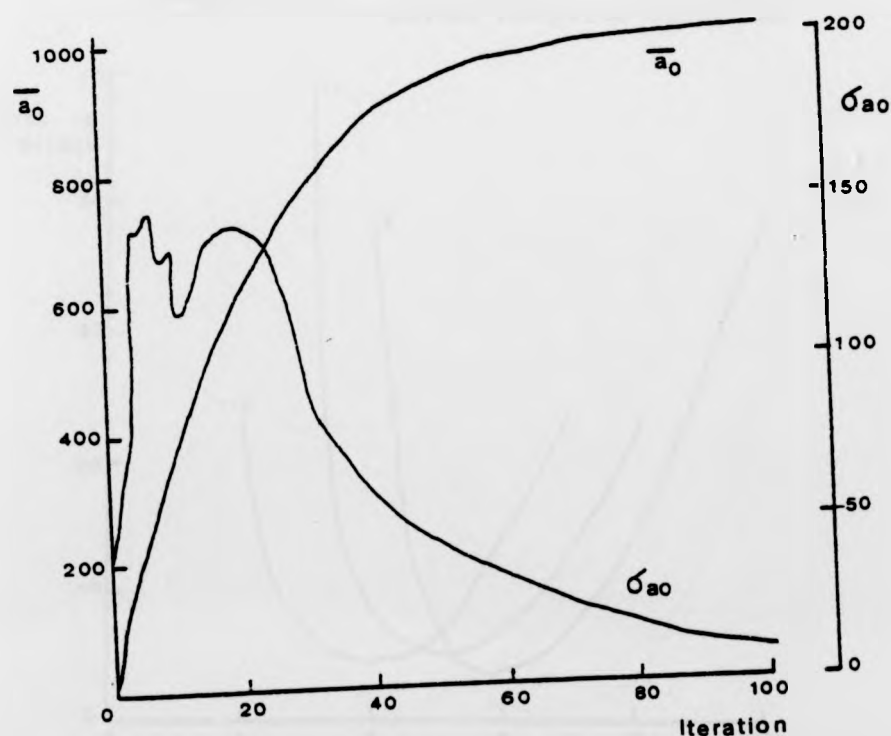
Figure 7.11: Convergence of $\bar{a}_0$ and σa_0 Using the Linear Adaption Algorithm
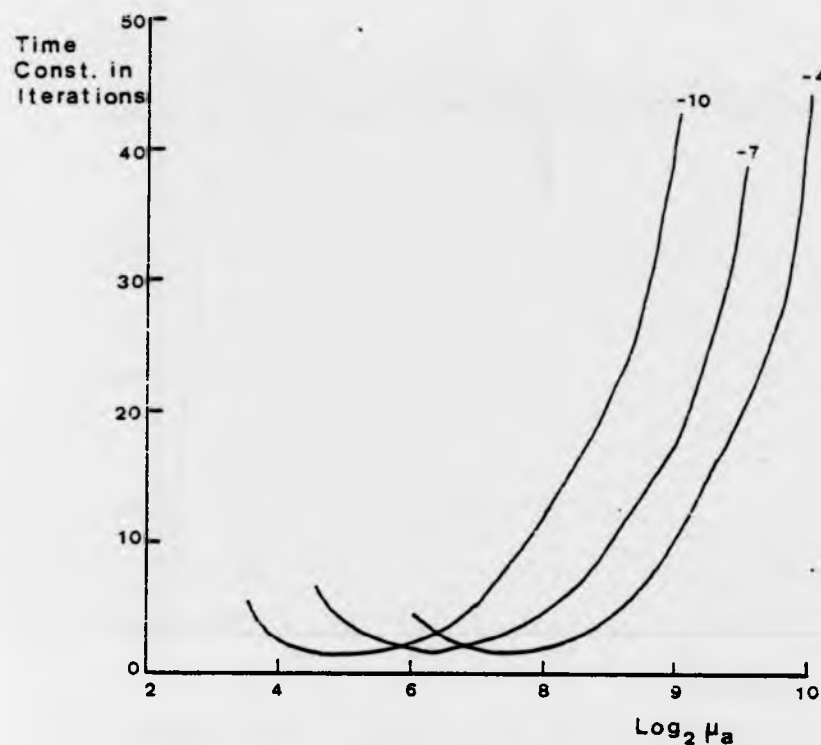
Figure 7.12a: Convergence of $\bar{a}_0$ Using the
Linear Adaption Algorithm
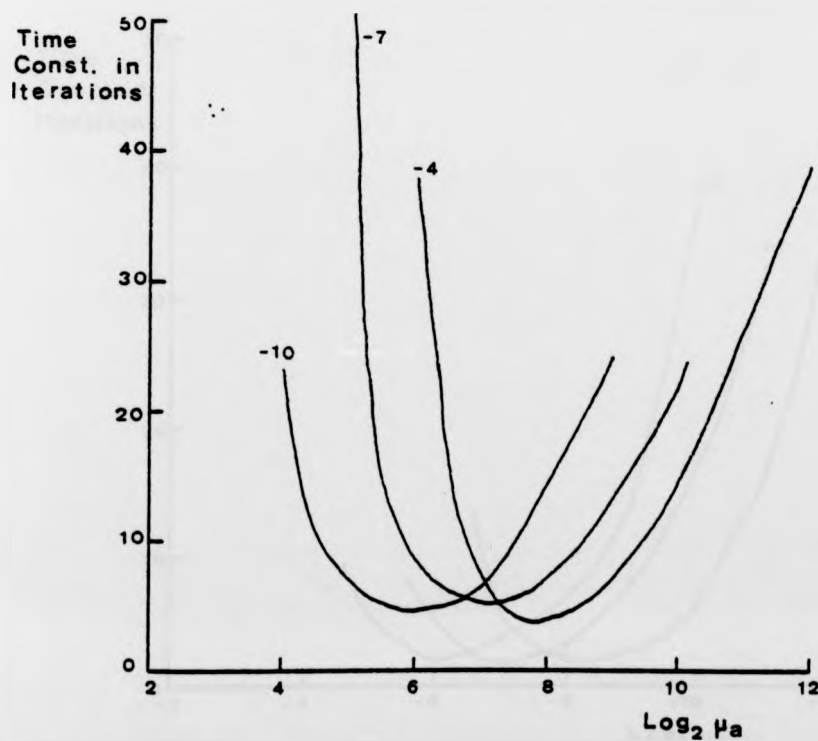
Figure 7.12b: Convergence of δa_0 Using the
Linear Adaption Algorithm
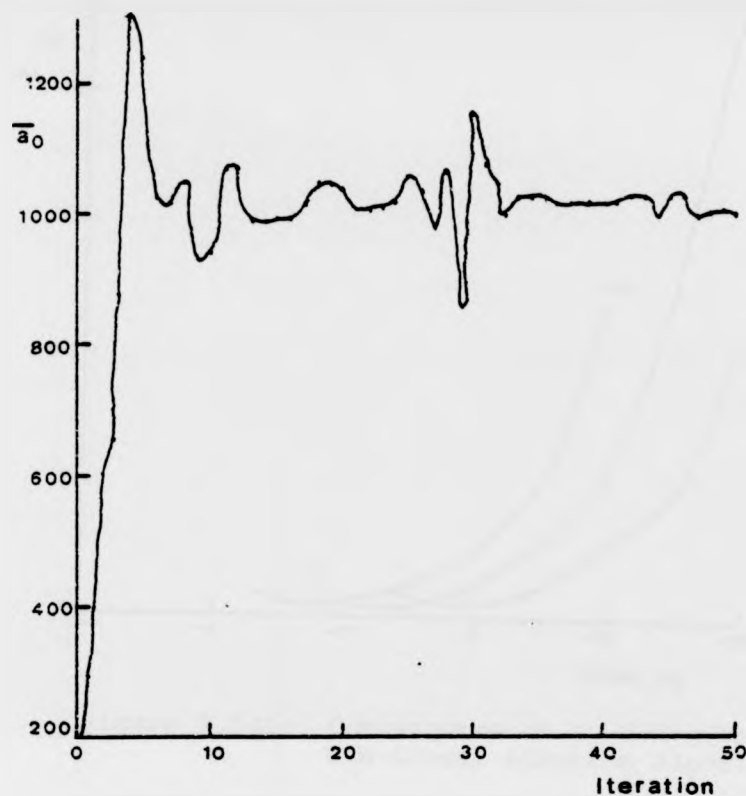
Figure 7.13: Convergence of the Adaptive Filter
Showing "Hunting" of the Coefficient
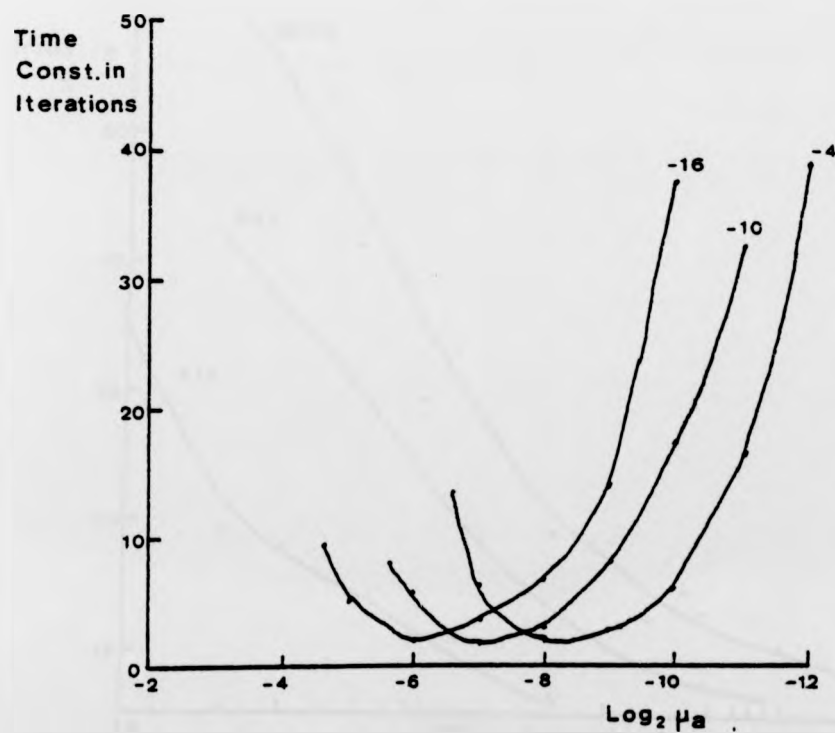
Figure 7.14a: Convergence of δa_0 Using the
Non-Linear Adaption Algorithm
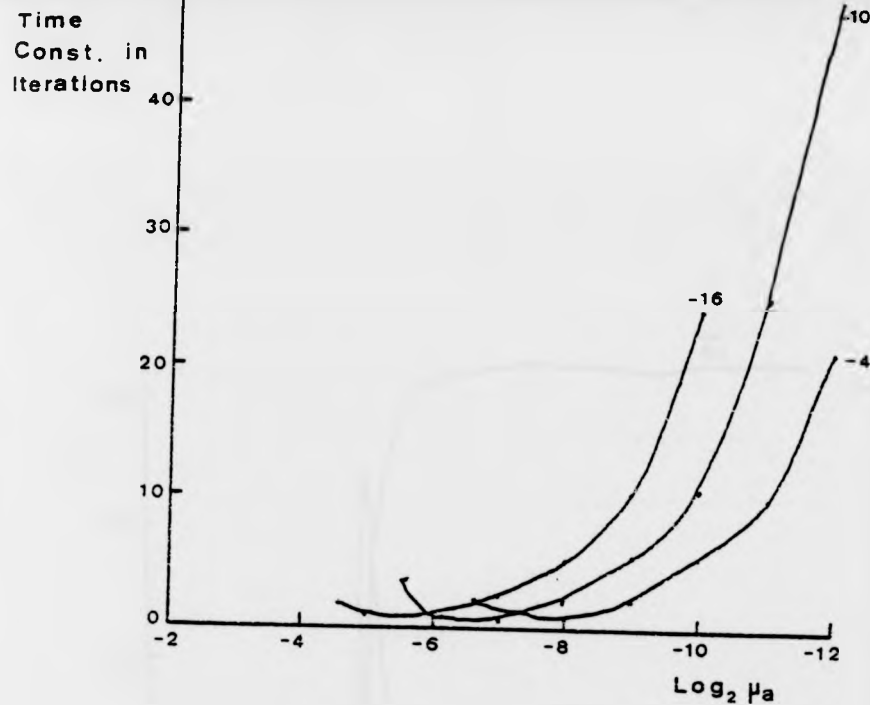
Figure 7.14b: Convergence of a_O Using the
Non-Linear Adaption Algorithm
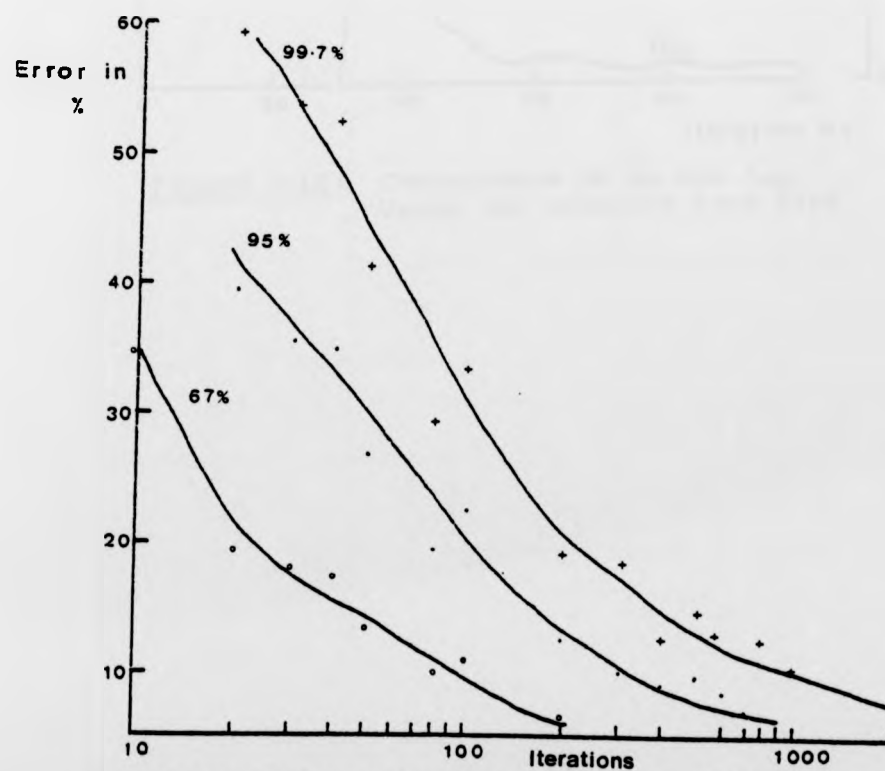
Figure 7.15:   Percentage Error in Calculating
the Power of the Input Signal
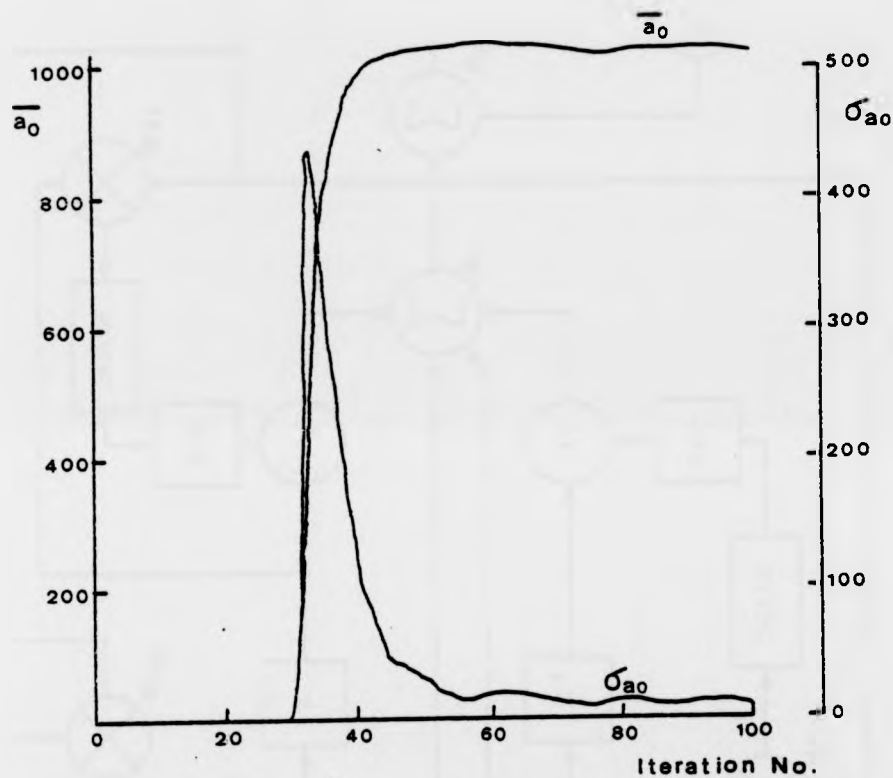
Figure 7.16:   Convergence of $\overline{a}_0$ and σ_{ao}
                Using the Adaptive Step Size
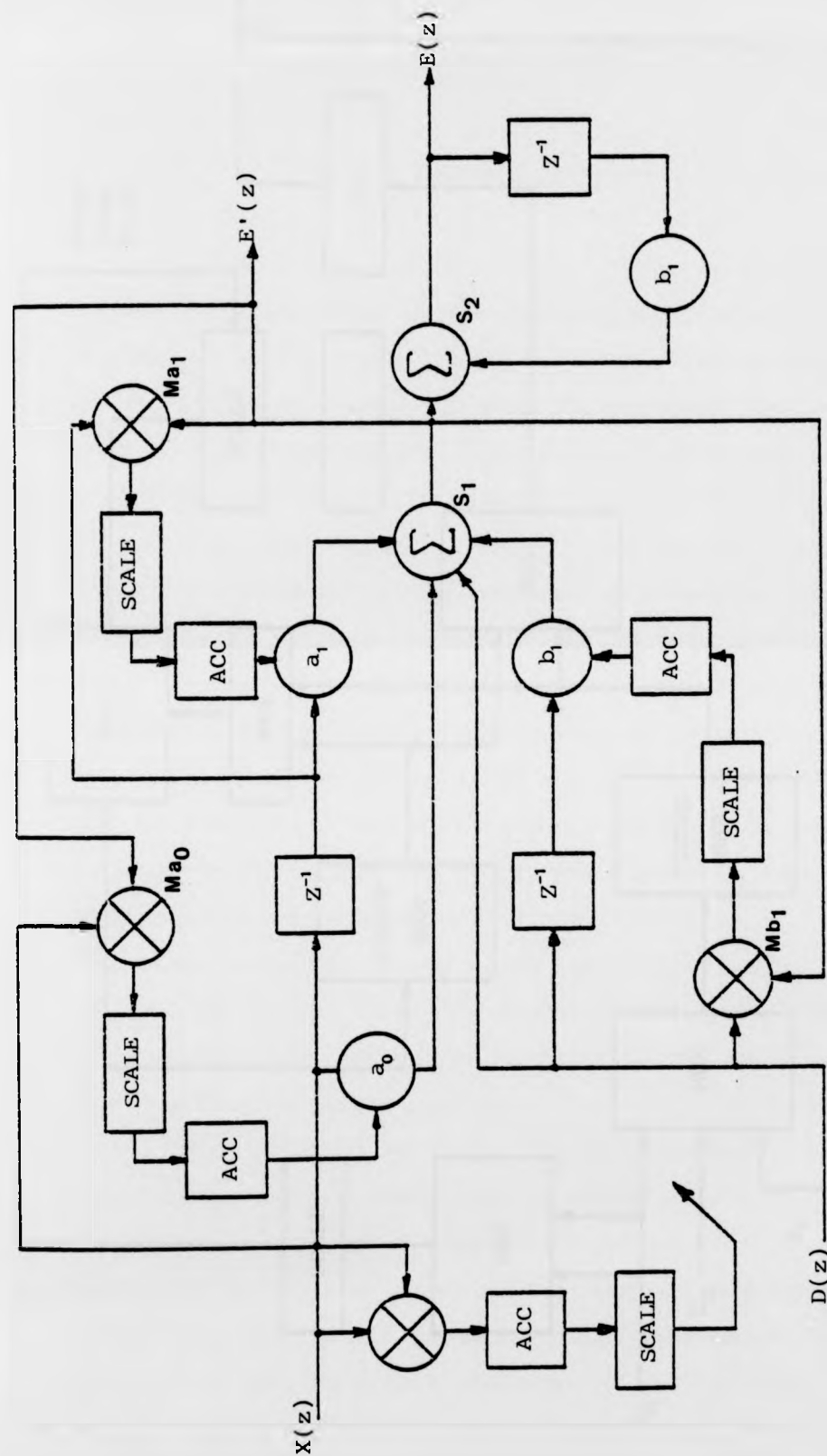
Figure 7.17: A Block Diagram of the Proposed Digital Adaptive Filter
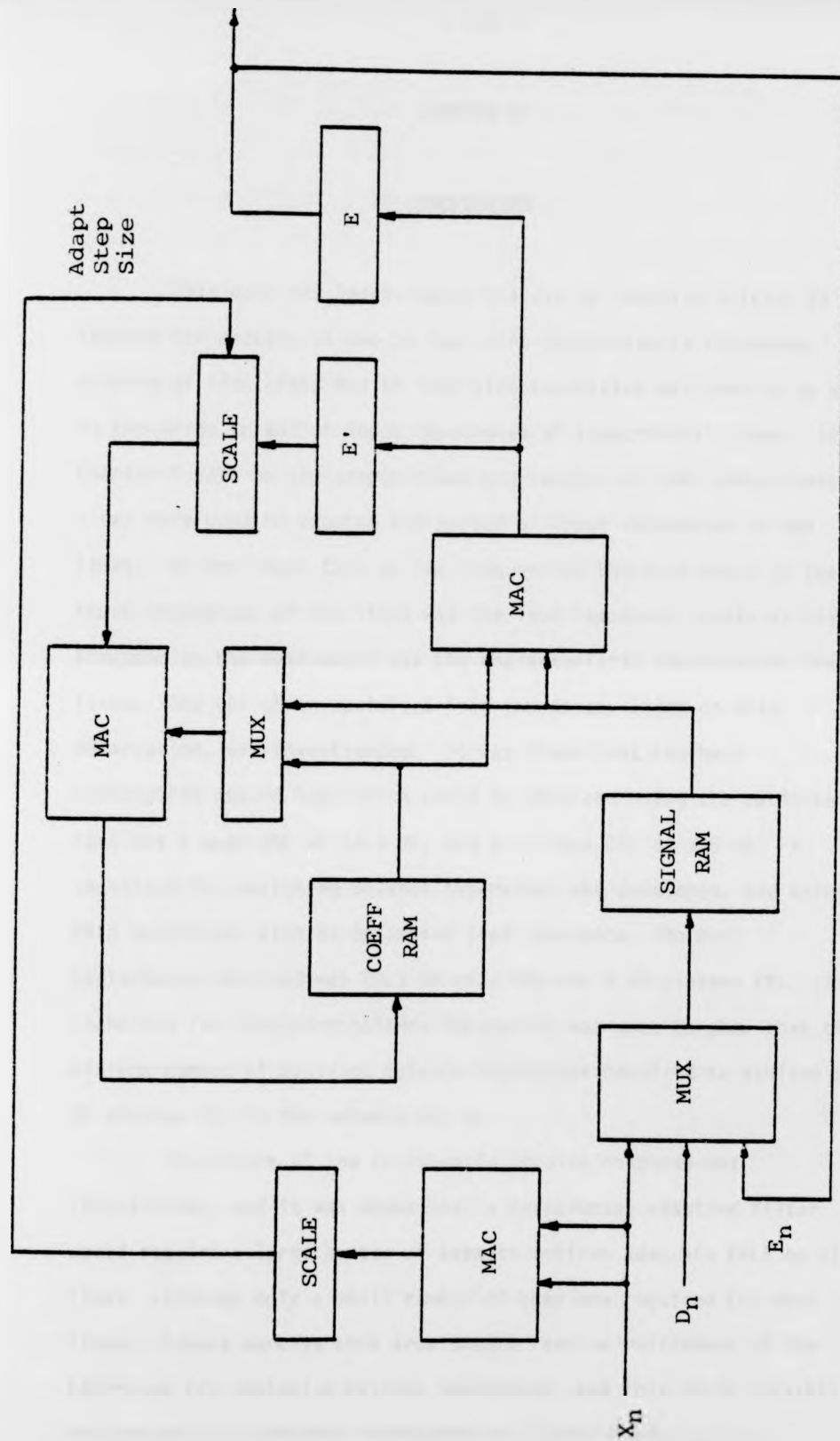
Figure 7.18: A Suggested Implementation of the Proposed Digital Adaptive Filter
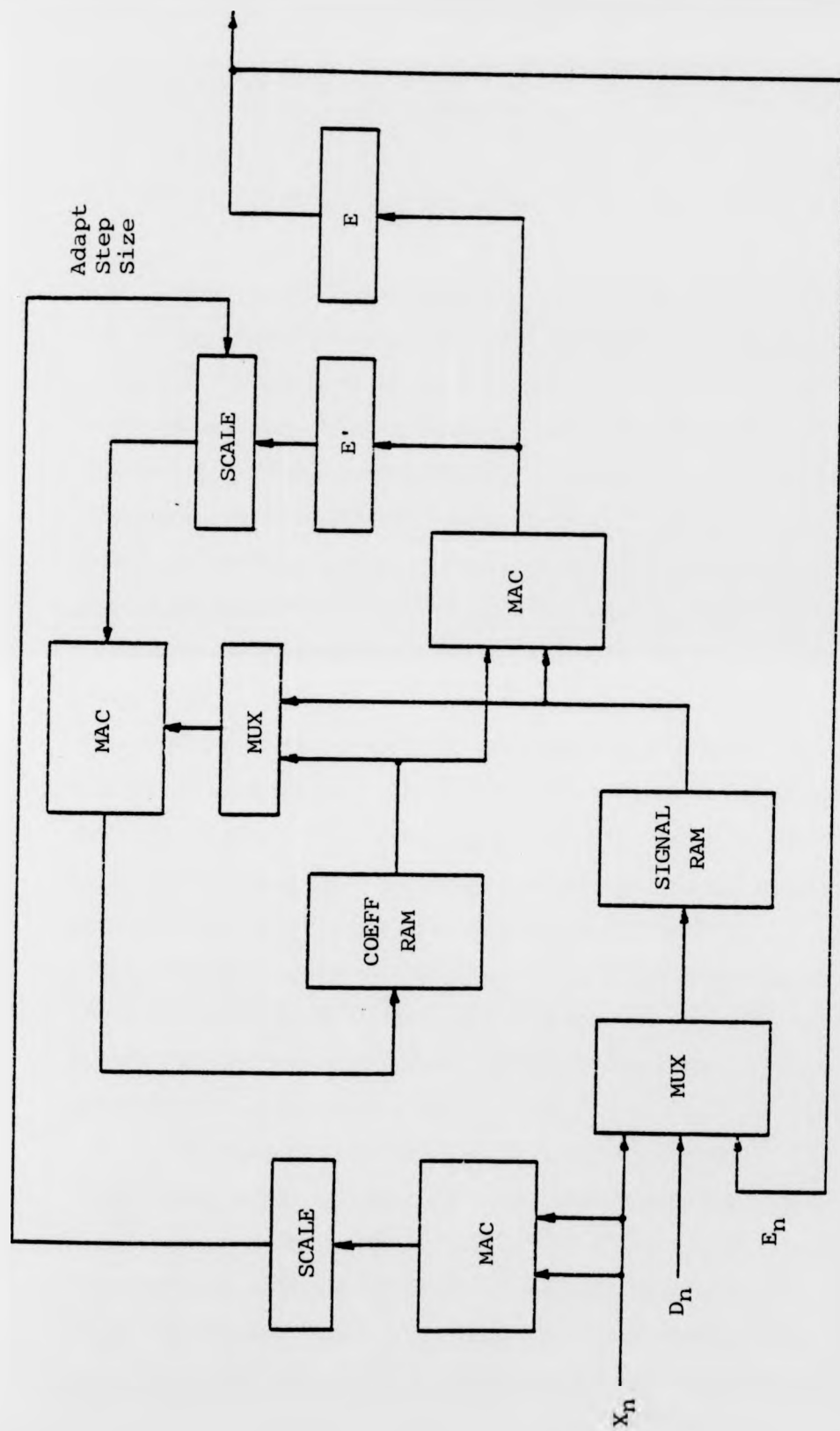
Figure 7.18: A Suggested Implementation of the Proposed Digital Adaptive Filter

CHAPTER 8

CONCLUSIONS

This work has investigated the use of adaptive filters to improve the process of two to four wire conversion in telephony. The problem of inaccurate two to four wire conversion was seen to be due to the large spread of input impedances of subscribers' lines. In Chapter 2 data on the compositions and lengths of 1845 subscribers' lines were used to examine the spread of input impedances of the lines. It was shown that at low frequencies the best match to the input impedances of the lines was the load impedance, while at high frequencies the best match was the characteristic impedance of the lines. The use of an optimised load impedance, based on this observation, was investigated. It was shown that the best transhybrid return loss which could be obtained using the optimised load was a mean ERL of 18.3 dB, and a minimum ERL of 9.5 dB. A technique for designing balance impedances was developed, and using this technique, with an optimised load impedance, the best performance obtained was 23.9 dB mean ERL and 9 dB minimum ERL. The technique for designing balance impedances was used to show that the minimum number of distinct balance impedances required to achieve 10 dB minimum SRL in the network was 3.

The nature of the transhybrid impulse response was investigated, and it was shown that a transversal adaptive filter would require a large number of taps to achieve adequate ERLE on all lines, although only a small number of taps are required for most lines. Future work in this area should involve refinement of the technique for designing balance impedances, and this could possibly be achieved by using the techniques of Cluster Analysis (see

CHAPTER 8

CONCLUSIONS

This work has investigated the use of adaptive filters to improve the process of two to four wire conversion in telephony. The problem of inaccurate two to four wire conversion was seen to be due to the large spread of input impedances of subscribers' lines. In Chapter 2 data on the compositions and lengths of 1845 subscribers' lines were used to examine the spread of input impedances of the lines. It was shown that at low frequencies the best match to the input impedances of the lines was the load impedance, while at high frequencies the best match was the characteristic impedance of the lines. The use of an optimised load impedance, based on this observation, was investigated. It was shown that the best transhybrid return loss which could be obtained using the optimised load was a mean ERL of 18.3 dB, and a minimum ERL of 9.5 dB. A technique for designing balance impedances was developed, and using this technique, with an optimised load impedance, the best performance obtained was 23.9 dB mean ERL and 9 dB minimum ERL. The technique for designing balance impedances was used to show that the minimum number of distinct balance impedances required to achieve 10 dB minimum SRL in the network was 3.

The nature of the transhybrid impulse response was investigated, and it was shown that a transversal adaptive filter would require a large number of taps to achieve adequate ERLE on all lines, although only a small number of taps are required for most lines. Future work in this area should involve refinement of the technique for designing balance impedances, and this could possibly be achieved by using the techniques of Cluster Analysis (see

Ambikairajah, 1982) to group together those lines whose imput impedances as a function of frequency are similar.

Chapter 3 described the implementation of a line and hybrid simulator, which when used with the data on the 1845 subscribers' lines allows both analog and digital adaptive filters to be tested realistically. The accuracy of the simulator was estimated by using it to simulate known frequency responses. This simulator is considerably more flexible than previous methods using artificial lines, etc, and is also suitable for automated measurements.

The theory of recursive analog adaptive filters was developed in Chapter 4, and it was shown that simple filters could be implemented by using a filtered error signal to control the filter parameters. The effect of the error filtering on the performance of the filter was analysed. The use of estimates of the gradient of the filtered error signal was investigated, and it was shown that on average the gradient estimates were correct, provided that the filter parameters were not updated. Relaxing this condition was shown not to interfere with the convergence of the filter, and the use of the gradient estimates considerably simplified the implementation of the filters. Various possible filter structures were analysed in terms of suitability for use in an adaptive hybrid, and three filters; an adaptive gain circuit, a single pole filter, and a first order pole-zero filter, were proposed for implementation. A technique for analysing the convergence of analog adaptive filters was developed. This technique was used to study the factors affecting the convergence of the proposed filters.

Chapter 5 described the implementation of the proposed filters, and the effects of non-ideal circuit components on the performance of the filters were examined. It was shown that high loop gains were needed to overcome the effect of the input offsets to

the control integrators, and that this limited the maximum cancelled
return loss which could be achieved. In the case of the single pole
filter, it was found that the constraints imposed by the stability of
the differentiator severely restricted the maximum time constant
against which the filter could adapt. Neither the single pole filter
nor the adaptive gain circuit provided significant ERLE against the
responses due to most subscribers' lines. The pole-zero filter was
shown to be theoretically capable of modelling infinite time
constants, but incapable of modelling a range of small time
constants. The signal integrators in the pole-zero filter were
designed to limit the effects of this anomaly. It was shown that the
pole-zero filter could be calibrated, allowing it to be used for
system identification. When the filter adapted against subscribers'
lines, this allowed the poles and zeros of the responses to be
estimated. The pole-zero filter performed well against subscribers'
lines, the mean value of cancelled ERL achieved was 35.3 dB, while
the minimum value was 28.4 dB.

The dynamic performance of the pole-zero filter was found to
be inadequate unless some method of storing a set of initial
conditions for the parameters of the filter was used. This
requirement can be achieved, however it is also necesary to control
the size of the input offsets to the signal multipliers. In
addition, the effect of error filtering on near-end speech must be
compensated. This adds considerably to the complexity of the analog
adaptive hybrid, and also requires strict control over the input
offset to the b_1 control multiplier. For these reasons the
implementation of the analog adaptive hybrid, using the single pole
filter, was deemed impractical. Future work on continuous analog
recursive adaptive filters should investigate simplifications to the
adaption algorithms for applications where the disadvantages referred

to above are insignificant. For example, in adaptive noise cancellation there is no near-end signal problem, and the transfer function of the adaptive filter is irrelevant, provided that the error signal power is minimised. Thus there is no need to compensate for the effect of error filtering.

The effects of the process of A/D and D/A conversion, and of the analog filters, on the complexity of the response to be modelled by a digital adaptive hybrid were investigated in Chapter 6. Analog filters were designed to meet the filtering requirements for various intermediate sampling frequencies, and the effects of the filters on the ERL and SRL which can be achieved by an adaptive hybrid, without additional complexity, were investigated. The introduction of simple fixed digital filters to compensate for the responses of the analog filters and the converters was proposed, and the effect of component tolerances on the performance which can be achieved was investigated. It was shown that at intermediate sampling rates as low as 32 kHz, proper choice of the order and cutoff frequency of the analog filter allows a single period pure time delay to be used to compensate for its response. Thus the use of a digital adaptive hybrid need not add much further complexity to the response to be matched by the digital filter.

In Chapter 7 the suitability of various adaptive digital filters for use in a digital adaptive hybrid was assessed, and the direct form recursive filter, with error filtering, was seen to allow easy adaption of the filter coefficients. The implementation of an experimental digital recursive adaptive filter, of up to 3rd order, was described. The filter includes a recursive section to compensate for the effects of error filtering on near-end speech. To allow flexibility in the choice of adaption algorithms, the adaption of the filter coefficients is performed by computer. Results were presented

for the performance of recursive digital adaptive filters of various orders against the 1845 subscribers' lines. Of the low order filters, the first order recursive filter gave the best performance, achieving 33.6 dB mean ERL and 26.0 dB minimum ERL. The dynamic performance of this filter against subscribers' lines was measured, using a set of stored initial coefficients. It was shown that 52% of lines had initial cancelled ERL greater than 20 dB, and this value of cancelled ERL was achieved for all lines within 100 iterations.

An adaption algorithm using an adaptive step size was developed, and it was shown that this algorithm considerably increased the speed of convergence of a 0th order transversal filter at low input signal levels. In the final section of Chapter 7 it was shown to be possible to implement a practical digital adaptive hybrid, based on the first order digital adaptive filter, using currently available technology.

In this thesis the effects of near-end speech on the performance of the adaptive filters have not been investigated. It has been assumed that a near-end speech detector can be used to prevent adaption of the filter coefficients during double talking. This proposition should be investigated further for the proposed digital adaptive filter and adaption algorithm. Results reported by Mackechnie (1970) and Ochiai et al (1977) however, indicate that simple solutions to the problem can be found.

In the results of Chapter 7 the mean values of the distributions of the filter coefficients were used as initial coefficients for the filter. The possibility of improving the initial value of cancelled ERL by altering the choice of initial coefficients should be investigated.

The results reported for the performance of the proposed adaptive filter were for subscribers' lines terminated in the input

impedance of the telephone. The effects of alterations of the load impedance on the performance of the filter should also be examined.

The number of bits required to represent the filter coefficients in the adaptive hybrid should be investigated, as this may lead to large savings in both the required data storage and the speed of the multipliers. Similarly, it may be possible to use coarsely quantised data words in the adaption algorithm, resulting in further savings in the complexity of the adaptive hybrid. A final area for suggested future work is in simplifying the techniques used to measure the power of the input signal for the adaptive step size algorithm.

APPENDIX 1

A1.1 Windowing and the inverse FFT

A1.2 Testing of the inverse FFT

A1.3 Gradient Estimates for the Steepest Descent Algorithm

A1.1 Windowing and the inverse FFT

In this appendix the derivation of the inverse fast Fourier transform (FFT) from the inverse Fourier transform is considered, and the effects of using a non-rectangular window in the frequency domain are discussed.

The expression for the inverse Fourier transform of any complex transfer function $H(j\omega)$ is given by:-

$$h(t) = \int_{-\infty}^{\infty} H(j\omega)e^{j\omega t} \qquad\qquad 1$$

This equation gives the value of $h(t)$, the impulse response, at any time t, $-\infty < t < \infty$, where the transfer function $H(j\omega)$ must be specified for all ω, $-\infty < \omega < \infty$. The expression for the inverse discrete Fourier transform is obtained by approximating the above integral by a summation over intervals $\Delta\omega$ in the frequency domain, thus:-

$$h_1(t) = \Delta\omega \sum_{k=-\infty}^{\infty} h(jk\Delta\omega)e^{jk\Delta\omega t} \qquad\qquad 2$$

$H(j\omega)$ is now represented by its samples at intervals $\Delta\omega$ over the entire frequency range, and the expression gives an approximation to the actual impulse response for all t. To examine the accuracy of this approximation, the process of "discretising" the transfer function can be considered as multiplying it by a set of impulses given by:-

$$S(\omega) = \sum_{k=-\infty}^{\infty} \delta(\omega - k\Delta\omega) \qquad\qquad 3$$

The effect of this process is that the approximate impulse response $h_1(t)$ is the actual impulse response $h(t)$ convolved with $s(t)$, the

A1.1 Windowing and the inverse FFT

In this appendix the derivation of the inverse fast Fourier transform (FFT) from the inverse Fourier transform is considered, and the effects of using a non-rectangular window in the frequency domain are discussed.

The expression for the inverse Fourier transform of any complex transfer function $H(j\omega)$ is given by:-

$$h(t) = \int_{-\infty}^{\infty} H(j\omega)e^{j\omega t} \qquad\qquad 1$$

This equation gives the value of $h(t)$, the impulse response, at any time t, $-\infty < t < \infty$, where the transfer function $H(j\omega)$ must be specified for all ω, $-\infty < \omega < \infty$. The expression for the inverse discrete Fourier transform is obtained by approximating the above integral by a summation over intervals $\Delta\omega$ in the frequency domain, thus:-

$$h_1(t) = \Delta\omega \sum_{k=-\infty}^{\infty} h(jk\,\Delta\omega)e^{jk\,\Delta\omega t} \qquad\qquad 2$$

$H(j\omega)$ is now represented by its samples at intervals $\Delta\omega$ over the entire frequency range, and the expression gives an approximation to the actual impulse response for all t. To examine the accuracy of this approximation, the process of "discretising" the transfer function can be considered as multiplying it by a set of impulses given by:-

$$S(\omega) = \sum_{k=-\infty}^{\infty} \delta(\omega - k\,\Delta\omega) \qquad\qquad 3$$

The effect of this process is that the approximate impulse response $h_1(t)$ is the actual impulse response $h(t)$ convolved with $s(t)$, the

inverse Fourier transform of the the sampling function $S(\omega)$. $s(t)$ can be obtained by substituting $2\pi/T_p = \Delta\omega$ into the time sampling Fourier transform pair:-

$$\sum_{k=-\infty}^{\infty} \delta(t-kT_p) \longleftrightarrow \sum_{k=-\infty}^{\infty} \delta(\omega-2\pi k/T_p) \qquad 4$$

Thus the inverse Fourier transform of the frequency sampling function is a time sampling function:-

$$s(t) = \delta(t - 2\pi k/\Delta\omega) \quad k = \ldots.-2,-1,0,1,2,\ldots. \qquad 5$$

and assuming $h(t) = 0$ outside the interval $0 < t < T_p$, the approximation is accurate.

Equation 2 thus allows accurate calculation of impulse responses up to time T_p, provided that they have decayed to zero in this time interval. The effect of sampling the transhybrid frequency reponse on the calculated transhybrid impulse response is illustrated in Figures A1.1(a) and A1.1(b). It can be seen that in the case illustrated some overlap error occurs because $\Delta\omega$ is insufficiently small. This overlap error which can occur as a result of sampling in the frequency domain is analogous to the aliasing error which can occur due to sampling in the time domain.

Equation 2 requires that samples of the transfer function $H(j\omega)$ be available for all ω where $H(j\omega) \neq 0$. In many cases this computation would be impractical and it is of interest to examine the effect on the calculated impulse response of limiting the range over which frequency response samples are required. Suppose samples of $H(j\omega)$ outside the range $-\omega_s/2 < \omega < \omega_s/2$ are assumed to be zero. This assumption is equivalent to multiplying $H(j\omega)$ by the window function:-

$$W(\omega) = 1, \quad -\omega_s/2 < \omega < \omega_s/2$$
$$= 0, \text{ otherwise} \qquad 6$$

The equation used to calculate the impulse response in this case is:-

$$h_2(t) = \Delta\omega \sum_{k=-k_1}^{k_1} h(jk\,\Delta\omega)e^{jk\,\Delta\omega t} \qquad\qquad 7$$

where $k_1 = \omega_s/(2\Delta\omega)$.

The effect in the time domain is that the calculated response is convolved with the inverse transform of the window function $w(t)$, where:-

$$w(t) = \frac{\omega_s \sin(\omega_s t/2)}{\omega_s t/2} \qquad\qquad 8$$

The calculated impulse response therefore is:-

$$h_2(t) = \omega_s \int_{-\infty}^{\infty} \frac{\sin(\omega_s \tau/2)}{(\omega_s \tau/2)} h_1(t-\tau)d\tau \qquad\qquad 9$$

i.e. the periodic approximate impulse response $h_1(t)$ convolved with a Sinc function whose main lobe width is $T_1 = 4\pi/\omega_s$. The effect of the convolution with the main lobe is a "smearing out" of the calculated impulse response, limiting the time resolution to T_1. Convolving the approximate impulse response with the side lobes of the Sinc function leads to a smaller smearing out effect, known as "leakage". Figure A1.1(c) shows the effect of the rectangular window function on the calculated impulse response. Since $h_1(t)$ is periodic there is also an edge effect due to the main lobe of the Sinc function smearing the initial portion of the impulse response into the final portion.

The ratio of the height of the first side lobe of the Sinc function to the height of its main lobe is 0.212 or -13.3 dB. Use of a rectangular window function could thus lead to impulse responses appearing longer than they actually are, for example the convolution of an impulse with a Sinc function is a Sinc function, which only decays to zero in infinite time. To achieve higher side lobe rejection, it is necessary to use a frequency domain window function which tapers to zero at the point where a discontinuity is introduced by the rectangular window function. Use of such windows involves

trading-off the smearing effect against the leakage effect, as lower relative side lobe heights of the transform of the window function mean greater main lobe widths.

Two windows which are simple to compute are the Hanning and Hamming windows, which have rejections of first side lobes of -31 dB and -41 dB respectively, and whose main lobe widths are $8\pi/\omega_s$

Equation 7 allows computation of the impulse response at any time t, where $-\infty < t < \infty$. If however the windowed frequency response $H_w(j\omega)$ is considered periodic, rather than zero, outside the interval $-\omega_s/2 < \omega < \omega_s/2$, the expression for the resultant impulse response is:-

$$h_3(t) = \int_{-\infty}^{\infty} \sum_{k=-\infty}^{\infty} H_w(j(\omega+k\omega_s))e^{j\omega t}d\omega \qquad 10$$

Exchanging the order of integration and summation, and changing the variable of integration gives:-

$$h_3(t) = \sum_{k=-\infty}^{\infty} e^{-jk\omega_s t} \int_{-\infty}^{\infty} H_w(j(\omega+k\omega_s))e^{jt(\omega+k\omega_s)} \, d(\omega+k\omega_s)$$

$$= \sum_{k=-\infty}^{\infty} e^{-jk\omega_s t} h_2(t)$$

$$= \delta(t+2\pi k/\omega_s)h_2(t) \qquad 11$$

Thus assuming the frequency response to be periodic outside $-\omega_s/2 < \omega < \omega_s/2$ has the effect of making the calculated impulse response sampled in nature. This process is analogous to considering the Fourier series of the periodic spectrum, where the calculated impulse response is of the form $h(i\Delta T)$. The effect of assuming the frequency response to be periodic is shown in Figure A1.1(d).

The equation used to calculate the impulse response samples from the frequency response samples therefore is:-

$$h(nT_S) = \Delta\omega \int_{k=-N/2}^{N/2} H(jk\,\omega_S/N)e^{2\pi jkn/N} \quad n = 0,1,\ldots\ldots N-1 \qquad 12$$

where $T_S = \Delta T = 2\pi/\omega_S$. This calculation can be performed efficiently using a fast Fourier transform routine.

Appendix A1.2 describes some measurements of the effects of the Hanning and Hamming windows on the calculation of simple impulse responses.

A1.2 Measurement of the effects of using non-rectangular windows in calculating impulse responses

To determine the effects of the non-rectangular window functions on the accuracy of the impulse response calculation, test calculations were performed on impulse responses due to first order systems.   The impulse response of a first order system is:-

$$h(t) = (e^{-t/a})/a$$

where the frequency response is:-

$$H(\omega) = 1/(1+j\omega a)$$

The time taken for the impulse response to decay to p% of its peak value is:-

$$t_p = a.\log_e(100/p)$$

Thus to generate a cumulative distribution of test impulse response decay times, the parameter a is stepped through appropriate values. For each value of 'a' the frequency response $H(\omega)$ is calculated, and inverse Fourier transformed to produce the impulse response.   The time taken for the envelope of the impulse response to decay to various percentages of its peak value is then calculated.

Figure A1.3 shows the cumulative distribution of decay times to 5%, 1% and 0.5% of peak value, for 100 first order systems whose decay times to 5% of peak should vary linearly between 0 and 16 mS. In this case a simple rectangular frequency window was used in the

calculation. Figure A1.2 shows the decay times for the same 100 first order systems, where the frequency response was multiplied by a Hamming window prior to computation of the impulse response. The true distributions are also shown on both figures. It can be seen that using the Hamming window, all decay times are sligthly lengthened. This is due to the smearing out effect of the transform of the window function. The rectangular window function gives accurate results for decay times to 5% of peak, however, when lower values of impulse response amplitude are measured, the side lobes of the Sin(x)/x function cause the decay times to appear longer than the true values. The Hamming window function is used in calculating impulse response decay times in the line survey because its transform has much lower side lobe amplitudes than those of the Sin(x)/x due to the rectangular window.

A1.3 Estimating the error gradients for the steepest descent algorithm

In this appendix it is shown that in an average sense, the gradient of the instantaneous error squared is equal to the gradient of the mean error squared, i.e:-

$$\overline{\frac{\partial e^2(t)}{\partial a}} = \frac{\partial \overline{e^2(t)}}{\partial a} \qquad 13$$

where e(t) is the error signal and 'a' is any of the parameters of the adaptive filter. The assumption made in this derivation is that the error signal is statistically stationary, thus the x(t) and d(t) signals are assumed to be stationary, and the filter parameters are assumed to be constant with time. This assumption therefore precludes adjustment of the filter parameters, as though knowledge of the gradient terms were required to design a fixed filter which would minimise the error signal for a given x(t) and d(t).

Using the chain rule on the left hand side of equation 13 gives:-

$$\overline{\frac{\partial e^2(t)}{\partial a}} = \overline{2e(t)\frac{\partial e(t)}{\partial a}} \qquad 14$$

The general form of Parseval's theorem is:-

$$\overline{s_1(t)s_2(t)} = \int_{-\infty}^{\infty} s_1(t)s_2(t)dt = \int_{-\infty}^{\infty} S_1(\omega)S_2(-\omega)d\omega \qquad 15$$

and

$$\frac{\partial e(t)}{\partial a} = \frac{\partial}{\partial a}\int_{-\infty}^{\infty} E(\omega)e^{j\omega t}d\omega = \int_{-\infty}^{\infty} \frac{\partial E(\omega)}{\partial a}e^{j\omega t}d\omega$$

where the dependence of $E(\omega,a)$ on 'a' is implicit. Thus:-

$$\frac{\partial e^2(t)}{\partial a} = 2\int_{-\infty}^{\infty} E(\omega)\frac{\partial E(-\omega)}{\partial a}d\omega \qquad 16$$

Let $E(\omega) = U(\omega) + jV(\omega)$ $\qquad\qquad$ 17

where $U(\omega) = Re[E(\omega)]$

and $\quad V(\omega) = Im[E(\omega)]$

Similarly:-

$$\partial E(\omega)/\partial a = Re\{\partial E(\omega)/\partial a\} + jIm\{\partial E(\omega)/\partial a\}$$

$$= P(\omega) + jQ(\omega) \qquad 18$$

and

$$\partial E(-\omega)/\partial a = P(\omega) - jQ(\omega),$$

treating $\partial E(\omega)/\partial a$ as the spectrum of a real signal. Thus from equation 16:-

$$\partial e^2(t)/\partial a = 2\int\{U(\omega)P(\omega) - jU(\omega)Q(\omega) + jV(\omega)P(\omega) + V(\omega)Q(\omega)\}d\omega \qquad 19$$

but differentiating equation 17 gives:-

$$\frac{\partial E(\omega)}{\partial a} = \frac{\partial U(\omega)}{\partial a} + j\frac{\partial V(\omega)}{\partial a} \qquad 20$$

and comparing equations 20 and 18 gives:-

$$P(\omega) = \frac{\partial U(\omega)}{\partial a} \text{ and } Q(\omega) = \frac{\partial V(\omega)}{\partial a} \qquad 21$$

Substituting equation 21 into equation 19 gives:-

$$\overline{\frac{\partial e^2(t)}{\partial a}} = 2 \int \{ U(\omega) \frac{\partial U(\omega)}{\partial a} - j U(\omega) \frac{\partial V(\omega)}{\partial a}$$

$$+ j V(\omega) \frac{\partial U(\omega)}{\partial a} + V(\omega) \frac{\partial V(\omega)}{\partial a} \} \, d\omega$$

$$= 2 \int \{ U(\omega) \frac{\partial U(\omega)}{\partial a} + V(\omega) \frac{\partial V(\omega)}{\partial a} \} d\omega$$

$$- 2j \int \{ U(\omega) \frac{\partial V(\omega)}{\partial a} - V(\omega) \frac{\partial U(\omega)}{\partial a} \} d\omega$$

22

The first integral of equation 22 can be written as:-

$$\int \left[\frac{\partial U^2(\omega)}{\partial a} + \frac{\partial V^2(\omega)}{\partial a} \right] d\omega$$

$$= \int \frac{\partial |E(\omega)|^2}{\partial a} \, d\omega$$

$$= \frac{\partial}{\partial a} \int |E(\omega)|^2 d\omega$$

$$= \frac{\partial}{\partial a} \overline{e^2(t)}$$

To show that the second integral of equation 22 is zero, consider:-

$$\overline{\frac{\partial e^2(t)}{\partial a}} = 2 \, E(-\omega) \frac{\partial E(\omega)}{\partial a} d\omega, \text{ from Parseval's theorem.}$$

In this case $E(-\omega) = U(\omega) - jV(\omega)$

and $\frac{\partial E(\omega)}{\partial a} = P(\omega) + jQ(\omega) = \frac{\partial U(\omega)}{\partial a} + j \frac{\partial V(\omega)}{\partial a}$, as before.

Thus:-

$$\overline{\frac{\partial e^2(t)}{\partial a}} = 2 \int U(\omega) \frac{\partial U(\omega)}{\partial a} + j U(\omega) \frac{\partial V(\omega)}{\partial a}$$

$$- j V(\omega) \frac{\partial U(\omega)}{\partial a} + V(\omega) \frac{\partial V(\omega)}{\partial a} \, d\omega$$

Therefore:-

$$\overline{\frac{\partial e^2(t)}{\partial a}} = 2 \int \frac{\partial}{\partial a} U^2(\omega) + \frac{\partial}{\partial a} V^2(\omega) \, d\omega$$

$$+ 2j \int U(\omega) \frac{\partial V(\omega)}{\partial a} - V(\omega) \frac{\partial U(\omega)}{\partial a} \, d\omega$$

23

Comparing equations 23 and 22 gives:-

$$\int U(\omega)\frac{\partial V(\omega)}{\partial a} - V(\omega)\frac{\partial U(\omega)}{\partial a} \, d\omega = 0$$

and equation 13 has been proven.

$$\int U(\omega)\frac{\partial V(\omega)}{\partial a} - V(\omega)\frac{\partial U(\omega)}{\partial a} \, d\omega = 0$$

and equation 13 has been proven.
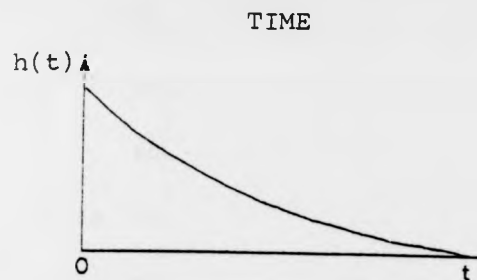
TIME   FREQUENCY

Figure A1.1a: Continuous   Continuous Doubly-
                Impulse Response   Infinite Response
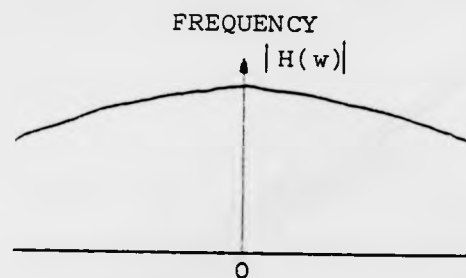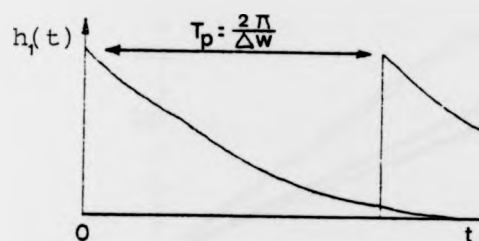
Figure A1.1b: Periodic   Discrete Doubly-
                Impulse Response   Infinite Spectrum
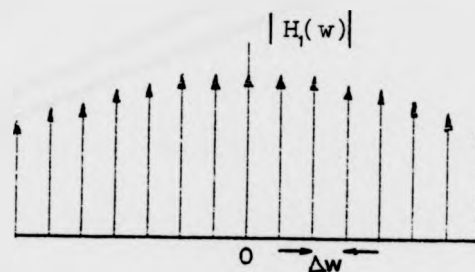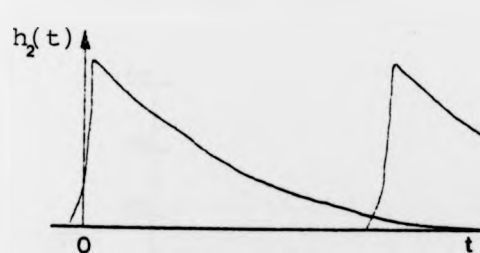
Figure A1.1c: The Effect of a Rectangular Frequency
                Window on the Impule Response
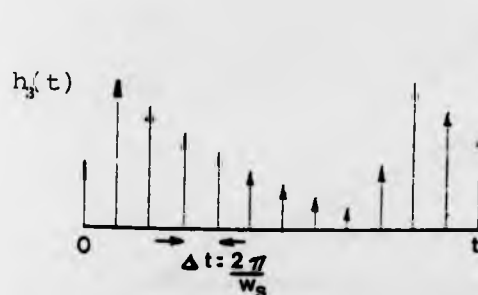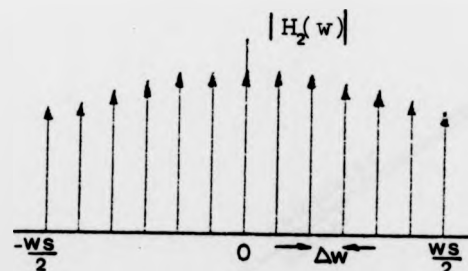
Figure A1.1d: The Effect of Assuming the Frequency
                Response to be Periodic
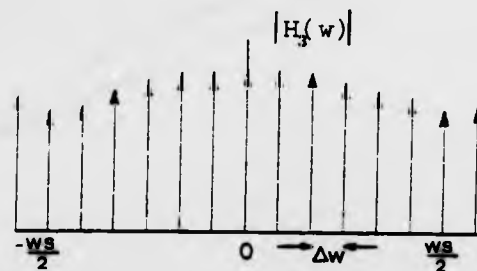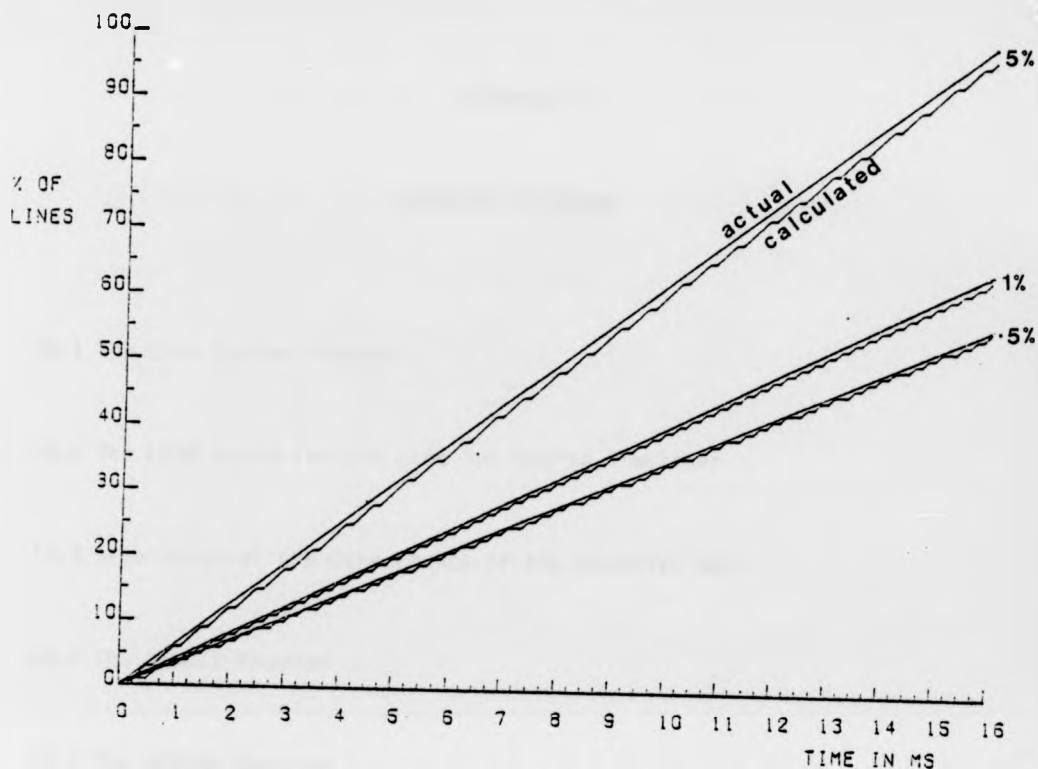
Figure A1.2: Test Decay Time Distributions Using the Hamming Window
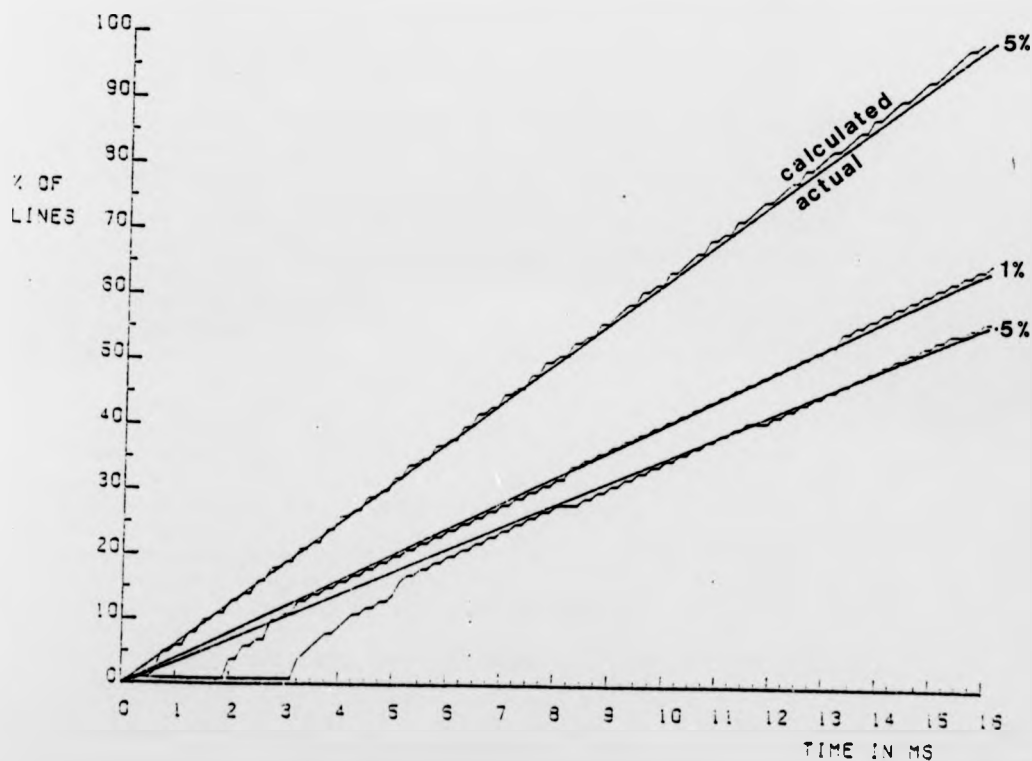
Figure A1.3: Test Decay Time Distributions Using a Rectangular Window
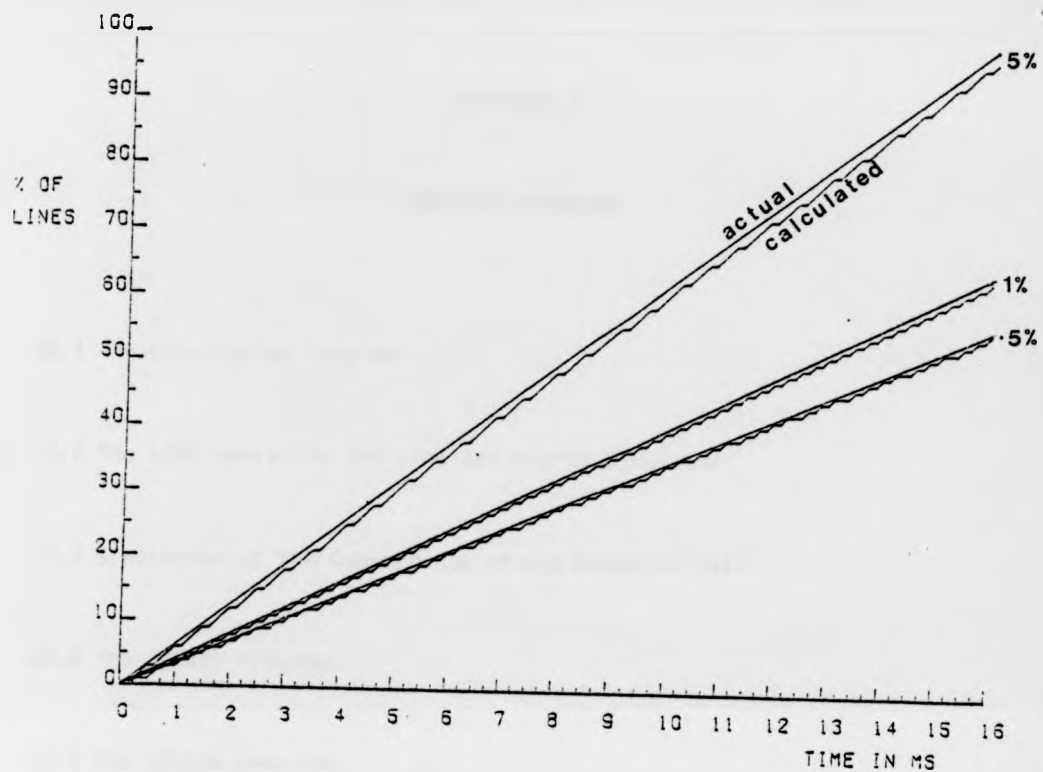
Figure A1.2: Test Decay Time Distributions
Using the Hamming Window
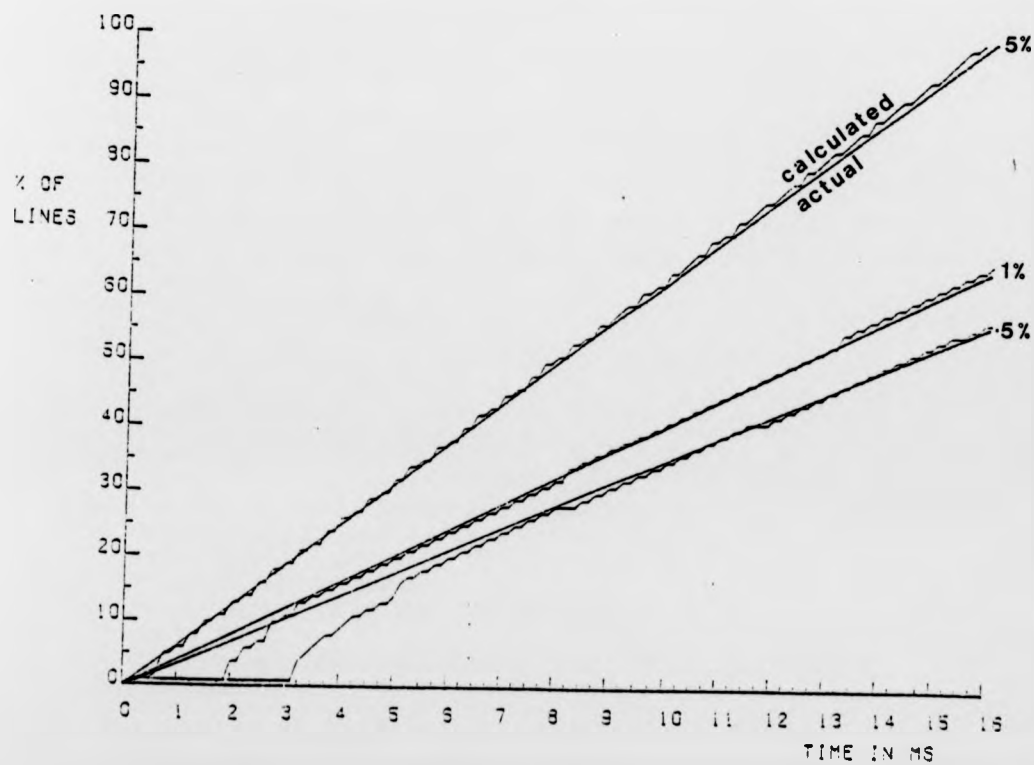
Figure A1.3: Test Decay Time Distributions
Using a Rectangular Window

APPENDIX 2

COMPUTER PROGRAMS

A2.1 The Line Survey Program

A2.2 The LOAD macro for the Line and Hybrid Simulator

A2.3 Simulation of the Convergence of the Adaptive Gain

A2.4 The AFWRIT Program

A2.5 The AFREAD Program

A2.6 The ADHYB Program

Appendix A2.1 The Line Survey Program

```
C
C-----------------------------------------------------------------------
C
C PROGRAM LINES CALCULATES THE TRANSHYBRID ERL AND SRL, AND THE IMPULSE
C RESPONSE DECAY TIMES, DUE TO SUBSCRIBERS' LINES. THE FOLLOWING FILES
C ARE USED BY THE PROGRAM:-
C      LDAT  : LINE SURVEY DATA BASE
C      ZOGMA : TABULATED CHARACTERISTICS OF THE VARIOUS LINE TYPES
C      TELE  : TABULATED IMPEDANCE OF THE TELEPHONE
C      RES   : RESULTS FOR ERL, SRL AND DECAY TIMES FOR EACH LINE
C      PLOT  : RESULTS FOR ERL, SRL AND DECAY TIME DISTRIBUTIONS
C
C-----------------------------------------------------------------------
C
       PROGRAM LINES(INPUT,OUTPUT,ZOGMA,PLOT,TELE,RES,LDAT
      1,TAPE5=INPUT,TAPE6=OUTPUT,TAPE7=ZOGMA,TAPE12=PLOT
      2,TAPE9=TELE,TAPE10=RES,TAPE11=LDAT)
       COMMON NLINES,ERLMN,SRLMN,FL(256)
       DIMENSION W(129),PK(128),IPK(128),L(17),TYP(17),FL(256)
       DIMENSION WIND(129),LMN(6)
       COMPLEX Z0(129),ZB(129),TC,TCC,GMA(129),ZT(129),ZOT(2193),
      1 GMAT(2193),ZTEL(129),ZI(256)
       PI2=8.0*ATAN(1.0)
C SET THE FREQUENCY RESOLUTION
       WINC=31.25*PI2
C READ THE NUMBER OF LINES TO BE ANALYSED AND THE VALUES OF THE 3-ELEMENT
C BALANCE AND TERMINATING IMPEDANCES.
       READ(5,*)NLINES
       READ(5,*)RST,RPT,CT
       READ(5,*)RSB,RPB,CB
       WRITE(10,*)RST,RPT,CT,RSB,RPB,CB
       T1=CT*WINC*RPT*1.0E-06
       T2=CB*WINC*RPB*1.0E-06
       T3=PI2/256.
C CALCULATE THE WINDOW RESPONSE AND THE VALUES OF THE BALANCE AND
C TERMINATING IMPEDANCES.
       DO 10 I=1,129
       WIND(I)=0.54+0.46*COS(FLOAT(I-1)*T3)
       ZT(I)=CMPLX(RST,0.0)+CMPLX(RPT,0.0)/CMPLX(1.0,T1*(I-1))
       ZB(I)=CMPLX(RSB,0.0)+CMPLX(RPB,0.0)/CMPLX(1.0,T2*(I-1))
   10 CONTINUE
       READ(5,*)ITEL,IWINDO
       WRITE(10,*)ITEL,IWINDO
C JUMP IF LOAD IMPEDANCE IS OTHER THAN THE TELEPHONE
       IF(ITEL.NE.1)GO TO 35
       READ(9,*)TELENO
       READ(9,240)(ZTEL(I),I=1,129)
  240 FORMAT(4(E13.6))
       GO TO 30
C READ VALUES OF THE 3-ELEMENT LOAD IMPEDANCE
   35 READ(5,*)RST,RPT,CT
       WRITE(10,*)RST,RPT,CT
       T1=CT*WINC*RPT*1.0E-06
C CALCULATE THE VALUES OF THE LOAD IMPEDANCE
       DO 50 I=1,129
       ZTEL(I)=CMPLX(RST,0.0)+CMPLX(RPT,0.0)/CMPLX(1.0,T1*(I-1))
   50 CONTINUE
```

```fortran
C READ THE PROPOGATION CONSTANT AND CHARACTERISTIC IMPEDANCE DATA
C FOR ALL THE LINE TYPES
   30 READ(7,240)(GMAT(I),I=1,2193)
      READ(7,240)(ZOT(I),I=1,2193)
C INITIALISE VARIABLES TO CALCULATE MEAN RETURN LOSSES
      ERLMN=0.0
      SRLMN=0.0
      DO 800 IX=1,6
      LMN(IX)=0
  800 CONTINUE
C LOOP FOR EACH SUBSCRIBERS' LINE
      DO 300 ILIN=1,NLINES
C PUT THE INPUT IMPEDANCE OF THE OTH LINE SECTION EQUAL TO THE
C LOAD IMPEDANCE
      DO 20 I=1,129
      ZI(I)=ZTEL(I)
   20 CONTINUE
C READ DETAILS OF A LINE FROM THE DATA BASE
      READ(11,*)LINO,RD,(FL(I),I=1,16)
C LOOP FOR EACH SECTION OF LINE
      DO 130 ISECT=1,16
C CONVERT DATA TO LENGTH AND TYPE OF LINE
      L(ISECT)=IFIX(FL(ISECT))
      TYP(ISECT)=FL(ISECT)-L(ISECT)
C JUMP IF END OF LINE
      IF(L(ISECT).LT.0)GO TO 140
C CALCULATE INDEX INTO LINE DATA TABLE (ZOGMA)
      IF(TYP(ISECT).GE.0.1075.AND.TYP(ISECT).LE.0.1101)N=0
      IF(TYP(ISECT).GE.0.1175.AND.TYP(ISECT).LE.0.1201)N=129
      IF(TYP(ISECT).GE.0.1675.AND.TYP(ISECT).LE.0.1701)N=258
      IF(TYP(ISECT).GE.0.2075.AND.TYP(ISECT).LE.0.2101)N=387
      IF(TYP(ISECT).GE.0.2475.AND.TYP(ISECT).LE.0.2501)N=516
      IF(TYP(ISECT).GE.0.3075.AND.TYP(ISECT).LE.0.3101)N=645
      IF(TYP(ISECT).GE.0.3175.AND.TYP(ISECT).LE.0.3201)N=774
      IF(TYP(ISECT).GE.0.3975.AND.TYP(ISECT).LE.0.401)N=903
      IF(TYP(ISECT).GE.0.4075.AND.TYP(ISECT).LE.0.4101)N=1032
      IF(TYP(ISECT).GE.0.4975.AND.TYP(ISECT).LE.0.501)N=1161
      IF(TYP(ISECT).GE.0.5075.AND.TYP(ISECT).LE.0.5101)N=1290
      IF(TYP(ISECT).GE.0.6075.AND.TYP(ISECT).LE.0.6101)N=1419
      IF(TYP(ISECT).GE.0.6275.AND.TYP(ISECT).LE.0.6301)N=1548
      IF(TYP(ISECT).GE.0.8075.AND.TYP(ISECT).LE.0.8101)N=1677
      IF(TYP(ISECT).GE.0.8975.AND.TYP(ISECT).LE.0.901)N=1806
      IF(TYP(ISECT).GE.0.6975.AND.TYP(ISECT).LE.0.701)N=1935
      IF(TYP(ISECT).GE.0.7475.AND.TYP(ISECT).LE.0.7501)N=2064
C LOOP FOR EACH FREQUENCY POINT
      DO 250 IF=1,129
C LOOK UP LINE DATA
      ZO(IF)=ZOT(N+IF)
      GMA(IF)=GMAT(IF+N)
      GMA(IF)=GMA(IF)*L(ISECT)
C CALCULATE INPUT IMPEDANCE OF THE LINE SECTION
      TCC=CMPLX(-AIMAG(GMA(IF)),REAL(GMA(IF)))
      TC=CSIN(TCC)/CCOS(TCC)
      TCC=CMPLX(-AIMAG(TC),REAL(TC))
      ZI(IF)=(ZI(IF)-ZO(IF)*TCC)/(CMPLX(1.0,0.0)-ZI(IF)*TCC/ZO(IF))
  250 CONTINUE
C NEXT LINE SECTION
  130 CONTINUE
  140 CONTINUE
C ZI IS NOW THE INPUT IMPEDANCE OF THE LINE
```

```
C CALCULATE THE TRANSHYBRID RESPONSE
      DO 160 IF=1,129
      ZI(IF)=(ZB(IF)/(ZB(IF)+ZT(IF)))-(ZI(IF)/(ZI(IF)+ZT(IF)))
      ZI(IF)=ZI(IF)*CMPLX(2.0,0.0)
  160 CONTINUE
C ZI NOW SPECIFIES THE TRANSHYBRID RESPONSE
C EVALUATE THE ERL AND SRL
      CALL EVAL(ZI,TYP(9),TYP(13))
C UPDATE THE RUNNING TOTALS FOR MEAN ERL AND SRL
      ERLMN=ERLMN+TYP(9)
      SRLMN=SRLMN+TYP(13)
C JUMP IF WINDOW NOT REQUIRED
      IF(IWINDO.NE.1)GO TO 560
C WINDOW THE FREQUENCY RESPONSE
      DO 550 IK=1,129
      ZI(IK)=ZI(IK)*WIND(IK)
  550 CONTINUE
  560 CONTINUE
C MIRROR THE RESPONSE AROUND HALF THE SAMPLING FREQUENCY, EVEN REAL
C PARTS, ODD IMAGINARY PARTS, TO PRODUCE A REAL IMPULSE RESPONSE
      DO 450 I=1,127
  450 ZI(257-I)=CMPLX(REAL(ZI(I+1)),-AIMAG(ZI(I+1)))
      ZI(129)=CMPLX(REAL(ZI(129)),0.0)
      CALL FFT(ZI,256,1,FL)
C FIND PEAK AMPLITUDE OF IMPULSE RESPONSE, HELD IN FL
      VM=0.0
      DO 510 I=1,129
      F=ABS(FL(I))
      IF(F.GE.VM)VM=F
      FL(I)=F
  510 CONTINUE
C SET LEVELS TO WHICH THE RELATIVE DECAY TIMES ARE REQUIRED
      TYP(3)=VM*0.5
      TYP(2)=VM*0.01
      TYP(1)=VM*0.005
C LOOP FOR EACH LEVEL
      DO 540 K=1,3
      V=TYP(K)
C STARTING FROM THE LAST IMPULSE RESPONSE SAMPLE, FIND THE FIRST
C SAMPLE WHERE THE LEVEL IS EXCEEDED
      DO 520 I=1,129
      J=130-I
      IF(FL(J).GE.V)GO TO 530
  520 CONTINUE
  530 L(4-K)=J
  540 CONTINUE
C REPEAT FOR DECAY TIMES TO ABSOLUTE LEVELS
      TYP(3)=0.1*0.05
      TYP(2)=0.1*0.01
      TYP(1)=0.1*0.005
      DO 640 K=1,3
      V=TYP(K)
      DO 620 I=1,129
      J=130-I
      IF(FL(J).GE.V)GO TO 630
  620 CONTINUE
  630 L(7-K)=J
  640 CONTINUE
C CALCULATE MEAN DECAY TIMES
      DO 820 IX=1,6
```

```
C CALCULATE THE TRANSHYBRID RESPONSE
      DO 160 IF=1,129
      ZI(IF)=(ZB(IF)/(ZB(IF)+ZT(IF)))-(ZI(IF)/(ZI(IF)+ZT(IF)))
      ZI(IF)=ZI(IF)*CMPLX(2.0,0.0)
  160 CONTINUE
C ZI NOW SPECIFIES THE TRANSHYBRID RESPONSE
C EVALUATE THE ERL AND SRL
      CALL EVAL(ZI,TYP(9),TYP(13))
C UPDATE THE RUNNING TOTALS FOR MEAN ERL AND SRL
      ERLMN=ERLMN+TYP(9)
      SRLMN=SRLMN+TYP(13)
C JUMP IF WINDOW NOT REQUIRED
      IF(IWINDO.NE.1)GO TO 560
C WINDOW THE FREQUENCY RESPONSE
      DO 550 IK=1,129
      ZI(IK)=ZI(IK)*WIND(IK)
  550 CONTINUE
  560 CONTINUE
C MIRROR THE RESPONSE AROUND HALF THE SAMPLING FREQUENCY, EVEN REAL
C PARTS, ODD IMAGINARY PARTS, TO PRODUCE A REAL IMPULSE RESPONSE
      DO 450 I=1,127
  450 ZI(257-I)=CMPLX(REAL(ZI(I+1)),-AIMAG(ZI(I+1)))
      ZI(129)=CMPLX(REAL(ZI(129)),0.0)
      CALL FFT(ZI,256,1,FL)
C FIND PEAK AMPLITUDE OF IMPULSE RESPONSE, HELD IN FL
      VM=0.0
      DO 510 I=1,129
      F=ABS(FL(I))
      IF(F.GE.VM)VM=F
      FL(I)=F
  510 CONTINUE
C SET LEVELS TO WHICH THE RELATIVE DECAY TIMES ARE REQUIRED
      TYP(3)=VM*0.5
      TYP(2)=VM*0.01
      TYP(1)=VM*0.005
C LOOP FOR EACH LEVEL
      DO 540 K=1,3
      V=TYP(K)
C STARTING FROM THE LAST IMPULSE RESPONSE SAMPLE, FIND THE FIRST
C SAMPLE WHERE THE LEVEL IS EXCEEDED
      DO 520 I=1,129
      J=130-I
      IF(FL(J).GE.V)GO TO 530
  520 CONTINUE
  530 L(4-K)=J
  540 CONTINUE
C REPEAT FOR DECAY TIMES TO ABSOLUTE LEVELS
      TYP(3)=0.1*0.05
      TYP(2)=0.1*0.01
      TYP(1)=0.1*0.005
      DO 640 K=1,3
      V=TYP(K)
      DO 620 I=1,129
      J=130-I
      IF(FL(J).GE.V)GO TO 630
  620 CONTINUE
  630 L(7-K)=J
  640 CONTINUE
C CALCULATE MEAN DECAY TIMES
      DO 820 IX=1,6
```

```
       LMN(IX)=LMN(IX)+L(IX)
   820 CONTINUE
   810 WRITE(10,760)LINO,(L(I),I=1,6),TYP(9),TYP(13)
   760 FORMAT(I4,1X,6(I3,1X),2(F7.2,1X))
   300 CONTINUE
       FLINES=FLOAT(NLINES)
       ERLMN=ERLMN/FLINES
       SRLMN=SRLMN/FLINES
       DO 790 IX=1,6
       FL(IX)=FLOAT(LMN(IX))/FLINES
   790 CONTINUE
       WRITE(10,780)(ERLMN,SRLMN,(FL(IX),IX=1,6))
       WRITE(6,780)(ERLMN,SRLMN,(FL(IX),IX=1,6))
   780 FORMAT(2(F8.3,2X),6(F7.2,2X))
C CALL SUBROUTINE ANL TO FORM CUMULATIVE DISTRIBUTIONS
       CALL ANL
       STOP
       END
C
C----------------------------------------------------------------------
C
C SUBROUTINE EVAL EVALUATES THE ERL (B) AND SRL (C) DUE TO A TRANSHYBRID
C FREQUENCY RESPONSE (A)
C
C----------------------------------------------------------------------
C
       SUBROUTINE EVAL(A,B,C)
       COMPLEX A(256)
       DIMENSION D(129)
       C=-200.0
       DO 10 I=11,110
       T=CABS(A(I))
       IF(T.LT.1.0E-11)T=1.0E-11
       D(I)=20.0*ALOG10(T)
       IF(D(I).GT.C)C=D(I)
    10 CONTINUE
       B=0.0
       DO 20 I=17,81
       B=B+D(I)
    20 CONTINUE
       B=B/65.0
       RETURN
       END
C
C----------------------------------------------------------------------
C
C SUBROUTINE FFT CALCULATES FORWARD AND INVERSE FAST FOURIER TRANSFORMS
C ISI = 1 FOR INVERSE, IN WHICH CASE THE IMPULSE RESPONSE IS ASSUMED
C REAL AND HELD IN RESULT
C
C----------------------------------------------------------------------
C
       SUBROUTINE FFT(DATA,N,ISI,RESULT)
       COMPLEX DATA(N),TEMP,W,CN
       REAL RESULT(N)
       PI=4.0*ATAN(1.0)
       FN=N
       J=1
       DO 80 I=1,N
       IF(I-J)30,40,40
```

```fortran
   30 TEMP=DATA(J)
      DATA(J)=DATA(I)
      DATA(I)=TEMP
   40 M=N/2
   50 IF(J-M)70,70,60
   60 J=J-M
      M=(M+1)/2
      GO TO 50
   70 J=J+M
   80 CONTINUE
      MMAX=1
   90 IF(MMAX-N)100,130,130
  100 ISTEP=2*MMAX
      DO 120 M=1,MMAX
      THETA=PI*FLOAT(ISI*(M-1))/FLOAT(MMAX)
      W=CMPLX(COS(THETA),SIN(THETA))
      DO 110 I=M,N,ISTEP
      J=MMAX+I
      TEMP=W*DATA(J)
      DATA(J)=DATA(I)-TEMP
      DATA(I)=DATA(I)+TEMP
  110 CONTINUE
  120 CONTINUE
      MMAX=ISTEP
      GO TO 90
  130 IF(ISI)160,140,140
  140 DO 150 I=1,N
      RESULT(I)=REAL(DATA(I))/FN
  150 CONTINUE
  160 CONTINUE
      END
C
C---------------------------------------------------------------------
C
C SUBROUTINE ANL ANALYSES THE DATA ON ERL, SRL AND DECAY TIMES FOR
C EACH LINE CONTAINED IN "RES" AND FORMS THE CUMULATIVE DISTRIBUTIONS
C
C---------------------------------------------------------------------
C
      SUBROUTINE ANL
      COMMON NLINES,ERLMN,SRLMN,FL(256)
      DIMENSION M1(129,3,2),R1(129,3,2),L(6),T1(129,3,2),LP(3)
      REAL TVAR(6),M3(61,2),T(2),R3(61,2)
      FLINES=FLOAT(NLINES)/100.
      REWIND 10
      LP(1)=5
      LP(2)=1
      LP(3)=0
C READ DETAILS OF HYBRID AND LOAD AND COPY TO PLOT FILE
      READ(10,*)RST,RPT,CT,RSB,RPB,CB
      WRITE(12,*)RST,RPT,CT,RSB,RPB,CB
      READ(10,*)ITEL,IWINDO
      WRITE(12,*)ITEL,IWINDO
      WRITE(6,40)RST,RPT,CT,RSB,RPB,CB
   40 FORMAT(' RST=',F7.2,2X,'RPT=',F7.2,2X,'CT=',E10.3,/
     1,' RSB=',F7.2,2X,'RPB=',F7.2,2X,'CB=',E10.3)
      WRITE(6,160)IWINDO
  160 FORMAT(' IWINDO = ',I1)
      IF(ITEL.NE.1)GO TO 50
      WRITE(6,210)
```

```
  210 FORMAT(/,' LOAD IS TYPICAL 706-TYPE TELEPHONE')
      GO TO 20
   50 READ(10,*)RST,RPT,CT
      WRITE(12,*)RST,RPT,CT
      WRITE(6,220)RST,RPT,CT
  220 FORMAT(/,' RSL=',F7.2,2X,'RPL=',F7.2,2X,'CL='E10.3)
C INITIALISE VARIABLES FOR RETURN LOSS DISTRIBUTION CALCULATIONS
C M3 IS AN ARRAY OF RETURN LOSS VALUES AGAINST WHICH ACTUAL RETURN
C LOSSES ARE CHECKED
   20 DO 10 I=1,2
      DO 10 J=1,61
      M3(J,I)=30.5-FLOAT(J)*0.5
      R3(J,I)=0.0
   10 CONTINUE
C INITIALISE VARIABLES FOR DECAY TIME CALCULATIONS
      DO 30 I3=1,2
      DO 30 I2=1,3
      DO 30 I1=1,129
      M1(I1,I2,I3)=I1
      R1(I1,I2,I3)=0.0
   30 CONTINUE
C INITIALISE VARIABLES TO CALCULATE STD. DEVIATIONS OF RETURN LOSSES
C AND DECAY TIMES
      ERLVAR=0.0
      SRLVAR=0.0
      DO 480 IX=1,6
      TVAR(IX)=0.0
  480 CONTINUE
C LOOP FOR EACH LINE
      DO 200 ILINE=1,NLINES
      READ(10,65)LINO,(L(I),I=1,6),T(1),T(2)
   65 FORMAT(I4,1X,6(I3,1X),2(F7.2,1X))
C UPDATE RUNNING TOTALS FOR STD. DEV. CALCULATIONS
      P1=ERLMN-T(1)
      P2=SRLMN-T(2)
      ERLVAR=ERLVAR+(P1*P1)
      SRLVAR=SRLVAR+(P2*P2)
      DO 490 IX=1,6
      P3=FLOAT(L(IX))-FL(IX)
      TVAR(IX)=TVAR(IX)+(P3*P3)
  490 CONTINUE
      I1=0
C LOOP FOR ABSOLUTE AND REALTIVE (TO PEAK AMPLITUDE) DECAY TIMES
      DO 62 I3=1,2
C LOOP FOR EACH VALUE TO WHICH THE DECAY TIME DISTN. IS REQUIRED
      DO 61 I=1,3
      J=1
C JUMP IF DECAY TIME LESS THAN CHECK TIME
   70 IF(L(I1+I).LE.M1(J,I,I3))GO TO 80
C INCREASE CHECK TIME
      J=J+1
      IF(J.LE.129)GO TO 70
C DECAY TIME TO THIS VALUE IS GREATER THAN 16 MS, SKIP TO NEXT VALUE
      GO TO 61
C INCREMENT TOTAL NUMBERS OF LINES WITH DECAY TIMES LESS THAN
C CHECK TIMES
   80 DO 60 M=J,129
      R1(M,I,I3)=R1(M,I,I3)+1.0
   60 CONTINUE
   61 CONTINUE
```

```
            I1=3
      62 CONTINUE
C LOOP ONCE FOR ERL, AGAIN FOR SRL
         DO 200 I=1,2
         J=1
C JUMP IF LOSS GREATER THAN MARKER

      75 IF(-T(I).GT.M3(J,I))GO TO 85
C INCREMENT MARKER
         J=J+1
         IF(J.LE.61)GO TO 75
         GO TO 68
C INCREMENT TOTAL NUMBERS OF LINES
      85 DO 95 M=J,61
         R3(M,I)=R3(M,I)+1.0
      95 CONTINUE
      68 CONTINUE
     200 CONTINUE

C OUTPUT RESULTS FOR DECAY TIMES TO VARIOUS PERCENTAGES OF PEAK
         P2=FLOAT(NLINES-1)
         DO 510 IX=1,6
         TVAR(IX)=SQRT(TVAR(IX)/P2)
     510 CONTINUE
         DO 90 I=1,3
         DO 90 J=1,129
         R1(J,I,1)=R1(J,I,1)/FLINES
         T1(J,I,1)=FLOAT(M1(J,I,1))/8.0
      90 CONTINUE
C OUTPUT RESULTS FOR RETURN LOSSES
         DO 300 I=1,3
         DO 300 J=1,129
         R1(J,I,2)=R1(J,I,2)/FLINES
         T1(J,I,2)=FLOAT(M1(J,I,2))/8.0
     300 CONTINUE
         DO 310 I=1,2
         DO 310 J=1,61
         R3(J,I)=R3(J,I)/FLINES
     310 CONTINUE
         DO 400 I=1,2
         DO 420 J=1,3
         WRITE(12,450)(R1(K,J,I),K=1,129)
     450 FORMAT(8(F7.2,1X))
         WRITE(12,500)FL(J+(I-1)*3),TVAR(J+(I-1)*3)
         WRITE(6,500)FL(J+(I-1)*3),TVAR(J+(I-1)*3)
     500 FORMAT(2(F8.3,4X))
     420 CONTINUE
     400 CONTINUE
         DO 430 I=1,2
         WRITE(12,450)(R3(J,I),J=1,61)
     430 CONTINUE
         SRLVAR=SQRT(SRLVAR/P2)
         ERLVAR=SQRT(ERLVAR/P2)
         WRITE(12,470)ERLMN,ERLVAR,SRLMN,SRLVAR
         WRITE(6,470)ERLMN,ERLVAR,SRLMN,SRLVAR
     470 FORMAT(2(F8.3,4X,F7.4,4X))
         STOP
         END
```

```
                ;MACRO-11 ROUTINE TO LOAD COEFFICIENTS FROM ARRAY
                ;IN MAINPROGRAM INTO FILTER RAM.
                ;ADDRESSES FOR THE FILTER RAMS MUST BE
                ;COMPLEMENTED DURING LOADING. DRV-11 BOARD SHOULD
                ;BE PATCHED AT ADDRESS 167770. FILTER IS HALTED
                ;AND LOADING STARTS AT RAM LOC 127,
                ;CONTINUING TO RAM LOC 0. FINALLY RAM LOC
                ;128 IS CLEARED AND THE FILTER RETURNED TO THE
                ;STATE DEFINED BY FIRST ARG OF MAINPROGRAM CALL.

        .TITLE LOAD LHS COEFFICIENTS
        .IDENT /V01/

                ;SET UP ADDRESSES FOR DRV-11 AS FOLLOWS,
CNTRL=167770    ;CONTROL-REGISTER'S ADDRESS
CMEM=167772     ;RAM-DATA-REGISTER'S ADDRESS
CCNTR=167774    ;RAM-LOC-REGISTER'S ADDRESS

FHALT=100000    ;DEFINE CONTROL WORD TO HALT FILTER
SMADD=000200    ;DEFINE RAM LOC 128
CZER0=177777    ;DEFINE DATA TO CLEAR ABOVE

LOAD::  MOV  #SMADD,R0       ;PREPARE TO ADDRESS RAM LOC 127
        DEC  R0
        MOV  #FHALT,@#CNTRL  ;HALT FILTER
        MOV  (R5)+,R1        ;GET NO. OF ARGS IN MAINPROG CALL
        MOV  @(R5)+,R1       ;GET 1'ST ARG (CONTROL WORD) FROM MAINPROGRAM
        MOV  (R5)+,R3        ;GET ADDRESS OF 2'ND ARG (FIRST COEFFICIENT) IN
                             ; M/C MEMORY
LAB1:   MOV  R0,R4           ;COPY RAM ADDRESS INTO R4
        COM  R4              ;COMPLEMENT ADDRESS TO ALLOW FOR BUFFERS
        MOV  R4,@#CCNTR      ;ADDRESS RO'TH LOC IN RAM
        MOV  (R3)+,R2        ;GET COEFFICIENT FROM M/C MEMORY
        MOV  R2,@#CMEM       ;WRITE COEFFICIENT INTO RO'TH RAM LOC
        DEC  R0              ;PREPARE TO ADDRESS NEXT RAM LOC
        BPL  LAB1            ;CONTINUE UNLESS RAM LOC 0 HAS BEEN LOADED
```

```
        MOV     #SMADD,R0       ;IF SO THEN CLEAR RAM LOC 128
        COM     R0              ;COMPLEMENT FOR BUFFERS
        MOV     R0,@#CCNTR      ;ADDRESS RAM LOC 128
        MOV     #CZERO,@#CMEM   ;CLEAR RAM LOC 128
        MOV     R1,@#CNTRL      ;OUTPUT 1'ST ARG (CONTROL WORD) FROM MAINPROGRAM
                                ;TO CONTROL REGISTER
        RTS     PC              ;RETURN TO MAINPROGRAM
        .END LOAD
```

```
MOV     #SMADD,RO                ;IF SO THEN CLEAR RAM LOC 128

COM     RO                       ;COMPLEMENT FOR BUFFERS
MOV     RO,@#CCNTR               ;ADDRESS RAM LOC 128
MOV     #CZERO,@#CMEM            ;CLEAR RAM LOC 128
MOV     R1,@#CNTRL               ;OUTPUT 1'ST ARG (CONTROL WORD) FROM MAINPROGRAM
                                 ;TO CONTROL REGISTER
RTS     PC                       ;RETURN TO MAINPROGRAM
.END LOAD
```

```
C
C-----------------------------------------------------------
C
C PROGRAM ADGAIN SIMULATES THE CONVERGENCE OF THE
C ADAPTIVE GAIN FILTER. THE MAXIMUM    NUMBER OF
C SAMPLES IS 512, IE: THE MAXIMUM TIME FOR
C WHICH THE OPERATION OF THE FILTER CAN BE
C SIMULATED IS 64 MS AT 8 KHZ. THE UNKNOWN
C SYSTEM IS SPECIFIED AS A SIMPLE GAIN/LOSS, AND THE
C INPUT SIGNAL IS SPECIFIED AS A SINE WAVE OR SUM OF
C SINE WAVES.
C
C-----------------------------------------------------------
C
      REAL X(512),D(512),EOLD(512),ENEW(512),AO(512)
      DATA X/512*0.0/,D/512*0.0/
      PI2=8.0*ATAN(1.0)
C SET DEVICE LIBRARY FOR GRAPHICS AND SCALE DRAWING AREA
      CALL DEVBEG
      CALL UNITS(1.0)
      CONV=180.0/PI2
C TIME RESOLUTION IS 0.25 MS
      TRES=0.25E-03
      NPTS=512
C SPECIFY THE UNKNOWN SYSTEM
   50 WRITE(2,10)
   10 FORMAT('INPUT G ')
      READ(1,*)G
      AOM=G
      WRITE(2,130)AOM
  130 FORMAT('THE OPTIMUM AO VALUE IS : ',F6.3,)
C SPECIFY THE SIGNAL SOURCE, SINE WAVE OR SUM OF
C SINES
      WRITE(2,70)
   70 FORMAT('INPUT FREQ,FREQ STEP,AMPLITUDE,NUMBER OF STEPS')
      READ(1,*)W,DW,AMP,NW
C CALCULATE THE POWER OF X
      PX=AMP*AMP*FLOAT(NW)/2.0
      W=W*PI2
      DW=DW*PI2
C LOOP FOR EACH FREQUENCY
      DO 80 IW=1,NW
      PHRAND=(RANDOM(1.)-0.5)*PI2
      T2=W*TRES
C LOOP FOR EACH SIGNAL SAMPLE
      DO 20 I=1,NPTS
      P1=T2*FLOAT(I-1)-PHRAND
      T1=AMP*SIN(P1)
      X(I)=X(I)+T1
      D(I)=D(I)+G*T1
   20 CONTINUE
      W=W+DW
   80 CONTINUE
C CALCULATE POWER OF D
      PD=PX*G*G
      WRITE(2,120)PX,PD
  120 FORMAT(' INPUT POWER = ',F7.4,' UNKNOWN POWER = ',F7.4,)
      T1=0.0
  150 WRITE(2,60)
   60 FORMAT('INPUT CONTROL AMPLIFIER GAINS')
```

```
C AX IS THE INPUT SIGNAL AMPLIFIER GAIN
C AE IS THE ERROR SIGNAL AMPLIFIER GAIN
C AI IS THE INTEGRATOR TIME CONSTANT
      READ(1,*)AX,AE,AI
      T2=0.0
      T1=0.0
      P1=TRES/AI
C SET FIRST APPROXIMATION TO THE ERROR AND CALCULATE THE
C POWER IN D
      DO 180 I=1,NPTS
      EOLD(I)=D(I)
      T2=T2+D(I)*D(I)
  180 CONTINUE
      D2AVG=T2*TRES/FLOAT(NPTS)
      P3=TRES/AI
      T2=T2*1.0E-05/FLOAT(NPTS)
C BEGIN PICARD ITERATION
      ITER=0
C INITIALISE T3 FOR INTEGRATION AND T4 TO CALCULATE
C THE MEAN SQUARE DIFFERENCE IN ERROR BEFORE AND
C AFTER EACH ITERATION.
   30 T3=0.0
      T4=0.0
      DO 40 I=1,NPTS
      T3=T3+EOLD(I)*AX*X(I)*P3
      AO(I)=T3
      ENEW(I)=D(I)-(X(I)*T3)
      T5=ENEW(I)-EOLD(I)
      T5=T5*T5
      T4=T4+T5
   40 CONTINUE
C UPDATE THE ERROR APPROXIMATION
      DO 90 I=1,NPTS
      EOLD(I)=ENEW(I)
   90 CONTINUE
      ITER=ITER+1
      T4=T4/FLOAT(NPTS)
C OUTPUT THE ITERATION NUMBER AND THE MEAN SQUARE DIFFERENCE
C IN ERROR.
      WRITE(2,*)ITER,T4
C JUMP IF NOT CONVERGED AFTER 80 ITERATIONS
      IF(ITER.GT.79)GO TO 150
C JUMP IF NOT CONVERGED ENOUGH
      IF((T4.GT.T2).OR.(ITER.LT.10))GO TO 30
C PLOT ERROR SIGNAL
      CALL PLOT(ENEW,NPTS,1,'ERROR*.')
      WRITE(2,110)
  110 FORMAT(' PLOT COEFFICIENT?,1/0')
      READ(1,*)FTEST
      IF(FTEST.EQ.1.)CALL PLOT(AO,NPTS,1,'AO*.')
  190 CONTINUE
C CALCULATE THE AVERAGE AO VALUE OVER THE FINAL N POINTS
      N=49
      T1=0.0
      DO 200 I=NPTS-N,NPTS
      T1=T1+AO(I)
  200 CONTINUE
      AOF=T1/FLOAT(N+1)
C CALCULATE ERROR POWER FOR THIS VALUE OF AO
      T1=0.0
```

```fortran
          DO 210 I=1,NPTS
          ER=D(I)-AOF*X(I)
          T1=T1+ER*ER
      210 CONTINUE
C CALCULATE ERLE ACHIEVED
          ERP=T1*TRES/FLOAT(NPTS+1)
          ERLE=20.0*ALOG10(D2AVG/ERP)
C CALCULATE THE TIME CONSTANT
          TX=AOF/AOM
          IF(TX.GE.0.995)GO TO 100
          TC=-FLOAT(NPTS)*TRES/(ALOG(1-TX))
      100 WRITE(2,230)AOF,ERLE,TC
      230 FORMAT('AO FINAL = ',E10.3,' ERLE = ',F7.2,' TC = ',
         1E10.3)
          WRITE(2,160)
      160 FORMAT('INPUT 0 TO END')
          READ(1,*)FTEST
          IF(FTEST.NE.0.0)GO TO 150
          CALL DEVEND
          STOP
          END
C
C
C
C-----------------------------------------------------
C
C SUBROUTINE PLOT PLOTS UP TO N DATA POINTS FROM ARRAY
C A ON THE Y AXIS. THE X AXIS REPRESENTS TIME. N MAX IS
C 512. IAX IS 1 IF AXES ARE REQUIRED, AND YLAB IS AN
C ARRAY CONTAINING THE LABEL FOR THE Y AXIS. THE PROGRAM
C USES SUBROUTINES FROM THE GINO GRAPHICS LIBRARY.
C
C-----------------------------------------------------
C
          SUBROUTINE PLOT(A,N,IAX,YLAB)
          DIMENSION A(512),C(512),B(512),YLAB(4)
          CALL PICCLE
          DO 20 I=1,N
          B(I)=FLOAT(I-1)
          C(I)=A(I)*100.
       20 CONTINUE
C     SWITCH OFF ANY PREVIOUS TRANSFORMATIONS
          CALL TRANSF(-1)
C     SET X RIGHT LIMIT
          XR=512.
C     SET X LEFT LIMIT
          XL=0.0
C     SET Y TOP
          YT=100.
C     SET Y BOTTOM
          YB=-100.
          XRNG=ABS(XR-XL)
          YRNG=ABS(YT-YB)
C     NRES IS NUMBER OF UNITS OF Y PER TICK
C     NINT IS NUMBER OF TICKS PER NUMBER
          NRES=10
          NINT=2
          CALL SHIFT2(35.0,35.0)
C     SCALE TO REQUIRED DIMENSIONS
          CALL SCALE2(100./XRNG,100./YRNG)
```

```fortran
              CALL MOVTO2(0.0,0.0)
C             SHIFT FOR REQUIRED ORIGIN
              CALL SHIFT2(-XL,-YB)
C
C             DRAW Y AXIS,NUMBERING FROM TOP TO BOTTOM
C
              CALL LINTO2(XL,ABS(YT))
              TICENL=XL+XRNG/50.
              TICENS=XL+XRNG/100.
C             SET LOCATION OF AXIS LABEL AND NUMBERS
              PNUM=XL-XRNG/6.
              PLAB=XL-XRNG/4.
C             SET NUMBERING INTERVAL
              J=NINT
              DO 110 I=1,INT(YRNG+1.5),NRES
              TICEN=TICENS
              F=ABS(YT)-FLOAT(I-1)
              IF(J.NE.NINT)GO TO 120
              FM=(YT+1-I)/100.0
              J=0
              TICEN=TICENL
              CALL MOVTO2(PNUM,F)
C             PRINT NUMBER
              CALL CHAFIX(FM,6,-2)
       120    CALL MOVTO2(XL,F)
C             TICK AXIS
              CALL LINTO2(TICEN,F)
              J=J+1
       110    CONTINUE
              CALL MOVTO2(PLAB,YB+YRNG*0.77)
C             LABEL AXIS
              CALL CHAARR(YLAB,2,4)
C
C             DRAW X AXIS,NUMBERING FROM RIGHT TO LEFT
C
              NRES=8
              NINT=8
              CALL MOVTO2(XL,YB)
              CALL LINTO2(XR,YB)
              TICENL=YB+YRNG/50.
              TICENS=YB+YRNG/100.
              PNUM=YB-YRNG/20.
              PLAB=YB-YRNG/10.
              J=NINT
              DO 210 I=1,XRNG+1,NRES
              TICEN=TICENS
              F=XR-FLOAT(I-1)
C             JUMP IF NUMBER NOT REQUIRED
              IF(J.NE.NINT)GO TO 220
              J=0
              M=INT(0.5+INT(F/4.0))
              TICEN=TICENL
              CALL MOVTO2(F,PNUM)
C             PRINT NUMBER
              CALL CHAINT(M,-4)
       220    CALL MOVTO2(F,YB)
              CALL LINTO2(F,TICEN)
              J=J+1
       210    CONTINUE
              CALL MOVTO2(XL+XRNG*0.75,PLAB)
```

```
C       LABEL AXIS
        CALL CHAHOL(11HTIME (MS)*.)
C
        CALL MOVTO2(B(1),C(1))
        CALL POLTO2(B,C,N)
        CALL CHAMOD
        RETURN
        END
```

```
;MACRO-11 PROGRAM TO LOAD A NEW SET OF COEFFICIENTS INTO THE ADAPTIVE
;FILTER. THE DRV-11 INTERFACE BOARD SHOULD BE PATCHED AT ABSOLUTE M/C
;ADDRESS 167760. A HALT REQUEST IS MADE AND THE PROGRAM WAITS FOR THE
;CORRECT FILTER STATE. COEFFICIENT LOADING STARTS AT
;ADDRESS 0 IN THE COEFFICIENT RAMS, AND CONTINUES TO ADDRESS 11.
;DATA WRITTEN TO THE ADDRESS COUNTER IS COMPLEMENTED TO ALLOW FOR THE CABLE
;BUFFERS.  FINALLY THE RAM ADDRESS COUNTER IS SET TO ZERO AND THE
;FILTER RETURNED TO A STATE DEFINED BY THE FIRST ARGUMENT OF THE
;MAINPROGRAM CALL.
        .TITLE AFWRIT
        .IDENT /V01/

        ;SET UP DRV-11 PORT ADDRESSES AS FOLLOWS,
CNTRL=167760    ;ADDRESS OF CONTROL PORT
ADDCNT=167762   ;ADDRESS OF RAM-ADDRESS COUNTER
SIGDAT=167764   ;ADDRESS OF SIGNAL-RAM DATA PORT
COEDAT=167766   ;ADDRESS OF COEFFICIENT-RAM DATA PORT
        ;
FHALT=040000    ;DEFINE HALT CONTROL WORD
ZERO=000000     ;DEFINE ZERO
ELEVEN=000013   ;DEFINE LAST RAM ADDRESS
MASK1=010000    ;DEFINE MASK FOR HALT BIT
        ;
AFWRIT::MOV #FHALT,@#CNTRL  ;REQUEST FILTER HALT
        MOV (R5)+,R0    ;GET NUMBER OF ARGUMENTS IN MAINPROGRAM CALL
        MOV @(R5)+,R0   ;GET FIRST ARG (CONTROL WORD) ROM MAINPROG.
        MOV (R5)+,R1    ;GET ADDRESS OF 2-ND ARG (1-ST FILTER COEFF)
        MOV #ZERO,R2    ;INITIALISE A REGISTER TO ADDRESS FILTER RAM
WAIT:   MOV @#SIGDAT,R3 ;READ INPUT DATA
        BIT #MASK1,R3   ;MASK ALL EXCEPT HALT BIT
        BEQ WAIT        ;JUMP UNLESS FILTER HALTED
        MOV @#SIGDAT,R3
        BIT #MASK1,R3
        BEQ WAIT
LOOP:   MOV R2,R3       ;COPY RAM ADDRESS INTO R3
        COM R3          ;COMPLEMENT FOR CABLE BUFFERS
```

```
MOV R3,@#ADDCNT        ;ADDRESS THE R2'TH RAM LOCATION
MOV (R1)+,R3           ;GET COEFFICIENT FROM M/C MEMORY
MOV R3,@#COEDAT        ;WRITE COEFFICIENT INTO R2-TH COEFFICIENT LOC.
INC R2                 ;NEXT RAM ADDRESS
CMP #ELEVEN,R2         ;RAM ADDRESS GREATER THAN 11?
BPL LOOP               ;JUMP IF 11-TH LOC NOT YET ADDRESSED
MOV #ZERO,R3           ;
COM R3                 ;
MOV R3,@#ADDCNT        ;CLEAR ADDRESS COUNTER
MOV R0,@#CNTRL         ;OUTPUT FIRST ARG (CONTROL WORD) FROM MAINPROG
                       ;TO CONTROL PORT

RTS PC
.END AFWRIT
```

```
;MACRO-11 PROGRAM TO READ THE INPUT,DESIRED INPUT, ERROR AND
;FILTERERD ERROR SIGNAL SAMPLES FROM THE ADAPTIVE
;FILTER. THE DRV-11 INTERFACE BOARD SHOULD BE PATCHED
;AT ABSOLUTE M/C ADDRESS 167760. A HALT REQUEST IS MADE AND THE
;PROGRAM WAITS FOR THE CORRECT FILTER STATE. DATA READING STARTS AT
; ADDRESS 0 IN THE SIGNAL AND RAMS, AND CONTINUES TO ADDRESS 11.
;THE FILTERED ERROR SIGNAL SAMPLE IS READ BY ADDRESSING LOCATION 16.
; DATA WRITTEN TO THE ADDRESS COUNTER IS COMPLEMENTED TO
;ALLOW FOR THE CABLE BUFFERS. 12-BIT DATA READ FROM THE FILTER RAMS IS
;COMPLEMENTED TO ALLOW FOR THE INVERSION THROUGH THE RAMS, AND SIGN EXTENDED TO
;16 BITS. FINALLY THE RAM ADDRESS COUNTER IS SET TO ZERO AND THE FILTER RETURNED
; TO A STATE DEFINED BY THE FIRST ARGUMENT OF THE MAINPROGRAM CALL.
;
;
;
        .TITLE AFREAD
        .IDENT /V01/
;
                        ;SET UP DRV-11 PORT ADDRESSES AS FOLLOWS,
CNTRL=167760            ;ADDRESS OF CONTROL PORT
ADDCNT=167762           ;ADDRESS OF RAM-ADDRESS COUNTER
SIGDAT=167764           ;ADDRESS OF SIGNAL-RAM DATA PORT
;
FHALT=040000            ;DEFINE HALT CONTROL WORD
ZERO=000000             ;DEFINE ZERO
FLEVEN=000013           ;DEFINE LAST RAM ADDRESS
FEBUFF=177757           ;DEFINE COMPLEMENT OF FILTERED ERROR BUFFER ADDRESS
MASK1=010000            ;DEFINE MASK FOR HALT BIT
MASK2=004000            ;DEFINE MASK FOR SIGN BIT OF 12-BIT DATA
MASK3=170000            ;DEFINE MASK FOR SIGN EXTENSION
;
AFREAD::MOV #FHALT,@#CNTRL   ;REQUEST FILTER HALT
        MOV (R5)+,R0         ;GET NUMBER OF ARGUMENTS IN MAINPROGRAM CALL
        MOV @(R5)+,R0        ;GET FIRST ARG (CONTROL WORD) FROM MAINPROG.
        MOV (R5)+,R4         ;GET ADDRESS OF 2-ND ARG (1-ST SIGNAL SAMPLE)
        MOV #ZERO,R2         ;INITIALISE A REGISTER TO ADDRESS FILTER RAM
WAIT:   MOV @#SIGDAT,R3      ;READ INPUT DATA
```

```
        BIT #MASK1,R3           ;MASK ALL EXCEPT HALT BIT
        BEQ WAIT               ;JUMP UNLESS FILTER HALTED
        MOV @#SIGDAT,R3        ;CHECK AGAIN
        BIT #MASK1,R3
        BEQ WAIT
LOOP:   MOV R2,R3             ;COPY RAM ADDRESS INTO R3
        COM R3                ;COMPLEMENT FOR CABLE BUFFERS
        MOV R3,@#ADDCNT       ;ADDRESS THE R2'TH RAM LOCATION
        MOV @#SIGDAT,R3       ;READ SIGNAL SAMPLE FROM R2-TH SIGNAL RAM LOC.
        JSR PC,SIGNEX         ;SIGN EXTEND 12 BITS OF R3 TO 16 BITS
        MOV R3,(R4)+          ;WRITE SIGNAL SAMPLE INTO M/C MEMORY
        INC R2                ;NEXT RAM ADDRESS
        CMP #ELEVEN,R2        ;RAM ADDRESS GREATER THAN 11?
        BPL LOOP              ;JUMP IF 11-TH LOC NOT YET ADDRESSED
        MOV #FEBUFF,@#ADDCNT  ;ADDRESS FILTERED ERROR SIGNAL BUFFER
        MOV @#SIGDAT,R3       ;READ FILTERED ERROR SIGNAL
        COM R3                ;NO RAM INVERSION TO BE ALLOWED FOR
        JSR PC,SIGNEX         ;SIGN EXTEND
        MOV R3,(R4)+          ;STORE IN M/C MEMORY
        MOV #ZERO,R3          ;
        COM R3                ;
        MOV R3,@#ADDCNT       ;CLEAR ADDRESS COUNTER
        MOV R0,@#CNTRL        ;OUTPUT FIRST ARG (CONTROL WORD) FROM MAINPROG
                             ;TO CONTROL PORT
        RTS PC
;
SIGNEX: COM R3                ;COMPLEMENT SIGNAL SAMPLE
        BIT #MASK2,R3         ;MASK ALL EXCEPT SIGN BIT
        BEQ POS              ;JUMP IF SIGN BIT CLEAR
        BIS #MASK3,R3        ;SET MS 4 BITS
        RTS PC              ;RETURN
POS:    BIC #MASK3,R3        ;CLEAR MS 4 BITS
        RTS PC              ;RETURN
;
        .END AFREAD
```

```
C-------------------------------------------------------------------------
C
C PROGRAM ADHYB TESTS THE PERFORMANCE OF DIGITAL RECURSIVE ADAPTIVE
C FILTERS AGAINST SIMULATED SUBSCRIBERS LINES.
C
C-------------------------------------------------------------------------
C
      REAL WIND(129),TYP(16),FL(257),RES(129),RESC(129)
      INTEGER ICOEFF(257),L(16),LENGTH
      COMPLEX ZL(257),ZT(257),ZB(257),Z1,Z2,ZI(257),GMA(257),ZO(257)
     1,TC,TCC
      COMMON/DATLHS/LHS(129)
      COMMON/AFDATA/IAF(12),IAFDAT(13),NDEL,ICOMP
C LHS CONTAINS THE COEFFICIENTS OF THE LHS, IAF CONTAINS THE
C COEFFICIENTS OF THE ADAPTIVE FILTER, IAFDAT CONTAINS THE
C SAMPLES OF DATA FROM THE FILTER IN THE ORDER:-
C
C X(N),X(N-1),X(N-2),X(N-3), D(N),D(N-1),D(N-2),D(N-3),
C E(N-1),E(N-2),E(N-3),E(N-4), E'(N-1)
C
C NDEL CONTROLS THE LENGTH OF THE DELAY INTRODUCED BY MACRO SDEL,
C AND ICOMP IS 1 FOR COMPENSATION FOR THE EFFECTS OF ERROR
C FILTERING.
      TYPE 510
  510 FORMAT(/,'   **** DIGITAL ADAPTIVE HYBRID PERFORMANCE  **** ',/)
C     NPTS IS THE NUMBER OF FREQUENCY POINTS USED TO REPRSENT THE TRANS-
C     HYBRID SPECTRUM IN THE RANGE 0 TO HALF THE SAMPLING FREQUENCY.
      NPTS=129
      NPTS1=NPTS-1
      NPTS2=NPTS1*2
      NPTS3=NPTS2+1
      PI=4.0*ATAN(1.0)
      PI2=8.0*ATAN(1.0)
      SCANG=PI2/360.
      TZ=PI2/FLOAT(NPTS2)
C     FS IS THE SAMPLING FREQUENCY, FINC IS THE FREQUENCY RESOLUTION
      FS=16000.
      FINC=FS/FLOAT(NPTS2)
      WINC=PI2*FINC
      SC=8000./FS
      NF=INT((NPTS1*SC)+1.5)
      NDF=INT((250.0/FINC)+0.5)
      IRECSZ=NPTS*4
      CALL ASSIGN (1,'DY1:ZOGMA.DAT',15,'RDO')
      DEFINE FILE 1(35,IRECSZ,U,IREC1)
      CALL ASSIGN (3,'DY1:HYB.DAT',13,'RDO')
      DEFINE FILE 3(3,IRECSZ,U,IREC3)
C     READ THE HYBRID ZT AND ZB
      READ(3'1)HYBNO
      READ(3'2)(ZT(I),I=1,NPTS)
      READ(3'3)(ZB(I),I=1,NPTS)
      CLOSE (UNIT=3)
      MAXREC=1850
      IRECSZ=36
C FILE LDAT CONTAINS THE LINE SURVEY DATA BASE
      CALL ASSIGN (2,'DY1:LDAT.DAT',14,'RDO')
```

```
C------------------------------------------------------------------
C
C PROGRAM ADHYB TESTS THE PERFORMANCE OF DIGITAL RECURSIVE ADAPTIVE
C FILTERS AGAINST SIMULATED SUBSCRIBERS LINES.
C
C------------------------------------------------------------------
C
      REAL WIND(129),TYP(16),FL(257),RES(129),RESC(129)
      INTEGER ICOEFF(257),L(16),LENGTH
      COMPLEX ZL(257),ZT(257),ZB(257),Z1,Z2,ZI(257),GMA(257),ZO(257)
     1,TC,TCC
      COMMON/DATLHS/LHS(129)
      COMMON/AFDATA/IAF(12),IAFDAT(13),NDEL,ICOMP
C LHS CONTAINS THE COEFFICIENTS OF THE LHS, IAF CONTAINS THE
C COEFFICIENTS OF THE ADAPTIVE FILTER, IAFDAT CONTAINS THE
C SAMPLES OF DATA FROM THE FILTER IN THE ORDER:-
C
C X(N),X(N-1),X(N-2),X(N-3), D(N),D(N-1),D(N-2),D(N-3),
C E(N-1),E(N-2),E(N-3),E(N-4), E'(N-1)
C
C NDEL CONTROLS THE LENGTH OF THE DELAY INTRODUCED BY MACRO SDEL,
C AND ICOMP IS 1 FOR COMPENSATION FOR THE EFFECTS OF ERROR
C FILTERING.
      TYPE 510
  510 FORMAT(/,'    **** DIGITAL ADAPTIVE HYBRID PERFORMANCE  **** ',/)
C     NPTS IS THE NUMBER OF FREQUENCY POINTS USED TO REPRSENT THE TRANS-
C     HYBRID SPECTRUM IN THE RANGE 0 TO HALF THE SAMPLING FREQUENCY.
      NPTS=129
      NPTS1=NPTS-1
      NPTS2=NPTS1*2
      NPTS3=NPTS2+1
      PI=4.0*ATAN(1.0)
      PI2=8.0*ATAN(1.0)
      SCANG=PI2/360.
      T2=PI2/FLOAT(NPTS2)
C     FS IS THE SAMPLING FREQUENCY, FINC IS THE FREQUENCY RESOLUTION
      FS=16000.
      FINC=FS/FLOAT(NPTS2)
      WINC=PI2*FINC
      SC=8000./FS
      NF=INT((NPTS1*SC)+1.5)
      NDF=INT((250.0/FINC)+0.5)
      IRECSZ=NPTS*4
      CALL ASSIGN (1,'DY1:ZOGMA.DAT',15,'RDO')
      DEFINE FILE 1(35,IRECSZ,U,IREC1)
      CALL ASSIGN (3,'DY1:HYB.DAT',13,'RDO')
      DEFINE FILE 3(3,IRECSZ,U,IREC3)
C     READ THE HYBRID ZT AND ZB
      READ(3'1)HYBNO
      READ(3'2)(ZT(I),I=1,NPTS)
      READ(3'3)(ZB(I),I=1,NPTS)
      CLOSE (UNIT=3)
      MAXREC=1850
      IRECSZ=36
C FILE LDAT CONTAINS THE LINE SURVEY DATA BASE
      CALL ASSIGN (2,'DY1:LDAT.DAT',14,'RDO')
```

```
                DEFINE FILE 2(MAXREC,IRECSZ,U,IRECS2)
                IRECSZ=20
                DEFINE FILE 3(MAXREC,IRECSZ,U,IREC3)
C       READ THE DEFAULT LOAD IMPEDANCE
                CALL ASSIGN(4,'DY1:ZTELE.LST',15,'RDO')
                READ(4,*)TELENO
                READ(4,220)(ZL(I),I=1,NPTS)
         220 FORMAT(4(E13.6))
                CLOSE (UNIT=4)
C       CALCULATE WINDOW RESPONSE UP TO FS/2
                DO 5 IPT=1,NPTS
                V=FLOAT(IPT-1)*T2
                WIND(IPT)=0.54+0.46*COS(V)
           5  CONTINUE
C
C
C
C SET THE STEP SIZES FOR THE ADAPTION ALGORITHM
                FL1=1024.
                FL2=FL1
                GL1=1.0/FL1
                GL2=1.0/FL2
C RETURN LOSSES ARE CALCULATED OVER NBLKS BLOCKS OF 4 SAMPLES,
C NITER IS THE NUMBER OF ITERATIONS AFTER WHICH THE CANCELLED ERL
C IS MEASURED. NA IS THE NUMBER OF TRANSVERSAL COEFFICIENTS,
C NB IS THE NUMBER OF RECURSIVE COEFFICIENTS
                NBLKS=100
                NDEL=100
                NITER=500
                NA=4
                NB=0
C NAVG IS THE NUMBER OF ITERATIONS OVER WHICH MEASUREMENTS ARE
C AVERAGED, AND AN INITIAL MEASUREMENT IS MADE AFTER NINIT
C ITERATIONS.
                NAVG=50
                NINIT=100
                WRITE(5,370)
         370 FORMAT(' INPUT STARTING LINENO AND FINISHING LINENO')
                READ(2,*)NLINS,NLINF
                NLINES=NLINF+1-NLINS
                MAXREC=1850
                IRECSZ=18
                DEFINE FILE IFILE(MAXREC,IRECSZ,U,IREC4)
                WRITE(IFILE'1)FL1,FL2,NA,NB
             1,NBLKS,NAVG,NINIT,NITER,NDEL
                WRITE(IFILE'2)NLINES
C
C
C
                LIND=3-NLINS
                DO 190 LINE = NLINS,NLINF
                DO 35 IPT=1,NPTS
                ZI(IPT)=ZL(IPT)
          35  CONTINUE
                READ(2'LINE)LINO,RD,(FL(I),I=1,16)
```

```
   70 FORMAT(/,' LINE ',I4,/,' LINE NUMBER = ',I4,/)
      TYPE 70,LINE,LINO
C      PRINT 80
   80 FORMAT(' LENGTH      TYPE ')
      TYPE 80
      LENGTH=0
      DO 130 ISEC = 1,16
      L(ISEC)=IFIX(FL(ISEC))
      TYP(ISEC)=FL(ISEC)-L(ISEC)
      IF(L(ISEC).LE.0.0)GO TO 140
      LENGTH=LENGTH+L(ISEC)
C      PRINT 75,L(ISEC),TYP(ISEC)
   75 FORMAT(I6,5X,F5.2)
      TYPE 75,L(ISEC),TYP(ISEC)
C      LOOK UP ZO AND GMA
  100 IF(TYP(ISEC).GE.0.1075.AND.TYP(ISEC).LE.0.11)N=2
      IF(TYP(ISEC).GE.0.1175.AND.TYP(ISEC).LE.0.12)N=4
      IF(TYP(ISEC).GE.0.1675.AND.TYP(ISEC).LE.0.17)N=6
      IF(TYP(ISEC).GE.0.2075.AND.TYP(ISEC).LE.0.21)N=8
      IF(TYP(ISEC).GE.0.2475.AND.TYP(ISEC).LE.0.25)N=10
      IF(TYP(ISEC).GE.0.3075.AND.TYP(ISEC).LE.0.31)N=12
      IF(TYP(ISEC).GE.0.3175.AND.TYP(ISEC).LE.0.32)N=14
      IF(TYP(ISEC).GE.0.3975.AND.TYP(ISEC).LE.0.4)N=16
      IF(TYP(ISEC).GE.0.4075.AND.TYP(ISEC).LE.0.41)N=18
      IF(TYP(ISEC).GE.0.4975.AND.TYP(ISEC).LE.0.5)N=20
      IF(TYP(ISEC).GE.0.5075.AND.TYP(ISEC).LE.0.51)N=22
      IF(TYP(ISEC).GE.0.6075.AND.TYP(ISEC).LE.0.61)N=24
      IF(TYP(ISEC).GE.0.6275.AND.TYP(ISEC).LE.0.63)N=26
      IF(TYP(ISEC).GE.0.8075.AND.TYP(ISEC).LE.0.81)N=28
      IF(TYP(ISEC).GE.0.8975.AND.TYP(ISEC).LE.0.9)N=30
      IF(TYP(ISEC).GE.0.6975.AND.TYP(ISEC).LE.0.7)N=32
      IF(TYP(ISEC).GE.0.7375.AND.TYP(ISEC).LE.0.75)N=34
      READ(1'N)(GMA(I),I=1,NPTS)
      READ(1'N+1)(ZO(I),I=1,NPTS)
C      COMPUTE SENDING END IMPEDANCE
      DO 250 IF=1,NPTS
      GMA(IF)=GMA(IF)*L(ISEC)
      TCC=CMPLX(AIMAG(GMA(IF)),-REAL(GMA(IF)))
      TC=CSIN(TCC)/CCOS(TCC)
      TCC=CMPLX(-AIMAG(TC),REAL(TC))
      ZI(IF)=(ZI(IF)+ZO(IF)*TCC)/(CMPLX(1.0,0.0)+ZI(IF)*TCC/ZO(IF))
  250 CONTINUE
C      SENDING END IMPEDANCE BECOMES RECEIVING END IMPEDANCE FOR NEXT SECTION
  130 CONTINUE
  140 TYPE 200,LENGTH
  200 FORMAT(/,' LINE LENGTH = ',I7,' METRES')
C      ZI IS NOW THE IMPEDANCE PRESENTED TO THE HYBRID BY THE COMBINATION
C      OF SUBSCRIBERS APPARATUS AND LINE
C
C
C
C      COMPUTE THE TRANS-HYBRID FREQUENCY RESPONSE
C
      DO 170 IF=1,NPTS
      ZI(IF)=(ZB(IF)/(ZB(IF)+ZT(IF)))-(ZI(IF)/(ZI(IF)+ZT(IF)))
      ZI(IF)=ZI(IF)*CMPLX(2.0,0.0)
```

```
C      WINDOW THE RESPONSE USING HAMMING WINDOW
       ZI(IF)=ZI(IF)*WIND(IF)
  170 CONTINUE
       T=PI/FLOAT(NPTS2)
C      COMPUTE THE TRANS-HYBRID RESPONSE IN DB
C       CALL RESP(ZI,RES,RESC,T,NPTS)
C
C      MIRROR THE RESPONSE ABOUT FS/2 FOR REAL IMPULSE RESPONSE
C
       DO 450 I=1,NPTS1-1
  450 ZI(NPTS3-I)=CMPLX(REAL(ZI(I+1)),-AIMAG(ZI(I+1)))
       ZI(NPTS)=CMPLX(REAL(ZI(NPTS)),0.0)
C      COMPUTE ECHO-RETURN-LOSS (ERL) AND STABILITY-RETURN-LOSS (SRL)
C       CALL EVAL(RES,FINC,NPTS,ERL,SRL)
C
C      COMPUTE TRANS-HYBRID IMPULSE RESPONSE
C
       CALL FFT(ZI,NPTS2,1,FL)
C      SHIFT IMPULSE RESPONSE TO ACCOUNT FOR WIDTH OF MAIN LOBE OF WINDOW
C      IN TIME DOMAIN
       DO 270 I=1,NPTS
       J=I-1
       IF(J.LT.1)J=J+NPTS2
       ICOEFF(I)=INT(FL(J)*2047.)
  270 CONTINUE
C      CALL MACRO-11 ROUTINE TO LOAD LHS COEFFICIENTS
       CALL LOAD(0,ICOEFF(1))
C
C
C
C INITIALISE THE ADAPTIVE FILTER
       DO 300 J=1,12
       IAF(J)=0
  300 CONTINUE
       IAF(5)=-2048
C ALLOW FILTER TO ADAPT INITIALLY FOR NINIT ITERATIONS
       DO 310 ITER=1,NINIT
C WRITE COEFFICIENTS TO FILTER
       CALL AFWRIT(0,IAF(1))
       CALL SDELAY(NDEL)
C READ SIGNAL SAMPLES FROM THE FILTER
       CALL AFREAD(0,IAFDAT(1))
C CALCULATE NEW COEFFICIENTS USING LINEAR ALGORITHM
       CALL ADLIN1(GL1,GL2,NA,NB)
  310 CONTINUE
C CALCULATE RETURN LOSSES; OERL=ORIGINAL ERL, FERL = CANCELLED
C ERL, ERLE1 = INITIAL ERLE
       CALL AFRLOS(OERL,FERL,ERLE1,NBLKS)
       WRITE(5,380)NINIT,ERLE1
  380 FORMAT(' ERLE AFTER',I4,' ITERATIONS IS ',F6.1,' DB')
C FINISH ADAPTION
       DO 320 ITER=NINIT+1,NITER
       CALL AFWRIT(0,IAF(1))
       CALL SDELAY(NDEL)
       CALL AFREAD(0,IAFDAT(1))
       CALL ADLIN1(GL1,GL2,NA,NB)
```

```fortran
  320 CONTINUE
C INITIALISE VARIABLES TO MEASURE AVERAGE RETURN LOSSES AND
C COEFFICIENTS OVER NAVG ITERATIONS
      ERLE2=0.0
      OERL=0.0
      FERL=0.0
      A0=0.0
      A1=0.0
      B1=0.0
      A3=0.0
      DO 330 IAVG=1,NAVG
      CALL AFWRIT(0,IAF(1))
      CALL SDELAY(NDEL)
      CALL AFREAD(0,IAFDAT(1))
      CALL ADLIN1(GL1,GL2,NA,NB)
      A0=A0+FLOAT(IAF(1))
      A1=A1+FLOAT(IAF(2))
      B1=B1+FLOAT(IAF(3))
      A3=A3+FLOAT(IAF(4))
      CALL SDELAY(NDEL)
      CALL AFRLOS(A,B,C,NBLKS)
      OERL=OERL+A
      FERL=FERL+B
      ERLE2=ERLE2+C
      CALL SDELAY(NDEL)
  330 CONTINUE
      FAVG=FLOAT(NAVG)
      A0=A0/FAVG
      A1=A1/FAVG
      B1=B1/FAVG
      A3=A3/FAVG
      OERL=OERL/FAVG
      FERL=FERL/FAVG
      ERLE2=ERLE2/FAVG
      WRITE(5,390)OERL,FERL,ERLE2
  390 FORMAT(' OERL : ',F6.1,/,' FERL : ',F6.1,/,' ERLE : ',F6.1)
C STORE RESULTS FOR SUBSEQUENT PROCESSING
      WRITE(IFILE'LINE+LIND)LINO,LENGTH,OERL,FERL,ERLE1,ERLE2
     1,A0,A1,B1,A3
  190 CONTINUE
C     GO TO 296
      STOP'RIGHT, THATS IT, IVE HAD ENOUGH '
      END
C
C
C
C
C
C
C     THIS SUBROUTINE EVALUATES ERL AND SRL AND RETURNS THEM IN ARGUMENTS
C     B AND C RESPECTIVELY.
C
      SUBROUTINE EVAL(A,FINC,N,B,C)
      REAL A(N)
C     COMPUTE THE SAMPLE NUMBERS CORRESPONDING TO 300 HZ, 500 HZ, ETC
      IF1=INT(300./FINC)+1
```

```
      IF2=INT(500./FINC)+1
      IF3=INT(2500./FINC)+1
      IF4=INT(3400./FINC)+1
C     FIND THE MINIMUM LOSS OVER THE RANGE 300 TO 3400 HZ
      C=A(IF1)
      DO 10 I=IF1,IF4
      IF(A(I).GT.C)C=A(I)
   10 CONTINUE
      C=-C
C     COMPUTE THE AVERAGE LOSS OVER THE RANGE 500 TO 2500 HZ
      B=0.0
      DO 20 I=IF2,IF3
      B=B+A(I)
   20 CONTINUE
      B=-B/FLOAT(IF3-IF2+1)
      RETURN
      END
C
C
C
C
C
C
C
C     THIS SUBROUTINE COMPUTES THE FFT OR INVERSE FFT USING RADIX 2
C     DECIMATION IN TIME ALGORITHIM
C
      SUBROUTINE FFT(DATA,N,ISI,RESULT)
      COMPLEX DATA(N),TEMP,W,CN
      REAL RESULT(N)
      PI=4.0*ATAN(1.0)
      FN=N
      J=1
      DO 80 I=1,N
      IF(I-J)30,40,40
   30 TEMP=DATA(J)
      DATA(J)=DATA(I)
      DATA(I)=TEMP
   40 M=N/2
   50 IF(J-M)70,70,60
   60 J=J-M
      M=(M+1)/2
      GO TO 50
   70 J=J+M
   80 CONTINUE
      MMAX=1
   90 IF(MMAX-N)100,130,130
  100 ISTEP=2*MMAX
      DO 120 M=1,MMAX
      THETA=PI*FLOAT(ISI*(M-1))/FLOAT(MMAX)
      W=CMPLX(COS(THETA),SIN(THETA))
      DO 110 I=M,N,ISTEP
      J=MMAX+I
      TEMP=W*DATA(J)
      DATA(J)=DATA(I)-TEMP
      DATA(I)=DATA(I)+TEMP
  110 CONTINUE
```

```
      IF2=INT(500./FINC)+1
      IF3=INT(2500./FINC)+1
      IF4=INT(3400./FINC)+1
C     FIND THE MINIMUM LOSS OVER THE RANGE 300 TO 3400 HZ
      C=A(IF1)
      DO 10 I=IF1,IF4
      IF(A(I).GT.C)C=A(I)
   10 CONTINUE
      C=-C
C     COMPUTE THE AVERAGE LOSS OVER THE RANGE 500 TO 2500 HZ
      B=0.0
      DO 20 I=IF2,IF3
      B=B+A(I)
   20 CONTINUE
      B=-B/FLOAT(IF3-IF2+1)
      RETURN
      END
C
C
C
C
C
C
C
C     THIS SUBROUTINE COMPUTES THE FFT OR INVERSE FFT USING RADIX 2
C     DECIMATION IN TIME ALGORITHIM
C
      SUBROUTINE FFT(DATA,N,ISI,RESULT)
      COMPLEX DATA(N),TEMP,W,CN
      REAL RESULT(N)
      PI=4.0*ATAN(1.0)
      FN=N
      J=1
      DO 80 I=1,N
      IF(I-J)30,40,40
   30 TEMP=DATA(J)
      DATA(J)=DATA(I)
      DATA(I)=TEMP
   40 M=N/2
   50 IF(J-M)70,70,60
   60 J=J-M
      M=(M+1)/2
      GO TO 50
   70 J=J+M
   80 CONTINUE
      MMAX=1
   90 IF(MMAX-N)100,130,130
  100 ISTEP=2*MMAX
      DO 120 M=1,MMAX
      THETA=PI*FLOAT(ISI*(M-1))/FLOAT(MMAX)
      W=CMPLX(COS(THETA),SIN(THETA))
      DO 110 I=M,N,ISTEP
      J=MMAX+I
      TEMP=W*DATA(J)
      DATA(J)=DATA(I)-TEMP
      DATA(I)=DATA(I)+TEMP
  110 CONTINUE
```

```
    120 CONTINUE
        MMAX=ISTEP
        GO TO 90
    130 IF(ISI)160,140,140
C       INVERSE TRANSFORM : ASSUME THE TIME SERIES IS REAL
    140 DO 150 I=1,N
        RESULT(I)=REAL(DATA(I))/FN
    150 CONTINUE
    160 CONTINUE
        RETURN
        END
C
C--------------------------------------------------------------
C
C SUBROUTINE ADLIN1 IMPLEMENTS THE LINEAR STEEPEST DESCENT
C ALGORITHM AND UPDATES THE FILTER COEFFICIENTS. IF ICOMP = 1
C THEN THE ERROR FILTERING COMPENSATION COEFFICIENTS ARE
C ALSO UPDATED.
C
C--------------------------------------------------------------
C
        SUBROUTINE ADLIN1(GL1,GL2,NA,NB)
        COMMON/AFDATA/IAF(12),IAFDAT(13),NDEL,ICOMP
C LOOP FOR TRANSVERSAL COEFFICIENTS
        DO 10 IA=1,NA
        T1=IAF(IA)
        DEL=GL1*IAFDAT(IA)*IAFDAT(13)
        T1=T1+DEL
        IF(T1.GT.2047.)T1=2047.
        IF(T1.LT.-2048.)T1=-2048.
        IAF(IA)=INT(T1)
     10 CONTINUE
        IF(NB.LE.0)RETURN
C LOOP FOR RECURSIVE COEFFICIENTS
        DO 20 IB=1,NB
        T1=IAF(IB+5)
        DEL=GL2*IAFDAT(IB+5)*IAFDAT(13)
        T1=T1+DEL
        IF(T1.GT.2047.)T1=2047.
        IF(T1.LT.-2048.)T1=-2048.
        N1=INT(T1)
        IAF(IB+5)=N1
        IF(ICOMP.NE.1)GO TO 20
        IAF(IB+8)=-N1
     20 CONTINUE
        RETURN
        END
C
C--------------------------------------------------------------
C
C SUBROUTINE ADSGN1 IMPLEMENTS THE STEEPEST DESCENT
C ALGORITHM  USING ONLY THE SIGN BIT OF THE SIGNAL,
C AND UPDATES THE FILTER COEFFICIENTS. IF ICOMP = 1
C THEN THE ERROR FILTERING COMPENSATION COEFFICIENTS ARE
C ALSO UPDATED.
C
```

```
C----------------------------------------------------------
C
      SUBROUTINE ADSGN1(GL1,GL2,NA,NB)
      COMMON/AFDATA/IAF(12),IAFDAT(13),NDEL,ICOMP
      Q1=1024.*GL1
      Q2=1024.*GL2
C LOOP FOR TRANSVERSAL COEFFICIENTS
      DO 10 IA=1,NA
      T1=IAF(IA)
      DEL=Q1*IAFDAT(13)*ISIGN(1,IAFDAT(IA))
      T1=T1+DEL
      IF(T1.GT.2047.)T1=2047.
      IF(T1.LT.-2048.)T1=-2048.
      IAF(IA)=INT(T1)
   10 CONTINUE
      IF(NB.LE.0)RETURN
C LOOP FOR RECURSIVE COEFFICIENTS
      DO 20 IB=1,NB
      T1=IAF(IB+5)
      DEL=Q2*IAFDAT(13)*ISIGN(1,IAFDAT(IB+5))
      T1=T1+DEL
      IF(T1.GT.2047.)T1=2047.
      IF(T1.LT.-2048.)T1=-2048.
      N1=INT(T1)
      IAF(IB+5)=N1
      IF(ICOMP.NE.1)GO TO 20
      IAF(IB+8)=-N1
   20 CONTINUE
      RETURN
      END
```

APPENDIX 3

CIRCUIT DIAGRAMS

A3.1 Circuit Diagram of the Line and Hybrid Simulator

A3.2 Circuit Diagram of the Single Pole Adaptive Filter

A3.3 Circuit Diagram of the Pole-Zero Adaptive Filter

A3.4 Circuit Diagram of the Experimental Digital Recursive
Adaptive Filter
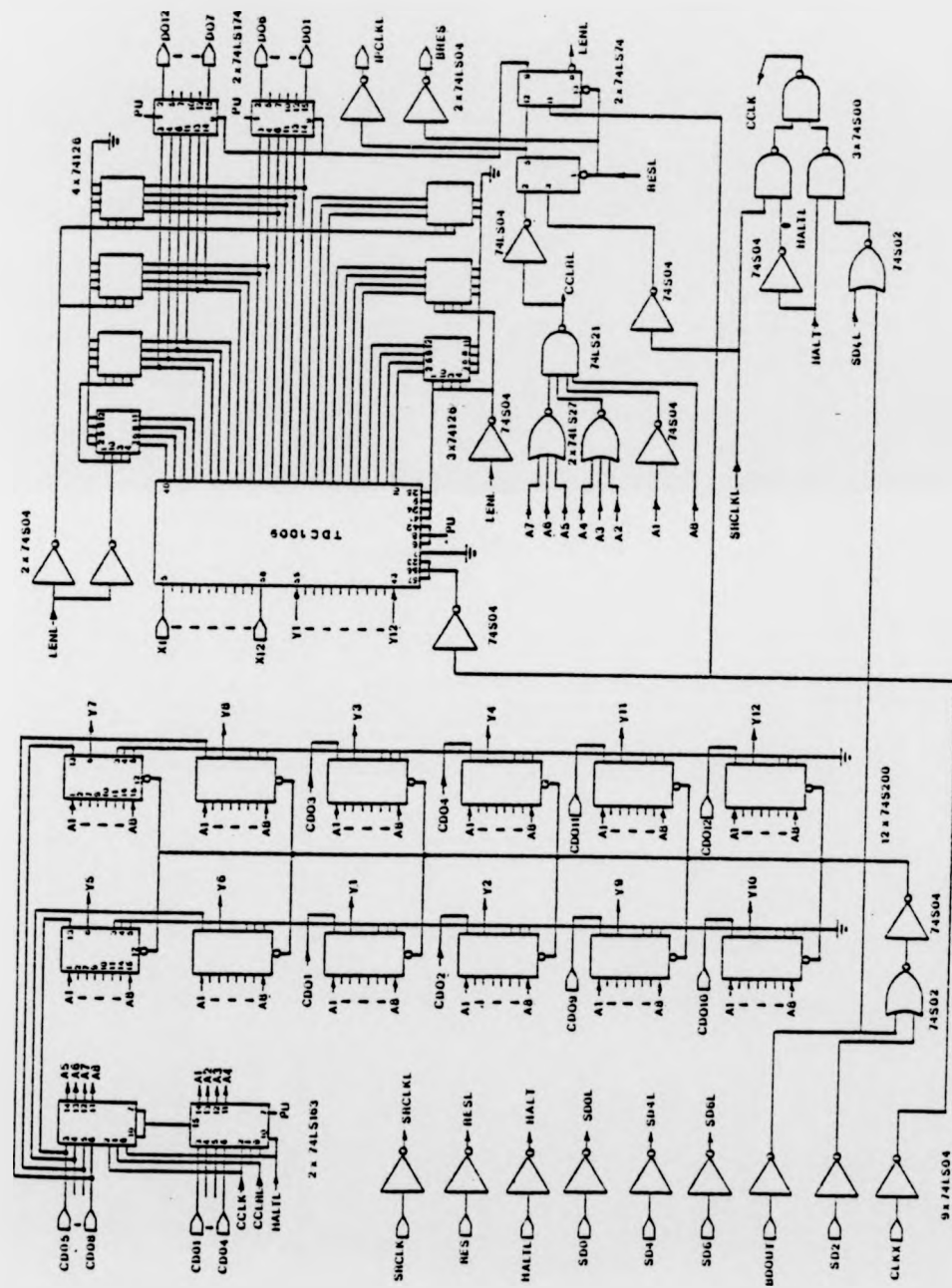
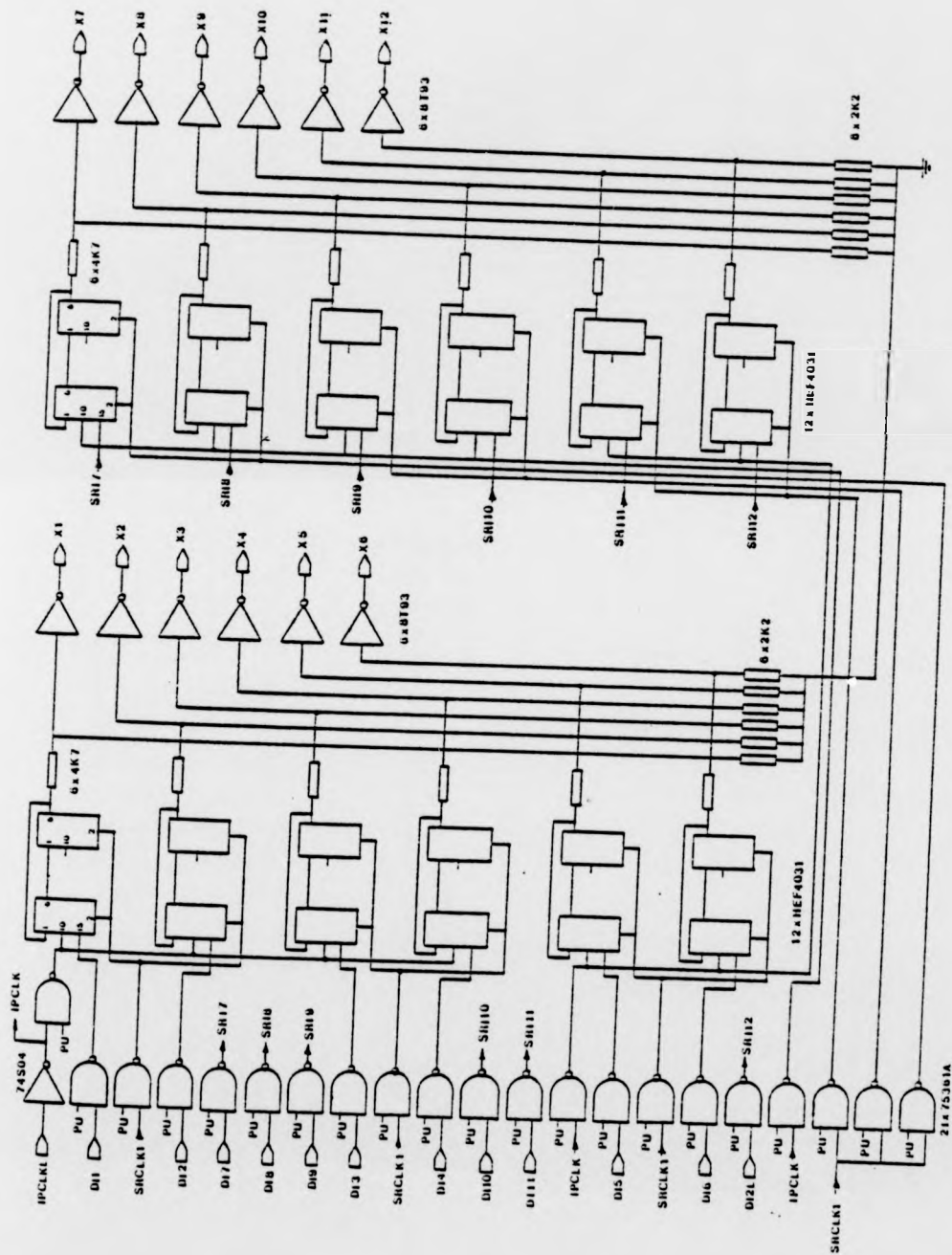Figure A3.1   Circuit Diagram of the Line and Hybrid Simulator
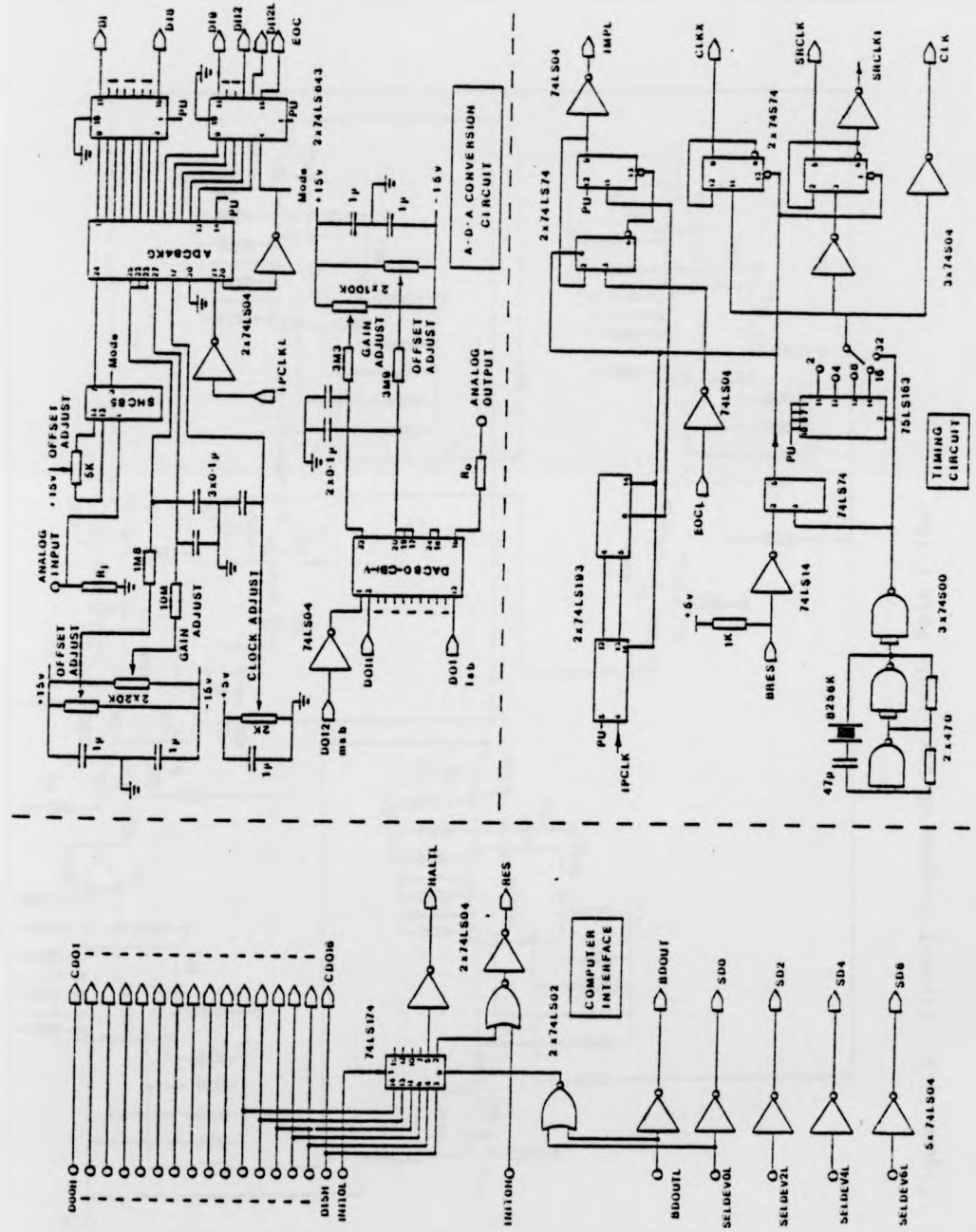
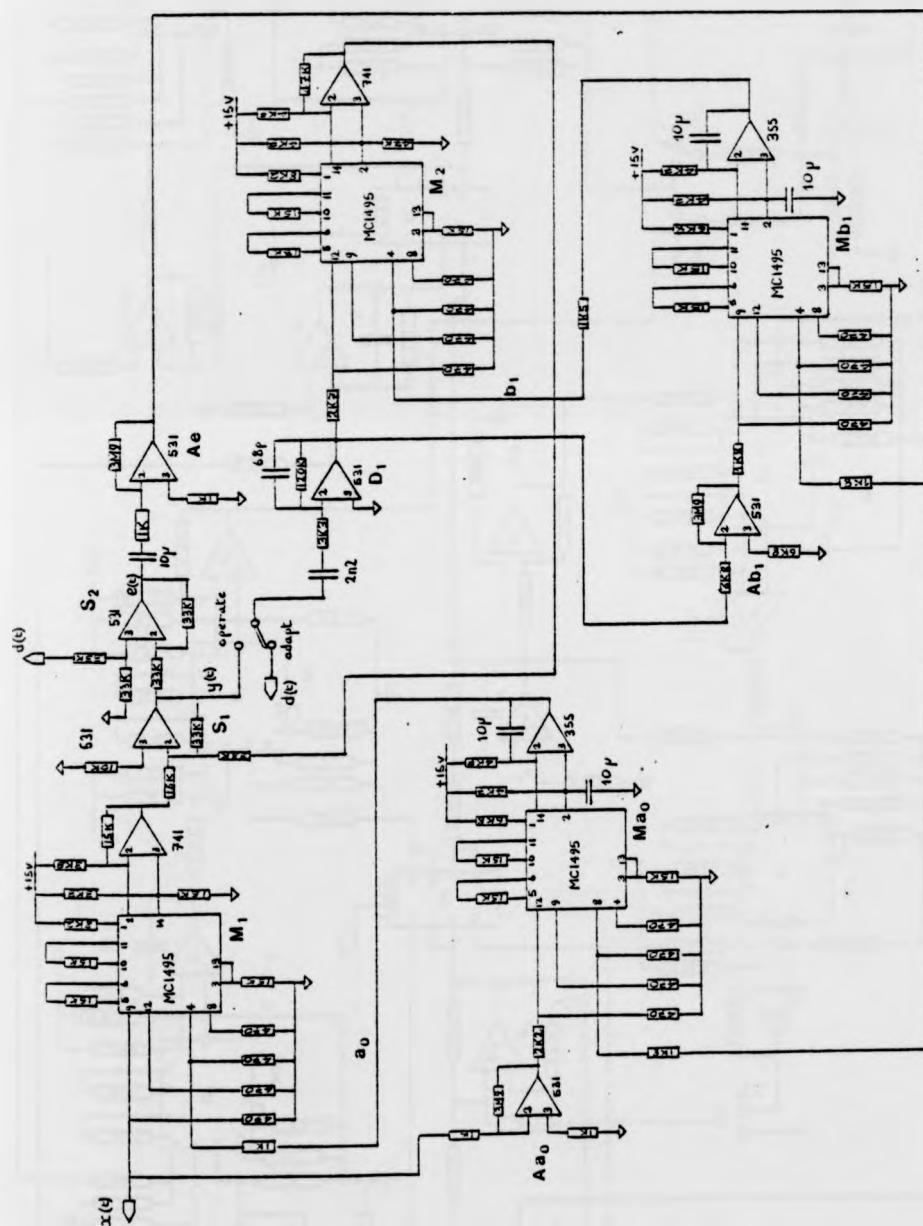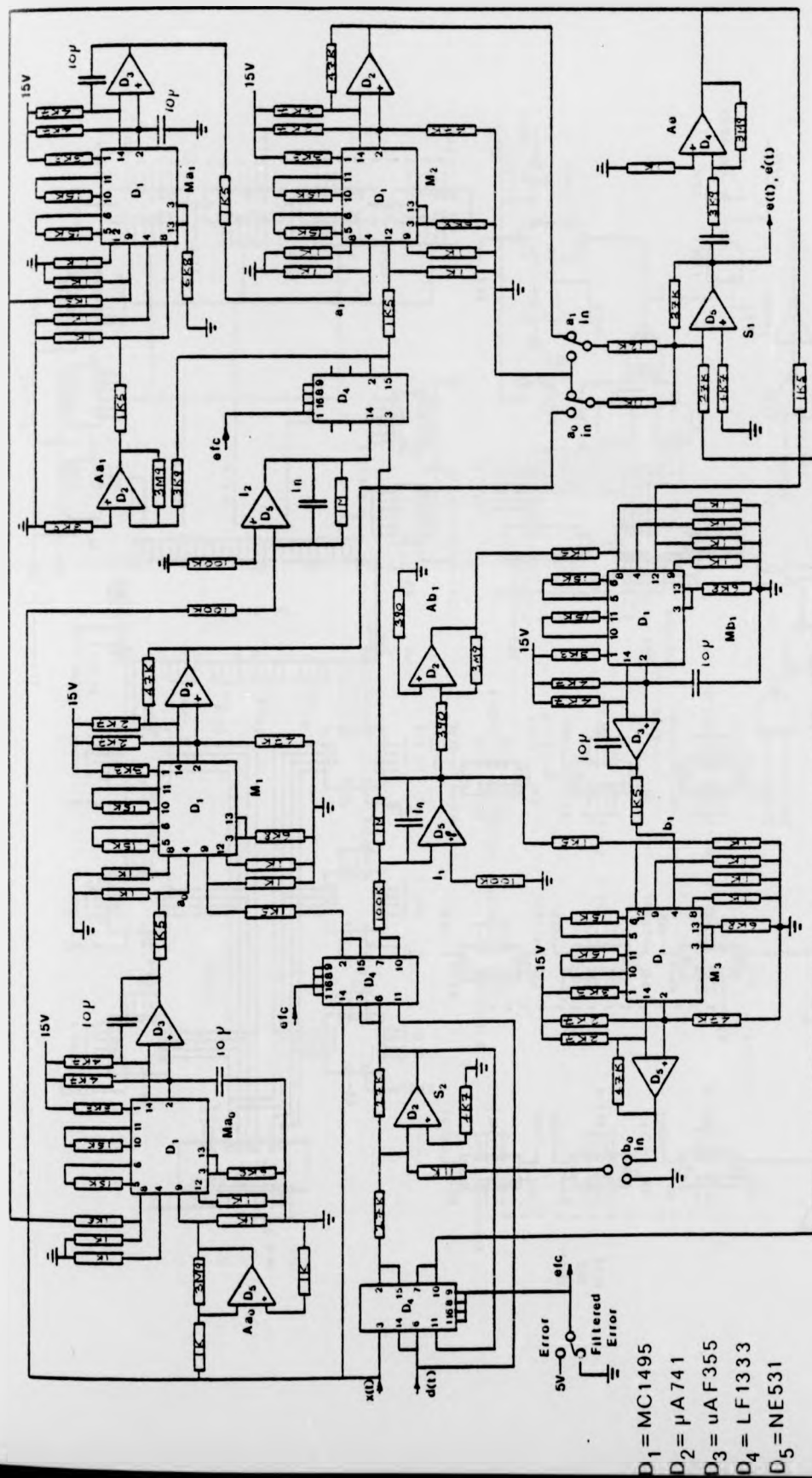Figure A3.1 - continued

Figure A3.1 - continued

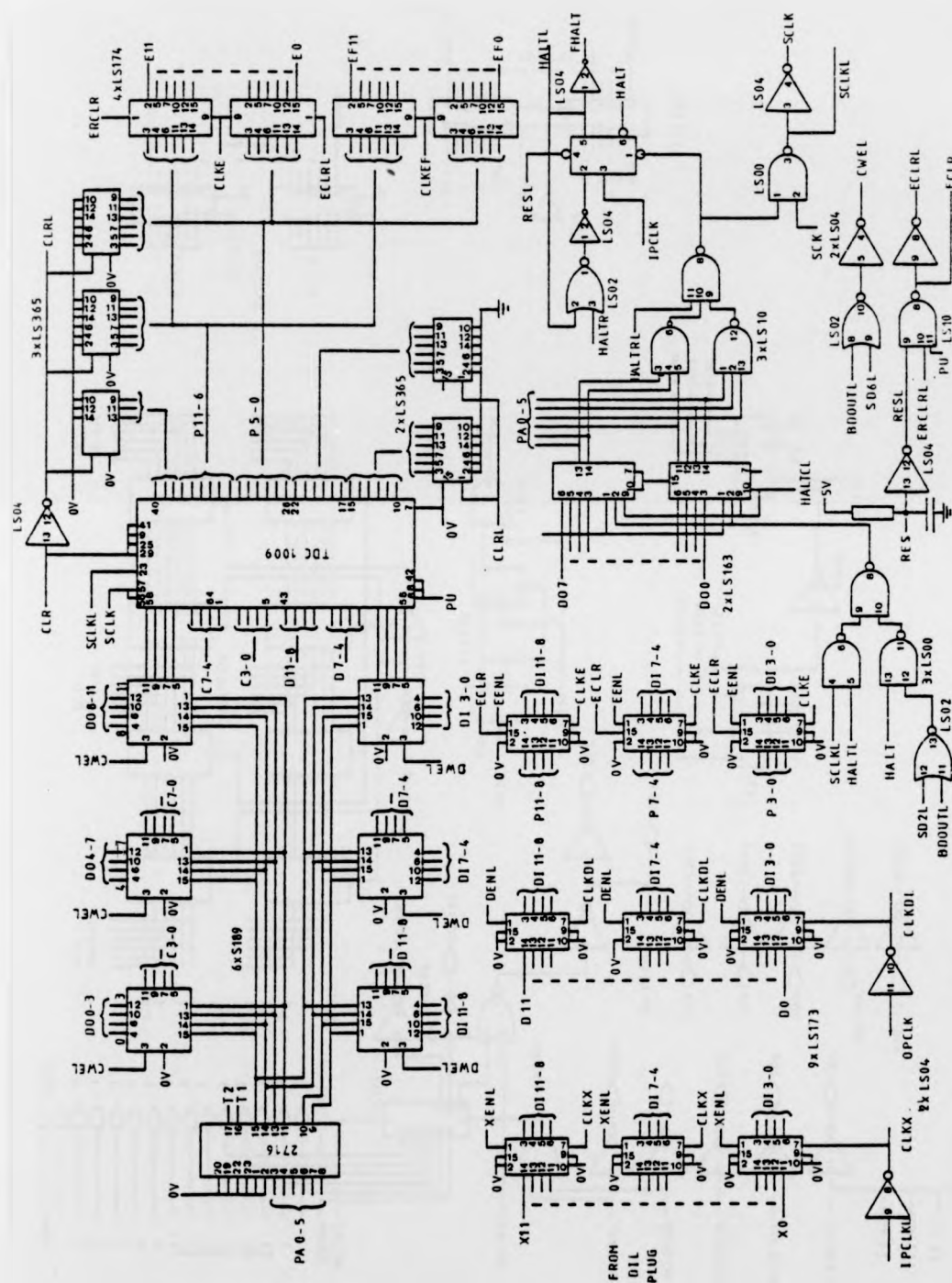Figure A3.2   Circuit Diagram of the Single Pole Filter

Figure A3.3 Circuit Diagram of the Pole-Zero Adaptive Filter

$D_1 = $ MC1495
$D_2 = \mu$A741
$D_3 = $ uAF355
$D_4 = $ LF1333
$D_5 = $ NE531

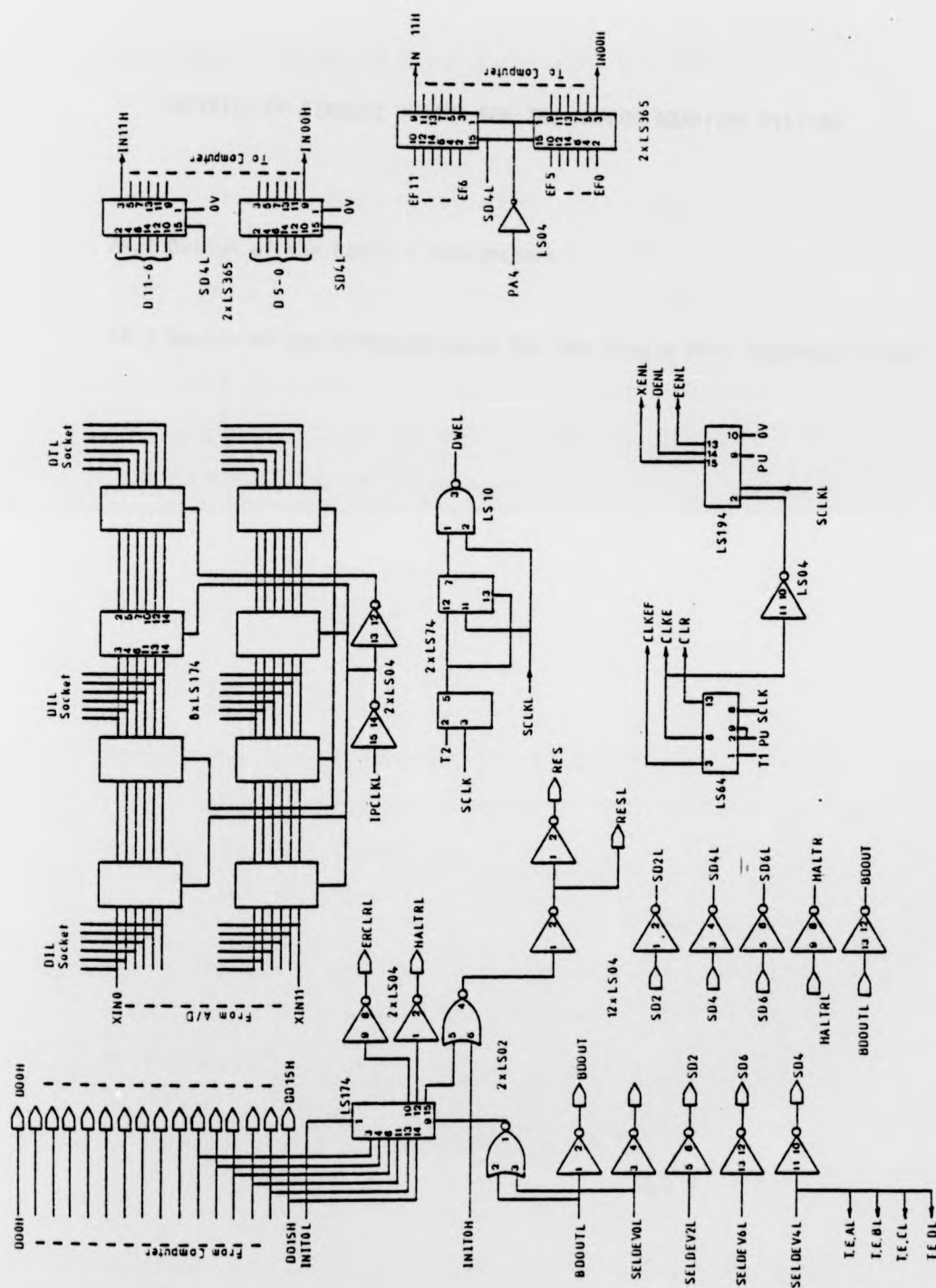Figure A3.4   Circuit Diagram of the Experimental Digital Recursive Adaptive Filter

Figure A3.4 - continued

APPENDIX 4

DETAILS OF CIRCUIT DESIGN FOR THE ANALOG ADAPTIVE FILTERS

A4.1 Design of the Control Integrators

A4.2 Design of the Differentiator for the Single Pole Adaptive Filter

A4.1 Details of the design of the control integrators for the analog adaptive filters

The frequency response of the integrators should be such that a.c. signals at the integrator output are sufficiently rejected, and do not cause harmonic distortion in the error signal. In the following analysis the effect of a given a.c. signal, superimposed on the parameter voltage of an adaptive gain circuit, on the return loss (RL) which can be achieved by the circuit is calculated. Figure A4.1 shows a diagram of the circuit, and the error signal can be written as:-

$$e(t) = \alpha x(t) - (\alpha + r(t))x(t)$$

$$= -r(t)x(t) \qquad\qquad 1$$

and

$$\overline{e^2(t)} = \overline{r^2(t)x^2(t)} \qquad\qquad 2$$

where it has been assumed that the filter has adapted correctly, and $r(t)$ is the a.c. voltage superimposed on the adaptive gain parameter. Equation 2 can be written as:-

$$\overline{e^2(t)} = \overline{x^2(t)}\,\overline{r^2(t)} + 2\,\overline{r(t)x(t)}^2 \qquad\qquad 3$$

$$\text{(Papoulis, 1965)}$$

The second term of equation 3 indicates that the power in the error signal depends on the correlation between $r(t)$ and $x(t)$. The RL can be written as:-

$$RL = \frac{\overline{x^2(t)}}{\overline{e^2(t)}} = \frac{\overline{x^2(t)}}{\overline{x^2(t)}\,\overline{r^2(t)} + 2\,\overline{r(t)x(t)}^2} \qquad\qquad 4$$

In the worst case $x(t)$ and $r(t)$ are perfectly correlated, ie: $r(t) = Ax(t)$, and under these circumstances the RL can be written as:-

$$RL = \frac{1}{3\ \overline{r^2(t)}}$$

5

Thus for 50 dB minimum RL, $\overline{r^2(t)} < 3.3*10^{-7}$. If the input signal is sinusoidal, then the integrator provides least rejection of a.c. signals at the lowest operating frequency (300 Hz). Thus the peak to peak a.c. signal at the integrator output should be less than 1.6 mV at 300 Hz.

Figure A4.2 shows the parameter control integrator, where the output currents of the control multiplier (I_1 and I_2) are applied directly to the inputs of the control integrator. If the operational amplifier is assumed to have a transfer function given by:-

$$H(s) = A/(1+sa)$$

6

then the integrator output can be shown to be:-

$$Vo(s) = \frac{[I_1(s) - I_2(s)]/sc}{1+((1+sa)/A)}$$

7

Thus if the frequency is such that the open loop gain of the amplifier is much greater than 1, then integration is accurate, irrespective of the value of C. The operational amplifier used in the integrator need not therefore have a very large gain-bandwidth product. Assuming:-

$$A/(1+sa) \gg 1$$

8

and using the equation for the transfer function of the multiplier, the output of the integrator is:-

$$v(t) = \frac{\alpha_e \alpha_x 2}{CR_x R_e I_{bias}} \int_0^t v_x(\tau)v_e(\tau)d\tau$$

9

where v_x and v_e are the input signals, α_x and α_e are input attenuators and R_x, R_e and I_{bias} control the scaling factor of the multiplier. The output of the integrator is attenuated by a factor

α_{a0} to form a_0. Thus the combination of multiplier and integrator can be represented by the equivalent circuit shown in Figure A4.3. The magnitude of the effective integrator transfer function is:-

$$\left| \frac{V_0}{V_i} \right| = \frac{\alpha_{a0}\alpha_e\alpha_x 2}{C R_x R_e I_{bias} \omega}$$

10

The values of the attenuators α_{a0}, α_e and α_x are fixed by signal handling considerations in the various amplifiers. The maximum value of I_{bias} is limited by the power dissipation of the multiplier, and the values of R_x and R_e are limited by the maximum signal voltages allowed in the multiplier. Thus the value of C is chosen such that a.c. signals at the output of the integrator are sufficiently rejected. Since the signals at the output of the equivalent circuit of the multiplier are at very high levels, then very high attenuation is required. For example, if the multiplier input signals are 10 V pk to pk, then a value of 10 µF for C gives a maximum pk to pk a.c. voltage of 1 mV at the integrator output.

To calculate O_3, the effective input offset voltage to the integrator, the rate of change of a_0 with respect to time can be written as:-

$$\frac{da_0(t)}{dt} = \frac{\alpha_{a0}I_3}{C}$$

11

where α_{a0} is the value of the attenuator at the output of the integrator, and I_3 is the output offset current of the multiplier. Thus the value of O_3 is:-

$$O_3 = \frac{I_3 R_x R_y I_{bias}}{2\alpha_x \alpha_y}$$

12

For the prototype adaptive gain filter, with maximum and minimum values of I_3, the effective offset voltages at the input to the integrator are 31 V and 154 V respectively. The maximum effective d.c. voltage due to the product at the integrator output is 225 V,

and it can be seen that O_3 can have a large effect on the convergence of the circuit. The effect of O_3 on the final level of RLE which can be achieved is small however, due to the high gain of the amplifier A_e.

A4.2 Details of the design of the differentiator for the single pole adaptive filter

In the block diagram of Figure 5.1 the response of the differentiator was taken to be:-

$$H(s) = -scr \qquad\qquad 13$$

i.e. an ideal differentiator response. In theory this response could be achieved by the use of a resistor, a capacitor, and an operational amplifier. In practice the non-ideal amplifier response causes the circuit to become unstable. This problem can be controlled by introducing two zeros into the open loop transfer function (OLTF) of the differentiator, resulting in the circuit of Figure A4.4. Assuming the response of the operational amplifier to be:-

$$G(s) = A/(1+sa) \qquad\qquad 14$$

then the closed loop transfer function (CLTF) of the circuit is:-

$$H'(s) = -H(s)/\{1 + (1+sa)(1+H(s))/A\} \qquad\qquad 15$$

where,

$$H(s) = \frac{sC_2R_1}{(1+sC_1R_1)(1+sC_2R_2)} \qquad\qquad 16$$

If it is assumed that the open loop gain of the amplifier at the frequencies of interest is much greater than 1, ie:-

$$(1+sa)/A \ll 1 \qquad\qquad 17$$

and further that:-

$$H(s)(1+sa)/A \ll 1 \qquad\qquad 18$$

then the response of the circuit is:-

$$H'(s) = -H(s)$$

If the maximum input frequency is such that the effect of the two compensation poles C_2R_2 and C_1R_1 can be neglected, then the the circuit has the transfer function of the ideal differentiator.

To ensure the stability of the differentiator, the compensating zeros of the OLTF should introduce phase lead before the total phase shift around the loop becomes 180° . The effect of this compensation is that at high frequencies the CLTF of the differentiator produces -90° phase shift. This could produce instability in the loop consisting of the components S1, D1 and M2 (Figure 5.1) if the error filtering were removed, i.e. if the loop were closed via Sw2. This loop will be referred to as the b_1 feedback loop. Removal of error filtering would be necessary once the filter has converged, to prevent near-end speech being effected by the error filtering function. With error filtering removed, any additional phase shift introduced by the operational amplifiers of the b_1 feedback loop could cause oscillation. Since the differentiator is the only element in the loop which requires a high closed loop gain, it contributes most of the phase shift around the loop. To ensure stability of the b_1 feedback loop with error filtering removed, the gain of the loop must be less than unity before significant phase shift is introduced by the differentiator operational amplifier.

The constraints governing the design of the differentiator can be illustrated as shown in Figure A4.5. The transfer function of the adaptive filter, using an ideal differentiator, is:-

$$G(s) = a_0/(1+b_1sC_2R_1) \qquad\qquad 20$$

and assuming b_1 has a maximum value of +1, then the maximum time constant to which the loop can adapt is C_2R_1. This is required to be as large as possible. Similarly the lower of the two pole frequencies, say $1/C_1R_1$, governs the maximum frequency at which

accurate differentiation is possible.   Typically $1/C_1R_1$ should be a decade above the maximum input frequency of the adaptive filter.   The frequency at which the gain of the differentiator should return to unity is determined by the stability requirement for the b_1 feedback loop.   To restrict the phase shift introduced by the the response of the operational amplifier in the differentiator, the maximum gain required of the differentiator should much less than the open loop gain of the amplifier (equation 18).   If a margin of 20 dB is taken as adequate, this requires that the upper unity-gain frequency of the differentiator be a decade below the unity-gain frequency of the open loop operational amplifier.

The restriction on the value of the upper unity-gain frequency thus requires that the maximum time constant to which the loop can adapt be traded off against the maximum input frequency for which good cancellation can be achieved.   In the prototype single pole adaptive filter it was found that an upper unity gain frequency of 2 MHz guaranteed the stability of the b_1 feedback loop, using an externally compensated operational amplifier.   By placing the differentiator compensation poles at 19.5 kHz and 21.9 Khz, the maximum time constant to which the filter can adapt is 264 µS.   This is reduced to 120 µS by attenuation around the b_1 feedback loop.

Figure A4.1: The Effect of a.c. Signals Superimposed on the Adaptive Gain Parameter on the Return Loss
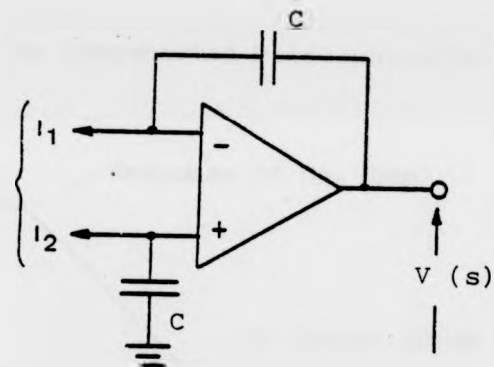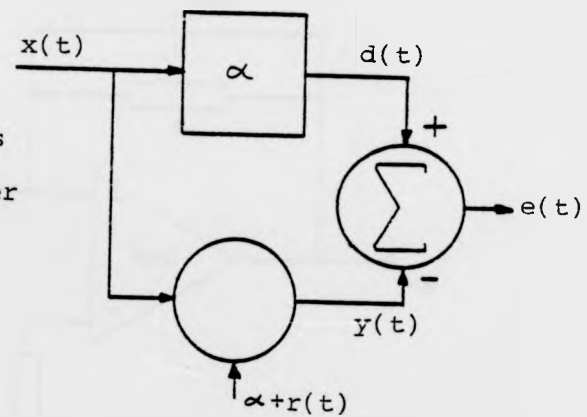
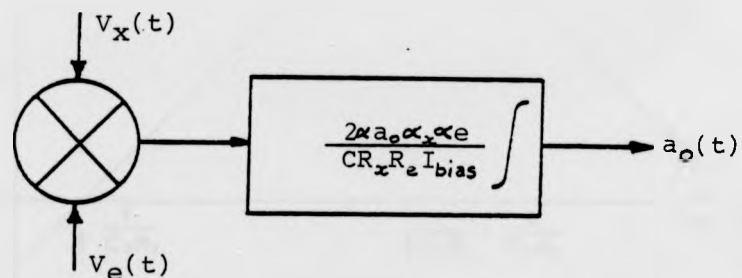

Figure A4.2: The Parameter Control Integrator

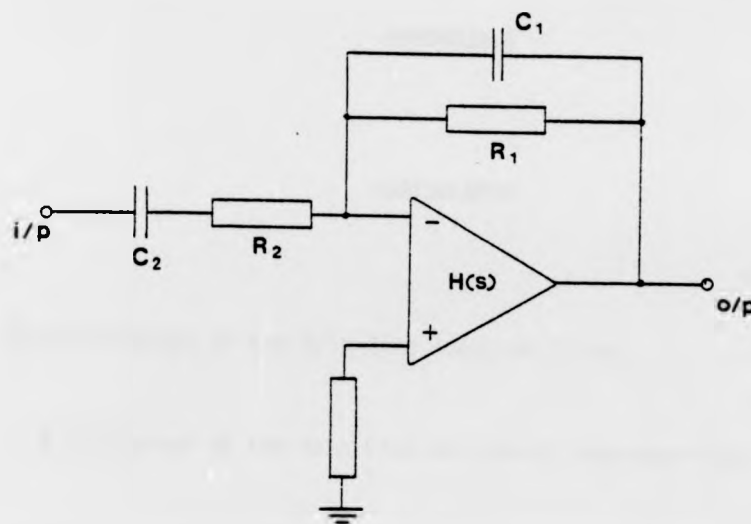Figure A4.3: An Equivalent Circuit of the Parameter Control Multiplier and Integrator

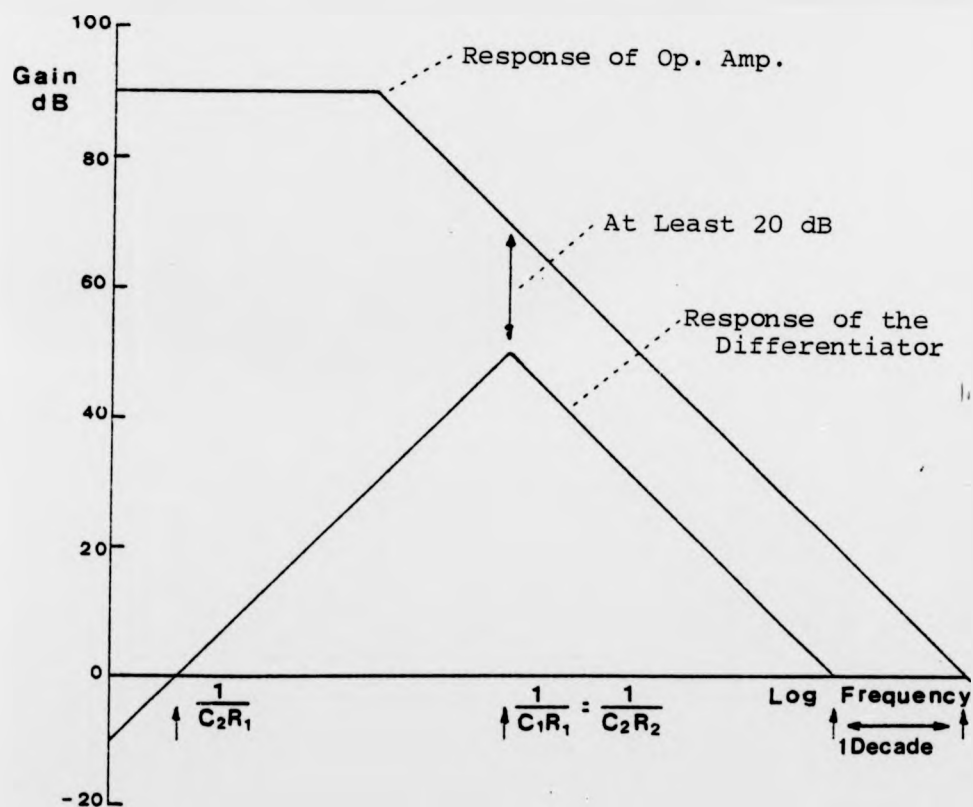Figure A4.4:   The Compensated Differentiator

Figure A4.5:   The Constraints Governing the
Design of the Differentiator
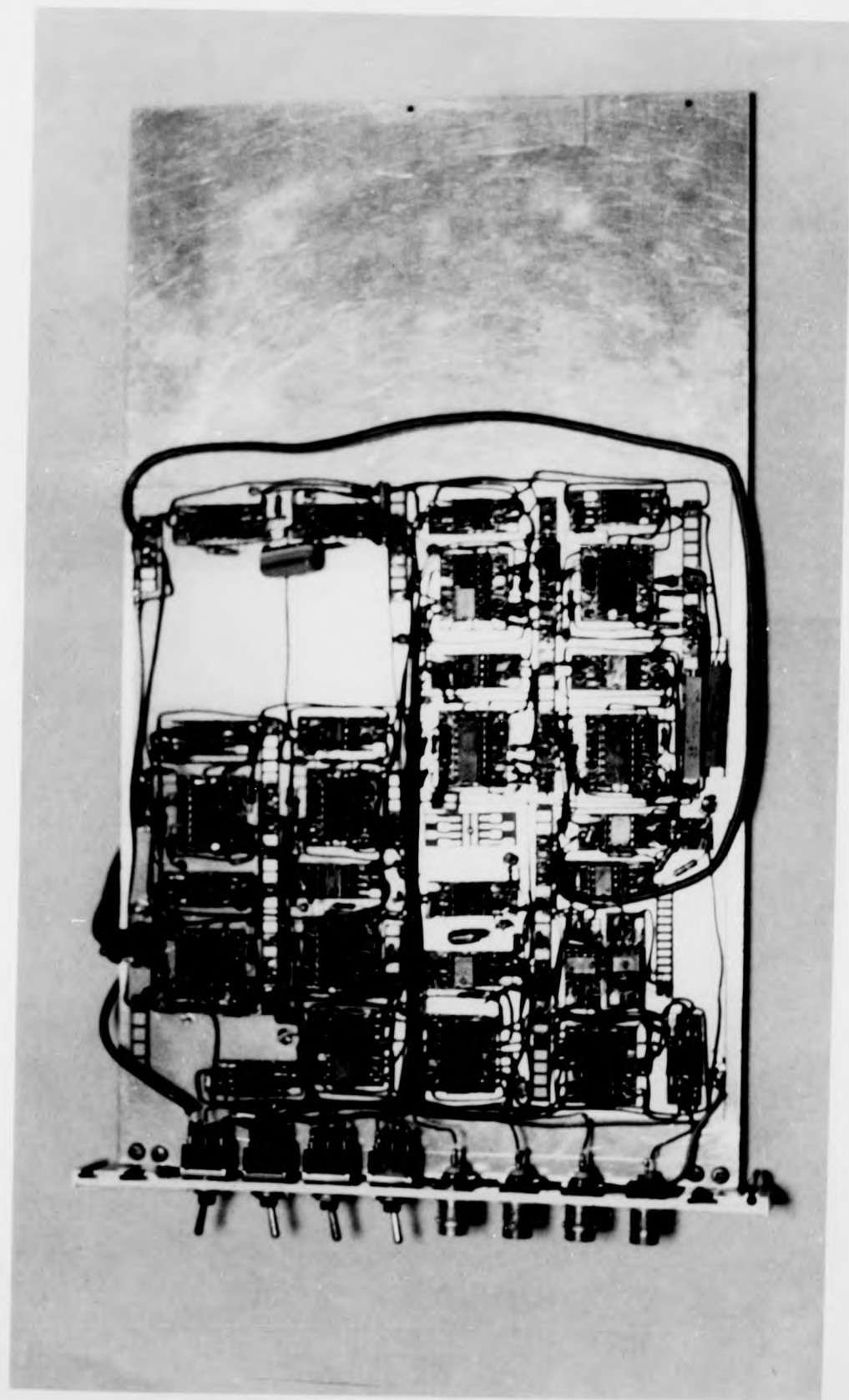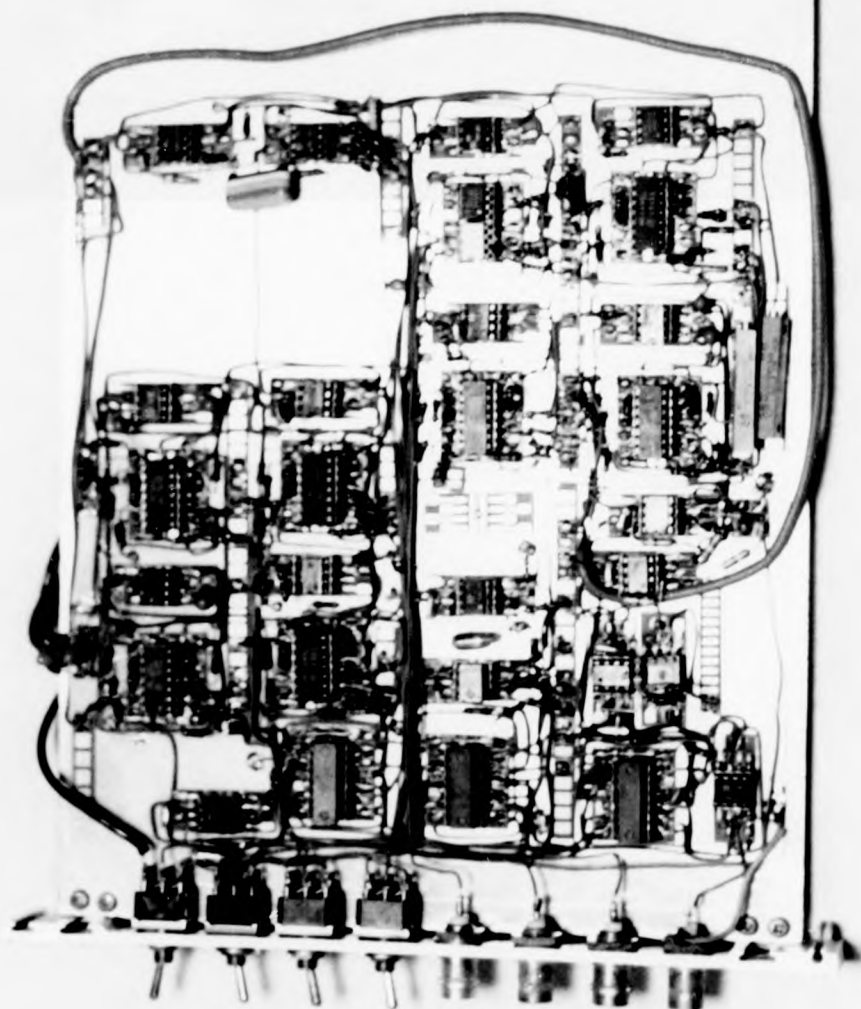
APPENDIX 5

PHOTOGRAPHS

A5.1 Photograph of the Pole-Zero Adaptive Filter

A5.2 Photograph of the main Line and Hybrid Simulator Board
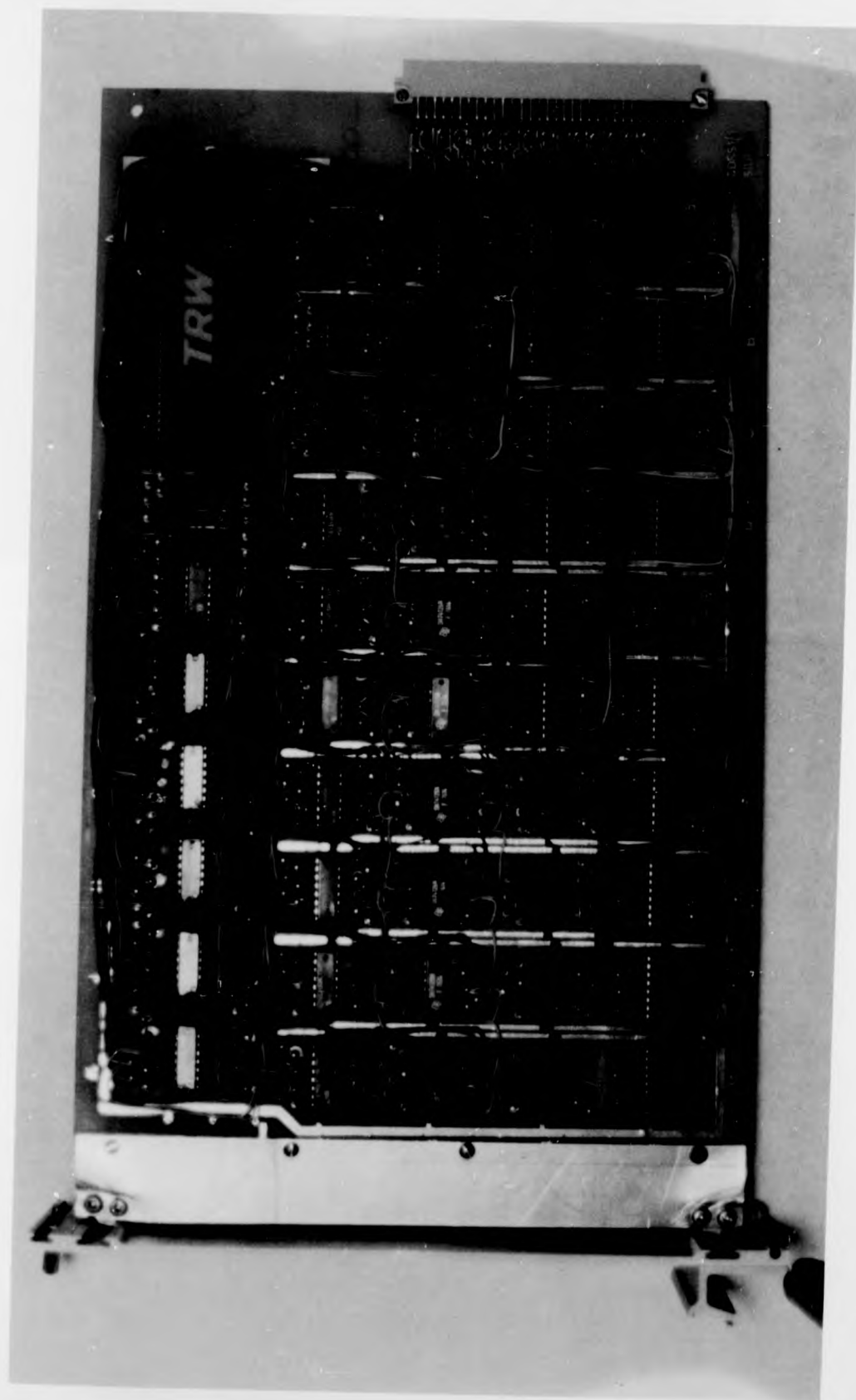
A5.3 Photograph of the Experimental Digital Recursive Adaptive
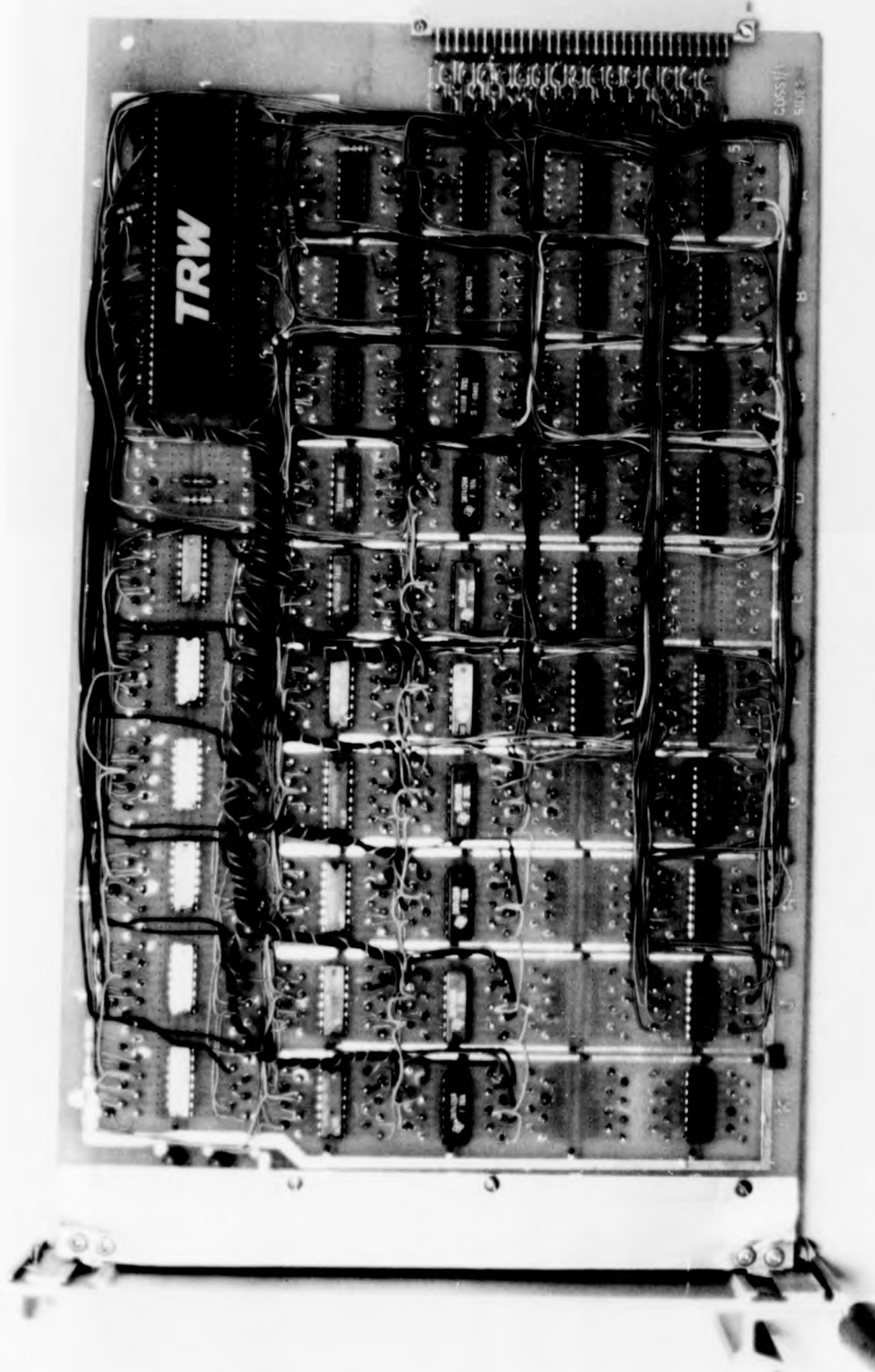Filter

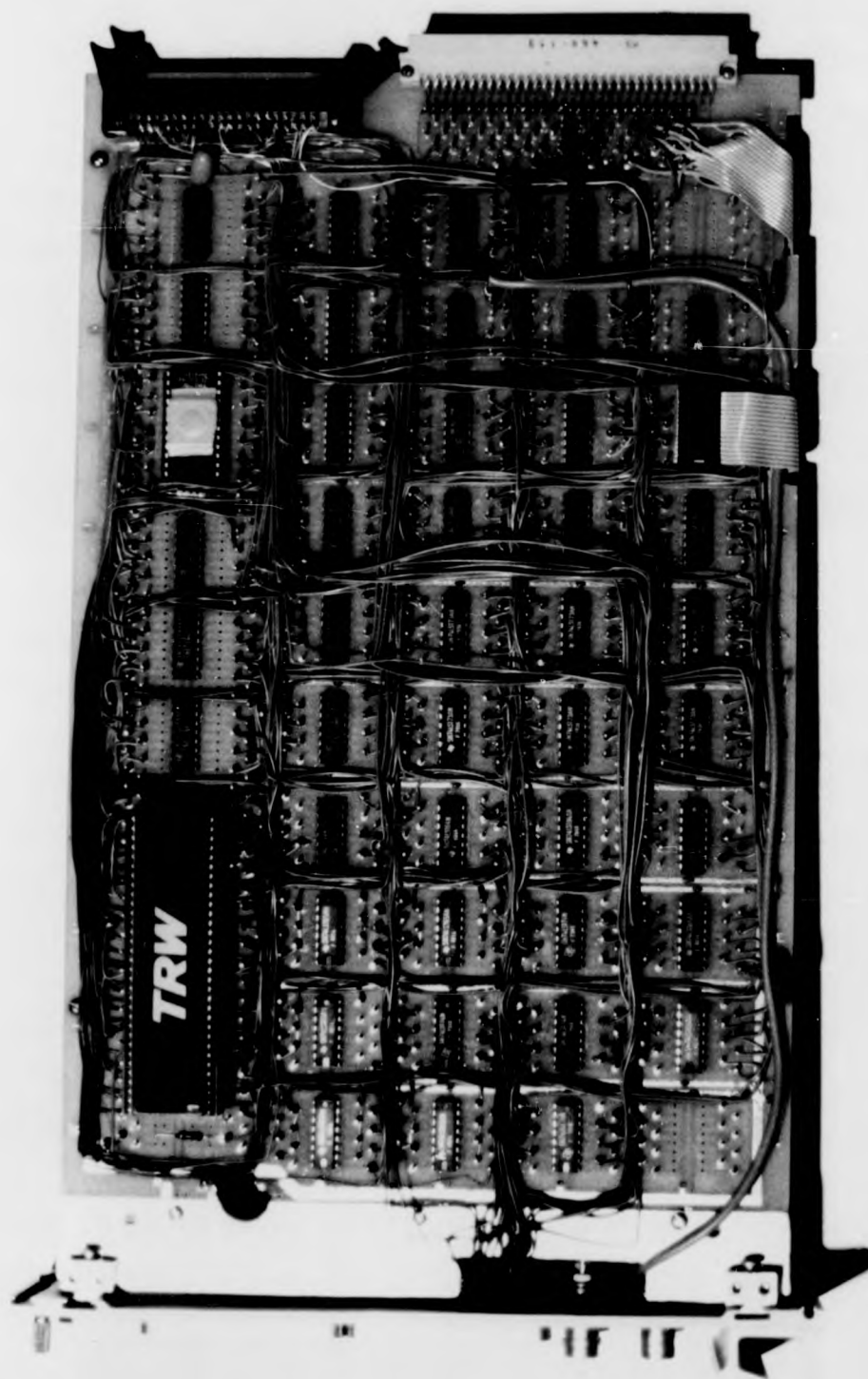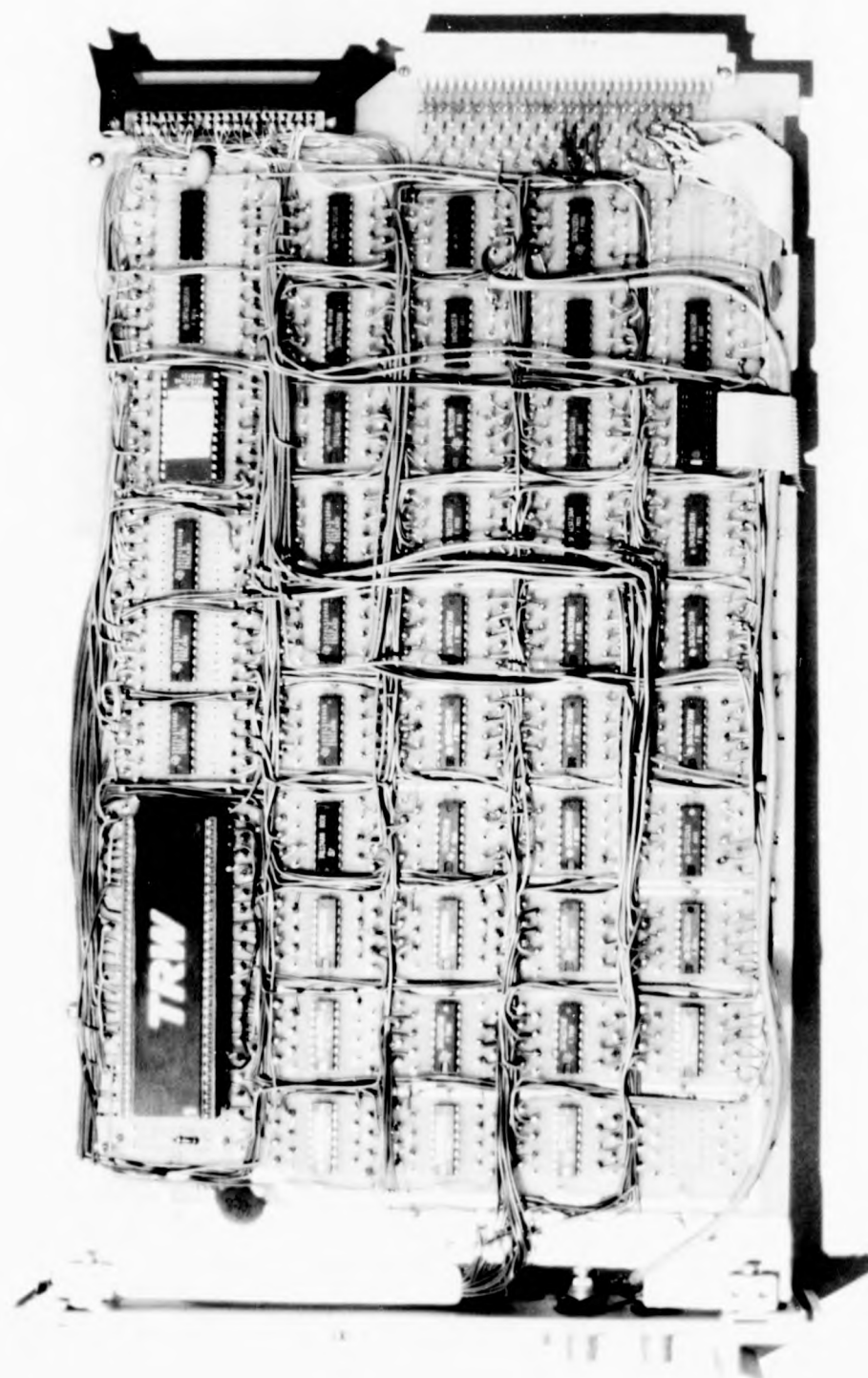<u>A5.1</u> A Photograph of the Pole-Zero Adaptive Filter

<u>A5.2</u> A Photograph of the Main Line and Hybrid Simulator Board

A5.3 A Photograph of the Experimental Digital Recursive Adaptive
Filter

REFERENCES

Adams, P.F., Harbridge, J.R., and Macmillan, R.H., "An MOS IC for Digital Filtering and Level Detection", IEEE Jour. Solid State Circuits, SC-16, No.3, pp.183-190, June 1981

Ahmed, N. Hummels, D.R., et al, "A Short-term Sequential Regression Algorithm", IEEE Trans. Acoust. Speech and Signal Processing, ASSP-27, No.5, pp.453-457 October, 1979

Ambikairajah, E., Private Communication, October 1981

Ambikairajah, E., "Efficient Digital Techniques for Speech Processing", Ph.D. thesis, University of Keele, 1982

Ames, J.R., "Survey of Transmission Problems in Introducing 4-Wire Digital Exchanges", International Switching Symposium ISS'81, Montreal, Canada, 21-25 Sept., 1981.

Ayala, I.L., "On a New Adaptive Lattice Algorithm for Recursive Filters", IEEE Trans. Acoust. Speech and Signal Processing, ASSP-30, No. 2, p.316, April 1982.

Becker, F.K., and Rudin, H.R., "Application of Automatic Transversal Filters to the Problem of Echo Suppression", B.S.T.J. Briefs, Vol. XLII, No. 10, pp.1847-1850, Dec. 1966.

Brady, P.T., and Helder, G.K., "Echo Suppressor Design in Telephone Communications", B.S.T.J., Vol. XLII, No. 6, pp.2893-2917, Nov. 1963

Bunker, R.L., Scida, F.J., and Mc. Cabe, R.P., "Line Matching Networks to Support Zero Loss Operation in Class 5 Offices", Int. Symp. on Subscriber Loops and Services, pp.166-171, Atlanta, Georgia, 1979.

Cavanaugh, J.R., Hatch, R.W., and Neigh, J.L., "A Model for the Subjective Effects of Listener Echo on Telephone Connections", B.S.T.J., Vol. 59, No. 6, pp.1009-1060, July 1980.

CCITT, Green Book, Vol. III-1, 5th Plenary Assembly, Geneva, 1972.

CCITT Recommendation P75, CCITT Red Book, Vol. 5, p.76.

Demytko, N., and English, K.S., "Echo Cancellation on Time Variant Circuits", Proc. IEEE., Vol. 65, No. 3, pp.444-453, March 1977.

Demytko, N., and Mackechnie, L.K., "A High Speed Adaptive Echo Canceller", Aust. Telecom. Res., Vol. 7, No. 1, p.20, 1973.

Dotter, B.E., De la Plaza, A., et al, "Implementation of an Adaptive Balancing Hybrid", IEEE. Trans. on Comm., Com. 28, No. 8, pp.1408-1416, Aug. 1980.

Duttweiler, D.L., "A Twelve Channel Digital Echo Canceller", IEEE. Trans. Comm., Com. 26, No. 5, p.647, May 1978.

Emling, J.W., and Mitchell, D., "The Effect of Time Delay and Echos on Telephone Conversations", B.S.T.J., Vol. XLII, No. 6, pp.2869-2891, Nov. 1963.

Everard, J.D., "A Single Channel PCM Codec", I.E.E.E. Jour. Solid State Circuits, Vol. SC-14, No.1, p.25, Feb. 1979.

Feintuch, P.L., "An Adaptive Recursive LMS Filter", Proc. IEEE, Vol. 64, No. 11, p.1622, Nov. 1976.

Feintuch, P.L., and Bershad, N.J., "Reply to 'Comments on and Additions to an Adaptive Recursive LMS Filter'", Proc. Lett., Proc. IEEE, Vol. 65, No. 9, pp.1401-1402, Sept. 1977.

Gibson, C.J., and Haykin, S., "Learning Characteristics of a Adaptive Lattice Filtering Algorithms", IEEE Trans. on Acoust. Speech and Signal Processing, ASSP. 28, No. 6, p.681, Dec. 1980.

Gray, A.H., and Markel, J.D., "Digital Lattice and Ladder Filter Synthesis", IEEE Trans. on Audio and Electroacoustics, AU-21, No. 6, pp.491-500, Dec. 1973.

Hildebrand, F.B., "Advanced Calculus for Applications", Prentice Hall Inc., N.J., 1962.

Hoge, H., "Analysis of an Adaptive Echo Canceller with Optimised Gradient Gain", Siemens Forsch. u. Entwickl. Ber., Bd. 4, Nr. 3, p.127, 1975

Horna, O.A., "Echo Canceller with Adaptive Transversal Filter Utilising Pseudo-logarithmic Coding", COMSAT Tech. Rev., Vol. 7, No. 2, p.393, Fall 1977.

Johnson, C.R., Landau, I.D., Taylor, T., and Dugard, L., "On Adaptive IIR Filters and Parallel Identifiers with Adaptive Error Filtering", Int. Conf. on Acoust. Speech and Signal Processing ICASSP-81, Atlanta, p.538, 1981.

Johnson, C.R., and Larimore, M.G., "Comments on and Additions to 'An Adaptive Recursive LMS Filter'", Proc. Letters, Proc. IEEE, Vol. 65, No. 9, p.1399, Sept. 1977.

Johnson, C.R., Larimore M.G., Treichler, J.R., and Anderson, B.D., "SHARF Convergence Properties", IEEE Trans. on Circuits and Systems, CAS-28, No. 6, p.499, June 1981.

Kanwal, A., "Linear Integral Equations (Theory and Technique)", Academic Press, London, 1971.

Kato, Y. et al, "A Digital Adaptive Echo Canceller", N.E.C. Res. and Dev., No. 31, p.32, Oct. 1973.

Kreyszig, E., "Advanced Engineering Mathematics", Wiley, 1972.

Landau, I.D., "Unbiased Recursive Identification using Model Reference Adaptive Techniques", IEEE Trans. Auto. Control, AC-21, no. 2, p.194, April 1976.

Larimore, M.G., "Hyperstability and Adaptive Filtering", IEEE Trans. Acoust. Speech and Signal Processing, ASSP-29, No. 2, p.319, April 1981.

Ljung, L., "Analysis of Recursive Stochastic Algorithms", IEEE Trans. Auto. Control, AC-22, No. 4, p.551, Aug. 1977.

Lucky, R.W., "Automatic Equalisation for Digital Communication", B.S.T.J., Vol. XLVIV, No. 4, p.547, April 1965.

Mackechnie, L.K., "Continuously Adaptive Echo Cancellers", Elect. Lett., Vol. 6, No. 3, p.69, 5th Feb. 1970.

Mantey, P.E., "Convergent Automatic Synthesis Procedures for Sampled Data Networks with Feedback", TA. No. 7663-1, Stanford Electronics Lab., CA., Oct. 1964.

Mark, J.W. and Yeung, K.L., "A Coupling Scheme for Adaptive Echo Cancellation", Proc. IEE, Vol. 123, Part 6, pp.477-489, June 1976.

Mc. Clellan, J.H., et al, "A Computer Program for Designing Optimum FIR Linear Phase Digital Filters", IEEE Trans. on Audio and Electroacoust., AU-21, No. 4, pp.354-366, Aug. 1973.

Mitchell, O.M.M., and Berkley, D.A., "A Full Duplex Echo Suppressor using Centre Clipping", B.S.T.J., Vol. 50, No. 5, p.1619, May/June 1971.

Miura, A., et al, "A Blockless Echo Suppressor", Electron. Comm. Japan, Vol. 51-A, No. 7, p.10, 1968.

Naglib, "NAG Fortran Library Manual, Mark 9", Chapter E02 - Curve and Surface Fitting, Numerical Applications Group, Oxford, 1977.

Ochiai, K., Araseki, T., and Ogihara, T., "Echo Canceller with Two Echo Path Models", IEEE Trans. on Comms., COM-25, No. 6, pp.587-594, June 1977.

Papoulis, A., "Probability, Random Variables, and the Stochastic Process", McGraw Hill, New York, 1965.

Parikh, D. and Ahmed, N., "A Sequential Regression Algorithm for Recursive Filters", Elect. Lett., Vol. 14, No. 9, p.266, 27th April, 1979.

Parikh, D., Ahmed, N., and Stearns, S.D., "An Adaptive Lattice Algorithm for Recursive Filters", IEEE Trans. Acoust. Speech and Signal Processing, ASSP-28, No. 1, p.110, Feb. 1980.

Popov, V.M., "Hyperstability of Control Systems", Springer-Verlag, Berlin, 1973.

Rabiner, L.R., and Gold., "Theory and Application of Digital Signal Processing", Prentice Hall Inc., N.J., 1975.

Rabiner, L.R., and Schafer, R.W., Digital Processing of Speech Signals, Prentice-Hall, N.J., 1978.

Riesz, R.R. and Klemmer, E.T., "Subjective Evaluation of Delay and Echo Suppressors in Telephone Communications", B.S.T.J., Vol. XLII, No. 6, p.2919, Nov. 1963.

Sondhi, M.M., "An Adaptive Echo Canceller", B.S.T.J., Vol. XLVI, No. 3, p.497, March 1967.

Sondhi, M.M., and Presti, A.J., "A Self Adaptive Echo Canceller", B.S.T.J. Briefs, Vol. XLV, No. 10, p.1851, Dec. 1966.

Stearns, S.D., "Error Surfaces of Adaptive Recursive Filters", Sandia National Lab., SAND-80-1348, Dec. 1980.

Stearns, S.D., Elliott, G.R., and Ahmed, N., "On Adaptive Recursive Filtering", Proc. 10th Asilomar Conf. on Circuits and Systems, p.5, 1976.

Tattersall, G.D., "Linear Phase Analog Active Filters with Equiripple Passband Responses", IEEE Trans. on Circuits and Systems, CAS-28, No. 9, p.925, Sept. 1981.

Tattersall, G.D. and Carey, M.J., "Digital Bandlimiting Filters for PCM Transmission Systems", IEEE Trans. on Comms., COM-27, NO. 1, p.240, Jan. 1979.

Tou, J., "Modern Control Theory", Mc. Graw Hill, 1964.

Treichler, J.R., Larimore, M.G., and Johnson, C.R., "Simple Adaptive IIR Filtering", Proc. IEEE Int. Conf. Acoust. Speech and Signal Processing, Tulsa, O.K., p.118, 1978.

TRW, Data Sheet on TDC1009J Multiplier-Accumulator, 1979.

White, S.A., "An Adaptive Recursive Digital Filter", Proc. 9th Asilomar Conf. on Circuits and Systems, p.21, 1975.

Widrow, B., "Adaptive Filters 1 - Fundamentals", Stanford Electronics Lab. Tech. Rept., No. 6764-6, Dec. 1966.

Widrow, B., and Mc. Cool, J.M., "Comments on 'An Adaptive Recursive LMS Filter'", Proc. Letters, Proc. IEEE, Vol. 65, No. 9, p.1402, Sept. 1977.

Zverev, A.I., "Handbook of Filter Synthesis", Wiley, N.Y., 1967.